Environmental modelling and spatial ecology with focus on invasive *Aedes* mosquitoes and emergent mosquito-borne pathogens

vorgelegt von

M. Sc.

Matteo Marcantonio

geb. in Fondi, Italy

Von der Fakultät VI – Planen Bauen Umwelt
der Technischen Universität Berlin
zur Erlangung des akademischen Grades

Doktor der Naturwissenschaften
Dr. rer. nat.

genehmigte Dissertation

Promotionsausschuss:
Vorsitzende: Prof. Dr. Eva Nora Paton
Gutachterin: Prof. Dr. Birgit Kleinschmit
Gutachter: Prof. Dr. Chris Barker

Tag der wissenschaftlichen Aussprache: 04.11.2016

Berlin 2017

Così, se non proprio visto,
era immaginato,
visto con gli occhi della mente.

Stefano D'Arrigo, *Horcynus Orca*

Acknowledgements

I would like to acknowledge all of the people who have supported me along the marvellous journey that brought me to conclude this project. I am pleased to have had the chance to meet all of you. The healthy and stimulating environment in every research group that hosted me played a pivotal role in shaping my positive attitude towards science and life. Emily, thanks a lot for having gloriously withstood my lunacy in the last months and for having proofread my English so many times!

I want to emphasise my gratitude to Dr. Markus Neteler and Dr. Annapaola Rizzoli, my supervisors at the Fondazione Edmund Mach, as well as to Prof. Dr. Birgit Kleinschmit and Dr. Michael Förster for their continuous support at the Technical University of Berlin.

I am grateful to Fondazione Edmund Mach (FIRST), the European Commission (Eurowestnile), the National Aeronautics and Space Administration (DDS-Mosquitos), the Provincia Autonoma di Trento (LExEM) and The Research Council of Norway (IRSAE) as co-funders of projects that provided me administrative and financial support. Furthermore, I wish to thank the European Centre for Disease Prevention and Control for the fruitful collaboration and data exchange on West Nile virus.

Summary

Biological invasions are a side effect of globalisation and human modification of natural systems. Invasive mosquitoes and the pathogens that they carry are leading causes of human suffering. Mosquito vectors of pathogens are often ecologically plastic and able to exploit human movements to disperse. As such they spread across wide geographical areas and are among the most successful species to have become invasive. Mosquito-borne pathogens have complex life cycles which involve a rich set of reservoir and vector hosts. They are evolutionarily very dynamic, ready to take advantage of new opportunities offered by anthropogenic environmental changes. Many pathogens associated with mosquitoes are indeed changing their ecology or modifying their geographical and biological distribution, being considered as invasive species. Despite this impressive plasticity, invasive mosquitoes and mosquito-borne pathogens are still part of a natural system, and as such are limited by environmental conditions.

The main target of my research was to apply ecological theory and environmental modelling to gain knowledge on these limiting conditions, by establishing mechanistic and correlative associations between the environment, invasive vectors and pathogen demographics, as well as physiological and spatial dynamics. Understanding these mechanisms is key to design effective health policies which aim to mitigate the emergence of new pathogens, mainly by hindering the population that vectors them.

The core of this thesis is formed by a series of stand-alone scientific papers, published, submitted or close to submission to peer-reviewed journals; the core chapters are backed by the General Introduction, and the General Summary and Outlook.

Chapter 1 (General Introduction) depicts the state of the knowledge of the thesis research topic, delineating the research context and objectives. The relevance of mosquitoes as vector species and of emerging pathogens, combined with the need to use environmental modelling in investigating their ecology, is exposed;

Chapter 2 looks at the environmental factors associated with the re-emergence of West Nile Virus (WNV) in the Old World. The association between WNV incidence in humans and a wide range of predictors was assessed through an automatic statistical approach. By identifying key environmental drivers of WNV, this chapter aims to both lay the foundations for the development of models able to predict WNV risk at a continental scale and to highlight the weakness of available data on WNV in the Old World;

Chapter 3 deals with the estimation of habitat suitability and potential spread velocities of *Ae. koreicus* in Italy, through statistical modelling. The integration of the developed suitability map with transportation network data and the observed species dispersal rate, allowed to characterise *Ae. koreicus* potential pattern of range expansion. Results showed that the study area is widely suitable for *Ae. koreicus*, and this mosquito was predicted to fill the suitable niche in a relatively short time. This scenario opens the way to an enriched entomological landscape with three container-breeding mosquitoes interacting and thus complicating the epidemiological status of vector-borne pathogens;
Chapter 4 presents a new model framework to simulate, with ecologically robust foundations, the introduction, life cycle, population and spatial dynamics of *Ae. albopictus* in urban landscapes. The developed model was applied to investigate the mechanisms underlying *Ae. albopictus* invasion dynamics in a newly invaded urban area. We found that *Ae. albopictus* introduction in the study area was more likely to have happened in spring or summer, and that the derived population remained at low density for a long time. These findings support the hypothesis that the recent *Ae. albopictus* invasion of the study area may derive from an old introduction event;
Chapter 5 explores *Ae. albopictus* invasion dynamics as a function of the configuration of urban vegetation. Vegetation is an important component of urban areas and it has also been suggested as important for *Ae. albopictus* invasion dynamics. We applied the model developed and proposed in chapter 4 to synthetic urban landscapes with different vegetation configurations. Results supported the expectation that vegetation affects *Ae. albopictus* invasion dynamics, with a spread vegetation configuration causing increased mosquito dispersal and density in urban areas;
Chapter 6 presents data from an experimental design implemented to acquire information on the thermal characteristics of aboveground *Ae. albopictus* micro-habitats. The acquired data was used to estimate temperature difference distributions between micro-habitats which are generalisable to other locations. We investigated how the use of micro-habitat data rather than generic temperature changes estimated *Ae. albopictus* life cycle durations. We found that the latter may be sub-optimal when modelling *Ae. albopictus* population dynamics. The reported temperature dataset can be exploited to make opportunistic temperature data appropriate for *Ae. albopictus* population dynamics modelling;
Chapter 7 (General Summary and Outlook) lay the key findings of the core chapters forming the thesis into a general context, and outlines directions for future research for using environmental modelling in studies of emergent mosquito-borne pathogens and invasive mosquito species.

Zusammenfassung

Biologische Invasionen sind ein Nebeneffekt der Globalisierung und der menschlichen Modifizierung von natürlichen Systemen. Invasive Stechmücken und die Krankheitserreger, die sie in sich tragen, sind die Hauptursache menschlichen Leidens. Moskito-Vektoren von Krankheitserregern zeigen oft ökologische Plastizität und können die menschliche Mobilität ausnutzen, um sich zu verteilen. Aus diesen Gründen sind sie über weite geographische Gebiete verteilt und gelten als einige der erfolgreichsten invasiven Arten weltweit. Stechmücken, die Krankheitserreger übertragen, haben komplexe Lebenszyklen, die viele Reservoir- und Vektor-Wirte beinhalten. Sie sind in Bezug auf ihre Evolution sehr dynamisch und nutzen die Vorteile, die ihnen anthropogene Umweltveränderungen bieten. Viele Krankheitserreger, die mit Stechmücken in Verbindung gebracht werden, sind dabei, ihre Ökologie oder ihre geografische und biologische Verteilung zu verändern und werden deshalb als invasive Arten betrachtet. Trotz dieser beeindruckenden Plastizität sind invasive Stechmücken und übertragen übertragene Krankheitserreger immer noch Teil eines natürlichen Systems, und dementsprechend immer noch durch Umweltbedingungen eingeschränkt. Das Hauptziel meiner Untersuchungen war es, ökologische Theorie und Umweltmodellierung anzuwenden, um Erkenntnisse über diese einschränkenden Bedingungen zu gewinnen. Hierzu wurden mechanistische und korrelative Assoziationen zwischen Umwelt, invasiven Vektoren und der Demographie der Krankheitserreger hergestellt sowie die physiologische und räumliche Dynamik analysiert. Das Verständnis dieser Mechanismen ist der Schlüssel dazu, effektive Strategien einer Gesundheitspolitik zu entwickeln, die das Auftreten neuer Krankheitserreger vermindern sollen, indem sie vor allem die Krankheitsvektoren an der Ausbreitung hindern. Der Kern dieser Arbeit besteht aus eigenständigen wissenschaftlichen Arbeiten (scientific papers), die bei Zeitschriften mit peer-review-Verfahren eingereicht wurden oder sich kurz vor der Einreichung befinden. Die Kernkapitel werden von einer allgemeinen Einführung und Zusammenfassung und einem Ausblick begleitet.

Kapitel 1 (Allgemeine Einführung) stellt den Kenntnisstand zum Forschungsthema der Doktorarbeit dar und umreißt den Forschungskontext und die Ziele. Die Relevanz von Mücken als Vektoren von neu auftretenden Krankheitserregern werden dargelegt, kombiniert mit der

Notwendigkeit der Verwendung von Umweltmodellierung, um die Ökologie der Mücken zu untersuchen.

Kapitel 2 befasst sich mit den Umweltfaktoren, die mit dem Wiederauftreten von West-Nil-Virus (WNV) in der Alten Welt verbunden sind. Die Verbindung von WNV-Vorkommen bei Menschen und einer Vielzahl von Vorhersage-Anzeichen wurde durch einen automatischen statistischer Ansatz bestimmt. Durch die Identifizierung der wichtigsten ökologischen Faktoren von WNV zielt dieses Kapitel sowohl auf die Grundlagen für die Entwicklung von Modellen, die das Risiko für WNV auf kontinentaler Ebene voraussagen sollen, als auch die Schwäche der verfügbaren Daten über WNV in der Alten Welt ab.

Kapitel 3 befasst sich mit der Einschätzung der Habitateignung und möglicher Ausbreitungsgeschwindigkeiten von *Aedes koreicus* in Italien mittels statistischer Modellierung. Die Einbindung von Transportnetzwerkdaten und Ausbreitungsraten der beobachteten Arten in die hier entwickelte Eignungskarte erlaubte es, das Potentialmuster der Ausbreitung von *Aedes koreicus* zu charakterisieren. Die Ergebnisse zeigten, dass das Untersuchungsgebiet für *Aedes albopictus* weitestgehend geeignet ist, und es wurde vorhergesagt, dass diese Stechmückenart die entsprechende Nische in relativ kurzer Zeit füllen wird. Dieses Szenario zeigt das Potential einer reicheren entomologischen Landschaft auf mit drei sich in Behältern vermehrenden Stechmückenarten, die in Wechselwirkung zueinander stehen und den epidemiologischen Status der Vektor-übertragenen Pathogene verkomplizieren wird.

Kapitel 4 stellt ein neues Rahmenmodell vor, welches mit ökologisch stabilen Kenntnissen die Einführung, den Lebenszyklus, die Bevölkerungs- und räumliche Dynamik von *Aedes albopictus* in urbanen Landschaften simuliert. Das entwickelte Modell wurde eingesetzt, um die der Dynamik der Invasion von *Aedes albopictus* zugrunde liegenden Mechanismen in einem neu befallenen Stadtgebiet zu untersuchen. Wir fanden heraus, dass die Einbringung von *Aedes albopictus* in das Untersuchungsgebiet vermutlich eher im Frühjahr oder Sommer geschehen war und dass die daraus entstandene Population lange bei niedriger Dichte blieb. Diese Ergebnisse stützen die Hypothese, dass sich die neueste *Aedes albopictus* Ausbreitung im Untersuchungsgebiet von einer alten Einführung abgeleitet werden kann.

Kapitel 5 untersucht die *Aedes albopictus* Invasionsdynamik in Abhängigkeit von der Zusammensetzung der Stadtvegetation. Vegetation ist ein wichtiger Bestandteil städtischer Gebiete und wurde auch als wichtig für die Invasionsdynamik von *Aedes albopictus* angenommen. Wir verwendeten das in Kapitel 4 entwickelte und vorgeschlagene Modell für synthetische Stadtlandschaften mit verschiedenen Vegetations-Konfigurationen. Die Ergebnisse unterstützten die Erwartung, dass die Vegetation die *Aedes albopictus* Invasionsdynamik beeinflusst, und zwar mit einer sich ausbreitenden Vegetationszusammensetzung, die eine erhöhte Moskitoausbreitung und -dichte in städtischen Gebieten verursacht.

Kapitel 6 stellt Daten aus einem experimentellen Design dar, das Informationen über die thermischen Eigenschaften der überirdischen Mikrohabitate von *Aedes albopictus* implementieren sollte. Die erfassten Daten wurden verwendet, um die Verteilung von Temperaturdifferenzen zwischen Mikrohabitaten zu schätzen, die auf andere Standorte übertragen werden können. Wir untersuchten, wie der Einsatz von Mikrohabitat-Daten die Lebenszyklusdauer von *Aedes albopictus* besser als generelle Temperaturmessungen schätzen kann. Wir fanden heraus, dass letztere zur Modellierung der Populationsdynamik von *Aedes albopictus* suboptimal sind. Der dargestellte Temperatur-Datensatz kann genutzt werden, um opportunistische Temperaturdaten für eine dynamische Modellierung der *Aedes albopictus* Population geeignet zu machen.
Kapitel 7 (Allgemeine Zusammenfassung und Ausblick) stellt die wichtigsten Ergebnisse der Kernkapitel dieser Doktorarbeit in einen allgemeinen Kontext und umreißt Ziele (Zielrichtungen) für zukünftige Forschung unter Verwendung von Umweltmodellierung in Studien zu neu auftretenden Stechmücken-übertragener Pathogene und invasiver Mückenarten.

Contents

List of Figures

List of Tables

Nomenclature

Acronyms / Abbreviations

AICc	An Information Criterion corrected for small sample sizes
BANOVA	Bayesian Analysis of Variance
CrI	Credible Interval
DIC	Deviance Information Criterion
GLM	Generalized Linear Model
HDI	High Density Interval
iSDM	invasive Species Distribution Model
logBAY	logistic regression with Bayesian inference
LST	Land Surface Temperature
MaxEnt	Maximum Entropy
MCMC	Markov Chain Monte Carlo
MM	Mechanistic Model/Population dynamics model
NDVI	Normalized Difference Vegetation Index
NDWI	Normalized Difference Water Index
PHY	GIS physiology-based
PPD	Posterior Probability Distribution
SDM	Species Distribution Model
SM	Suitability model/Correlative model
TSS	True Skill Statistics
UL	Urban Landscape
WNE	West Nile meningitis
WNV	West Nile encephalitis
WNF	West Nile fever
WNV	West Nile virus
WS	Weather Station

Chapter 1

Introduction

1.1 General introduction: Invasive species and emerging infectious pathogens

Invasive species are a global threat for biological diversity [Simberloff et al., 2013], economics [Pimentel, 2011] and human health [Daszak et al., 2000]. They are an important determinant of the current generalised loss of biological diversity and alteration of ecosystem services [Drake, 1989; Hejda et al., 2009]. The economy of entire production sectors is impacted by invasive agricultural pests, as well as invasive parasites of domestic animals and wildlife [Pimentel et al., 2005; Ancona et al., 2010]. Notwithstanding the heavy impact on biodiversity and economics, the most perceived consequences of biological invasions are the health risks associated with the spread of these pathogenic species or the species which vector the pathogens [Crowl et al., 2008; Hulme, 2015]. Emerging pathogens are defined as pathogens "that have newly appeared in a population [emergent – Ed.] or have existed previously but are rapidly increasing in incidence or geographic range [re-emergent – Ed.]" [Morens et al., 2004]. Emerging pathogens can be considered as another class of invasive species that spread into new host populations, species or communities [Hatcher et al., 2012]. Prevention or management of invasive species relies on a deep understanding of the processes that lead to introduction and invasion [Dunn and Hatcher, 2015]. Policies which aim to control the spread of invasive species are weakly implemented at national and international levels. With the exception of some sporadic examples (i.e. EU Regulation 1143/2014; The Ballast Water Management Convention at international level; New Zealand and Australia invasive species policies, at national level), these policies have low priority and lack adequate funds [Simberloff, 2014]. As a consequence, environmental modelling and risk assessments, which enable us to gain knowledge on mechanisms and processes leading to invasions, are critical for identifying high-risk scenarios and for targeting resources accordingly. The general aim of this thesis is to gain insights into the association between emerging pathogens, invasive vector species and environmental conditions. To reach this main goal this thesis focuses on developing and applying statistical and mathematical models as well as experimental designs to the re-emergence of West Nile virus (WNV) in the Old World, the invasion pattern of *Aedes koreicus* (Edwards; the "Korean tiger mosquito") in Northern Italy and the mechanisms underpinning *Aedes albopictus* (Skuse; the "Asian tiger mosquito") invasion in urban areas.

1.2 Mosquitoes as vector of infectious pathogens

Mosquitoes are a moderately diverse taxon, counting about 3200 species [Becker, 2010]. They live on all the human inhabited continents and provide many ecosystem services, such as

pollination and recycling of detritus in aquatic ecosystems [Fang, 2010]. The female of some mosquito species are entomophagous insects which use the blood of a host not only as a protein food source but also to regulate metabolic processes (e.g. eggs maturation; Clements [1992]). They have evolved a set of physiological adaptations to overpass the animal skin barrier and take blood meals that can reach three times their mean body weight [Nayar and Sauerman, 1975]. These physiological adaptations are exploited by a wide group of pathogens to efficiently pass from host to host blood vessels, giving mosquitoes the infamous title of "the deadliest animal in the world" [Gates, 2016] or "the best known disease vector" [WHO, 2016]. The mosquito-borne pathogens are part of a wider class of pathogens, the vector-borne pathogens, and as such are characterised by an indirect transmission, requiring an intermediate host, the mosquito, to complete their life cycle. Every year more than 1 million deaths are caused by vector-borne pathogens such as malaria parasites and dengue virus [WHO, 2016], making the biology, ecology and control of these pathogens as well as of their vector populations a central topic in the scientific and educational literature.

1.3 Re-emerging vector-borne pathogens, West Nile virus as a model

Vector-borne pathogens have always plagued humans [Morens and Fauci, 2013], and today, in our overcrowded world, about half of the world's population lives under the risk of becoming infected by them [Bhatt et al., 2013]. Some of these pathogens, defined as re-emerging, besides expanding their geographical distribution, are also changing their ecology in historical distribution areas, rapidly increasing in incidence and, thus, causing serious public health issues (Figure 1.1).

There are often multiple and interconnected causes underpinning the re-emergence of vector-borne pathogens, such as mutation in the pathogen genome, new disease-host systems (i.e. novel ecosystems; Corlett [2015]) and human-related environmental or climatic changes [Morens et al., 2004; Reisen, 2013; Dunn and Hatcher, 2015]. Among the most recent and renowned example of re-emergent vector-borne pathogens is the West Nile virus (WNV). This virus belongs to the *Flavivirus* genus [Kuno et al., 1998] and was first discovered in Uganda in 1937, on the West side of the Nile river [Smithburn et al., 1940]. WNV has a multi-host enzootic (i.e. maintained in the animal population) life cycle where mosquitoes are the bridge vector between vertebrate hosts. *Culex pipiens* Assemblage (hereafter, Pipiens Assemblage; Harbach [2012]), is the main vector taxon while a wide diversity of vertebrate taxa are reservoir hosts, but birds of the family *Passerinidae* (Illiger) are considered to be the principal. Humans

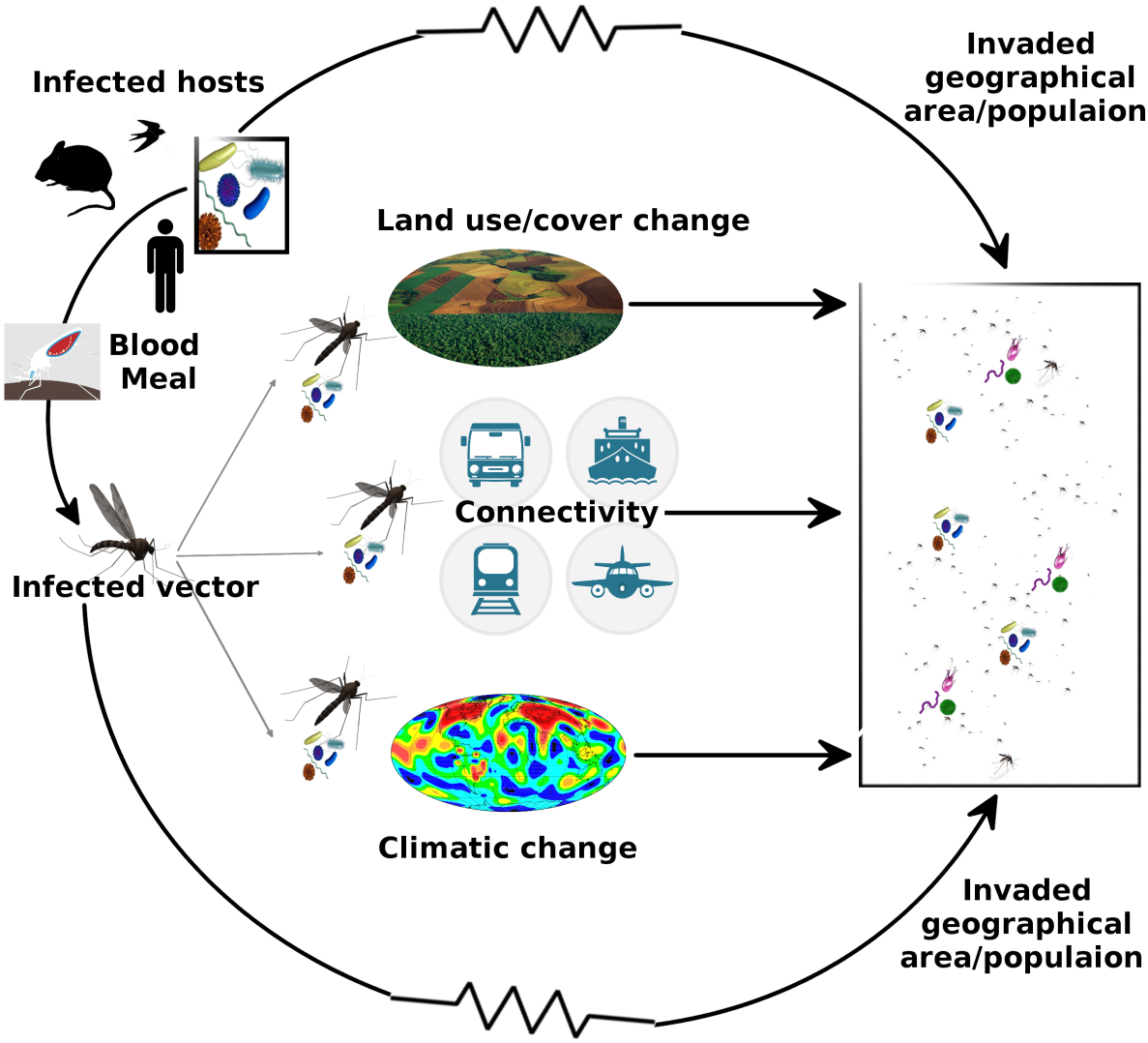

Figure 1.1: The introduction pathways of vectors and vector-borne pathogens. In the top pathway, the pathogen is introduced through its hosts. The receiving environment has already competent vectors that allow the pathogen spread. In the bottom pathway, the introduction of the arthropod vector is contemporary or follows the introduction of the pathogen. Both the introduction pathways are mediated by human factors, such as land use/cover change, increased connectivity and climate change, which break ecological "resistance" factors or conditions previously insurmountable for vectors and pathogens.

and horses can become incidentally infected and develop a mild-to-severe-disease. They are dead-end hosts, meaning that they are not able to transmit the virus to other mammals or mosquitoes during infection. About 80 % of the infections in humans by this virus are asymptomatic. Among the clinical cases, 99 % develop flu-like symptoms known as West Nile fever (WNF), while approximately 1 % develop severe, and potentially fatal, neuro-invasive diseases (meningitis and/or encephalitis; WNM ,WNE). Documented sporadic and localised WNV outbreaks in human populations have been documented since the 1960s in Europe and Africa, but in the last 2 decades a change in its epidemiological trend has arisen [Reisen, 2013; Rizzoli et al., 2015]. This emerging trend was underpinned by: *i)* an increased frequency of outbreaks in human and domestic horses populations, *ii)* increased reported encephalitis and meningitis cases in humans and *iii)* a dramatic expansion of the geographical range of outbreaks [Murray et al., 2011]. Indeed, WNM and WNE outbreaks, once restricted to Europe, Asia and Africa (hereafter the Old World; Cambridge Dictionary [2016]), have been reported in the United States since 1999 and in Australia since 2011 [Reisen, 2013; Prow et al., 2016]. For the above-listed reasons, WNV has abruptly become a focus of scientific research, and in turn has emerged as a model for understanding the potential risk factors associated with emerging pathogens worldwide [Artsob et al., 2009]. Variation in land use, climate, habitat structure, ecological community, human socio-economic status or behaviour have all been indicated as affecting the spatio-temporal trend of WNV occurrence in the Old World [Paz and Semenza, 2013; Semenza, 2015]. However, the scientific literature on this trend focused on occurrence at course spatial scales [Tran et al., 2014], a limited time span [Paz et al., 2013] or a limited geographical extension [Valiakos et al., 2014]. A quantitative characterisation of WNV epidemiological trend determinants across Europe throughout a multi-year time span would instead provide important insight into the epidemiological context of those geographical areas which have long been invaded by this pathogen. This quantitative characterisation may serve as a prelude to the development of eco-epidemiological models which would effectively predict WNV transmission in the Old World [Smith et al., 2014].

1.4 The worldwide spread of *Aedes* mosquitoes

The remarkable geographical expansion of WNV after introduction in the New World, was undoubtedly facilitated by the prior presence of a competent vector, the Pipiens Assemblage. However, in other cases, the emergence of pathogens in new geographical areas or populations has been boosted by the contemporary or subsequent introduction of competent vectors (Figure 1.1; Charrel et al. [2014]). This is the case of emergent pathogens such as chikungunya, dengue and Zika virus, all transmitted by *Aedes* (Meigen) mosquitoes [Simmons et al., 2012; Charrel

et al., 2014; Weaver et al., 2016]. These pathogens, once constrained by the geographical distribution of their vectors, now menace millions of often immunologically naive people worldwide [Brady et al., 2013]. *Aedes* mosquitoes are among the species which have most expanded their geographical range in the last century. Those *Aedes* mosquitoes native of the tropical and subtropical zones or temperature territories of Southern-West Asia, have now colonised all the human inhabited continents, and their distribution spans from as South as Argentina to as North as Northern United States. Some of these species have long established populations in areas outside their native range. As an example, *Aedes aegypti* (Linnaeus), the most significant vector of dengue, chikungunya and yellow fever viruses, native of Southern-east Asia, was successfully introduced in the New World and Europe sometimes between the 15-18th centuries, possibly in multiple occasions [Tabachnick, 1991; Brown et al., 2014]. Other *Aedes* species, such as *Aedes japonicus* (Theobald), *Aedes koreicus* and *Aedes albopictus* were only able to significantly expand their geographical distribution more recently [Medlock et al., 2015].

The change in the geographical distribution of *Aedes* species follows a well established biological invasion pattern, common to a set of hardy generalist species able to exploit human-mediated environmental changes [Williamson and Fitter, 1996]. This pattern is consequential of a complex interplay between socio-economical trends and environmental factors [Brown et al., 2014]. Among these determinants, the opening and intensification of new connections and goods exchange between previously ecologically isolated areas has played a leading role in the impressive worldwide invasion of *Aedes* mosquitoes [Tatem et al., 2006].

1.4.1 *Aedes koreicus*, a new invasive vector of pathogens

Among *Aedes* mosquitoes, *Ae. koreicus*, which is native of Southern-West Asia temperate regions was reported for the first time outside its native range in Belgium and Italy, in 2008 and 2011, respectively [Versteirt et al., 2012; Capelli et al., 2011]. This species has also been recently found in Switzerland, Black sea's Russian territories, Germany and Hungary [Suter et al., 2015; Ganushkina et al., 2016; Werner et al., 2016; Kurucz et al., 2016]. *Aedes koreicus* is cold resistant and can exploit urban habitats, however little more that this is known about its biology and ecology [Capelli et al., 2011]. The sparse information we have and the phylogenetic similarities with *Ae. japonicus* (see Reinert et al. [2009]) is however enough to hypothesise that this species will colonise a wide geographical range in the next decades [Kaufman and Fonseca, 2014]. The range expansion of *Ae. koreicus* may also have an impact on human and animal health, as it is a potential vector of *Dirofilaria immitis* [Morchón et al., 2012; Montarsi et al., 2015a] and Japanese encephalitis virus [Miles, 1964]. While the population introduced in Belgium has not shown further expansion since the year of discovery, the Italian *Ae. koreicus*

population is in moderate expansion [Montarsi et al., 2015b]. A rapid assessment of potential suitable areas and the velocity of spread in Italy are needed to prioritise where and when monitoring efforts should be applied to have a greater chance of success in mitigation of this mosquito species.

1.4.2 *Aedes albopictus*, a globally invasive vector of pathogens

While *Ae. koreicus* is at the beginning of a potentially wide expansion of its geographical distribution, *Ae. albopictus* range expansion is still continuing after four decades [Benedict et al., 2007]. The native geographical range of *Ae. albopictus* is restricted to some parts of Southeast Asia [Caminade et al., 2012; Medlock et al., 2012]. In the last 40 years it has unremittingly spread to Europe (1979; Adhami and Reiter [1998]), North America (1985; Hawley et al. [1987]), South America (1986; Forattini [1986]) and Africa (1990; Cornel and Hunt [1991]). This species is a competent vector of at least three of the most globally important vector-borne pathogens: chikungunya, dengue and Zika viruses [Grard et al., 2014]. The resulting volume of research on this species has been staggering, as evident from a search in August 2016 for Web of Science publication titles containing "*Aedes albopictus*" which returned 3436 results. Among this set of publications, *Ae. albopictus* continental or global distribution has been modelled several times. With some variation due to input data and model algorithms, these model outputs' show that *Ae. albopictus* climatic suitability expands from Argentina to Northern European countries, with further potential expansion due to the global raising temperature trend [Benedict et al., 2007; Caminade et al., 2012; Brady et al., 2013; Kraemer et al., 2015; Proestos et al., 2015; Cunze et al., 2016]. On the one hand, this information is useful to raise attention of human effects on species ecology into the non-scientific arena, and to maximise resources for surveillance in areas where disease and entomological reporting remains poor, or which are currently uninvaded [Sinclair et al., 2010; Manica et al., 2016]. On the other hand, little is known about the mechanisms that determine the introduction, colonisation and spread of this species at local spatial scales. Shedding light on these mechanisms is the keystone of implementing operational control or mitigation actions, especially in urban areas [Unlu et al., 2016]. Urban areas are indeed considered as "ticking time bombs" for emerging vector-borne pathogens transmission [Lederberg et al., 1992; Patz et al., 2004], not least because they are hot spots for populations of pathogen vectors, such as *Ae. albopictus* [Li et al., 2014; Samson et al., 2015; Manica et al., 2016]. The availability of man-made micro-habitats certainly increases the number of potential mosquito breeding sites in urban areas [Paupy et al., 2009]. Several studies demonstrated the extremely broad variety, from cans to concrete tanks, of aboveground breeding sites exploited by *Ae. albopictus* larvae in urban areas [Bartlett-Healy et al., 2012]. These breeding sites represent a wide range of environmental conditions, with those in shadow

Figure 1.2: Vegetation in urban areas affects the suitability of breeding and resting sites as well as the energetic input of breeding sites. Breeding sites partially or totally sheltered by vegetation are fertilised and thus bacterial or protozoan populations, food for mosquito larvae, can develop. Evaporation is limited in shadow conditions, increasing the micro-habitat capacity of sustaining the successful development of larvae in adults (6-8 days is the minimum time span from the hatching of eggs to emergence of adults.

or half-shadow conditions reported as more suitable for developing mosquito larvae (Figure 1.2; Beier et al. [1983b]).

Natural shade lowers temperature, by limiting the direct solar radiation reaching the water. Moreover, if the shadow is provided by vegetation (i.e. trees or shrubs), fallen leaves and debris collect in the containers [Eaton et al., 1973]. As a consequence, the water is fertilised and colonies of microorganisms develop, providing food for mosquito larvae [Schultz, 1989]. Furthermore, vegetation provides resting sites and sugar food as well as a higher diversity of potential hosts [Manica et al., 2016]. The importance of urban vegetation for *Ae. albopictus* is also derivable from its ecological niche in the native distribution range, where it is a forest tree-hole dweller [Hawley, 1988]. The association between this species and urban vegetation has been quantitatively demonstrated in the scientific literature [Mercado-Hernandez et al., 2003; Vezzani et al., 2005; Cianci et al., 2015; Manica et al., 2016]. Most of these studies investigated this association in an indirect way, while projects that directly target this association are still missing. Manica et al. [2016] investigated how the micro-geographic features of an urban areas affect *Ae. albopictus* population abundances, finding a positive association between *Ae. albopictus* abundance and vegetation cover just around the trapping sites (20 m circular buffer), but a negative association with vegetation coverage in a 300 m circular buffer. This result can be due to the spatial configuration of vegetation around the trapping sites more than its abundance (coverage). Indeed, the configuration of suitable breeding and resting habitats

provided by vegetation in urban areas, can potentially affect the movement of adults mosquitoes with consequence on their spread and local abundances [Villard et al., 1999; Pita et al., 2009; Haenke et al., 2014]. For example, given the biological features of this species, an urban matrix with small patches of vegetated areas, overall a low vegetation cover, may favour *Ae. albopictus* introduction, invasion and population abundance. As a consequence, the structure of the urban landscape may be an important factor in understanding and explaining the urban ecology of *Ae. albopictus*, and as such targeted research on this topic is needed to shed light on what the involved ecological mechanisms are.

As stated above, vegetation in urban areas provides shadow, potentially enhancing the suitability of *Ae. albopictus* breeding habitats [Bartlett-Healy et al., 2012]. Temperature drives the life cycle of poikilothermic insects like *Ae. albopictus*. As a consequence, a marginal change in micro-habitats temperature has a profound effect on the spatial and temporal pattern of their occurrence and abundance. The human made micro-habitats preferred by *Ae. albopictus* mosquitoes often represent a variety of thermal characteristics [Bartlett-Healy et al., 2012]. As an example, in conditions of direct solar irradiation, these micro-habitats may become sub-optimal or deadly for *Ae. albopictus* larvae, that have an optimal development temperature between 15 °C and 25 °C [Delatte et al., 2009; Waldock et al., 2013]. In addition, the conditions of artificial micro-habitats usually differ from those in the surrounding environment. It derives that collecting temperature data at the micro-habitat scale is essential to an accurate understanding and modelling of *Ae. albopictus* suitability, population or spread dynamic [Hannah et al., 2014]. In regard to this, Vallorani et al. [2015] recently measured temperature of aboveground micro-habitats showing that the application of this data instead of generic temperature data causes heavy changes in the *Ae. albopictus* estimated life cycle duration. In the same way, Paaijmans et al. [2010], measuring the water temperatures in water pools, found that the population growth of *Anopheles gambiae* (Giles), the major malaria vector in Africa, is underestimated when using generic air temperature, while population growth projections under future climate changes may be overestimated. Therefore, studies that provide quantitative and robust estimates of temperature differences for *Ae. albopictus* aboveground micro-habitats are needed. A detailed description of micro-habitat thermal characteristics in urban areas would widely improve our understanding of *Ae. albopictus* invasion dynamics, with certain positive consequences on the control of this vector species noxious for human health [Evans et al., 2015].

1.5 Environmental modelling

Environmental modelling is an "umbrella" definition for the application of computational techniques to model or simulate environmental processes or patterns. Environmental modelling has long been applied in physics (i.e. to simulate atmospheric processes), while its application in life sciences is relatively new. In the latest decades, environmental modelling has been exploited to investigate and predict the spatio-temporal distribution of species, emerging in an array of sophisticated modelling applications known under the name of "Species Distribution Models" (SDMs). SDMs simulate or relate the occurrence/abundance of species making use of species observations or known physiological, ecological constraints combined with quantitative and/or qualitative measures describing environment conditions. SDMs can be split in two main groups: correlative SDMs (see Elith and Leathwick [2009]) and process-based SDMs. Correlative SDMs relate species occurrence or abundance to a variety of environmental data sets. This class of SDMs is useful for exploring possible species-environment associations, and embraces a set of model algorithms relatively quick to implement but often not generalisable to different environmental conditions. On the other hand, process-based SDMs integrate the ecology of species through mathematical functions of which the species' occurrence or abundance is an emergent consequence. The latter set of models explicitly consider the mechanisms underpinning processes, is not linked to specific conditions, thus being more generalisable [Chevalier et al., 2014]. However, the flexibility of process-based SDMs comes at the price of requiring detailed data which are expensive to derive or available only for a restricted set of organisms [Evans et al., 2015]. In spite of the differences, these two groups of models can be considered as extremes of a common correlation-process continuum (Figure 1.3), that spans from a purely correlative (e.g. Generalised Linear Models) to a purely process-based approach (i.e. forward models; Dormann et al. [2012])

1.5.1 Ecology before modelling, a Bayesian inference

The trend in species distribution modelling moves towards increasingly automatic methods that leave the users with the only annoyance of collecting the broadest possible set of predictor variables. Ensemble modelling approaches [Araújo and New, 2007], which consist in the aggregation of results from multiple model algorithms in a "consensus" output, summarises this trend [Thuiller et al., 2009]. Despite of being undoubtedly useful to explore the environmental suitability for species whose ecology is not known sufficiently, or when rapid prediction is the desired output, automatic approaches sometimes lead to advance in ecological knowledge, and often generate confusion [Zhang et al., 2015; Pacifici et al., 2015]. This idea has been skilfully summarised by the "Bigfoot Problem" posed by Lozier et al. [2009].

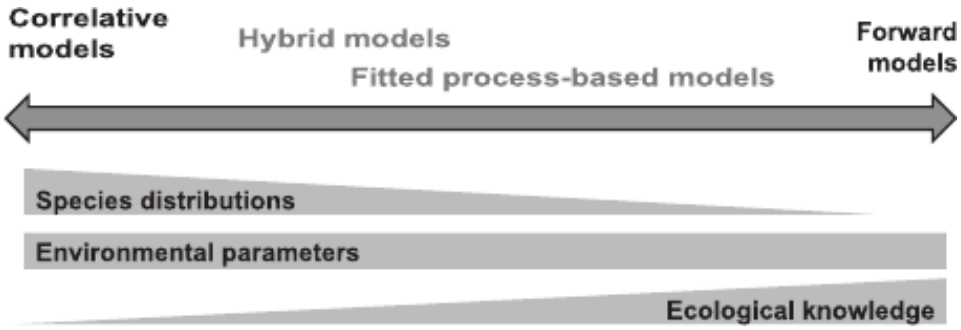

Figure 1.3: The correlation-process continuum of SDMs. Observations on species distribution is key for correlative models, whereas detailed information on species physiology (ecological knowledge) is vital for pure mechanistic models (forward models). Reproduced with permission from Dormann et al. 2012.

In the latest 15 years, Bayesian methods are penetrating the scientific literature with potential positive effect also on SDMs. Bayesian methods represent a totally different way of thinking about research methods, with the researcher's knowledge and experience having a key role on inference and decision-making [McCarthy and Masters, 2005; Ellison, 2004]. The Bayesian research method is based on empirical observations and on accumulated experience of the researcher [Martinez and Achcar, 2014]. Experience and prior knowledge represent a massive set of data that is often neglected in ecological modelling. In Bayesian inference, this "prior knowledge" needs to be formalised in a prior probability distribution of model parameters that, interacting with the maximum likelihood function, emerges in the parameters posterior probability distributions [Gelman and Hill, 2006]. Ecological and epidemiological data is commonly structured in groups. Hierarchical models are hence appropriate for the analysis of this data structure, and are naturally handled using Bayesian methods, which also provide intuitive and direct estimates of uncertainty around parameter values [Link and Sauer, 2002]. For the above-listed (see Kruschke [2015a] for a complete list of the advantageous linked with Bayesian analysis), in this thesis Bayesian inference is extensively exploited, and not just for modelling species distribution. However, the reader may notice a transformation of statistical beliefs that took place in this thesis's author, from the blind belief in automatic statistical methods to the re-discovery of the central role of *eco*-logical knowledge to answer scientific questions with statistical tools [Ginzburg et al., 2007].

1.6 Experimental design and semi-controlled environments

Experimental design is used in the scientific method to determine whether a factor causes changes in the status of a variable. Experimental designs are usually performed under controlled

environmental conditions, by manipulating the levels of all the relevant conditions that may affect the system under investigation. This experimental setting improves the internal validity of the research, removing potential confounding effects. However, results obtained from an experimental design where too much control has been applied are often not generalisable as they are only relevant to the specific study conditions (lower external validity). To reduce the limitations associated with controlled experimental research the experiment may be performed under a more natural environment. Experimental designs with this characteristic are often defined as "semi-controlled".

In this thesis, we used a semi-controlled experimental design to quantify the temperature variability in *Ae. albopictus* micro-habitats. We simulated artificial *Ae. albopictus* breeding and resting habitats while controlling for the exposition to direct solar radiation and the volume of water forming the micro-habitat. The variability in temperature experienced by different mosquito life stages was also controlled, considering the temperatures of water (the habitat of mosquito larvae), external water (eggs) and air (adults). By controlling for those conditions that most impact micro-habitat temperature and by allowing their levels to vary around a broad range of realistic values, we aimed to minimise the internal validity of the experimental design while maximising the transferability of the outcomes in different environmental settings.

Chapter 2

Identifying the Environmental Conditions Favouring WN Virus Outbreaks in Europe

Marcantonio, M, Rizzoli, A, Metz, M, Rosà, R, Marini, G, Chadwick, E, Neteler, M, (2015). Identifying the Environmental Conditions Favouring West Nile Virus Outbreaks in Europe. *PLoS ONE*, 10(3).

doi: 10.1371/journal.pone.0121158

Abstract

West Nile Virus (WNV) is a globally important mosquito borne virus, with significant implications for human and animal health. The emergence and spread of new lineages, and increased pathogenicity, is the cause of escalating public health concern. Pinpointing the environmental conditions that favour WNV circulation and transmission to humans is challenging, due both to the complexity of its biological cycle, and the under-diagnosis and reporting of epidemiological data. Here, we used remote sensing and GIS to enable collation of multiple types of environmental data over a continental spatial scale, in order to model annual West Nile Fever (WNF) incidence across Europe and neighbouring countries. Multi-model selection and inference were used to gain a consensus from multiple linear mixed models. Climate and landscape were key predictors of WNF outbreaks (specifically, high precipitation in late winter/early spring, high summer temperatures, summer drought, occurrence of irrigated croplands and highly fragmented forests). Identification of the environmental conditions associated with WNF outbreaks is key to enabling public health bodies to properly focus surveillance and mitigation of West Nile virus impact, but more work needs to be done to enable accurate predictions of WNF risk.

2.1 Introduction

West Nile virus (WNV) is a multi-host mosquito borne virus belonging to the Japanese encephalitis (JE) antigenic complex (genus *Flavivirus*, family *Flaviridae*) [Murray et al., 2011]. Although the majority ($\sim$ 80%) of human WNV infections are sub-clinical and can pass unnoticed, some 20 % of patients experience flu-like symptoms known as West Nile fever (WNF), while approximately 1 % develop a severe, and potentially fatal, neuro-invasive disease [Artsob et al., 2009]. While clinical trials for human vaccines are underway [Iyer and Kousoulas, 2013] prevention currently depends on organized, sustained vector (mosquito) control campaigns and risk communication [Arnold, 2012; Dauphin et al., 2004; Martín-Acebes, 2012; Reisen, 2013].

Sporadic cases of WNV have been documented in Europe and Africa since it was first identified in Uganda in 1937 [Smithburn et al., 1940], but until the 1990s it was considered a low risk for humans and domestic animals. Since then however, WNV has spread rapidly across all populated continents and it is now the most widespread arthropod borne virus in the world [May et al., 2011; Ozdenerol et al., 2013]. In Europe, human cases of WNF have been notified in almost all Eastern, Central, and Southern European countries [Sambri et al., 2013] with hotspots in Italy since 2008 [Barzon et al., 2013], Greece since 2010 [Papa, 2013] and continuous transmission in Russia and Romania since 1996 [Tsai et al., 1998]. The number of WNF cases and the impacts on public health are, so far, limited in Europe relative to other vector borne infection (in 2013, 783 cases of WNF were reported by ECDC in Europe and neighbouring countries, as compared to 45,854 Lyme borreliosis reported by the World Health Organization between 2010 and 2013). However, both escalating case load and increased pathogenicity (e.g. substitution of the NY99 genotype with the more pathogenic WN02 in the USA Moudy et al. [2007]) are contributing to increased risk. Financial costs associated with the prevention of virus transmission to humans through blood and tissue transplantation are mounting (Blood safety regulation; see Semenza and Domanović [2013]).

WNV is maintained in enzootic cycles involving several species of birds, and mosquitoes belonging principally to the Pipiens Assemblage [Martín-Acebes, 2012; Jimenez-Clavero, 2012; Paz and Semenza, 2013; Petersen LR et al., 2013; Petersen and Marfin, 2002]. Humans and horses are accidental and dead end hosts since they do not develop a viraemic titre sufficient to infect mosquitoes and amplify the transmission cycle [Petersen and Marfin, 2002]. In Europe, the common house mosquito, *Cx. pipiens* (Linnaeus, 1758), is considered the principal bridge vector of WNV between birds and mammals (horses and humans), although at least 60 other mosquito species can be found infected with the virus [Martín-Acebes, 2012; Petersen LR et al., 2013; Petersen and Marfin, 2002; Gomes et al., 2013]. *Culex pipiens* occurs in two biological forms, *Cx. pipiens pipiens* and *Cx. pipiens molestus*, which can hybridise. Both behaviour and host preference vary between forms, with major implications for risk of transmission to

humans depending on their relative abundance [Gomes et al., 2009; Osório et al., 2013]. WNV ecology in the Old World is complex and several aspects of the WNV transmission cycle are as yet poorly quantified. The co-circulation of at least five lineages with variable pathogenicity and the overlap of new introductions with endemic circulation, render the quantification of the parameters necessary to develop transmission models challenging [May et al., 2011; Bakonyi et al., 2013; Calzolari et al., 2013].

Although favourable environmental conditions for virus transmission seem to occur extensively in the Old World and a widespread circulation of the virus has been demonstrated by serological screening of wildlife and sentinel animals, clinical emergence in humans tends to be unpredictable, sporadic and clustered [Sambri et al., 2013]. The occurrence of spatially and temporally localised hot-spots in emergence is likely to reflect the coincidence of circulating virus strain with favourable environmental (biotic and abiotic) conditions which modulate the interaction between virus, mosquito, and hosts, consequently leading to locally altered pathogen amplification, transmission and disease risks [Dobson and Foufopoulos, 2001; Karesh et al., 2012]. Variation in land use, climate, habitat structure, animal community, human socio-economic status or behaviour can all significantly affect the risk of infection—for example, via impacts on the spatial and temporal distribution of the competent reservoir host assemblages and their immune status, as well as on the local abundance and genetic population structure of mosquito vectors and their vectorial capacity [Colborn et al., 2013; Dowling et al., 2013; Morin and Comrie, 2013; Patz et al., 2004; Paz and Semenza, 2013].

At the same time, the availability of simultaneous information on the infection pattern in vectors and birds is lacking at a wide spatial scale, while the cost of integrated surveillance, and the economic and social disparities which affect several EU countries, limit the capacity of high-level institutions to collect detailed and standardised ecological and epidemiological data [Mulatti et al., 2014]. Identification of the areas of potential emergence, and predicting temporal and spatial variation in WNV risk therefore remains challenging [Petersen and Marfin, 2002].

The current study aimed to identify environmental factors associated with WNF occurrence in humans across the Old World. We analysed the association between WNF incidence (derived from WNF number of cases as reported annually by the European Centre for Disease Prevention and Control, ECDC) and a wide range of potential predictors including climate, land use, indices of water, vegetation, conservation status, landscape fragmentation and human population density. By identifying key environmental drivers of WNF, we aim to lay the foundations for the development of statistical models able to predict WNF risk at a continental scale.

2.2 Methods

2.2.1 Epidemiological Data

Data used were provided by the European Centre for Disease Prevention and Control (ECDC), compiled from weekly WNF case reports from 146 areas defined at the Nomenclature of Territorial Units level 3 (NUTS3)/Global Administrative Unit Layers level 1 (GAUL1), originating from 16 different countries across western Asia, Europe and northern Africa (Figure 2.1). For nation specific details of data collection see [Paz and Semenza, 2013] and references therein. Weekly data were pooled, to provide annual totals for 2010 to 2012. Population data were obtained for each area using online national statistical databases (Table 2.1), so that the number of cases per 10×10^4 inhabitants (hereafter referred to as the 'incidence') of WNF could be calculated per head of population, per year. Areas with no reports of WNF were excluded from analysis, as it was not possible to discriminate between true negatives, and areas where reporting or diagnosis were inadequate.

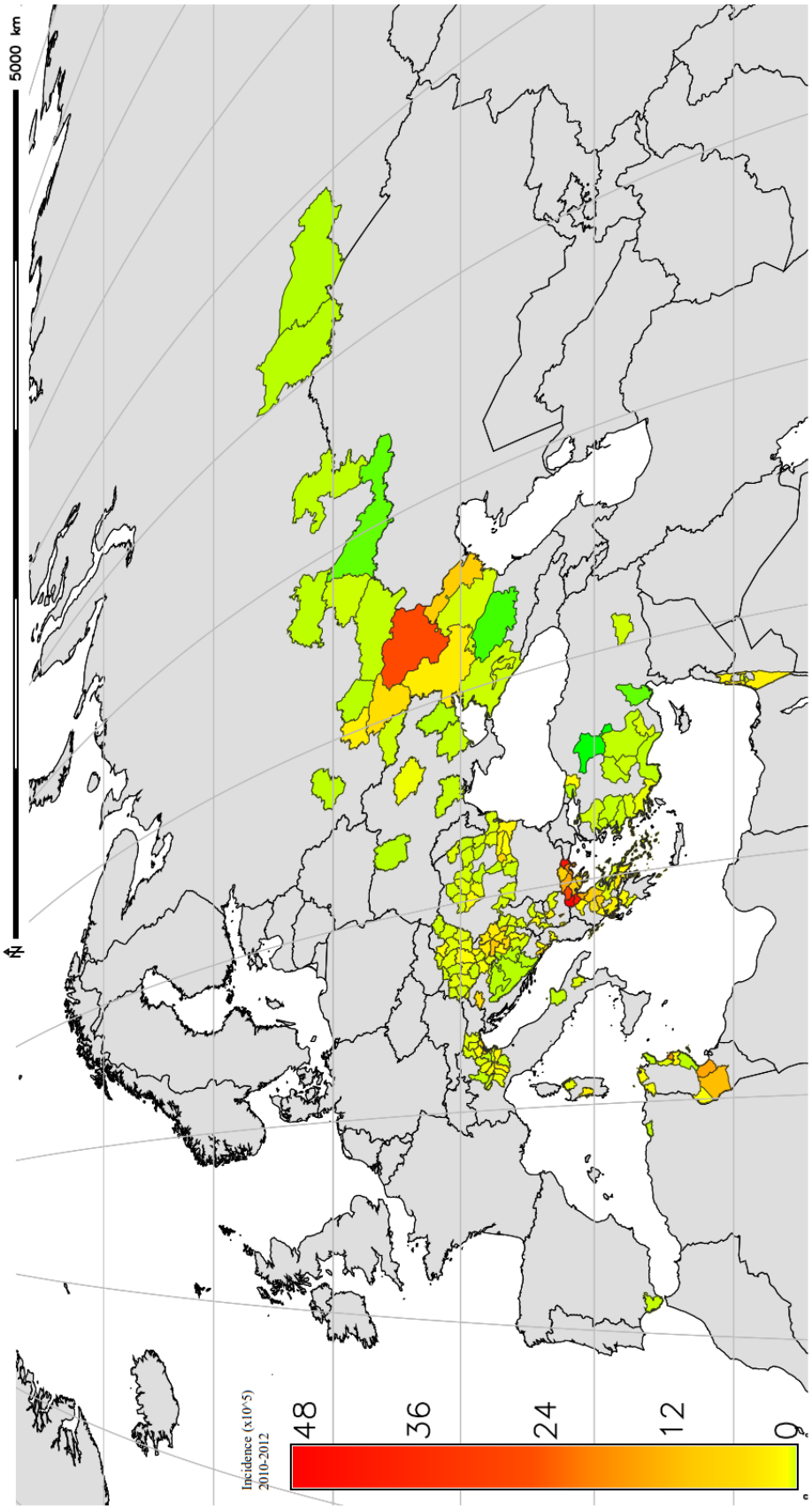

Figure 2.1: Spatial variation in cumulative WNF incidence (cases per 10×10^4 population) between 2010 and 2012 is indicated in colour, within areas delineated using NUTS3/GAUL1 administrative boundaries. Areas with no reported cases of WNF are shown in grey, and delineated using Country boundaries. Peak incidences are reported in red, these being in Volgograd Oblast, North Eastern Greece and Central Tunisia.

Table 2.1: Population data source per country is reported. The population data has been used to derive yearly WNF incidence per each NUTS3 area.

Country	Source[2]	Web link
Albania	INSTAT	http://www.instat.gov.al
Algeria	Office National des Statistiques	http://www.ons.dz
Israel	Central Bureau of Statistics	http://www.cbs.gov.il
Kosovo	Kosovo Agency of Statistics	http://esk.rks-gov.net
Macedonia	State Statistical Office	http://www.stat.gov.mk
Palestina	Palestinian Central Bureau of Statistics	http://www.pcbs.gov.ps
Russia	Federal State Statistics Service	http://www.gks.ru
Serbia	Statistical Office of the Republic of Serbia	http://webrzs.stat.gov.rs
Tunisia	National Institute of Statistics	http://www.ins.nat.tn
Ukraine	State Statistics Service of Ukraine	http://www.ukrstat.gov.ua
All other countries	Eurostat	http://epp.eurostat.ec.europa.eu

2.2.2 Climatic and environmental variables

All climatic and environmental variables were collated as either vector data (protected areas and water bodies) or gridded raster data (all other variables) for the entire study area, and processed using GRASS GIS [Neteler et al., 2012]. Full details of data sources, resolution, and all variables included in statistical analyses are reported in Table 2.2.

Raw data

Climatic variables were: *i)* Land Surface Temperature and *ii)* Precipitation (daily amount of precipitation, and number of days with precipitation). Environmental variables were: *i)* Vegetation index, *ii)* Water index, *iii)* Land use (land cover classes from GlobCover [Patrice et al., 2008] and 'Anthropogenic Biomes' (global ecological patterns created by sustained direct human interactions with ecosystems) from the Anthromes dataset [Ellis and Ramankutty, 2008], *iv)* Protected areas, *v)* Water bodies, and *vi)* Intensity of light at night (used as a proxy for human population density, [Elvidge et al., 1997; Zhuo et al., 2009; Small et al., 2011]).

[2] All population data were from 2009 except Algeria (2008), Kosovo (2011), Russia (2010) and Ukraine (2010).

Table 2.2: Population data source per country is reported. The population data has been used to derive yearly WNF incidence per each NUTS3 area.[2]Classes selected based on published evidence of their strong interactions with human incidence of vector-borne disease [Mack et al., 2000; Pradier et al., 2008; Chuang et al., 2012; Eisen et al., 2013; Valiakos et al., 2014], excluding those absent from the study area, or represented in less than 10 areas.[3]evidence weight < 0.8

/

Variable	Raw data source and resolution	Derived data	Into preliminary model	Into final model	Terms in set of best models
Temperature	Gap-filled daily MODIS Land Surface Temperature from MODIS satellite sensor products *MOD*11*A*1 and *MYD*11*A*1; 4 records per day aggregated to weekly average at 250 m resolution [Metz et al., 2014].	16 week aggregated average and standardised anomaly, calculated individually for nine periods: from weeks 1-16, 2-17, etc to weeks 9-24 in each year and area.	All variables for both Anomalies and Average across all 9 periods.	Ano.Temp3–6; Av.Temp6–9	Av.Temp6–9
Vegetation index	Gap-filled (after [Roerink et al., 2000]) Normalized Difference Water Index (NDWI, calculated from MODIS product *MOD*09*A*1), at a resolution of 500 m.			Ano.NDVI4–7	No
Water index	Gap-filled Normalized Difference Vegetation Index (NDVI, MODIS product *MOD*13*Q*1), at a pixel resolution of 500 m.			Av.NDWI4–7	Yes
Precipitation	Gridded ECA&D database, at 25 km resolution [Haylock et al., 2008].	16 week aggregated total precipitation, and days of rain; cumulative total and standardised anomaly for both measures, calculated individually for nine periods: from weeks 1-16, 2-17, etc to weeks 9-24 in each year and area.	All variables for both Anomalies and Cumulative, across all 9 periods – for both total precipitation and days of precipitation.	Av.PrecDays2–5	Yes
Land use.[2]	Land cover classes from GlobCover [Patrice et al., 2008], 300 m resolution.	Percentage of each land use category, calculated within each area.	Irrigated Croplands, Rainfed Croplands, Mosaic Croplands, Mosaic Vegetation, Closed Forests/Vegetation, Open Forests/Vegetation,Mosaic Forest, Mosaic Grasslands, Flooded Broadleaved Forests, Artificial surfaces, Water Bodies	Irrigated Croplands; Mixed Natural Vegetation	Irrigated Croplands;Mixed Natural Vegetation.[3]
		Pielou's index of heterogeneity.	Yes	Yes	Yes.[3]
		Number of land use patches.	Yes	Yes	No
	Anthromes dataset (Anthropogenic Biomes: global ecological patterns created by sustained direct human interactions with ecosystems) [Ellis and Ramankutty, 2008], 86 km resolution).	Percentage of each land use category, calculated within each area.	Urban, Dense settlement, Irrigated villages, Cropped pastoral villages, Rainfed villages, Rainfed mosaic villages, Residential irrigated cropland, Residential rainfed villages, Populated irrigated cropland, Populated rainfed cropland, Residential rangelands, Populated rangelands,Populated forests	Populated Forests; Populated Rangelands	Populated Forests
Protected areas	IUCN and UNEP, 2013; http://www.wdpa.org/.	Percentage within each area.	No	Yes	No
Water bodies	OpenStreetMap contributors 2013.	$m^2 ha^{-1}$	No	Yes	Yes.[3]
Light at night	Derived from The visible Infra-red Imaging Radiometer Suite (VIIRS) sensor aboard the Suomi National Polar-Orbiting Partnership (NPP). A first set of cloud free DNB data (observations from 2012/4/18-26 and 2012/10/11-23) acquired by VIIRS was released by NOAA for the year 2012. The VIIRS product is cloud free at 15″ spatial resolution and corrected for erroneous light sources (http://mapserver.ngdc.noaa.gov/viirs_data/viirs_composite/).	Mean and variance, within each area.	No	Yes	No
Year	Years 2010, 2011, 2012.		Yes (as random variable)	Yes (as random variable)	Yes
Area	146 areas defined at the NUTS3/GAUL1 level, from 16 different countries across western Asia, Europe and northern Africa.		Yes (as random variable)	Yes (as random variable)	Yes

Derived data

All variables were summarised within the NUTS3/GAUL1 areas, from which we derived a series of measures described below.

Seasonal averages and anomalies For datasets incorporating temporal as well as spatial variation (temperature, precipitation, NDVI, NDWI), data from each year and area were aggregated into nine 16 week periods, these being labelled using months instead of weeks, such as 1–4 (January-April), 2–5 (February-May), 3–6 (March-June),. . . , to 9–12 (September-December) [Rosà et al., 2014]. For each period, we calculated the average (for temperature, NDVI and NDWI) or the cumulative total (precipitation). From these average or cumulative totals we derived anomalies [Paz et al., 2013] as the difference between the average (or cumulative) value within the given time period, and the average (or cumulative) value for the same time period recorded in the preceding decade, 2001–2010. We then standardised the anomalies by dividing them by the 2001–2010 standard deviation. Standardised anomalies provide more information about the magnitude of the anomalies because influences of dispersion have been removed. This was repeated for each year (2010–2012). Where referred to in the text, each variable (Temp, PrecTot, PrecDays, NDVI, NDWI) is prefixed with Ano. or Av. for standardised anomaly or average, and the relevant period denoted in subscript (e.g. $\text{Ano.Temp}_{2\text{–}5}$ = weekly anomaly temperature during months 2–5).

Landscape For each land use class (GlobCover and Anthromes), protected areas, and water bodies, percentage cover was calculated within each NUTS3/GAUL1 area. Pielou's evenness index of diversity [Pielou, 1966], and the number of patches of homogeneous land use, were calculated using GlobCover data. For night light intensities, the mean and variance were calculated within each NUTS3/GAUL1 area, and are used as proxies for the average population density, and the fragmentation of the human population, respectively.

2.2.3 Statistical analyses

We investigated the association between incidence of WNF and a range of environmental predictors, measured across Europe and adjacent countries, using available epidemiological data from 2010–2012. For all analyses, we used as the response variable the log-transformed annual incidence of WNF, for each NUTS3/GAUL1 area, respectively. All analyses were performed using the R language and environment for statistical computing [R Core Team, 2014].

Preliminary analyses

In order to select the most appropriate time window for each temporally variable predictor, linear mixed-effects models (LMMs) were fitted to the response variable, for each time window in turn, for both the average and the standardised anomaly of each of the temporally variable environmental predictors. Year and area (NUTS3/GAUL1) were included as random variables. The inclusion of random factors in the model is needed to take under control the clustering of data in different areas and years [Zuur et al., 2009]. The best model was selected for each predictor using An Information Criterion (AICc), with small sample bias adjustment [Burnham and Anderson, 2002].

LMMs were fitted to test the association between WNF incidence and land use. Two models were created, testing in turn for associations with land cover (GlobCover data), and anthropogenic biomes (Anthromes data). Using a process of multi-model inference [Burnham and Anderson, 2002; Johnson and Omland, 2004; Buckland et al., 1997], we compared all possible models using the R package 'MuMIn' [Bartoń, 2013]. The best models were selected using a threshold of ΔAICc≤ 2 [Burnham and Anderson, 2002].

The full model

Following preliminary stages of variable selection, we developed further LMMs including all remaining environmental variables 2.2, with year and area included as random variables. As previously, all possible models were compared using multi-model selection. The consensus set of best models were selected using a threshold of ΔAICc≤ 2 [Burnham and Anderson, 2002], and differences in AICc (ΔAICc) between consecutively ranked models were used to calculate weights and relative evidence ratios for each variable. All variables included in the best models were ranked according to their importance, and the relative evidence weight for each model term was calculated (this being the sum of the IC weights of those models in which the term is included, [Buckland et al., 1997]). These data were used to calculate the model-averaged estimates of the coefficients and their standard error. Although we acknowledge that utilising a process of multi-model selection and inference can lead to the testing of spurious models (that we tried to filter out pre-selecting the variables used in the full model), it is an extremely powerful approach that enables us to present a consensus of landscape and weather predictors from multiple models, rather than only a single 'best' model, while also considering model selection uncertainty [Burnham and Anderson, 2002]. After testing the averaged model for multicollinearity using the Variance Inflation Factor (VIF) [Hair, 2009], we compared WNF incidence fitted values versus WNF incidence observed values to assess the averaged model goodness of fit.

In order to clarify effect size, predictions were made from the best models for each significant predictor variable in turn. All variables but one were fixed at their median values, and predictions made across the full range of the selected variable. For example, to test the association between temperature and WNF incidence, in a model where temperature, precipitation and NDWI were all significant predictors, precipitation and NDWI were added to the model as constants (fixed at their median measured value) while values for temperature were allowed to vary within their observed range.

2.3 Results

2.3.1 WNF incidence

The highest WNF incidences during the 2010–2012 period were reported in Volgograd Oblast, North Eastern Greece and Central Tunisia (Figure 2.1). Annual incidence across the entire study area varied from 1.31 cases per 10×10^4 people in 2011 to 2.66 in 2012 (incidence in 2010 reached an intermediate value of 1.68; 2.2. In 2010, the highest incidences were reported in eastern Europe, western Asia (Volgograd Oblast) and Greece. In 2011, the highest incidence was reported in Greece, but overall, incidence was low. In 2012 the average incidence was the highest in Greece and Tunisia.

2.3.2 Preliminary analyses

To predict incidence of WNF, the optimum periods over which to measure temperature, precipitation, NDWI and NDVI were late-winter early spring (Av.PrecDays$_{2–5}$ and $_{6–9}$, Ano.Temp$_{3–6}$) and summer (Av.NDWI$_{4–7}$, Ano.NDVI$_{6–9}$, Av.Temp$_{6–9}$), respectively. The anthropogenic biomes selected from the initial subset of 14 classes were "Populated Forests" and "Populated Rangelands" (forests or rangelands with scattered, low density human populations), and the land use classes selected from the initial subset of 13 classes were "Mosaic forests" (forests alternated with other land uses such as grasslands), "Irrigated Croplands" and "Mixed Natural Vegetation".

2.3.3 The full model

A total of 9 models were identified with ΔAICc≤ 2. Of the 14 explanatory variables considered in the full model, 8 were represented in the consensus set of best models. The Variance Inflation Factor of the full model was less than 2 for all variables, indicating that multicollinearity was not significant. The model-averaged fitted values explained 32 % ($R^2 = 0.32$) of the observed data, moreover the model averaged residuals did not show any evident pattern,

being normally distributed around 0. Model-averaged importance of terms and the estimation of their coefficients (2.3, 2.3) showed that the most important predictors affecting WNF incidence were climatic and land use factors. Water index (NDWI) proved a highly significant predictor, negatively correlated with incidence (cases per 10×10^5 inhabitants) of WNF such that a decrease in spring-early summer vegetation index ($\text{Av.NDWI}_{4\text{–}7}$) of 0.10 predicts an increase in incidence of approximately 47 (NDWI theoretically ranges from -1 to 1 but in our study area/years $\text{Av.NDWI}_{4\text{–}7}$ ranges between -0.13 and 0.04). Summer average temperatures $\text{Av.Temp}_{6\text{–}9}$) were positively correlated with WNF, such that an increase of 1.6°C (as predicted under climate change scenario RCP 2.6; [IPCC, 2013] predicts an increase in incidence of 2. Days of precipitation in late winter/early spring ($\text{CumulativePrecDays}_{2\text{–}5}$) were also positively correlated with WNF incidence, such that an additional 10 days of precipitation (in the four months considered) predict an increase in incidence of WNF of 29 (where the range within our dataset was between 0 and 58 days of rain in total for this period).

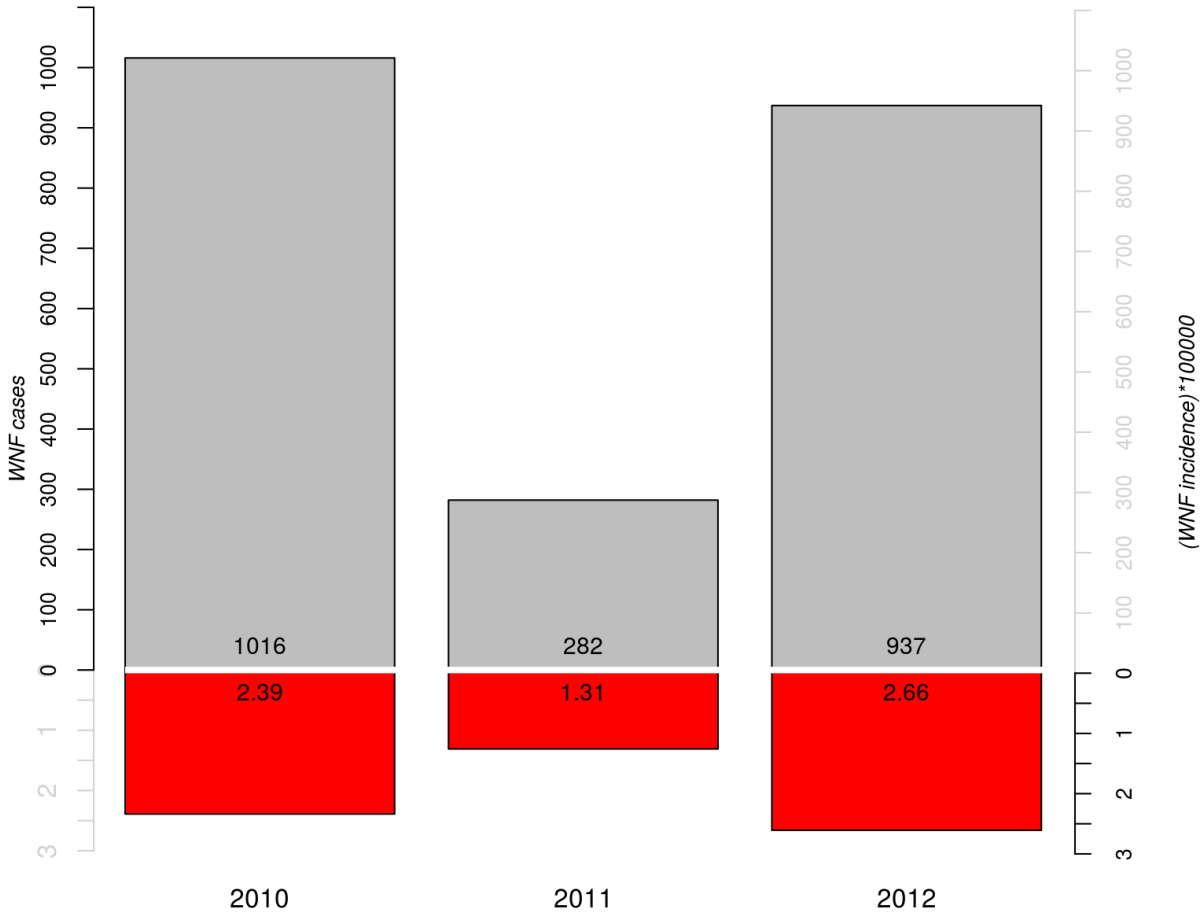

Figure 2.2: Barplot reporting the total number of cases (grey) and incidence (cases per 100000 population, red) of WNF in each year (2010, 2011, 2012).

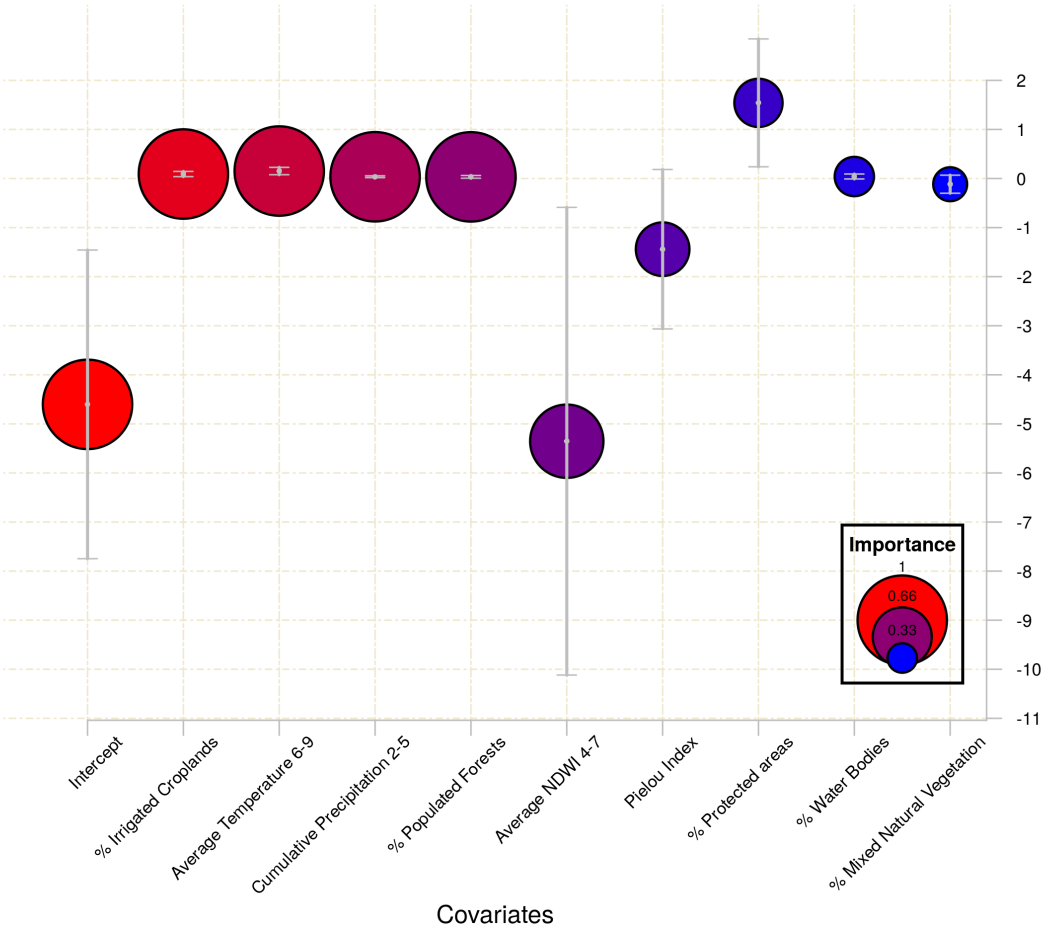

Figure 2.3: Summary statistics from the best 9 models ($\Delta AIC \leq 2$ from the best model) for log-transformed WNF incidence (from 2010 to 2012). The coefficients have been derived using multi-model averaging. The model term "Importance" is proportional to the number of times that the variable is included in the set of best models and is represented by the colour and size of the bubbles (red/bigger bubble = high importance; blue/smaller bubble = low importance). Where referred to in the figure, each variable (Temp, PrecTot, PrecDays, NDVI, NDWI) is prefixed with Ano. or Av. for standardised anomaly or average, and the relevant period denoted in subscript (e.g. $\text{Ano.Temp}_{2\text{–}5}$ = weekly anomaly temperature during months 2–5).

Of the land use variables, the most significant predictors were the percentage of area covered by irrigated croplands, or by populated forests, both of which were positively correlated with incidence of WNF. An increase of 5 % in the area cultivated as irrigated croplands predicts an increase in incidence of 113 (in the current study, the average area cultivated in this way varied between 0 and 26 % of each NUTS3/GAUL1 area), while an increase of 5 % in the area of

[0] All population data were from 2009 except Algeria (2008), Kosovo (2011), Russia (2010) and Ukraine (2010).

Table 2.3: Population data source per country is reported. The population data has been used to derive yearly WNF incidence per each NUTS3 area.

Model term	Model-averaged coefficient	Unconditional variance	Evidence Weight
Intercept	−4.71	1.26	1.00
% Populated Forests	0.03	0.01	1.00
% Irrigated Croplands	0.10	0.03	1.00
$\text{Av.Temp}_{6–9}$	0.15	0.04	1.00
$\text{Av.PrecDays}_{2–5}$	0.04	0.01	1.00
$\text{Av.NDWI}_{4–7}$	−5.35	3.32	0.82
Pielou Index	−1.44	0.83	0.60
% Protected areas	1.54	0.66	0.54
% Water Bodies	0.04	0.03	0.44
% Mixed Natural Vegetation	−0.12	0.09	0.38

populated forests predicts an increase of 36 per 100 000 people (in our study, the average area of populated forest varied between 0 and 47 %).

Remaining variables were given an evidence weight <0.8, and were not considered significant [Calcagno and de Mazancourt, 2010].

2.4 Discussion

West Nile virus is spreading in Europe and neighbouring countries at an increasing rate, with new lineages and variants emerging into new territories. Several factors contribute to the current epidemiological picture, amongst which urbanisation, variation in land use and climate are considered among the most important [Paz and Semenza, 2013; Bradley and Altizer, 2007; Chase and Knight, 2003; Dohm et al., 2002; Kilpatrick, 2011]. To our knowledge the current study is the first attempt to model WNF human incidence at a continental scale in the Old World, including the whole of Europe, northern Africa and western Asia. Despite the large number of studies set in North America, differences in vectors and reservoir host species, in the degree of human exposure and wildlife immune status, suggest that the ecological processes driving WNV ecology in the New World (e.g. [Reisen, 2013]) can be only partly considered to apply to the Old World system. In this system, perhaps because of the far longer history of WNV circulation and the recognition of at least five co-circulating lineages with variable pathogenicity, WNV epidemiology and ecology seem to be more complex.

It is well established that climate affects many components of the WNV biological cycle (e.g. [Dohm et al., 2002; Kilpatrick, 2011]), and that the carrying capacity for both vector and host populations differs with land use [Chuang and Wimberly, 2012]. The interplay between biotic and abiotic variables that drive WNV in humans forms a complex and dynamic ecological system, and to adequately describe those dynamics across a large scale, requires a comprehensive set of predictors within a modelling framework. The current study makes use of remote sensing and GIS to enable collation of multiple types of environmental data over a continental spatial scale, at sufficient temporal and spatial resolution to test associations with WNF incidence. The number of studies utilising such tools are increasing [Chuang et al., 2012; Brown et al., 2008b] but although a plethora of studies on WNV have been published since the New York outbreak of 1999, only a few authors applied statistical modelling techniques to study spillover potential (i.e. [Paz and Semenza, 2013; Chuang et al., 2012; Brown et al., 2008b; Landesman et al., 2007; Chuang and Wimberly, 2012; Bowden et al., 2011]). Only a small subset of these studies use human cases as the response variable and environmental factors as predictors, and most are conducted at a local or regional spatial scale [Chuang et al., 2012; Chuang and Wimberly, 2012; Bowden et al., 2011; Harrigan et al., 2010; LaBeaud et al., 2008]. Only two studies [Paz and Semenza, 2013; Tran et al., 2014] have made an attempt to model WNV outbreaks in humans in the Old World at a regional scale while others modelled WNV circulation in horses [Pradier et al., 2008].

Climatic anomalies are considered among the most important drivers of WNV emergence, and ambient temperature can be a determinant of outbreaks [Barzon et al., 2013]. Permissive meteorological conditions are necessary for the persistence of active transmission [Paz and Semenza, 2013], and empirical studies suggest that temperature is a key factor influencing WNV evolution and dissemination [Kilpatrick et al., 2008]. Indeed, the relationship between temperature and increased WNV incidence in humans has repeatedly been confirmed both at national and multinational scales [Tran et al., 2014; Pecoraro et al., 2007; Soverow et al., 2009]. In the current study, by using spatially continuous input data, we managed to avoid weak interpolation methods which only employ sparse point data. We found that average summer temperatures between the months of June and September ($Av.Temp_6 - -9$) are positively correlated with WNF human incidence, in concurrence with [Paz and Semenza, 2013] who found that the summer temperature anomaly before the upsurge was the main driver. Similarly, [Tran et al., 2014] found a significant relationship between summer temperature anomalies and WNV risk in Europe. The effect of temperature is likely to be mediated through its impact on the distribution, behaviour and survival of the mosquito vector, via direct impacts on the virus and on its' extrinsic incubation period in the competent vectors (which is reduced at higher temperatures [Kilpatrick et al., 2008]), and via impacts on host distribution and behaviour.

The nature of the association with temperature is therefore complex—for example, although warmer temperatures may have a negative effect on mosquito survival, they increase mosquito biting and development rates, and pathogen replication [Kilpatrick et al., 2008] and can lead to increased human exposure risk through altered human activity patterns [Reisen, 2013].

Previously, [Paz and Semenza, 2013] found no significant correlation between WNF incidence and either precipitation or humidity in Europe. In the present study, however, we observe positive associations between WNF incidence and the total number of days with precipitation in late winter-spring ($Av.Rain_{2–5}$), and the percentage of irrigated croplands, suggesting a strong link to spring precipitation, and the presence of standing water. Standing water is a prerequisite for larval development of the mosquito vector, without which they cannot complete their biological cycle [Townson, 1993; Becker, 2010]. WNV transmission to humans is inefficient and infrequent [Kilpatrick et al., 2008], and cases of WNF occurs more often when mosquito population density rises (i.e. see [Colborn et al., 2013]). While [Paz and Semenza, 2013] found no link to precipitation, their data were limited to 2010, and landscape structure was not considered [Pérez-Rodríguez et al., 2013]. Furthermore, the authors used point source climatic data (meteorological stations) which may not represent spatial and temporal variations as well as global earth observations [Chuang et al., 2012]. We believe the results of the current study are a more robust representation of the association between human incidence of WNF and spring precipitation/standing water in Europe, but recognise also that the nature of this association is likely to vary across the geographic range of the virus and the precipitation regimes, as reflected by conflicting evidence in literature (e.g. a positive correlation between precipitation and human incidence in eastern US, but a negative correlation in the west [Landesman et al., 2007], in southern Florida [Shaman et al., 2005] and Israel [Aharonson-Raz et al., 2014]).

Although precipitation in spring is positively associated with WNF incidence, a strong negative association is seen between WNF incidence and summer NDWI (Av.NDWI4–7). [Tran et al., 2014] also report an association between NWDI and WNV risk in Europe, specifically a positive association with anomalies in early June. NDWI is a proxy for the amount of water in the ecosystem, and low NDWI may be indicative of drought. Recent research suggests that drought may lead to subsequent localised increases in mosquito numbers and disease outbreaks [Chase and Knight, 2003; Landesman et al., 2007]. Drought conditions may encourage the aggregation of both hosts (birds) and vectors (mosquitoes) at remaining water bodies, increasing rates of transmission [Schöning et al., 2013], while potentially also influencing their vector competence [Bakonyi et al., 2013]. *Culex pipiens* thrives during drought conditions by exploiting larval habitats with high organic matter (a consequence of drying content) and artificial containers not reliant on precipitation [Shaman et al., 2010]. Furthermore, drought conditions may force amplifier bird species into urban and suburban areas where water is more

freely available, thereby bringing competent hosts into contact with competent urban vectors [Reisen, 2013]. Associations between dry summers and increased WNV outbreaks have been indicated in a number of US studies [Epstein, 2001].

Wetlands [Young et al., 2013; Johnson et al., 2012; Liu et al., 2008], agricultural area [[LaBeaud et al., 2008; Deichmeister and Telang, 2011], and urban infrastructure [Bowden et al., 2011] have previously been reported to influence vector populations or WNV transmission [Gardner et al., 2014]. In the current study, the detailed resolution of land use classes allows a distinction to be made between irrigated, and rain-fed crop lands. Irrigated croplands were positively associated with WNF, in accordance with research in the US where an increased human incidence of WNF was found to be associated with crop land cover and water catchment depressions in the otherwise semi-arid environment of Texas [Warner et al., 2006]. Rain-fed crop lands in the current study show no significant association with WNF, possibly because the more variable water supply is less favourable to mosquito populations.

A positive association with urban infrastructure has been repeatedly demonstrated in the US (e.g. [Pecoraro et al., 2007; Brown et al., 2008a; Gómez et al., 2008], although with some exceptions and east-west differences e.g. [Bowden et al., 2011]. This association is not apparent in the current study, and has not been reported in other European studies, although the largest outbreaks in the Old World, as in the New, have occurred in urban areas (e.g. Bucharest in 1995, Volgograd in 1999; Belgrade 2012; [Platonov et al., 2008; Popović et al., 2013; Reiter, 2010]). This probably reflects significant differences in urban planning and infrastructures design, demonstrating the importance of region specific analyses. Indeed, US suburban areas are often characterised by assemblages of houses surrounded by vegetation (gardens, public parks, trees) which provide the optimal habitat for interaction of synantropic birds, mosquitoes and humans. On the other hand, Old World cities, especially those with a longer history, typically include far less green space. Instead, small buildings surrounded by vegetation are more common in rural areas of the Old World, where WNF cases are common.

In the current study, results indicate a clear positive association of WNF cases with populated forests. 'Populated forests' are defined as those with relatively low human population density (1–10 individuals km^2), and are characterised by a mixture of forest, human habitation, farmlands and transitional habitat, and usually occur in agricultural areas [Ellis and Ramankutty, 2008]. In such areas houses are usually scattered within forest patches which provide refuge, nesting and feeding opportunity for birds, including species which are considered highly competent reservoir hosts for WNV [Reisen, 2013]. The occurrence of natural and protected areas was not significantly associated with WNF, but it is likely that increased sprawl of urban settlements causes fragmentation of previously pristine forest systems, increasing contact rates between vectors (mosquitoes), competent reservoir hosts (birds) and dead-end hosts such as humans

[Chuang and Wimberly, 2012; Gardner et al., 2014], therefore enhancing transmission from the sylvatic cycle [Kilpatrick et al., 2006].

Landscape structure, patchiness and matrix organisation have previously been associated with variation in vector population and virus transmission at a local scale [Gardner et al., 2014; Deichmeister and Telang, 2011], but although our model suggests a negative association with an index of heterogeneity (the Pielou Index), the model support for this term is low and the result therefore inconclusive.

Increases in the risk of WNF emergence in humans may arise due to temporal extension of the transmission season, increased spatial extent of habitat suitable for hosts and vectors, or increased intensity of virus amplification and circulation among birds and mosquitoes. All of these variables are likely to vary with changes in climate, human population expansion and land use change. A better understanding of the environmental drivers of WNF may ultimately be used to map the spatial variation in risk across the continent. In conjunction with long range meteorological forecasts, environmental data might be used further, to forecast inter annual change. Together, these could be used to target public health actions and so mitigate risk from WNF emergence. At the current time however, a number of weaknesses in the data available mean that predictive modelling is unlikely to be accurate. In particular, the complexity of the viral transmission cycle remains poorly understood in the Old World, while human WNF incidence data are limited by geographic variation in the accuracy of diagnosis, the establishment of surveillance, and the organisation of national reporting systems.

Further research is needed, integrating interdisciplinary research across human, veterinary and environmental health (i.e. in line with the 'One Health' initiative [Coker et al., 2011]). In particular, enhanced monitoring of WNV circulation in the environment (via the combined use of sentinel birds and the virological screening of mosquitoes) and the recording of environmental variables [Kwan et al., 2012], and a European shared database collecting geo-localised reports of human WNF, would provide important advances in data quality. This combined with collection of socio-economic data, and enhanced environmental data (for example, inclusion of species specific bird density data or routes of migrations) would help the development of more reliable predictive models.

In conclusion, although further interdisciplinary research is required to develop accurate predictive models of WNF risk, the current study, making use of a multi model inference framework (for a complete overview on the topic please refer to the milestone paper on model selection by Johnson and Omland [2004]), provides a valuable starting point, and successfully identifies and confirms a number of variables which are associated with WNV emergence in Europe, Asia and North Africa.

Acknowledgments

We kindly thank Dr Bertrand Sudre of ECDC and three anonymous reviewers for precious insights on an earlier version of the manuscript. The PhD Scholarship of Matteo Marcantonio is supported by FIRS|T (FEM International Research School e Trentino). We acknowledge the E-OBS dataset from the EU-FP6 project ENSEMBLES (http://ensembles-eu.metoffice.com) and the data providers in the ECA&D project (http://www.ecad.eu). We are grateful to the NASA Land Processes Distributed Active Archive Center (LP DAAC) for making the MODIS LST data available.

Author Contributions

Conceived and designed the experiments: M. Marcantonio RR GM. Performed the experiments: M. Marcantonio AR. Analyzed the data: M. Marcantonio GM. Contributed reagents/materials/-analysis tools: M. Marcantonio EC M. Metz MN. Wrote the paper: M. Marcantonio AR EC MN RR M. Metz.

Chapter 3

First assessment of potential distribution and dispersal capacity of the emerging invasive mosquito *Aedes koreicus* in Northeast Italy

Marcantonio, M, Metz, M, Baldacchino, F, Arnoldi, D, Montarsi, F, Capelli, G, Carlin, S, Neteler, M, and Rizzoli, A (2016). First assessment of potential distribution and dispersal capacity of the emerging invasive mosquito Aedes koreicus in Northeast Italy. *Parasites & Vectors*, 9(1).

doi: 10.1186/s13071-016-1340-9

Abstract

Invasive alien species represent a growing threat for natural systems, economy and human health. Active surveillance and responses that readily suppress newly established colonies are effective actions to mitigate the noxious consequences of biological invasions. However, when an exotic species establishes a viable population in a new area, predicting its potential spread is the most effective way to implement adequate control actions. Emerging invasive species, despite monitoring efforts, are poorly known in terms of behaviour and capacity to adapt to the newly invaded range. Therefore, tools that provide information on their spread by maximising the available data, are critical. We apply three different approaches to model the potential distribution of an emerging invasive mosquito, *Aedes koreicus*, in Northeast Italy: 1) an automatic statistical approach based on information theory, 2) a statistical approach integrated with prior knowledge, and 3) a GIS physiology-based approach. Each approach possessed benefits and limitations, and the required ecological information increases on a scale from 1 to 3. We validated the model outputs using the only other known invaded area in Europe. Finally, we applied a road network analysis to the suitability surface with the highest prediction power to highlight those areas with the highest likelihood of invasion. The GIS physiological-based model had the highest prediction power. It showed that localities currently occupied by *Aedes koreicus* represent only a small fraction of the potentially suitable area. Furthermore, the modelled niche included areas as high as 1500 m a.s.l., only partially overlapping with *Aedes albopictus* distribution. The simulated spread indicated that all of the suitable portion of the study area is at risk of invasion in a relatively short period of time if no control policies are implemented. Stochastic events may further boost the invasion process, whereas competition with *Aedes albopictus* may limit it. According to our analyses, some of the major cities in the study area may have already been invaded. Further monitoring is needed to confirm this finding. The developed models and maps represent valuable tools to inform policies aimed at eradicating or mitigating *Aedes koreicus* invasion in Northeast Italy and Central Europe.

3.1 Background

An increasing number of species is rapidly spreading outside of their original distributional range and invading new territories, gaining the name of invasive species. The factors underpinning invasion processes are numerous and include socio-economical determinants linked to the intensified speed and density of transcontinental commercial and tourist fluxes [Wilson et al., 2009; Pyšek et al., 2010]. Among abiotic factors, anomalous climatic fluctuations [Stenseth et al., 2003] and landscape perturbations [Foley et al., 2005], mainly due to human exploitation of the environment, modify ecological conditions. These altered conditions trigger or facilitate species mixing at various spatial scales, at times resulting in novel ecosystems which are constituted by persistent assemblages of exotic and indigenous species [Hobbs et al., 2006; Lockwood et al., 2005]. Among the risks arising from the increased or shifted geographical distribution of species as well as from novel ecosystems [Pyšek et al., 2010; Lockwood et al., 2005; Lenoir and Svenning, 2014], the spread rate of infectious diseases is the most pressing for human health [Crowl et al., 2008]. Indeed, many vertebrate and invertebrate species are competent hosts for one or multiple zoonoses –infectious and parasitic diseases transmissible from animals to humans, whose distribution strictly follow the geographical range of their host species [Vora, 2008].

Bloodsucking arthropods, such as mosquitoes, represent the majority of the organisms able to transmit agents of infectious diseases to humans [Buck, 1988]. Indeed they constitute a system able to overpass the skin barrier and deliver the agent of the disease directly into the blood vessels. They use host blood not only as a food source but also to regulate metabolic processes that cause dramatic and key changes in their physiology [Lehane, 2005]. Among them, mosquitoes have been the most successful invasive disease-vector group in the 20th century, and are bridge-vectors of infectious pathogens (e.g. arboviruses) which have caused devastating anthropozoonosis. Some arboviruses, such as dengue fever, Rift Valley fever, yellow fever and chikungunya are transmitted by *Aedes* species. These are highly invasive container-breeding mosquitoes, with a native geographical distribution barycentre located in tropical and subtropical regions [Reinert et al., 2004].

During the last thirty years, *Aedes* have spread worldwide, recently becoming pests in several non-tropical countries [Medlock et al., 2015]. In Europe, Italy is the most heavily infested country [Medlock et al., 2015]. Here, the tiger mosquito *Aedes albopictus* (Skuse, 1894) has been recorded for the first time in 1990 [Sabatini et al., 1990] and is now well established [Carrieri et al., 2003; Bellini et al., 2005]. This species has been indicated as the primary vector for the first endemic outbreak of chikungunya in Europe [Rezza et al., 2007]. Furthermore, in France and Croatia *Ae. albopictus* has been blamed for the transmission of the first autochthonous dengue cases reported in Europe (in 2010 and 2013) in the last 80

years [La Ruche et al., 2010; Marchand et al., 2013]. However, in temperate countries, the distribution of *Aedes* species is limited by winter temperature [Roiz et al., 2011; Neteler et al., 2013], and in Italy, *Ae. albopictus* is mainly present in areas below 600–800 m a.s.l. [ECDC, 2012; Valerio et al., 2010]. In 2011, *Aedes koreicus* (Edwards, 1917), was found in Italy [Capelli et al., 2011]. This species is native of South Korea, Japan, parts of China and ex-USSR countries [Tanaka et al., 1979] and was recorded in 2008 in Belgium for the first time outside its native range [Versteirt et al., 2012]. *Aedes koreicus* forms a monophyletic *taxon* with *Aedes japonicus* (Theobald, 1901), which is another emerging invasive mosquito in USA and Europe. Given its ecological plasticity, *Ae. koreicus* has been proposed as the next global invasive mosquito species [Versteirt et al., 2012; Kaufman and Fonseca, 2014], with potential impact on human and animal health as the vector of *Dirofilaria immitis*, a heartworm, endemic in Northern Italy and the Japanese Encephalitis virus, mostly prevalent in Asia [Tanaka et al., 1979; Feng, 1930; Miles, 1964; Montarsi et al., 2015a].

According to the few data available about its native distribution, *Ae. koreicus* may be able to tolerate lower winter temperatures than *Ae. albopictus*. It is also better adapted to urban environments than the forest dwelling species *Ae. japonicus* [Tanaka et al., 1979; Versteirt et al., 2012]. An exploratory analysis performed using nine data points where *Ae. koreicus* was sampled in its native range (Koreas; Kim et al. [2006, 2010]) revealed that its native habitat has a yearly average temperature of 11.5 °C (sd 0.8) with the minimum average temperature of the coldest month of −9 °C (sd 1.7; Matteo Marcantonio, personal communication). With the highly competitive species *Ae. albopictus* well established in Italy, *Ae. koreicus* may presumably be outcompeted by *Ae. albopictus* in many areas with mild climate conditions (e.g. through larvae interspecific competition; [Juliano et al., 2004]), but new populations of *Ae. koreicus* might establish in areas too cold for *Ae. albopictus*. Following this scenario, a wider geographical range could be colonized by *Aedes* mosquitoes, potentially widening the spatial distribution of *Aedes*-borne diseases. Therefore, describing *Ae. koreicus* potential distribution is critical for proacting ecological management able to promptly respond to the threat posed by this emerging invasive species [Dunn and Hatcher, 2015].

The potential distribution of invasive species in a new geographical area can be assessed through mechanistic or correlative algorithms, generally referred to as invasive Species Distribution Models (iSDMs) [Guisan and Zimmermann, 2000; Guisan and Thuiller, 2005; Elith and Leathwick, 2009; Kearney and Porter, 2009]. The main challenge with correlative iSDM is that, while many spatial modelling techniques require species to be at equilibrium with their environment, emerging invasive species are by definition in a dynamic transition state in the invaded range [Crowl et al., 2008]. The equilibrium assumption may mislead predictions over broad areas since species' capacities to colonise previously unoccupied areas may affect relia-

bility of model prediction [Leroux et al., 2013]. Therefore, the reliability of some ecological modelling techniques is disputed in the scientific literature, with hybrid (mechanistic together with correlative approach) and adaptive frameworks being more and more explored [Kearney and Porter, 2009; Dormann et al., 2012; Uden et al., 2015; Barker et al., 2015]. However, choosing methods is often dictated by more practical reasons such as availability of field and laboratory data, knowledge of species biology, project deadlines and statistical or mathematical expertise. Purely automatic statistical approaches require minimal knowledge about the species' life history, ecology and physiology, making predictions easy to achieve. By contrast, other approaches make use of such knowledge to select parameters appropriate to model the physiological requirement of the investigated species or build mathematical representations of ecological processes. Such iSDMs require more effort but are more accurate when detailed physiological information is available or in circumstances that require in-depth understanding of survival and spread framework [Dormann et al., 2012; Uden et al., 2015]

As part of the L.E.xE.M. (Laboratory of Excellence for Epidemiology and Modelling, www.lexem.eu) project, we set a network of traps supported by larval searches in northern Italy. Using the collected data, we estimated the potential distribution of *Ae. koreicus* in Northeast Italy with three different iSDM approaches. First, we applied an automatic statistical approach, represented by the Maximum Entropy (MaxEnt) modelling [Phillips et al., 2006]. Second, we implemented a logistic regression model with Bayesian framework informed by using prior knowledge retrieved from literature on the ecologically similar and better studied species *Ae. albopictus*. The information derived from field data is therefore mediated by a-priori ecological information [McCarthy and Masters, 2005; Hooten and Wikle, 2007]. Third, we applied a Geographic Information System (GIS) physiology-based iSDM, solely relying on known environmental constraints of the species (e.g. the species cannot survive cold winter temperatures, etc.). Beyond describing species distributions, iSDMs have become an important and widely used decision making tool for a variety of applications, such as mapping risk of VBDs as well as their host spread, and determining locations that are potentially susceptible to invasion. Here, making use of multiple iSDMs, we aim to reliably estimate *Ae. koreicus* potential distribution in Northeast Italy, gathering insights into which iSDM should be preferred on the others. Our final goal was to investigate the future expansion of *Ae. koreicus* in the study area combining the developed habitat suitability map with available information about transportation networks and the observed species dispersal rate. Integrating the current and potential distribution of emerging invasive species with their preferred spread pathways is pivotal in identifying the most appropriate strategy to mitigate and control their invasion. In this paper, we hope to provide useful and validated spatial information about *Ae. koreicus*

spread to decision makers in order to support control strategies and develop proactive public health policies.

3.2 Study area

The study area is located in Northeast Italy (Figure 3.1; latitude N46.75, S45.59, longitude W10.38, E12.82; Datum WGS84). We investigated the presence of *Ae. koreicus* in two administrative units, Trentino and Veneto regions (EU NUTS2 code: ITD2 and ITD3). The area comprises the Eastern section of the Alps and the Northeastern part of the Po Valley. The altitude ranges from 0 to 3900 m a.s.l. The climate ranges from subartic climate (Köppen climate classification: Dwc) in the Northern-most mountainous part to oceanic climate (Cfc) in the central and southern low altitude and flat part of the study area. The annual average temperature ranges from -6.8 to 15.3 °C, the cumulative annual precipitation ranges from 439 to 1660 ml yr^{-1}, while the total population count was around 1.7 million with a very variable density, spanning from 0 to 1100 people km^{-2} [CIESIN - Columbia University, 2015]. The study area includes one of the most developed agricultural, industrial and commercial areas of Italy [Capelli et al., 2011] with dense connections between central and northern European commercial hubs. The area has already been invaded by *Ae. albopictus* which was first detected in 1991 to then gradually colonise all the suitable habitats.

3.3 Methods

3.3.1 Sampling design

We sampled a total of 394 locations from April to November in 2013 and 2014 using various collection methods such as larval searches, ovitraps, CDC-light traps and BG-sentinel traps (Biogents AG, Regenburg, Germany). We derived part of the data from entomological surveillance supported by Veneto Region. The sampling was implemented in order to acquire data on the current distribution of *Ae. koreicus* inside and at the boundary of its known invaded range. The sampled locations were checked every 2 weeks, except for larval search. Eggs collected from ovitraps were maintained in water for hatching, and larvae were reared until the fourth instar for identification [Becker, 2010; Montarsi et al., 2013]. Adults caught in CDC-light traps and BG-sentinel traps were identified and stored at −80 °C for molecular analysis. Expert entomologists identified each sample at species-level and organised data in a geodatabase. A location was considered positive (presence) if at least one individual was sampled during the sampling period. The presence/absence dataset was spatially aggregated in a 250 m pixel grid

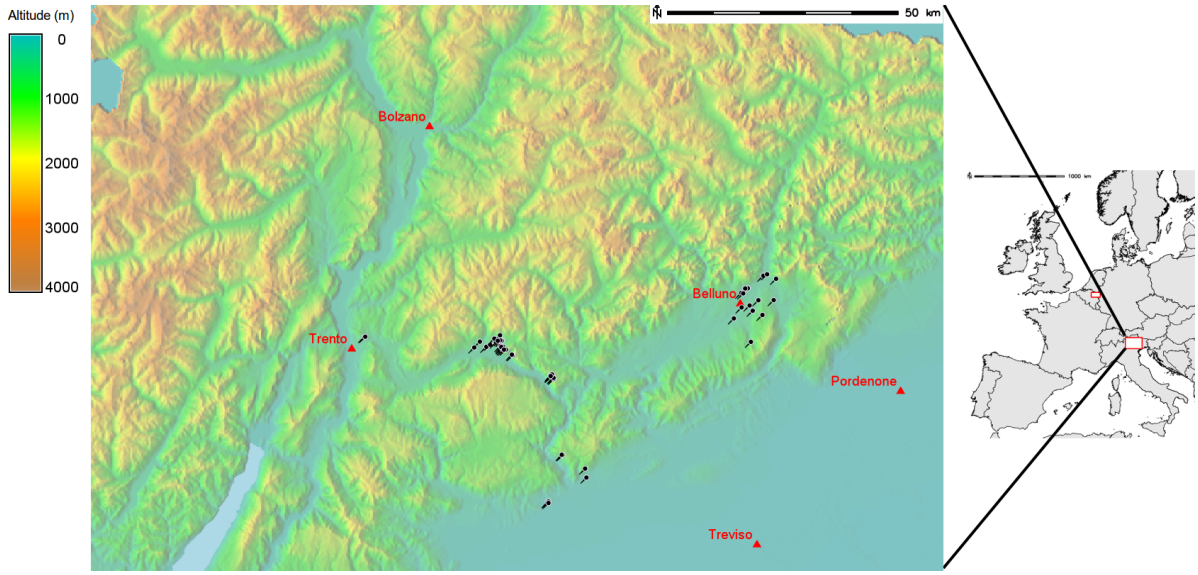

Figure 3.1: Right side: European map with the two red rectangles showing *Ae. koreicus* positive areas for *Ae. koreicus* in Italy (big rectangle) and in Belgium (small rectangle). For the statistical analysis, the Italian study area was used as the training area while the Belgian one as the test area. Left side: Zoom of the Italian study area showing trap locations and major cities, with the shaded digital elevation model as background

aligned to the EuroLST grid [Metz et al., 2014]. The grid cells containing both positive and negative locations were considered as positive. As a result, a total of 306 grid cells, of which 53 positive and 253 negative, were used in the following statistical analysis.

3.3.2 Environmental data sources and model predictors

To model the habitat suitability of *Ae. koreicus*, we used a set of environmental predictors based on a 10-years long average (2003–2012) derived from remote sensing (satellite) data at a spatial resolution of 250 m. Temperature variables have been derived from the EuroLST bioclim dataset, freely available at the EuroLST website (http://geodati.fmach.it/eurolst/). Those bioclim variables which integrate temperature together with precipitation were calculated by merging the EuroLST [Metz et al., 2014] dataset with precipitation data from the Climate Prediction Center (CPC) Morphing algorithm (CMORPH) Version 1.0 [Joyce et al., 2004] which we calibrated against data from the Global Precipitation Climatology Project (GPCP) Version 2.2 [Adler and Laurenroth, 2003]. Moreover, two additional temperature predictors were derived; average temperature of the coldest month ($Tavg_CM$) and average temperature of mosquito growing season ($Tavg_GS$). The two latter variables were considered in order to match the biology of *Aedes* spp. with temperature variables. Indeed, in the study area, the time period

Table 3.1: Description of the predictor variables. We reported source and spatial resolution of each group of predictor variables.

N	Variable	Source	Resolution
19	Bioclim 1-19[1]	MODIS LST and CMORPH	250 m
1	Avg. T of growing season	MODIS LST	250 m
1	Avg. T of the coldest month	MODIS LST	250 m
4	seasonal NDWI	MODIS LST	250 m
4	seasonal NDVI	MODIS LST	250 m

from April to September represents the most favourable conditions for *Aedes* population growth. Furthermore, cold temperatures under 0 °C are a limiting factor for diapausing egg survival. On the one hand, in the literature it is reported that *Aedes* cold-acclimated and diapausing eggs can survive very low temperature (−10,−12 °C) for a brief to moderate period of time [Hanson and Craig, 1995; Thomas et al., 2012]. On the other hand, long periods of average cold weather represent a chronic stress which may more strongly limit the fitness (e.g. hatching) of diapausing eggs. Therefore, the average temperature of the coldest month may be more effective to limit mosquitoes potential distribution than the average minimum temperature of the coldest month.

We obtained data on the vegetation biomass from the MODIS Normalised Difference Vegetation Index (NDVI; $MOD13Q1$) product [Neteler and Metz, 2014]. Vegetation indices, such as NDVI, have been extensively used to describe disease risk and habitat suitability for different species of mosquitoes [Brown et al., 2008a; Kleinschmidt et al., 2000; Lourenço et al., 2011]. The ecosystem water content might also limit mosquitoes habitat suitability, as water is a key component of their ecological niche. We calculated the Normalised Difference Water Index (NDWI; Gao [1996]), derived from the MODIS surface reflectance product ($MOD09A1$). NDWI and NDVI embed different wavelengths, and so they should be considered as complementary [Gao, 1996]. We averaged NDVI and NDWI values pixel-wise in four seasonal groups over a three month period each (January–March, April–June, July–September, October–December), in order to have a representation of the vegetation coverage and ecosystem water for each of the four seasons.

The initial set of 29 environmental predictors (19 EuroLST/CMORPH bioclim, 2 further temperature-based variables, 4 seasonal NDVI and 4 seasonal NDWI; Table 3.1) was used in different combinations as input for the modelling approaches described in detail in the next

[1] http://www.worldclim.org/bioclim

section. All the considered environmental parameters have already been shown as relevant for mosquito iSDMs [Eisen et al., 2010].

3.3.3 Modelling framework

SDMs are a set of algorithms which quantitatively describe areas that support the presence of a given species, based on experimental data, known presence/absence data and the associated environmental conditions. These models seek, despite some limitations, the species ecological niche in the Hutchinsonian sense [Hutchinson, 1957]. We made use of three different modelling approaches to estimate *Ae. koreicus* potential distribution in Northeast Italy. These three techniques rely on automatic statistical methods or on physiological knowledge of the species life history cycle. The target output of all these three modelling techniques was an environmental suitability indicator, expressed as a continuous value from 0 (no suitability) to 1 (complete suitability). We associated each suitability value to its respective EuroLST grid cell, at a resolution of 250 m. Therefore, we visualised the predicted environmental suitability (habitat suitability) in potential distribution maps.

Maximum Entropy (MaxEnt) approach to species distribution modelling

MaxEnt is a common modelling framework used in species distribution modelling [Phillips et al., 2006; Phillips and Dudı, 2008]. MaxEnt minimises the relative entropy between the probability density of the predictors estimated from the presence data and the probability density of the predictors estimated from the region of interest (background information). This means that the geographic extent and the number of background samples influence the results. After having tested different buffer sizes, we have placed a buffer of 5 km around the presence data, representative of locations accessible for *Ae. koreicus* via dispersal and which approximate the overall study area environmental conditions [Saupe et al., 2012; Merow et al., 2014]. The resultant region has been used as input for MaxEnt modelling. We used MaxEnt as machine learning algorithm, letting it decide which predictors were important through regularisation [Elith et al., 2011]. Therefore, we ran the MaxEnt model without any previous biologically-based selection of the predictor variables. However, since several predictors were highly correlated among them, we performed a correlation analysis in order to limit multicollinearity issues. We excluded all those predictors showing a correlation higher than 0.50 (Pearson's r). The predictors exclusion was performed selecting the most correlated couple, followed by a random draw to decide what to exclude of the two predictors. We carried out all the analysis in R [R Core Team, 2015], using dismo [Hijmans et al., 2015] package.

Bayesian logistic regression (logBAY) with Markov Chain Monte Carlo simulation

Logit-link Generalised Linear Models (GLMs) are standard regression methods to model habitat suitability in ecology [Elith et al., 2006]. The model regression output (x) is transformed through the logistic function ($1/(1+exp(-x))$) in a new interval $s, s \in [0,1]$, describing the probability s of the species presence given the model parameters. We wrapped the logistic

regression in a Bayesian framework using Just Another Gibbs Sampler (JAGS) [Plummer, 2003] in combination with rjags [Plummer, 2015] and coda [Plummer et al., 2006] R packages. We used presence or absence data as response variable, while as predictor variables we chose those environmental variables with the strongest credibility in shaping *Aedes* ecological niche, as follows: *i)* average temperature of mosquito growing season (*TavgGS*), *ii)* average annual temperature (*TavgY*), *iii)* average of the minimum temperature (*TavgM*); *iv) TavgCM*; *v)* cumulative annual precipitation (*PcumY*) and *vi)* spring NDWI (*NDWIavgS*) [Medlock et al., 2015; Neteler et al., 2013; Roiz et al., 2011; Versteirt et al., 2012; Montarsi et al., 2013; Hanson and Craig, 1995; Fischer et al., 2014; Rochlin et al., 2013; Caminade et al., 2012; Neteler et al., 2011; Medlock et al., 2006; Alto and Juliano, 2001]. All predictors were scaled using their mean and standard deviation as follows: $(x-\bar{x})/sd(x)$, where x is the predictor variable. Even though the role of precipitation as limiting factor for container-breeding mosquitoes is controversial [Rochlin et al., 2013], we included it among predictors since water availability do affect the aquatic stages of the mosquito life cycle [Caminade et al., 2012]. Moreover, a preliminary exploratory analysis showed a strong association between precipitation and *Ae. koreicus* presence/absence for our dataset. Nevertheless, the observed correlation may be a spurious pattern linked with a different detectability probability for different parts of the precipitation range [Krishna et al., 2008]. We used Gaussian distributed informed priors derived from [Neteler et al., 2013] for the temperature based variables, whereas non-informative priors (normal distribution with $\mu = 0; 1/SD = 10^{-12}$ for all the other variables (Table 3.2).

Table 3.2: Average and precision for informed and non informed priors. The precision of a distribution is the inverse of its standard deviation.

Predictor	**Average**	**Precision**
TavgGS[2]	2.580	0.835
TavgCM[2]	1.962	0.654
Others	0	10^{-12}

[2] Values from Roiz et al. [2011]

To select the combination of variables carrying the most information on mosquito distribution, we run all the models possible combining the six aforementioned predictor variables (including models with interactions between *TavgGS* or *TavgY* and *PcumY* and models with *TavgY* second order polynomial function). Each model was initialised using maximum likelihood estimates for each coefficient and 10000 burn-in Markov Chain Monte Carlo (MCMC) iterations to find a good starting point to sample a representative Posterior Probability Distribution (PPD). The models were therefore ranked using the Deviance Information Criterion (DIC) with 1000 MCMC iterations and thinning set of 5. The most informative model (lowest DIC) was used to sample 10 000 times with thinning set of 50 the PPD of model parameters and of *Ae. koreicus* occurrence in each pixel of the study area. The convergence of MCMC chains was monitored using Gelman and Rubin's convergence diagnostic between two MCMCs [Gelman and Rubin, 1992]. The PPD Highest Density Interval (HDI) was calculated using the function proposed in [Kruschke, 2010]. The average value of PPD was assigned to the correspondent pixel, resulting in the habitat suitability map for *Ae. koreicus*. Furthermore, the uncertainty linked to the average pixel prediction was assessed (and mapped; not reported) deriving the 95 % Bayesian confidence interval of the PPD of each pixel. We reported all the steps to reproduce the logBAY model as an R function in Appendix A.

GIS physiology-based (PHY) suitability modelling

This iSDM approach considers environmental parameters corresponding to physiological constraints of *Ae. koreicus*. The exact physiological constraints for this species are currently unknown. We used a conservative and parsimonious approach by assuming that the same environmental parameters which represent limiting factors for *Ae. albopictus* can be applied, most importantly: the average temperature of the coldest month (*TavgCM*) and the average temperature of the hottest quarter of the year (*TavgHQY*). The temperature of the coldest month determines overwintering suitability: if the coldest month is under a certain threshold, diapausing eggs will not survive and a persistent population can not be established. If the temperature of the hottest quarter of the year does not reach a certain value, larvae can not develop and adults can not reproduce. Additionally, precipitation can determine habitat suitability, but needs to be treated with caution because irrigation and small anthropogenic water reservoirs can compensate for low precipitation. Other environmental parameters of potential importance are the average temperature of the mosquito growing season (*TavgGS*) and annual average temperature (*TavgY*). *TavgY* has previously been used to model habitat suitability for *Ae. albopictus*, but can not be linked to a particular physiological constraint. Suitable summer temperatures might be averaged out by cold winter temperatures, and equally cold winter temperatures might be averaged out by hot summer temperatures. The specific

Table 3.3: Predictor variables used in the GIS physiology-based suitability model. The descriptive statistics refers to the location of all the positive traps in the study area

Parameter	**Average**	**Standard deviation**	**Lower bound of the 99% CI**
Tavg_{HQY} (°C)	21.41	10.76	18.63
Tavg_{CM} (°C)	0.38	1.33	−3.06
Pcum_{Y} (°C)	1182.00	105.00	912.00

threshold for the three environmental parameters (average temperature of the coldest month, average temperature of the hottest quarter of the year and annual precipitation) was estimated from the values observed at sampling locations with presence of *Ae. koreicus*. We used the lower bound of the 99 % confidence interval of each environmental parameter distribution as the low threshold for the environmental parameters (Table 3.3). The estimated thresholds were used to model *Ae. koreicus* habitat suitability, resulting in suitability maps. All temperature thresholds were transformed with a sigmoid function such that zero means not suitable, 0.5 corresponds to the actual threshold and 1 means highly suitable (Appendix C). A margin of 4 was applied to the sigmoid function for temperature. Moreover, for annual precipitation (*PcumY*), a margin of 200 $\text{mm}\,\text{yr}^{-1}$ was applied. Compared to MaxEnt, we defined a priori response curve for relevant environmental parameters, whereas such response curves are a diagnostic result of MaxEnt. The separate suitability indicators were multiplied in order to obtain a single general suitability index S, where:

$$S = \begin{cases} 0, & \forall X = 0. \\ (0,1), & \forall X > 0 \\ 1, & \forall X = 1 \end{cases} \tag{3.1}$$

Model performance accuracy

Model performance accuracy was measured assessing the error rate as a percentage (i.e. error rate (%) equals the number of incorrect cases divided by the total number of cases tested), as well as Cohen's kappa coefficient (k), which is a measure of agreement that takes into account chance effects [Manel et al., 2001] and True Skill Statistics (TSS; Allouche et al. [2006]), an accuracy index not sensitive to prevalence. The optimal thresholds to discriminate the continuous model outputs in the presence or absence category were estimated by maximising sensitivity together with specificity.

We performed a further qualitative validation of the models sensitivity predicting *Ae. koreicus* overall average suitability and standard deviation in the only other known invaded area in Europe, the Maasmechelen municipality in Eastern Belgium (Figure 3.1). In this locality, a viable hibernating *Ae. koreicus* population persists in a homogeneous 6 km industrial area since its first detection in 2008 [Versteirt et al., 2012]. When dealing with emerging invasive arthropods, absence points have a high likelihood to represent areas where the trap failed to catch entities of the species despite presence in the area, or areas that are inside the species ecological niche, but which have not yet been invaded (i.e. dispersal limitation). Therefore, we emphasised model sensitivity on specificity since it should be considered more effective to assess iSDM predictive power [Ward, 2006; Cianci et al., 2015; De Clercq et al., 2015].

3.3.4 *Aedes koreicus* spread analysis

To estimate the *Ae. koreicus* spread rate since introduction in the study area, we used information about its presence since 2011, when it was recorded for the first time in a small village near Belluno (Sospirolo village, 46.14°N; longitude 12.07°E, datum: WGS84; Capelli et al. [2011]). In absence of information about the presence of the species before 2011, we assumed this geographical location as the centre of gravity for the introduction point(s).

In addition, we calculated the centre of gravity for the coordinates of positive traps for 2013 and 2014 respectively. We assumed that the range expansion has been constant through time, therefore we divided the Euclidean distance between 2011, 2013, 2014 centres of gravity by 4, representing the years since the introduction, deriving an approximate spreading rate, defined as spread rate in kilometres per year ($km\,yr^{-1}$). Afterwards, we built a road network, weighted by the travelling distance between each road segment and the introduction point (root of the network, assumed to be the village Sospirolo). The road network was acquired from the OpenStreetMap project (openstreetmap.org), cleaned from tertiary roads, tracks and pathways which were assumed to be of low importance for mosquito dispersal. All the unconnected (not connected to the root of the network) road segments were also removed from the network.

The following step was to intersect the weighted road network with the habitat suitability map, to derive a distance-suitability weighted cost network. For the reference suitability map, we chose the one derived by the iSDM with the best predictive performance. This step was carried out to increase the cost for those locations that, despite being spatially close to the introduction location, were ecologically distant from *Ae. koreicus* ecological niche. We assumed that, for high suitability values (defined using the suitability threshold at which sensitivity plus specificity were maximised), the cost for the spread of the mosquito was the distance from the introduction point divided by the suitability value, while for suitability values below the threshold, the new weighted distance from the introduction location was the original

distance from the introduction location divided by the suitability values raised to the power of 1.5 (penalty derived from empirical observations of the invasion process).

Eventually, we split the distance-suitability weighted road network into invasion cost isolines according to the observed *Ae. koreicus* dispersal rate. This step was performed in order to estimate areas with the same probability to be invaded in a defined temporal span (in years).

All the spatial analysis were performed using GRASS GIS 7 [Neteler et al., 2012] modules (particularly v.net tool set).

3.4 Results

The potential distribution maps for *Ae. koreicus* derived from the three models are reported in 3.2.

3.4.1 MaxEnt modelling results

The output of the correlation analysis, which was a matrix with 9 predictors (Appendix A), was used as an input in the MaxEnt model.

Variable importance can be estimated by different means: percent contribution, permutation importance, and jacknife gain. These three measurements provide different rankings and are reported in Appendix A. According to the rank sum of the three different criteria, the two most important variables for the MaxEnt model were temperature seasonality (bio4) and maximum temperature of the warmest month (bio05). The response curve of bio4 suggests that *Ae. koreicus* presence probability is relatively constant until it drops suddenly in the localities where seasonality becomes extreme. Bio5 response curve implies a monotonic increase of presence probability in a temperature range between 22 and 28 °C, after which it assumes an asymptotic trend (Appendix A).

The *Ae. koreicus* potential distribution map derived from the MaxEnt model showed values ranging from 0 to 0.94, with an average suitability of 0.11 (Fig. 2a). According to the MaxEnt model, suitable areas are concentrated along the main Alpine valleys.

3.4.2 Bayesian logistic regression modelling results

The best logBAY model (lowest DIC; Table 3.4) comprised the average temperature of the growing season (April to September; *TavgGS*), the minimum temperature of the coldest month (*TavgDEC*) and the cumulative annual precipitation (*PcumY*). All the predictors were positively correlated with the presence of *Ae. koreicus*. The PPD of the model coefficients with their mean and 95 % HDI is showed for the best model in Appendix B. The 95 % HDI of *TavgGS*

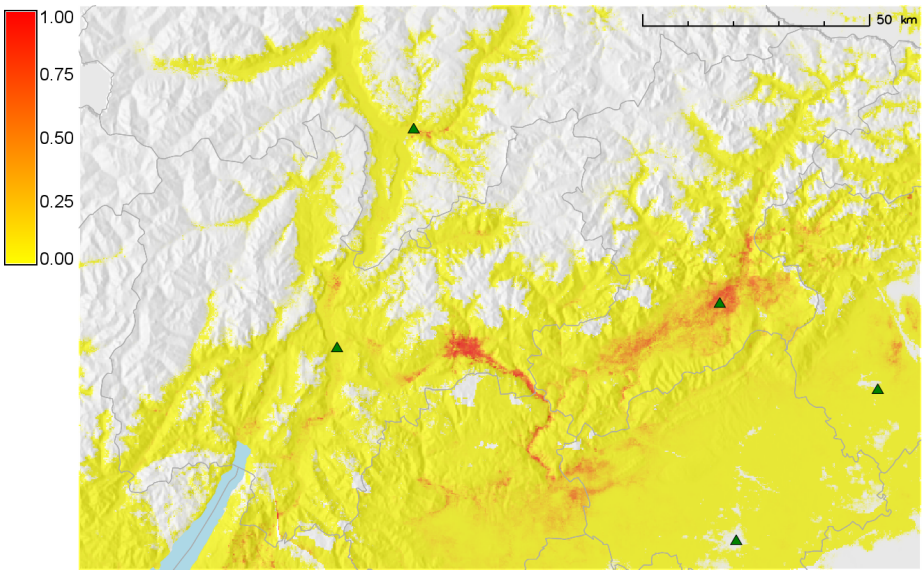

(a) MaxEnt potential distribution map

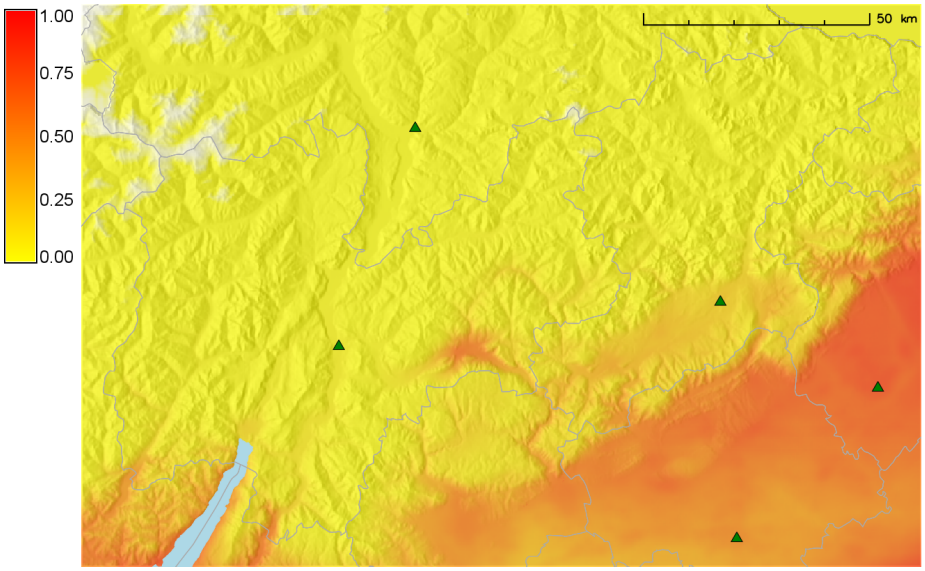

(b) Bayesian logistic regression potential distribution map

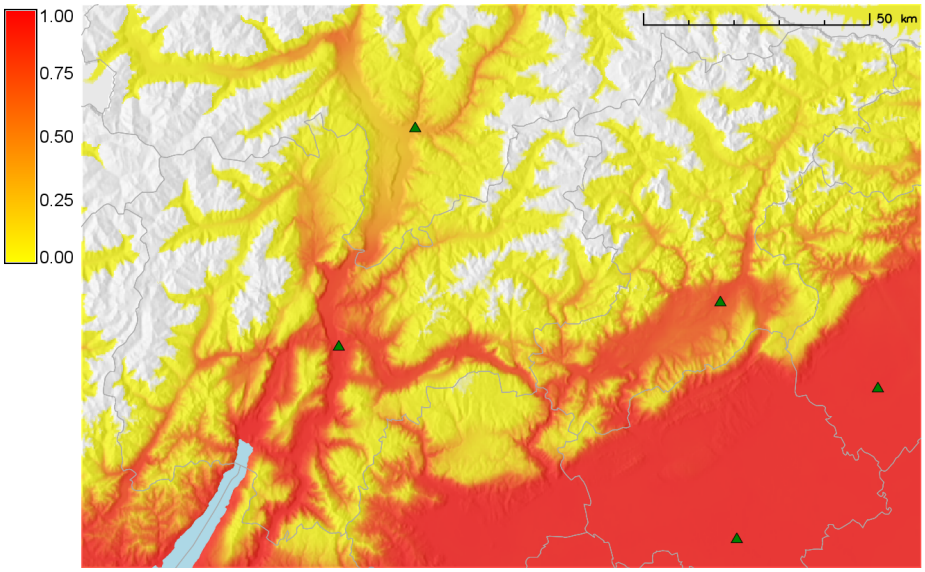

(c) GIS physiology-based potential distribution map

Figure 3.2: Potential distribution maps of *Ae. koreicus* . The green triangles represent the main cities in the area.

and *PcumY* did not include 0, meaning that the credible values of these model parameters are different than 0 (Appendix B).

Table 3.4: Model specifications and Deviance Information Criterion (DIC) for the best 15 logBAY models plus the full model.

Model N	Model Terms	DIC
1	T_{avgY}	272.0
2	P_{cumY}+$NDWI_s$	264.0
3	T_{avgDEC}+P_{cumY}	222.0
4	T_{avgDEC}+P_{cumY}	222.0
5	T_{avgM}+P_{cumY}	220.2
6	T_{avgY}+T_{min}+P_{cumY}	220.0
7	T_{avgGS}+T_{avgY}+T_{avgM}+T_{avgDEC}+P_{cumY}+$NDWI_s$ (full)	218.2
8	T_{min}+P_{cumY}	217.0
9	T_{avgY}+P_{cumY}	215.4
10	T_{avgY}+P_{cumY}	215.0
11	T_{avgY}+P_{cumY}+$NDWI_s$	215.0
12	T_{avgY}+T_{min}+P_{cumY}+$NDWI_s$	212.0
13	T_{avgGS}+T_{min}+P_{cumY}+$NDWI_s$	211.6
14	T_{avgGS}+T_{min}+P_{cumY}	210.8
15	T_{avgGS}+T_{avgM}+P_{cumY}	209.5
16	T_{avgGS}+T_{avgDEC}+P_{cumY}	208.3

The logBAY suitability map, built using the average of the PPD, showed values ranging from 0 to 0.83, with an average suitability of 0.14 (Fig. 2b). The suitability predicted by logBAY model cut the study area in two distinct sections: high suitability in the southern part, low suitability in the northern mountainous area. The highest suitability was indicated for Pordenone, Treviso provinces and on the surroundings of lake Garda.

3.4.3 Physiology-based modelling results

The PHY suitability surface resembles the one of MaxEnt, with the difference of a much higher absolute suitability value. By definition, the PHY suitability value for most known presence sites is one. The main difference between the PHY, logBAY models and MaxEnt is due to the upper threshold in the MaxEnt response curves, which are mainly composed of

parameters derived from temperature, whereas the other two models have not imposed an upper threshold on temperature (logBAY is a linear regression model, while for MaxEnt there is no physiological restriction for maximum monthly temperature in the study area, which rarely reaches more than 35 °C.

The suitability values predicted by PHY ranged from 0 to 1, with an average suitability of 0.32. PHY had the maximum average suitability value among the developed models, with more than 65 % of the studied areas having values higher than 0.50 (Figure 3.2c). Very high suitability was assigned to Po, Adige, Valsugana and Sarca valleys. Furthermore Piave, Isarco as well as other minor valleys were characterised by moderate to high suitability values.

3.4.4 Model validation

The suitability threshold at which sensitivity plus specificity were maximised for each model is reported in Table 3.5 together with Kappa statistics, TSS and percent error rate. The threshold at which sensitivity plus specificity were maximised varies considerably between the three models. After grouping the suitability values in suitable and not suitable classes using these thresholds, MaxEnt reported the highest error rate. On the contrary, logBAY and PHY had TSS and Kappa values indicating from substantial to almost perfect agreement with observed data [Landis and Koch, 1977]. PHY showed the highest sensitivity while logBAY the highest specificity.

Table 3.5: Suitability thresholds at which sensitivity plus specificity were maximised, Kappa statistics, TSS and error rate for each model.

Model	**Optimal threshold**	**Kappa**	**TSS**	**Predicted high Present**	**Predicted low Absent**	**Error rate (%)**
MaxEnt	0.13	0.87	0.67	$^{52}/_{56}$	$^{250}/_{338}$	27.2
logBAY	0.14	0.84	0.69	$^{53}/_{56}$	$^{251}/_{338}$	26.6
PHY	0.71	0.70	0.51	$^{52}/_{56}$	$^{191}/_{338}$	44.7

Applying the discriminant thresholds listed in Table 3.5 to the suitability maps, we found that 3 %, 26 % and 30 % of the study area was reported as suitable by MaxEnt, logBay and PHY models respectively.

The result of the cross-tabulation between elevation and suitable area is reported in Fig. 3. All the models agreed on the suitable area being concentrated at low altitude (0–800 m).

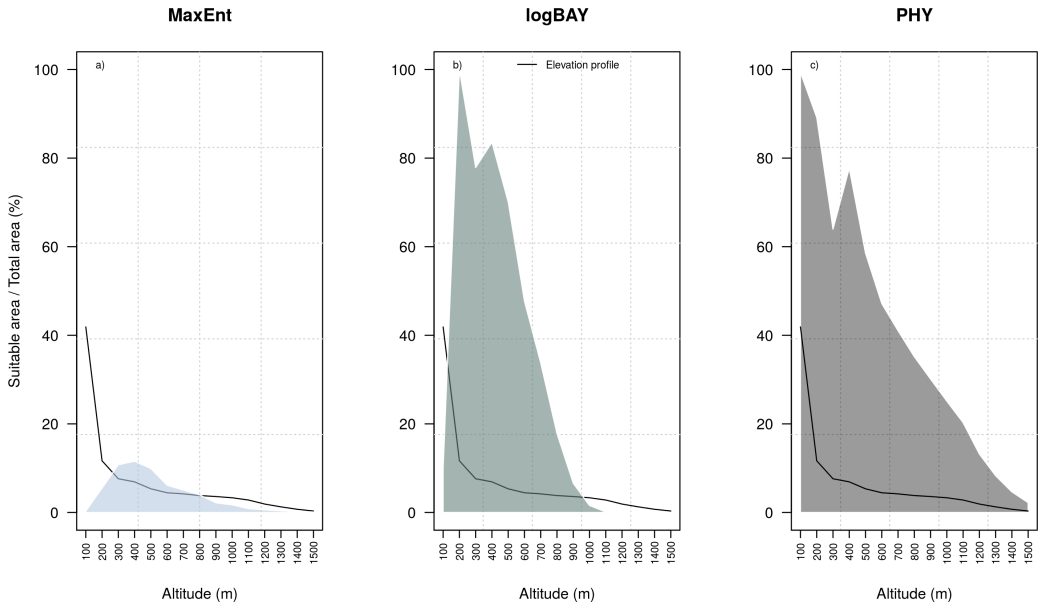

Figure 3.3: Altitude profile of suitable area: This figure depicts the percentage of suitable area over the total area for each altitude class for *a)* PHY; *b)* logBAY and *c)* MaxEnt model. The black line represents the percentage of area in each corresponding altitude class.

Half of the total area between 0 and 800 m was indicated as suitable according to logBAY and PHY. It is interesting to note that all the profiles in Figure 3.3 show a spike in suitability around 400–500 m. Moreover, PHY model predicted as suitable a remarkable percentage (16 %) in higher altitude area (above 800 m). To further validate the model using an independent set of data, we applied each model to the only other area invaded by *Ae. koreicus* in Europe: Maasmechelen municipality in Belgium (Figure 3.1). We reported the descriptive statistics of the predicted suitability distribution in Table 3.6. PHY model predicted high suitability, whereas logBAY very low suitability.

Table 3.6: Descriptive statistics of Maasmechelen municipality suitability for *Aedes koreicus* for all the three models.

Model	**Average suitability**	**Min. suitability**	**Max. suitability**
MaxEnt	0.21	0.01	0.59
logBAY	0.10	0.07	0.14
PHY	0.61	0.38	0.78

3.4.5 *Aedes koreicus* spread analysis

From 2011 to 2014, the average shift of the invaded area centroid was approximately 8 km yr^{-1}. The analysis performed to predict the spread of *Ae. koreicus* showed that the most likely dispersal direction was along Valsugana Valley (Figure 3.4). Furthermore, the mosquito may be already present in the northern part of Verona province (south-east of the study area; predicted to be invaded within 5-10 years after introduction). According to our results the mosquito spread might be rather fast in the southern part of the study area due to both the dense road connection with the introduction point and to the high habitat suitability. Even though the dispersal along the highly populated Adige Valley was found to be slower than in the southern part of the study area, probably due to its more rough topography, overall it will potentially be at high risk of invasion during the forthcoming decades.

3.5 Discussion

Aedes koreicus is an emerging invasive species in Europe, and is a nuisance and potential vector of pathogens [Tanaka et al., 1979; Montarsi et al., 2015a]. In this study, we assessed its habitat suitability in Northeast Italy, making use of iSDMs and a limited amount of field data supported by prior knowledge from related species. We also investigated the potential pathways and timing of future spread through a road network analysis. The main outcome was that the known distribution of *Ae. koreicus* is only a fraction of the potentially suitable area. However, we observed a rather variable characterisation of the suitable area, highly dependent on the considered iSDM. MaxEnt predicted the smallest suitable area, while PHY the largest. The observed differences are mainly due to the lack of upper temperature threshold limits for logBAY and PHY (Appendix A, C), which allows high suitability in the warmest section of the study area. Despite potential limitations due to the approximation of biological patterns with linear relations in ecological niche modelling, the lack of upper thresholds for temperature should not to be considered an artefact due to the studied species and the climatic characteristic of the study area. Indeed, *Ae. koreicus* is a temperate-continental taxon and the studied area is characterized by monthly average temperatures rarely exceeding 30 °C (therefore well inside the temperature niche of other *Aedes* species; Smith and Eliason [1989]). However, high temperatures might affect local abundance of *Ae. koreicus* (e.g. [Scott, 2003] observed a decrease of *Ae. japonicus* larvae survivorship at temperatures over 22 °C under laboratory conditions).

All the models were mainly driven by temperature variables, confirming what has already been found in literature for other *Aedes* species (e.g. [Roche et al., 2015]). The most important predictors for MaxEnt were bio4 and bio5, the best logBAY model included two temperature variables *TavgGS*, *TavgDEC* in addition to *PcumY*, while PHY was completely constrained by temperature (the included precipitation threshold was always exceeded in the study area). Mosquitoes are small-bodied poikilotherms, meaning that ambient temperature is the main abiotic factor limiting their ecological niche and, therefore, their geographical distribution [Alto and Juliano, 2001]. High temperature decreases embryonic (e.g. Trpis et al. [1973]) and larval (e.g. Teng and Apperson [2000]) development time, and the size of adults (e.g. [Rueda et al., 1990]), while cold winter temperatures have a severe impact on the survival of diapausing eggs [Thomas et al., 2012]. The lesser importance of environmental indicators other than temperature can be explained by the considered spatial scale (i.e. extension and grain), where vegetation variability might be less important than climatic conditions [95], and by the autoecology of *Aedes* mosquitoes, container-breeding species, able to develop independently of the regional precipitation trend and environmental variability. At a finer spatial scale and in urban habitats, vegetation may be more influential on *Aedes* life cycle. Indeed, in this setting, even small pockets of vegetation favour habitat heterogeneity, allowing mosquitoes to regulate extreme weather conditions [Meyer et al., 1990].

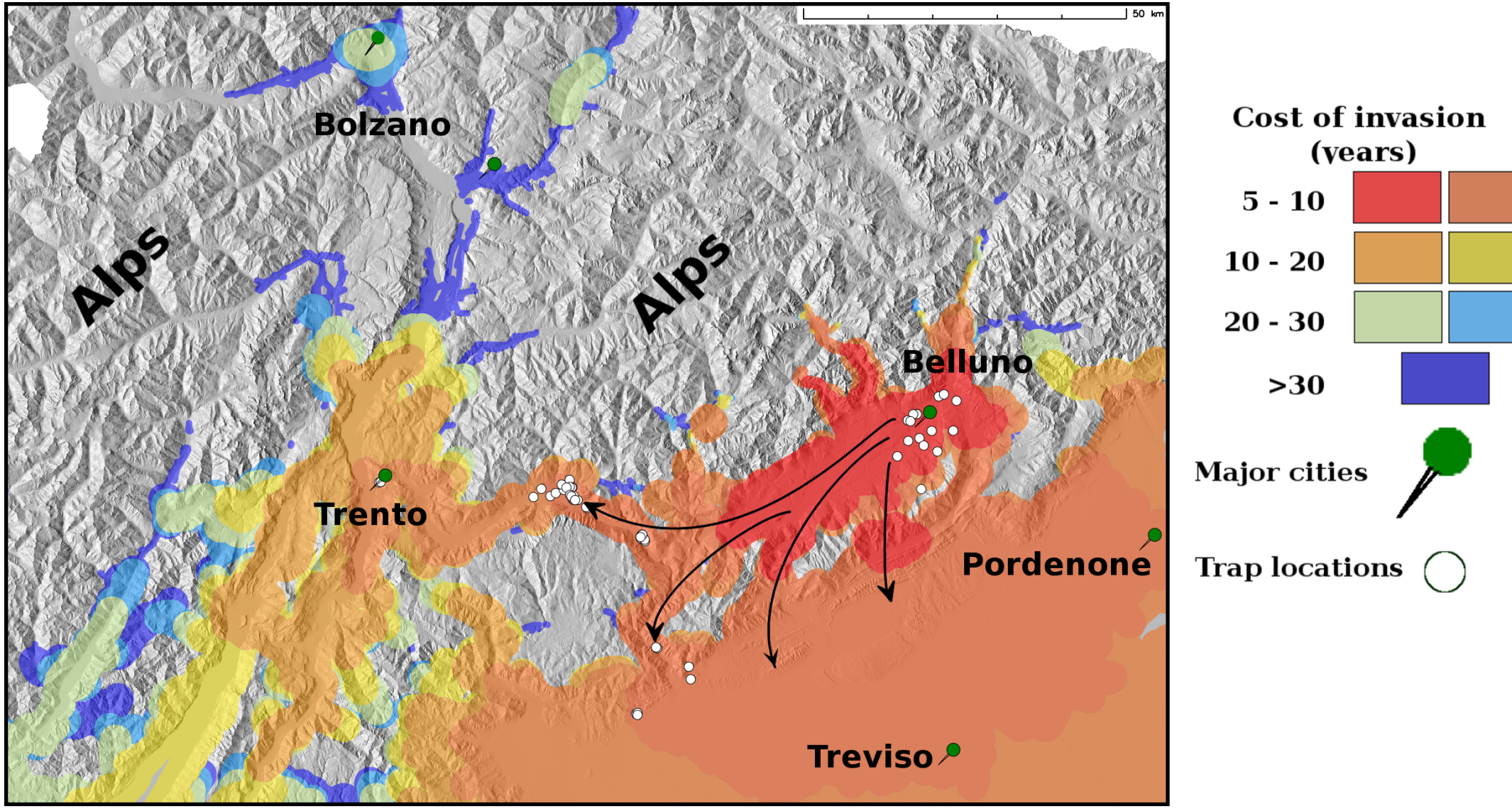

Figure 3.4: Potential spread of *Aedes koreicus* predicted through road network analysis: Areas with the same cost of invasion are displayed using a red-green-blue colour scale. The cost of invasion is expressed in years since the species' introduction (2011). Cost of invasion is a function of the travelling distance from the introduction point based on the observed rate of shift of the invaded range centroid and the predicted habitat suitability. Major cities (green pushpins) and sampling locations (white circles) are also reported.

We performed model validation with a two-step analysis, i.e. a classical accuracy assessment with a dependent set of data and a qualitative sensitivity analysis using an independent set of data. The classical accuracy analysis suggested logBAY as the best model. However, PHY indicated a moderate-to-high agreement with observed data, while MaxEnt performed poorly. All the three models predicted presence locations with high accuracy (high sensitivity). On the contrary, model specificity was relatively low for all three models. As extensively reported in the literature, absence data is the Achille's heel of SDM due to the high uncertainty linked to absence data veracity (see Hirzel et al. [2002]; Brotons et al. [2004]; Drake [2015]). This is especially true when dealing with emerging invasive arthropods, whose true absence is hard to identify (see Cianci et al. [2015]; De Clercq et al. [2015]). Therefore, to further assess the model accuracy, we decided to perform a further sensitivity analysis. MaxEnt and logBAY predicted low suitability for Maasmechelen municipality, despite this, the area has hosted a viable *Ae. koreicus* population at least since 2008 [Versteirt et al., 2012]. By contrast, PHY model predicted a moderate to high average suitability. This model, based on the construction of mechanistic overlay functions for climatic constraints, is partially independent from local datasets and thus tends to be more accurate for prediction on an independent dataset.

The percentage of the study area predicted as suitable varied from 3 to 30 %, encompassing different topographic and environmental conditions. To better characterize the predicted suitable area, we cross-tabulated it with a digital elevation model. PHY and logBAY indicated most of the low-altitude areas as highly suitable, while MaxEnt showed a peak in suitability distributed around moderate altitude (400 m). This outcome may be due to the buffer size (5 km) chosen around the presence points to derive background data, which may over-represent hilly areas, influencing the MaxEnt output. However, all three models showed a peak in suitability around 400–500 m, which may indicate optimal ecological conditions for *Ae. koreicus*. In support of this hypothesis, we noted that the trap with the highest *Ae. koreicus* abundance was located at an altitude of 451 m. Another interesting outcome is that PHY predicted as suitable areas between 600 and 1500 m. This altitudinal range represents a still empty niche for invasive *Aedes*, as 600 m is the altitudinal limit for *Ae. albopictus* distribution [Valerio et al., 2010] in Northeast Italy. As a result, the area between 600 and 1500 m suitable for *Ae. koreicus* should be particularly monitored as, here, the invasion would not be constrained by biotic interactions with species with similar evolutionary traits.

The accuracy assessment indicates PHY as the model with the highest prediction power, being in moderate-to-high agreement with observed data in the study area and predicting high suitability in a positive location with a different environmental setting. Therefore, PHY model was chosen as reference to investigate how *Ae. koreicus* may further spread in Northeast Italy. The spread analysis was achieved considering the observed dispersal rate since introduction,

the preferred dispersal pathways, study area connectivity and habitat suitability. *Aedes* species have a short flight range, with a flying dispersal capability of 200–300 m radius per week around the hatching location [Turell et al., 2005; Marini et al., 2010]. However, the short active dispersal range is generally compensated for by long distance used-tyres transportation and the plant nursery trade (*Dracaena* sp.) in the form of drought resistant eggs [Eritja et al., 2005]. The local dispersal in new invaded areas is also boosted by humans, through the movement of garden waste, moist vegetation and water containers that can hold eggs or larvae as well as dispersal in trucks transporting used tyres or private vehicle [Eritja et al., 2005; Lucientes-Curdi et al., 2014]. As a consequence, it can be inferred that the local dispersal probability in a newly invaded area is a function of the introduction point, local transportation network as well as habitat suitability. From these premises, we derived a distance-suitability weighted road network to predict which areas in Northeast Italy have the highest probability to be invaded. The results revealed how the centroid of the invaded range has been shifting approximately $8\,\mathrm{km\,yr^{-1}}$ since 2011 (putative introduction year). Assuming a constant invaded range shift and driving it along the shortest road pathway (lowest cost from the introduction point), weighted according to the suitability of each road segment, we built a potential dispersal network which represents a reliable dynamic description of the invaded area evolution in the next decades. The simulated spread predicted all the known presence locations (except one) as invaded in a time frame of 5–10 yr since its introduction. Moreover, it showed how the species may have already invaded the two major cities in the southern part of the study area, Treviso and Pordenone. However, a first investigation in July 2015 did not find positive locations in these cities [Montarsi et al., 2015b]. Furthermore, the simulated spread predicted the north part of Po Valley and the southern Adige Valley as invaded in the next decade. A favourable topography (continuous flat areas), mild climate and dense, congested road network underlie the predicted rapid spread in these parts of the study area. On the contrary, we noticed no predicted spread in the north side of the study area, apart from limited spots such as the southern Isarco and northern Adige Valleys, where temperature hotspots due to towns (Urban Heat Island) as well as high road connectivity may favour *Ae. koreicus* spread over the next years.

The simulated spread is a reliable approximation of the future expansion of *Ae. koreicus* distribution range since it integrates a validated suitability surface as well as the most likely dispersal pathways at local scale. A partial validation of the adopted spread analysis comes from a similar study on *Ae. albopictus* by [Roche et al., 2015]. The authors found that *Ae. albopictus* is currently surfing a dispersal wave in Southern France, with occasional "jumps" that did not result in new colonization fronts. However, it should be remembered that the proposed approach may underestimate the dispersal rate. This is due to the choice to consider the centroids as indication of the invaded area shift as well as the deterministic nature of our

approach which does not integrate stochastic events such as occasional introductions in spatially distant but ecologically close locations. Stochasticity in species distribution change underlies unpredictable events that sometimes strongly boost species dispersal and colonisation of new areas. Besides, in the southern part of the study area, biotic interactions and out-competition by *Ae. albopictus*, not considered in this study, may slow down *Ae. koreicus* spread [Juliano et al., 2004], modifying the outcome of the invasion process. Preliminary larval competition experiments suggested that the larval development of *Ae. koreicus* might be negatively affected by the presence of *Ae. albopictus* (Frédéric Baldacchino, personal communication).

3.6 Conclusion

Despite the rising concern about biological invasions after recent economic and human health issues due to invasive species (e.g. *Drosophila suzukii* (Matsumura, 1931) and *Xylella fastidiosa* Wells et al. [1987] as crop pests and *Ae. albopictus* as a vector of tropical pathogens; Rezza et al. [2007]; Cini et al. [2012]; Saponari et al. [2013]), at present there is no coordinated plan which aims to manage *Ae. koreicus* in the study area. Multiple control and mitigation strategies are available to eradicate, mitigate or control invasive species [Baldacchino et al., 2015]. At the beginning of an invasion, as is the case of *Ae. koreicus*, the most effective control strategy is through inspections followed by destruction of removable breeding sites (e.g. plastic drums) and treatment with larvicidae of fixed sites (e.g. concrete bins). This strategy is time consuming and might be improved in terms of cost-effectiveness by targeting the most productive breeding sites. However, there is often a limited understanding of the biology of emerging invasive species and, consequently, of the hazard they represent [Hulme, 2006]. Delays in early mitigation actions result in escalating costs of control, reduced economic returns from management actions and decreased feasibility of management [Dunn and Hatcher, 2015; Goedde, 1998; Simberloff, 2003]. iSDMs and spread pathway analysis are powerful tools to shed light on the present and future invader distribution and to inform on-ground control of the invasions [Adams et al., 2015]. We suggest that modelling and mapping the spatial distribution of invasive mosquitoes, validated by entomological surveys, should routinely support the implementation of control actions to limit their expansion. We hope that the results in this study serve as a foundation for design policies aiming to limit *Ae. koreicus* invasion in Northeast Italy.

Chapter 4

Modelling *Aedes albopictus* Skuse population and spatial dynamics in urban landscapes, an integrated approach.

Montecino, D, Marcantonio, M, Perkins, A, Barker, C, (submitted). Modelling *Aedes albopictus* Skuse population and spatial dynamics in urban landscapes, an integrated approach. Parasites & Vectors

Abstract

The Asian tiger mosquito, *Aedes albopictus*, is among the world's most invasive species. Its spread has been facilitated by rapid global transport of cargo and potentially by the warming of climate, and it is now established on every human inhabited continent except Antarctica. This species poses multiple threats to human health, being a day-biting pest, a competent vector of globally important dengue and chikungunya viruses, and a potential bridge vector of several zoonotic pathogens. As a result of its importance for public health, the biology of *Ae. albopictus* is well-studied, but the fine-scale processes by which it becomes established in a given location are poorly understood. This is because even intensive surveillance systems yield limited information during the early phase of invasions when densities are low, and detection often occurs after populations are relatively widespread. Fine-scale spatial models for mosquito dynamics and movement offer a way forward, combining our understanding of *Ae. albopictus* biology with surveillance paradigms and detailed data on the real landscapes where invasions occur. In this study we developed an integrated model where a hierarchical Bayesian framework was applied to predict suitability surfaces which, in turn, informed a stochastic dynamical/mechanistic model in order to infer population dynamics and spatial behaviour of *Ae. albopictus* across the El Monte villages in Los Angeles County. The hierarchical Bayesian/correlative model was fed using presence and absence data collected at land parcels in the study area from 2011 to 2016 as the response variable and fine resolution vegetation land cover and demographic data as predictors. The dynamical/mechanistic part consisted of a spatially explicit temperature-dependent process-based model, which was parametrised with life cycle estimates published in the scientific literature. The goal of this study was to simulate, with ecologically robust foundations, the introduction, life cycle, population and spatial dynamics of *Ae. albopictus* in a complex urban landscape using the developed integrated model. The model outputs effectively reproduced the spatio-temporal dynamics of introduced *Ae. albopictus* populations, giving insights into the mechanisms contributing to the invasion pattern in urban areas. The findings support the hypotheses that *Ae. albopictus* was actually introduced years before it was observed, resulting from a carry-over of a previous introduction which occurred in 2001. The developed model framework can be considered a valuable and flexible tool for investigating the invasion mechanisms of this species, and with further development and implementation will contribute to knowledge for operational control actions.

4.1 Background

The Asian tiger mosquito, *Aedes albopictus*, is one of the world's most invasive species, now found on every continent except Antarctica [Lowe et al., 2000]. It is a vector of pathogens that cause important human diseases, including dengue, chikungunya, Zika, West Nile, and La Crosse viruses [Mitchell et al., 1992; Turell et al., 1994; Gerhardt et al., 2001; Gratz, 2004; Hughes et al., 2006], and it has been the primary species implicated in recent dengue and chikungunya outbreaks in Hawaii and the Indian Ocean, respectively [Effler et al., 2005; Delatte et al., 2008; Rezza et al., 2007; Paupy et al., 2009]. Due to its vector competence and opportunistic feeding on a wide range of blood meal hosts [Sullivan et al., 1971; Richards et al., 2006; Valerio et al., 2010; Niebylski et al., 1994; Delatte et al., 2010], *Ae. albopictus* is also an often-suspected bridge vector capable of transmitting zoonotic arboviruses from highly competent non-human hosts to humans that may suffer from disease. Native to Southeast Asia [Gratz, 2004], *Ae. albopictus* are "container breeders" that require very little water to complete their aquatic development, which has permitted invasion of many new locations through international transport of goods and travel [Hawley, 1988]. The earliest records of *Ae. albopictus* in the continental United States were isolated introductions in used tires from Asian ports during 1946 [Pratt and Heterick, 1946]; however, this species successfully established in mainland United States in 1985 [Hawley et al., 1987]. This year *Ae. albopictus* was found to be both widespread and the most abundant container species encountered in Texas, suggesting that the species had been established for some time [Sprenger and Wuithiranyagool, 1986]. Thirty years after this introduction, this mosquito has spread to over at least 25 states and continues to expand its range in the United States northward and westward [Moore, 1999; Yee, 2008; Enserink, 2008; Rochlin et al., 2013; Kraemer et al., 2015].

In California, *Ae. albopictus* had been detected in the previous decades with brief persistence. During the second half of 1945 alive larvae and adults of this mosquito were introduced through one shipment with used military hardware returning to the port of Los Angeles, that originated in Batangas in the Philippine Islands, some 11 000 km apart. Later in April 1971 several larvae and pupae of *Ae. albopictus* were found in used tyres coming from Vietnam in a ship that arrived to the port of Oakland [Eads, 1972]. In 2001, this mosquito was discovered in Los Angeles in maritime shipments of the plant known as "Lucky Bamboo" (*Dracaena* spp.) arriving from China. Infestations were detected subsequently at 15 nursery distributors of this plant, and persisted until October 2002 [Linthicum et al., 2003]. On 14th September 2011, *Ae. albopictus* was found again in California, specifically in El Monte and later spread to South El Monte, both located in Los Angeles County [Fujioka and et al., 2012]. Populations of *Ae. albopictus* are now well-established in this area while spreading spatially at low rates [Zhong et al., 2013]. In order to mitigate the spread of this invasive mosquito at these locations,

ongoing surveillance and control response are currently conducted by the San Gabriel Valley Mosquito and Vector Control District (SGVMVC) and Greater Los Angeles Vector Control District (GLAVC), consisting mainly on public reports and door-to-door inspections.

Due to the spatial complexity and extension of the invaded area, these activities may result insufficient in responding to the invasion without information on the species population dynamics and spatial behaviour. This information can be approximated by modelling techniques which allow simulations of *Ae. albopictus* life cycle, population and spatial dynamics in the invaded range. Indeed, understanding these components may result vital for mosquito control as both a conceptual area and as quantitative approach.

Here, we developed an integrated model [Pagel and Schurr, 2012; Dormann et al., 2012] where a hierarchical logistic regression with Bayesian framework was used to model suitability surfaces which, in turn, informed a stochastic dynamical model to infer population dynamics and spatial behaviour of *Ae. albopictus* across the Real-Estate parcels (typically consisting in households and associated land) included in the study area (hereafter "parcels"). Presence and absence data collected at urban parcel level in the study area from 2011 to 2016 were used as response variable in the hierarchical model. Furthermore fine resolution vegetation land cover and demographic data were used as predictors, at parcel and block spatial scale, respectively. The dynamical/mechanistic part consisted in a spatially explicit temperature-dependent process-based model, parametrised with life cycle estimates published in the scientific literature. In this model, while feeding and laying eggs, mosquito movements occurred daily across parcels according to probabilities of staying or moving informed by: *i*) the estimated suitability surface, *ii*) distance, so that spreading to nearby parcels was more likely than to more distant ones, *iii*) size and shape of urban parcels, with small and elongated parcels more easy to leave than big and spherical-like ones.

The goal of this study was to simulate, with ecologically robust foundations, the introduction, life cycle, population and spatial dynamics of *Ae. albopictus* in an complex urban landscape using an integrated model. We hypothesise that the probability that *Ae. albopictus* successfully invade the study area, as well as its demographic and spatial dynamics, varies according to the season and development stage at the introduction. The objective of this paper is to present the model and identify the most likely time and life stage for *Ae. albopictus* introduction in the study area. We aim at showing that our model is able to catch the spatio-temporal variability of *Ae. albopictus* population dynamics in the study area.

4.2 Methods

4.2.1 The study area

The study area (Figure 4.1) included the cities of El Monte and South El Monte, two contiguous villages located in eastern Los Angeles County in Southern California (hereafter, El Monte villages) that have been foci of surveillance and detection of *Ae. albopictus* since its discovery on the 14th September 2011. The area includes a mix of residential, industrial and commercial land uses covering an area of 32.48 km^2 with a population of 134 462 people [Bureau, 2014]. The climate is mild, with daily low/high temperatures that vary from a daily mean of 14.7 °C in January to 24.2 °C in August with a mean precipitation of 374 $mm\,yr^{-1}$ concentrated in the cooler half of the year (1981-2010 normals, Anaheim weather station; 33.82°N, 117.92°E).

The study area was subdivided into census blocks [Bureau, 2014] and parcels within each block. Parcels were delineated by spatial data obtained from the Los Angeles County Assessor's office as of 2012. The cadastral and block spatial data were obtained as vector ESRI shapefile map. The cadastral map presented several overlapping polygons, therefore it was simplified by snapping boundaries with a threshold of 1 m using GRASS GIS v7 [Neteler et al., 2012]. After the simplification, the total number of parcels was reduced to 24 547.

4.2.2 Data sources and dataset construction

The SGVMVC and GLAVC are the agencies which manage *Ae. albopictus* surveillance activities within the study area. Their tasks include setting traps in domestic properties open areas, and sampling water containers present in these sites, such as: buckets, bottles, pools, pond, pots, tires and others. We used data from the surveillance activities obtained between the 11th September 2011 and the 25th April 2016. During this period, 2 type of traps were mainly used: Biogents-Sentinel® Professional Mosquito trap (Biogents AG, Germany) and ovitraps. Household addresses present in the surveillance records were geocoded using Google API and OpenStreetMap Nominatim https://nominatim.openstreetmap.org/, in order to assign them geographical coordinates. Those addresses geocoded with accuracy different than parcel level were checked for misspelling and corrected, or visually characterised using other address locator (yahoo map) in order to be identified in Google Earth 6.2.2.6613 and to record the corresponding coordinates. Those addresses still not geocoded at the parcel level were assigned to the nearest parcels in Euclidean space. The resulting dataset had 48 247 observations (6028 presence and 42 219 absence) in a total of 1128 parcels grouped in 461 blocks (Figure 4.1).

Spectral band 1 (red) and 4 (near-infrared) were obtained as raster files from the Digital Orthophoto Quarter Quads (DOQQ) of the study area (1 m spatial resolution) generated by the

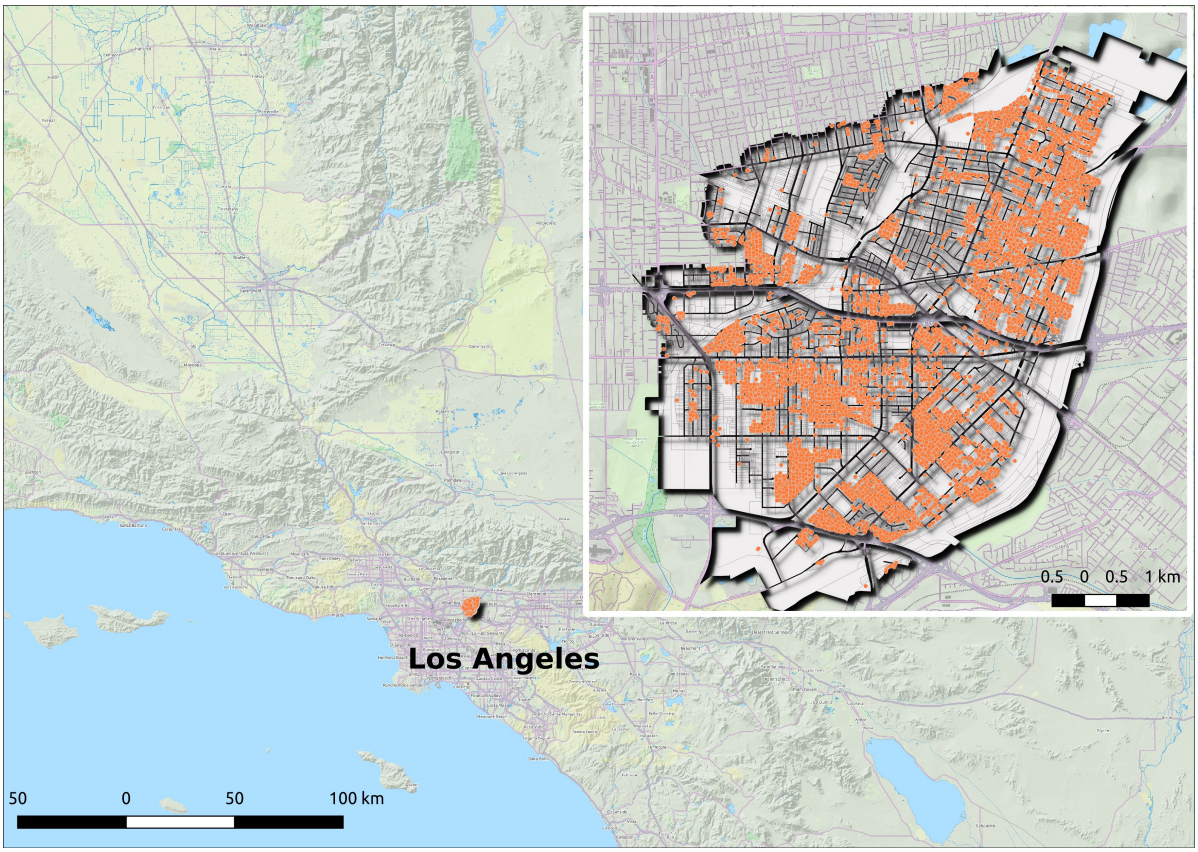

Figure 4.1: Study area (©OpenStreetMap). The map inset on the right highlights El Monte and South El Monte boundaries, with their road network. The orange points represent the 48 247 *Ae. albopictus* presence/absence observations collected between 2011 and 2016.

National Agriculture Imagery Program (NAIP 2014). We used these raster files to construct a 1 m spatial resolution Normalised Difference Vegetation Index (NDVI) raster map following Rouse [1974]. The NDVI is a numerical indicator of the biomass of live green vegetation that theoretically ranges $-1{,}1$, with healthy plants typically having values greater than 0.5 and non-vegetation classes, such as water or barren surface, having 0 or negative values. The NAIP data is acquired during the agricultural growing seasons in the continental United States (May), therefore, high NDVI values in an urban area in Mediterranean climate region correspond to irrigated areas that remains relatively constant throughout the year. Land cover data and land cover imperviousness data, were obtained from the 2011 National Land Cover Database (NLCD) [Homer et al., 2015] and the 2011 Percent Developed Imperviousness data (PDI) [Xian et al., 2011], respectively. The first one is a 16-class land cover classification scheme, but, based on *Ae. albopictus* behaviour, only those categories related with human settlements: 21, 22, 23, 24 and 71 were considered in the suitability modelling. Due the urban environment of the study area, categories 71 (Grassland, Herbaceous) and 21 (Developed, Open Space) were

assumed equal in terms of the study objective and merged when both present in a block. The PDI provides nationally consistent estimates of the amount of man-made impervious surfaces, such as roads, roofs and other paved features, present over a given area in a seamless form. Imperviousness values ranges from 0 to 100 %.

In order to assign raster values to the corresponding parcels under surveillance, we used the "r.mapcalc" tool in GRASS GIS 7 in combination with the "raster" [Hijmans, 2016] and "maptools" [Bivand and Lewin-Koh, 2016] packages in R 3.2.2 [R Core Team, 2015]. Demographic characteristics by blocks were obtained from the census TIGER data [Bureau, 2014]. Daily temperature data (Figure 4.2) was used to fit several parameters of *Ae. albopictus* life cycle. In order to have an accurate representation of the spatio-temporal temperature trend in the last years in the study area, we made use of air temperature recorded by the National Climatic Data Center weather station of Monrovia (daily time series; 34.14°N, −117.98°E) about 9 km away from the centroid of the study area.

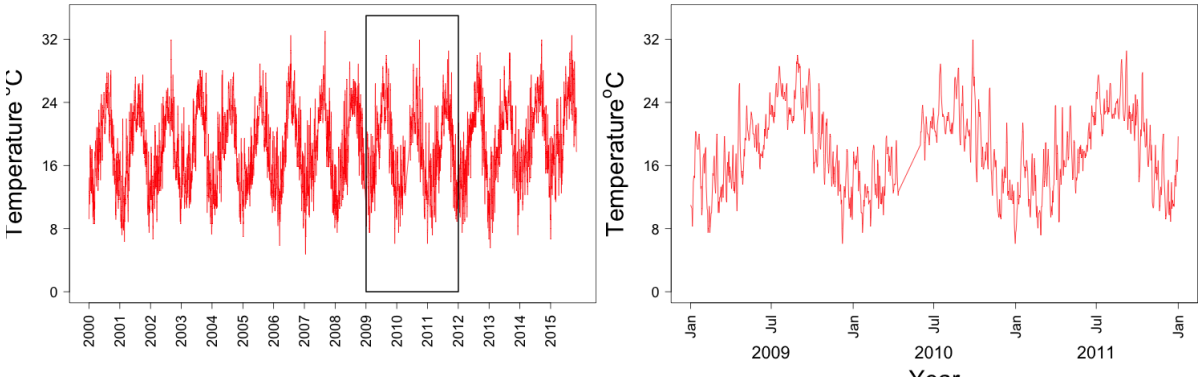

Figure 4.2: Daily average temperature time series from Monrovia weather station. The long time series was reported on the left, while a zoom in on the study period on the right.

4.2.3 The integrated model

A two-step integrated model to simulate the spread of *Ae. albopictus* was developed (Figure 4.3). A hierarchical logistic regression with Bayesian inference, to capture the heterogeneity in the probability of mosquito presence (hereafter, "SM") in each parcel, was used to inform a process based dynamical/mechanistic model (hereafter "MM") aiming at simulating mosquito population and spatial dynamics across the study area.

The hierarchical correlative model

The correlative model was constructed to define a realistic surface for *Ae. albopictus* spatial dynamics, associated with mosquito collection data since the initial detection. We estimated

suitability values for each parcel in Elmonte villages by modelling the probability of its presence, in any developmental stage, making use of all the observations i within parcel j within block k, through a hierarchical model of the form:

$$y_{jk} \sim Binomial(n_{jk}, p_{jk}) \tag{4.1}$$

The probability p_{jk} of *Ae. albopictus* presence in parcel j within block k, was related to a suite of fixed predictors x at the j parcel level.

$$logit(p_{jk}) = a_{jk} \tag{4.2}$$

where:

$\alpha_{jk} \sim Normal(a_k + bx_j, \sigma_{parcel})$
$\alpha_k \sim Normal(a_0 + bx_k, \sigma_{block})$

While α_k are random intercepts for parcel j belonging to block k, with fixed predictors measured in the k^{th} block. The fixed effects considered for model selection were maximum, mean and median NDVI values at the j^{th} parcel, demographic characteristics, mean PDI raster values, and the proportion of NLCD land use type at block k. We expected these fixed predictors to be representative for the spatial variability in artificial breeding habitats and vegetation settings appropriate for *Aedes* life cycle activities such as oviposition, food availability and resting sites in the study area.

Non-informative priors and hyperpriors were assigned for all the b's $[Normal(0, 25)]$, and σ's $[LogNormal(0, 1)]$. Models were fitted in JAGS version 4.0.0 [Plummer, 2003] using the "runjags" package [Plummer, 2015] in R 3.2.2 [R Core Team, 2015]. We scaled and centred the predictor variables in order to improve the efficiency of the MCMC process. Posterior probability distributions (PPDs) for all parameters were sampled from each of six chains for 10 000 Markov Chain Monte Carlo (MCMC) iterations following a 10 000 burn-in and 1000 adaptation iterations, with thinning set to 5, for a total of 60 000 samples. Each chain was assigned random start values from a Normal (0, 1) distribution for b's and a Uniform (0, 1) for σ's. Convergence was assessed by the Gelman-Rubin statistic [Gelman and Rubin, 1992]. Model selection was based on the deviance information criterion (DIC) [Spiegelhalter et al., 2002], and biological considerations. Regression parameters with 95 % credible intervals (CIs) that excluded 0 were considered to be credible.

Secondly, we used the best model (in terms of DIC and biological considerations) to estimate the probability distribution for *Ae. albopictus* presence in each of the 24 196 parcels. The predictive model was run using five chains for 2000 MCMC iterations following a 1000 burn-in and 1000 adaptation iterations, with thinning set to 5, for a total of 4000 samples.

Random draws from the posterior distributions for *Ae. albopictus* presence were then used to inform the mechanistic model about the environmental suitability of each parcel in the study area, s_i (see below).

The mechanistic model

The MM was built to simulate *Ae. albopictus* life cycle, population and spatial dynamics in a real urban landscape which suitability was informed by the SM. We used days (t) and parcels (i) as fundamental temporal and spatial units, respectively.

Aedes albopictus life stages are: egg, four larval instars, pupae, and adult [Hawley, 1988]. In the MM, we reduced the life cycle complexity, while retaining realistic development, by combining larval and pupal stages into a single immature stage (L) between egg (E) and adult (F) stages, resulting in a three-stage model. We considered only adult females (excluding males; hereafter reported simply as "adults") assuming that mating does not limit population dynamics. Indeed, F alternately fed and laid eggs at rates defined from literature, while daily "choosing" to stay within a parcel or moving into a neighbour one. If they moved from the current parcel, they "decided" their destination according to the distance between the origin parcel and its neighbour parcels, the suitability, shape and size of the neighbour parcels, s_i. Each MM simulation was initialised with a different suitability surface across the study area by randomly sampling the posterior distributions for *Ae. albopictus* presence in each parcel obtained from the correlative model. This step was implemented to account for the uncertainty linked with the estimated suitability surface when modelling *Ae. albopictus* population dynamics and spatial behaviour.

***Aedes albopictus* life cycle and population dynamics** As previously mentioned, the MM considered 3 life stages: E, L, and F. The first 2 were restricted to the parcel harbouring the container where E were laid. Within a specific parcel i, the amount of E at day t depended on the number eggs laid by F during day $t-1$, E that survived day $t-1$, and E that hatched in day $t-1$. Within a specific parcel i, the number of L at day t depends on E that hatched at day $t-1$, L that survived day $t-1$, and L that developed to F during day $t-1$. On the contrary, F were not restricted to specific parcels and their number in the i^th parcel at day t depended on F that survived day $t-1$ and stayed in parcel i, the number of F located in the i' neighbour parcel that survived day $t-1$ and moved into parcel i, and L that develop to F in the i^th parcel during day $t-1$.

Once E were laid by each F according to a Poisson$\sim$(40) [Hawley, 1988], they were subject to a daily mortality rate (μE_t) randomly drawn from a beta distribution, parametrised using epiR package [Nunes et al., 2016] in R 3.2.2 [R Core Team, 2015] with mode = 0.95, and 95 % confidence that $\mu\ E_t > 0.5$, accounting for the variability reported in literature [Hawley, 1988;

Delatte et al., 2010]. The waiting time between oviposition to hatching (W_{ELt}) was randomly drawn every day from a gamma distribution parametrised with shape $\alpha = 1.2$ and rate $\beta = 0.1$, implying a mean = 12, mode = 2, and standard deviation = 10.95. We chose this distribution to allow for a very broad range of oviposition-to-hatching time due to the ephemeral nature of hatching niches in Mediterranean climate urban environments, as this process is a function of a complex and often unknown interplay of factors such as flooding, age, desiccation, temperature changes and oxygen tension [Hawley, 1988]. Values of $W_{ELt} < 2$ are unlikely, thus we set 2, the minimum number of days for eggs to hatch found in the laboratory, as the lower threshold for W_{ELt} [Hawley, 1988].

L emerged in a 1 : 1 gender ratio; however, as mentioned previously, we only tracked the females. The L stage developed to F according to the temperature-dependent rate for aquatic immature development $1/W_{LF}(T)$, where $W_{LF}(T)$ is the daily typical aquatic immature development time from L to F. This daily rate was derived by firstly estimating the parameter values of the temperature-dependent enzyme kinetic function described by Sharpe and DeMichele [1977], using previous results on *Ae. albopictus* temperature-dependent development [Delatte et al., 2010] and an optimisation method proposed by Nelder and Mead [1965]; and secondly, using daily T values in the parametrised function. Also, the L stage was subject to a daily mortality rate ($\mu\ L_t$), which was the sum of the density independent larval mortality rate during day t ($-log(1-\mu\ di_L)$) and the density dependent larval mortality rate in parcel i during day t ($\mu\ dd_{Lit}$). The $\mu\ diLt$, the daily independent larval mortality probability, was set as a random draw from a beta distribution parametrised with mode = 0.92 and 95 % confidence that $\mu\ diLt > 0.5$ [Hawley, 1988; Delatte et al., 2010], while:

$$\mu\ dd_{Lit} = (EL_{it} - (-(log(1-\mu\ di_{Lt})) + W_{LF}(T)^{-1}) \times K) \times K^{-2} \tag{4.3}$$

where:

EL_{it-1}= the eggs at parcel i that hatch during day $t-1$.
K = the carrying capacity for L at the parcel level defined as 40, based on expert opinion.

For mosquitoes, it is likely that density dependent effects, if occur, act on or originate with larvae [Gilpin and McClelland, 1979]. Its regulation effect at immature stages appears to be most common in mosquitoes from container or highly ephemeral habitat [Juliano, 2007], such as *Ae. albopictus*.

Finally, the F stage laid eggs according to a temperature-dependent rate of gonotrophic development $1/Gp(T)$, derived as $1/W_{LF}(T)$. Moreover, this stage was subject to a temperature-dependent daily mortality probability ($\mu_F(T)$). We used laboratory temperature-dependent

survival data (from Armijos [2016]) to fit a parametric survival regression using T and T^2 as predictors (°C and $°C^2$, respectively) in order to estimate the temperature-dependent laboratory-based adult *Ae. albopictus* daily mortality rate $\lambda_{LAB}(T)$. Once this rate was converted to a survival probability as $exp(-\lambda_{LAB}(T))$, (hereafter, $(1-\mu_{LAB})(T)$, we subtracted a randomly selected value from a beta distribution parametrised as previously, with mode = 0.06 and 95 % confidence that it is less than 0.15. The result of this subtraction represents the field daily mortality probability (μ_{FIELDt}) that includes the combined action of natural enemies and other factors with inherent variability [Brady et al., 2013]. Therefore, the temperature dependent survival probability for females, $(1-\mu_F)(T)$, was $(1-\mu_{LAB})(T)-\mu_{FIELDt}$.

***Aedes albopictus* spatial dynamics** F were not restricted to specific parcels but they could "decide" to stay in the current parcel or move into a neighbour parcel according to st_i, the probability to stay in the i^th parcel.

$$sti = s_i \times sai_i^{0.5} \times a_i \tag{4.4}$$

where:

s_i = the suitability per parcel informed by the SM.
sai_i = the Shape Area Index of the i^th parcel [McGarigal and Marks, 1995]

As a result, parcels with an elongated shape are easier to leave than parcels with a globular shape (but to avoid overweighting of very elongated parcels we squared root the sai_i value); and a_i is a negative weight for those parcels with area larger or equal than the 97.5 quantile of parcel area distribution. Specifically, $a_i = 1$ or 0.75 depending on $parcelarea \geq 97.5$ of the parcel area distribution quantile or not (regardless their suitability, very large parcels are relatively more difficult to leave than smaller ones).

To establish the parcel of destination for those F_{it} that chose to move, we defined: *a)* the set of i' neighbour parcels for each parcel i by determining the maximum daily distance (max_d) an adult *Ae. albopictus* can fly daily, *b)* the vector of distances between the parcel of origin and the i' neighbour parcels (**dii'**), *c)* the parameter for an exponential decay in probability with respect to distance (λ_D), and the distance from the origin that a mosquito has equivalent probability to fly daily (d_e). We used a preliminary MM to simulate the introduction of 200 sterile adults in a random parcel and track their spread within a week, assuming that the landscape suitability was uniformly distributed at 1. We ran 1000 iterations for different combinations of max_d, λ and d_e values, and chose those that better reproduced the results reported in [Marini et al., 2010]. Moreover, we built a "synthetic" urban landscape made by 2 groups of 6 parcels divided by

a 130 m width flight barrier (i.e. highway), and released 50 females for 1000 iterations and recorded the number of times they crossed the highway after 1 d. With the results of these iterations we checked that the chosen λ value gave a reliable rate of F (i.e. very low) crossing this urban barrier over time.

With the chosen values we established the vectors of inverse weighted distances from parcel i to the corresponding set of i' neighbour parcels: $\mathbf{invd_{ii'}} = \mathbf{d_{ii'}}^{-\lambda}$, with equivalent $\mathbf{invd_{ii'}}$ for $\mathbf{d_{ii'}}$ when $0 \leq d_{ii'} \leq d_e$. These vectors, together with the s_i, the vector of suitability values of the i' neighbour parcels of parcel i, probabilistically informed the destination parcel of those F_{it} leaving the $i^t h$ parcel as,

$$\theta_{\mathbf{ii'}} = \frac{s_{i'} \times invd_{ii'}}{sum_{(s_{i'} \times \mathbf{invd_{ii'}})}} \tag{4.5}$$

where:

$\theta_{\mathbf{ii'}}$ = the vector per parcel i containing the probabilities to move to the i' neighbour parcel.
$s_{i'}$ = suitability of the i' neighbour parcel
$inv_{dii'}$ = the inverse weighted distance from parcel i to the i' neighbour

Therefore, the destination of F_{it} leaving parcel i was defined by a multinomial trial parametrised by F_{it} and $\theta_{ii'}$. As a consequence, while feeding and laying eggs, mosquitoes moved across parcels according to the probabilities of staying or moving to the neighbour parcels. The E_{it}, L_{it}, and F_{it} were defined stochastically by the addition or subtraction of random draws from appropriate discrete distributions:

$$E_{it} = Es_{it-1} + \sum_{FEit-1=1}^{FE_{it-1}} EL_{fe} \tag{4.6}$$

where:

ES_{it-1} = the eggs that survived time $t-1$ in parcel i defined as $Es_{it-1} \sim Bin(n,p)$
n = $E_{it-1} - EL_{it-1}$
p = $1 - exp(-(W_{ELt^{-1}}))$
$\sum_{FEit-1=1}^{FE_{it-1}} El_{fe}$= the summation of all eggs laid by each female that laid eggs in parcel i in time *t-1*
EL_{fe} $\sim P\lambda_E$
λ_E = 40
FE_{it-1} $\sim Bin(n,p)$
n = F_{it-1} (adults alive at $t-1$)

p $= 1 - e^{-G_p(T)}$ (the daily probability to lay eggs)

$$L_{it} = L_{it-1} - LF_{it-1} - Ld_{it-1} + EL_{it-1} \tag{4.7}$$

where:

L_{it-1} = the larvae from the previous day in parcel i
$LF_{it-1} \sim Bin(n,p)$
n $= L_{it-1}$
p $= 1 - exp(-(1/W_{LF}(T)))$
Ld_{it-1}= the larvae that did not survived at $t-1$ in parcel i, defined as $Ld_{it-1} \sim Bin(n,p)$
n $= L_{it-1} - LF_{it-1}$
p $= \mu_{Lt}$

$$F_{it} = LF_{it-1} + Fst_{it-1} + \sum_{i'=1}^{I'} Fmi_{i'it-1} \tag{4.8}$$

where:

Fst_{it-1} = the adults that survived the $t-1$, staying in their current parcel, defined as $Fst_{it-1} \sim Bin(n,p)$
n $= Fs_{it-1}$
p $= st_i$
Fmi_{it-1}= the adults at $t-1$ in parcel i that survived defined as $Fmi_{it-1} \sim Bin(n,p)$
n $= F_{it-1}$
p $= (1-\mu_F)(T)$

The last term of Equation 4.8 refers to the adults coming from the set of neighbour parcels of parcel i. $Fmi_{i'it-1}$ are the adults from parcel i' coming into parcel i in day $t-1$.

These sets of adult mosquitoes were defined by multinomial trial processes having as subject those adults from the neighbour parcels that survived the previous day but chose not to stay in their current parcel. As a consequence of this probabilistic sampling, every day a subset of adults from each i' neighbour parcel "chose" to move to parcel i. As an example, if we are interested in the adults from a single parcel i' moving into, specifically, parcel i, then $Fmi_{i'it-1} \sim Bin(n,p)$, where $n = Fs_{i't-1} - Fst_{i't-1}$ and $p = \theta_{i'i}$, or the corresponding probability value to move from the i' parcel into the i^{th} parcel. This probability is contained in the vector of probabilities for the i' parcel to move to its neighbour parcels $\theta_{i'i''}$. A comprehensive summary of the parameters defining the biological cycle and the movement of *Ae. albopictus* adults in the study area is given in Appendix E, while a schematic representation of the model is given in Figure 4.3.

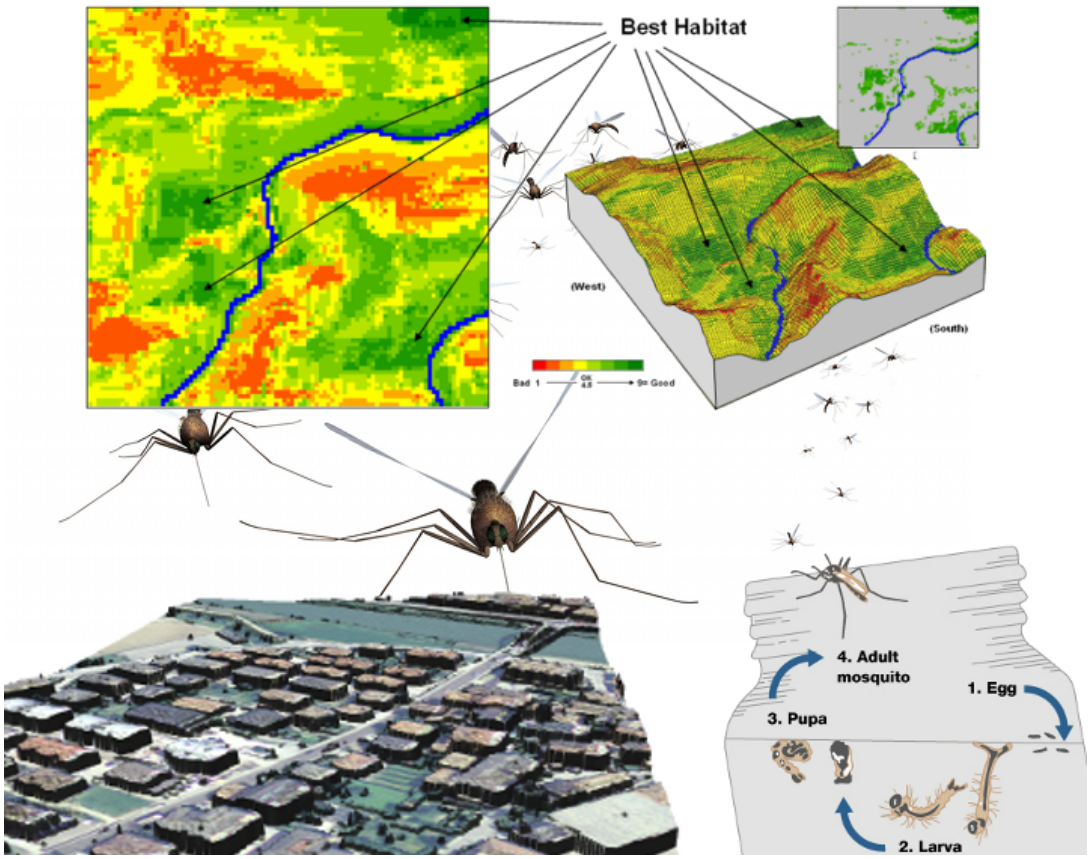

Figure 4.3: Graphical representation of the theoretical model structure. On the top row, the suitability surface is modelled through correlative approaches. On the bottom row, *Ae. albopictus* life cycle and movement are simulated across an urban landscape through a population dynamics model. (Images composite from Berry [2007], Shutterstock/Linda Bucklin and Nature Education) (http://www.nature.com/scitable/topicpage/dengue-transmission-22399758))

In order to evaluate the likelihood of successful invasion and the spread of *Ae. albopictus* in the study area, we introduced 40 eggs, or 25 larvae or 2 adults, and tracked the population every 1 week until the end of the following winter equinox since introduction (21st March 2011). Moreover, to evaluate the effect of the season of introduction in the likelihood of invasion, we repeated the introduction of each *Aedes* propagule at seasonal midpoints (winter = Feb 5, spring = May 5, summer = Aug 5, and fall = Nov 5) for a total of 12 introduction scenarios (3 stages times 4 seasons). We also estimated seasonal variations in the typical (median) and maximal ranges of *Ae. albopictus* movement since introduction and speed of spread. Given the stochastic nature of the model, each scenario was simulated 1000 times. To made this number of simulations possible, we coded the theoretical model as a parallelised R function using foreach [Analytics and Weston, 2015], doSNOW [Revolution Analytics and Weston, 2015], Rmpi [Yu, 2002], Matrix [Bates and Maechler, 2016] and parallelize.dynamic [Boehringer, 2013] R packages. We run the simulations on a 24 cores cluster computer, running time spanned from 5 to 15 h for different simulations.

We considered an introduction as successful only if, at the end of the following winter equinox since introduction (21st March 2011), there was at least one egg, larva or adult alive in the study area.

4.3 Results

4.3.1 The hierarchical Bayesian/correlative model

Results from the correlative modelling showed that the Bayesian hierarchical logistic regression with maximum NDVI (at parcel level) and NLCD 24 category (at block level) as the only fixed predictors, had the lowest DIC. The 3 MCMC chains for this model converged (Multivariate Gelman diagnostic = 1.01), therefore they can be assumed representative of the model parameter PPDs. The correlation between PPDs was low (Pearson's $r < 0.4$). Models containing housing by hectare, population by hectare, and imperviousness as only fixed predictors, increased the DIC and had parameter estimates close to zero. The mean and 95 % Credible Interval (CrI) of the PPDs from the best model are shown in Table 4.1.

The negative intercept α_0 revealed that when the predictors (that were centred) were at their average value *Ae. albopictus* probability of presence was near 0. The estimated NLCD 24 coefficient was negatively associated with the odds of *Ae. albopictus* presence. Those parcels in a block with only NLCD 24 category had a probability 0.03 times lower to host *Ae. albopictus* compared to those parcels located at blocks with a NLCD 24 proportion of zero. The mean of the PPD of standardised maximum NDVI showed that those parcels containing at least one

Table 4.1: Mean and 95 % CrI of the hierarchical logistic regression parameter PPDs

Parameter	**Mean**	**95 % CrI**
Maximum NDVI	0.50	0.41, 0.59
NLCD 24	−0.26	−0.44, −0.08
σ_{parcel}	3.22	2.87, 3.64
σ_{block}	2.22	1.84, 2.77
α_0	−5.01	−4.80, −5.25

cell with NDVI equal 1 had a probability 0.47 higher to host *Ae. albopictus* compared with parcels that contained the lowest NDVI value relatively to the study area (−0.150; with NLCD 24 proportion held constant at its average value, 0.21).

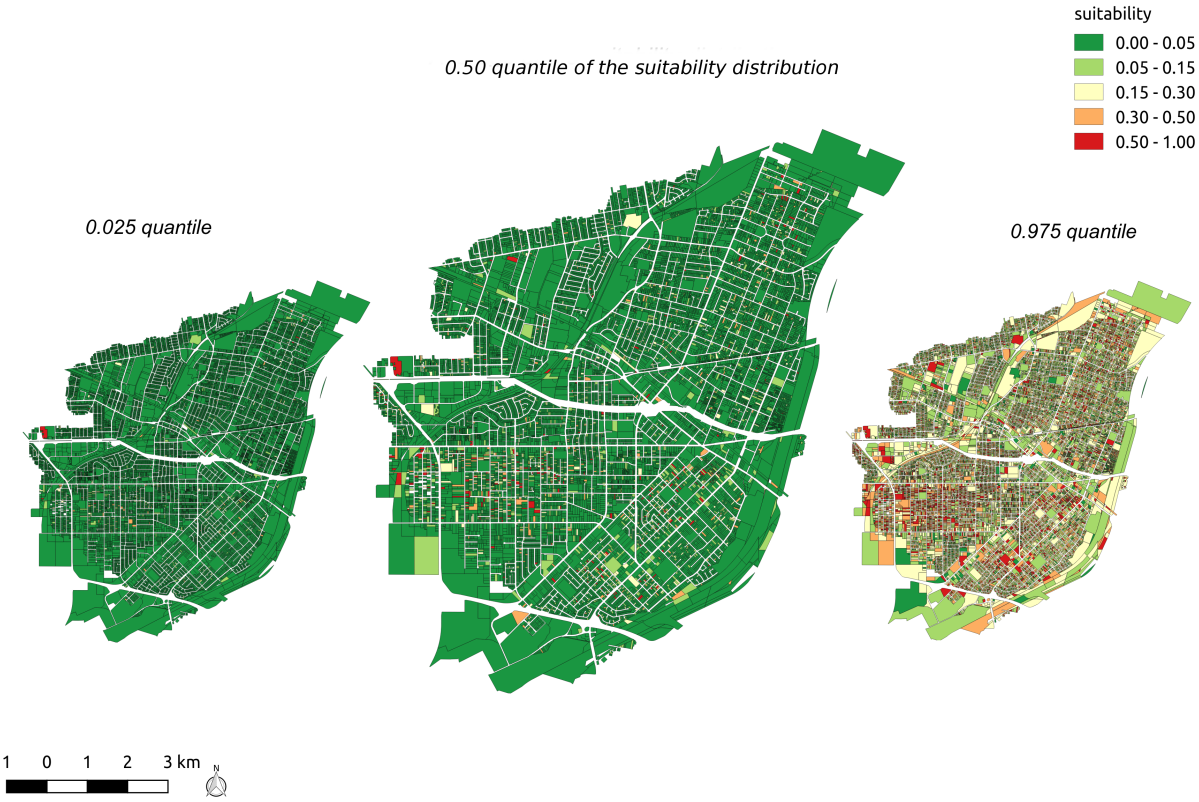

Figure 4.4: *Ae. albopictus* suitability for each real estate parcel in El Monte villages. We reported the 2.5 (left), 50 (centre) and 97.5 % (right) quantile of the suitability PPD.

The PPD for the standard deviation of block random intercepts σ_{block} and the standard deviation of parcels σ_{parcel} were not credibly different from zero but with an effect size bigger

for parcels than block intercepts. The variability among parcels within and among blocks for one realisation of the s_i's distributions is shown in Figure 4.4. This figure shows that the median probability of presence in the study area is generally low, with a low number of parcels highly suitable for *Ae. albopictus*, but with wide 95 % interquartile range of values.

4.3.2 The mechanistic model

Gonotrophic period and immature development period as a function of temperature

Parameter values obtained for $1/Gp(T)$ function were: $RHO25 = 0.201$, $HA = 14792.5$, $HH = 105759.7$ and $TH = 34.88$; while for $1/W_{LF}(T)$ function were: $RHO25 = 0.091$, $HA = 13601.05$, $HH = 91171.43$, and $TH = 34.17$. As a result, the expected $1/Gp(T)$ and $1/W_{LF}(T)$ decreased with higher temperatures until 30 °C inverting to at this point to longer periods. Similar results were obtained for daily larval survival. The mean daily temperature for the study area in the considered period (5th February 2010–21st March 2011) ranged from 6.1 °C to 30.0 °C, with a mean of 17.7 °C. Therefore, $W_{LF}(T)$ ranged from 8.33 d in warmer periods to 25.2 d during the colder season. Similarly, $Gp(T)$ ranged from 3.4 to 12.3 d, while the percentage of larvae surviving a day varied from 89 % – 96 % during the warm and cold seasons respectively (Figure 4.5).

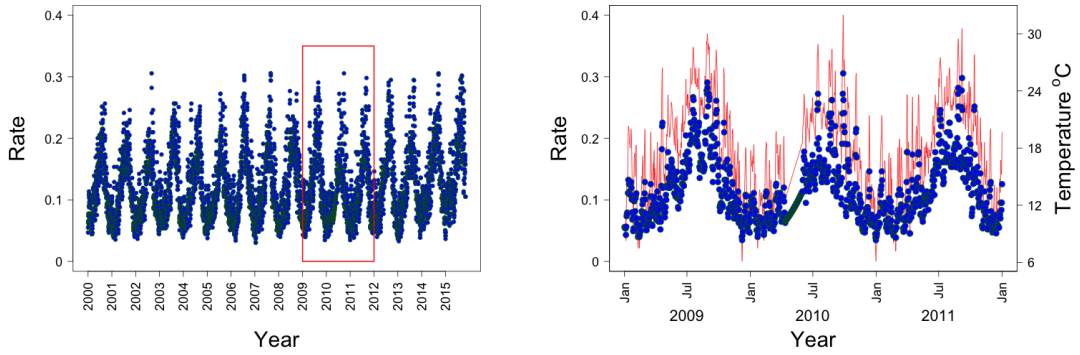

(a) Gonotrophic rate.

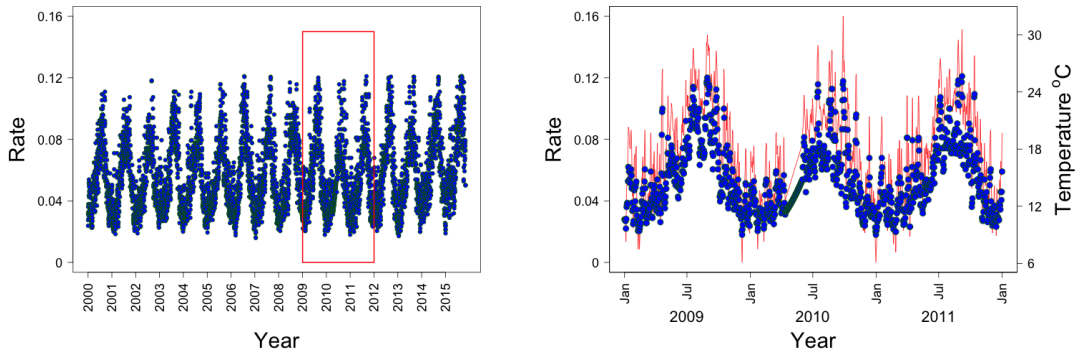

(b) Immature development rate.

Figure 4.5: Temporal trend for two life cycle rates estimated using the daily average temperature from the study area. *a)* gonotrophic rate and *b)* immature development rate, estimated for (left) the long term temperature series and (right) for the period considered in this study.

Distance to define neighbour parcels and probabilities to move from parcel *i*

The values that most closely reproduced the mark-recapture results [Marini et al., 2010] were 200 m for the maximum daily distance an adult female can fly, 6 for the λ_D parameter, and 20 m for the maximum distance having an equal probability of flight. The number of neighbours for each parcel within the 200 m were mainly between 100–200, with few parcels having over 300 neighbours. Considering the 1000 iterations run to tune the λ_D parameters, when set it at a value of 6, the mean distance reached at seventh day since introduction was 79.2 m, while the mean maximum distance was 302.7 m at this day. Besides, the probability of crossing a flight obstacle representing an highway was lower than 0.005.

Survival regression

The estimated coefficients for the intercept, and the predictors T and T^2 were 1.622, 0.209 and -0.005, respectively. The statistical test for this model reported a chi-square $= 31.66$ with 2 d.f. resulting in $p < 0.01$, meaning that the predictors informed the laboratory-based adult daily mortality rate ($\lambda_{LAB}(T)$) significantly at $\alpha = 0.05$. The estimated $1 - (\lambda_{LAB}(T))$ are presented in Figure 4.6.

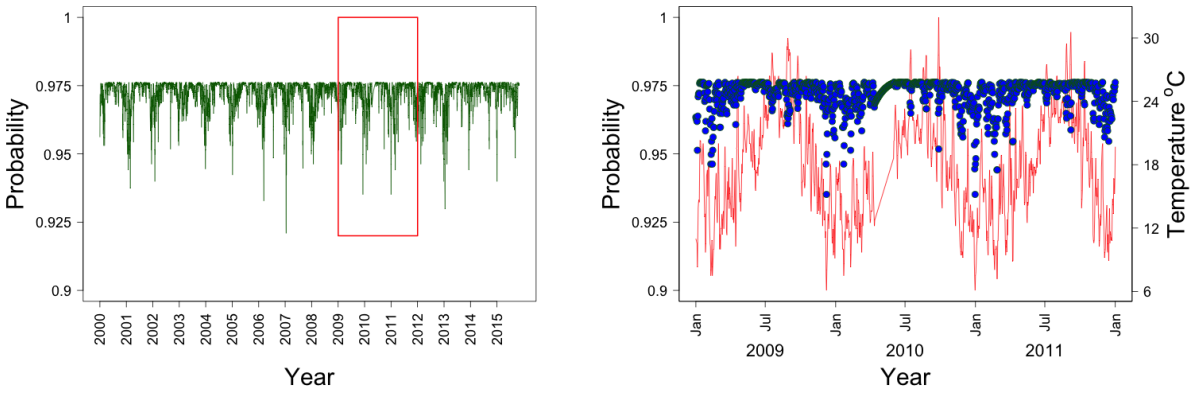

Figure 4.6: Temperature dependent laboratory-based adult *Ae. albopictus* daily survival probability estimated using the daily average temperature time series from the study area. On the left the long term daily survival probability temporal trend is reported, while on the right the daily adult survival probability for the period of interest is superimposed to the temperature time series.

Mosquito population dynamics

The simulations showed variability in *Ae. albopictus* invasion dynamics. Nevertheless, ecologically meaningful invasion patterns were evident. The extinction probability after introduction varied importantly by scenario. In general, *Ae. albopictus* introductions in autumn and winter had an extinction probability higher than 0.9, and over 0.8 for eggs and larvae introduced

Table 4.2: *Aedes albopictus* extinction probability for each simulated introduction scenario. The considered period to assess the extinction probability across simulations was the time span from introduction in the middle of each season to the end of the following Winter (March 21st).

Season of Introduction	**Stage Introduced**		
	Eggs	Larvae	Adults
Winter (60 weeks)	0.926	0.957	0.970
Spring (48 weeks)	0.833	0.995	0.417
Summer (35 weeks)	0.817	0.038	0.225
Autumn (21 weeks)	0.998	0.990	0.982

in spring. The lowest extinction probability was obtained for larvae and adults introduced during summer (0.04 and 0.23) and adults introduced in spring (0.42; Table 4.2). Results presented hereafter are based on the subset of simulations per scenario where *Ae. albopictus* was not extinct (in at least one stage) at the end of the corresponding observation period (see the methods section for more details on how we defined a successful invasion).

The simulated mosquito populations showed variable dynamics for different introduction scenarios (Figure 4.7). As expected, mosquito population density at the parcel level was higher for every scenario during or just after summer. The trends in population density underlies an interaction effect among the life stage introduced and the season of introduction, except for autumn. In this season indeed, regardless the introduced life stage, all the introductions generated very low densities. On the other hand, the introduction of eggs during winter generated the highest density value (peak of $\sim$60 eggs/parcel), while introduction of larvae and adults in this season generated much lower densities, but still the largest ones for these stages across all scenarios. Introductions in spring generated higher densities when adults were introduced in the system causing the second largest densities for all stages across all scenarios, but were unfavourable when larvae were introduced. Introduction in summer had similar densities when larvae or adults were introduced, but lower densities when eggs were introduced. All the stages, when introduced in summer, generated lower population densities compared to adults in spring or eggs in winter. All introductions in winter generated very low densities for all stages independently of the stage initially introduced. Importantly, all scenarios showed very low average population density at the parcel level by the end of the next winter.

Interesting to note is the time passed between the introduction event and the beginning of apparent population growth in summer. When not extinct, the mosquito populations introduced

Table 4.3: The mean and maximum (in brackets) rate of new parcels invaded per week for each simulated introduction scenario. The considered period to assess invasion rate across simulations was the time span from introduction in the middle of each season and the end of the following Winter (March 21st).

Season of Introduction	**Stage Introduced**		
	Eggs	Larvae	Adults
Winter (60 weeks)	2.4 (70.6)	0.3 (14.2)	0.4 (20.1)
Spring (48 weeks)	0.3 (15.0)	0.0 (0.5)	0.4 (15.5)
Summer (35 weeks)	0.1 (10.4)	3.4 (36.8)	0.7 (23.2)
Autumn (21 weeks)	0.0 (0.2)	0.0 (0.5)	0.0 (0.6)

in winter and spring could persist at very low density for a long period (20-25 weeks for winter). This time span decreased to 5 weeks in summer.

The introduction season heavily affected the number of new invaded parcels per week (Table 4.3). When considering the rate of new invaded parcels per week across all simulations, the introduction of eggs in winter brought about the highest maximum rate (70.6 parcels/week) and the second highest median rate. When adults were introduced in this season, it caused the second highest maximum rate for this life stage. Scenarios in spring were favourable in terms of new parcels invaded per week when eggs were introduced (second most successful scenario, in terms of median and maximum new parcels invaded). Summer introductions showed the highest median rate, with the second highest median and maximum rates across all scenarios when larvae were introduced. When adults were introduced, the summer season was the most favourable in terms of the median and maximum number of new parcels invaded per week. On the other hand, autumn introductions had the lowest rate across all the investigated life stages. Comparing the introduction of different stages, the advantage of one stage over the others was dependent on the season of introduction, with eggs favoured in winter, adults in spring and larvae in summer (Table 4.3).

Figure 9 reports the temporal trend of low, median and high quantiles of the distribution of the distances weekly travelled by adults *Ae. albopictus* for each introduction scenario. After a rapid initial dispersal in the first month, the median dispersal pattern across the urban landscape slowed down. The spread distance was similar when eggs were introduced in winter, spring

or summer, dispersing in median about 400 m by week 20. A similar pattern was found for population begun from larvae or adults. However, for the autumn introduction scenarios, the median spread showed unstable patterns with a marked reduction by the end of the 20th week, except when adults were introduced. Comparable results were observed when considering the 97.5 % quantile of the spread distance by the 20th week (Figure 4.8). The distance spread weekly reported in Figure 4.9 revealed that when mosquitoes did not vanish, the median weekly spread was not markedly different between introduction scenarios (about 10 m week^{-1}), just somewhat higher for eggs introduced in winter and larvae introduced in summer, consistent with results shown in Table 4.2. However, when considering the most mobile fraction of the mosquito population (the 97.5 % quantile), the introduction of eggs in winter, and larvae and adults in summer, caused the highest values (about 30 m week^{-1}). For the remaining scenarios, this value was about 15 m week^{-1} (Figure 4.9).

4.4 Discussion

In this project we combined remotely sensed, weather station, literature, field and laboratory data in an integrated modelling framework [Dormann et al., 2012] to simulate *Ae. albopictus* population and spatial dynamics. We aimed at presenting the developed model by using it to better describe the fine scale *Ae. albopictus* invasion dynamics in an urban area (El Monte villages) where *Ae. albopictus* was found in September 2011, and which is at risk of *Aedes*-borne pathogens transmission to human populations [Zhong et al., 2013]. Understanding the population and spatial dynamics of *Ae. albopictus* in this location and other newly invaded areas, is a critical step towards contrasting its spread and thus limiting pathogens transmission risk [Benedict et al., 2007; Faraji and Unlu, 2016]. Indeed, for animal and public health end-users, predictions of models of pathogens vectors need spatio-temporal accuracy to assess current and future disease risks, and for operationally useful early-warning and/or forecasting tools [Ogden and Lindsay, 2016]. We modelled the habitat suitability surface of the study area, using real data from *Ae. albopictus* surveillance, to characterize the "attractiveness" of each real estate parcel of El Monte villages for *Ae. albopictus* adults. This suitability surface was then used in a population dynamics model in order to inform the mosquitoes movements from parcel to parcel. The resulting surface showed that the suitability was generally low in the study area (however, the distribution of suitability values per parcel had a wide 95 % interquartile range, indicating high variability).

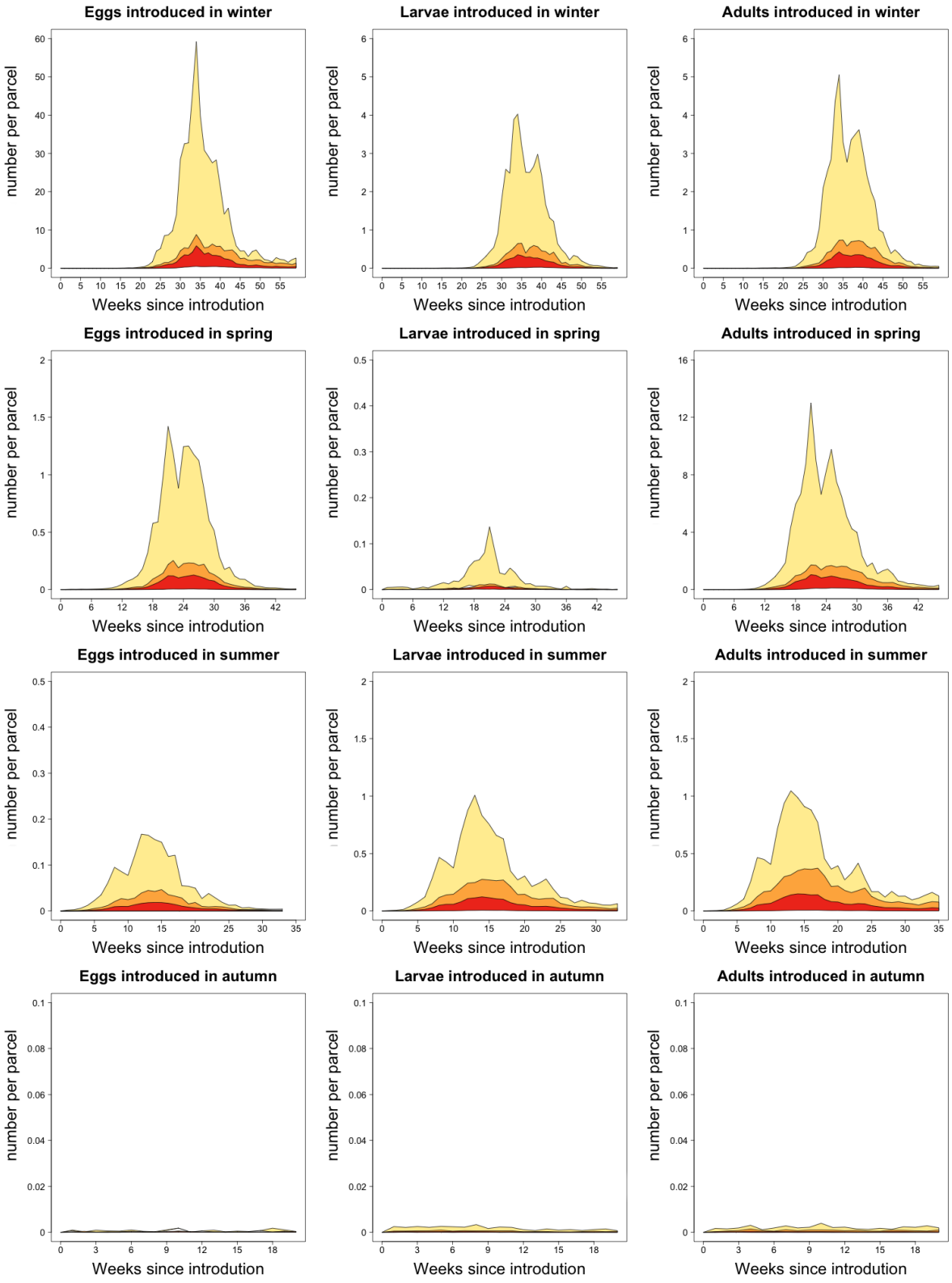

Figure 4.7: The temporal trend of *Ae. albopictus* density at the parcel level for each introduction scenario. The yellow, orange and red areas represent the median number of eggs, larvae and adults per parcel per week.

This conclusion is in agreement with the urban characteristics of El Monte villages, where most of the area is highly developed and the availability of breeding and resting habitats, linked with urban vegetation, is irregular. Our results indicate that *Ae. albopictus* presence in the study area is positively associated with pockets of vegetation at real estate parcel spatial scale, and negatively associated with high developed areas (apartment complexes, row houses and commercial/industrial; Homer et al. [2015]) at city block scale. This pattern is consistent with the scientific literature on the topic and it is justified by *Ae. albopictus* ecology in its native and invaded geographical range. The presence of vegetation (i.e. small green islands) has been repeatedly found to be positively related to *Aedes* infestation in urban areas [Vezzani et al., 2001; Mercado-Hernandez et al., 2003; Cianci et al., 2015; Manica et al., 2016]. Vegetation in urban areas combines a whole set of key features favourable for *Ae. albopictus* environment suitability as it provides shelter, hiding places from predators as well as stepping-stones towards new areas for colonisation. It also provides breeding habitats as it promotes water accumulation mainly in artificial containers actively, as requiring constant watering, or passively, through rainfall interception. These breeding habitats are optimal since the plant debris improves their quality [Schultz, 1989; Kling et al., 2007]. In addition, vegetation represents a source of sugar food and a higher proportion of potential blood meals for mosquitoes given the higher host abundance and diversity in these areas. Finally, when the climatic conditions of the host urban environment diverges from the optimal ecological niche of the invader, vegetation can be used as an environmental buffer [Meyer et al., 1990; Bartlett-Healy et al., 2012; Beier et al., 1983b]. On the contrary, highly developed areas with scarce vegetation may represent too harsh host environments for *Ae. albopictus*.

We modelled *Ae. albopictus* life history. For this purpose, we used temperature-dependent functions when data were available to parametrise them. This was the case for the gonotrophic and immature development period and the adult daily survival. The outputs from these three functions were in line with the known biology of the species, the first two showing a decrease with temperature until 30 °C to increase with higher temperature [Hawley, 1988; Delatte et al., 2009; Becker, 2010], while the third resulting in a concave shaped trend with inflection point around 20 °C [Waldock et al., 2013]. Besides these deterministic functions, stochasticity was integrated through the use of probability distributions instead of point estimates for life history parameters. Stochasticity is part of the complex invasion process under investigation and its integration provides more accurate parameter estimates and even useful insight on the invasion process itself [Calder et al., 2003].

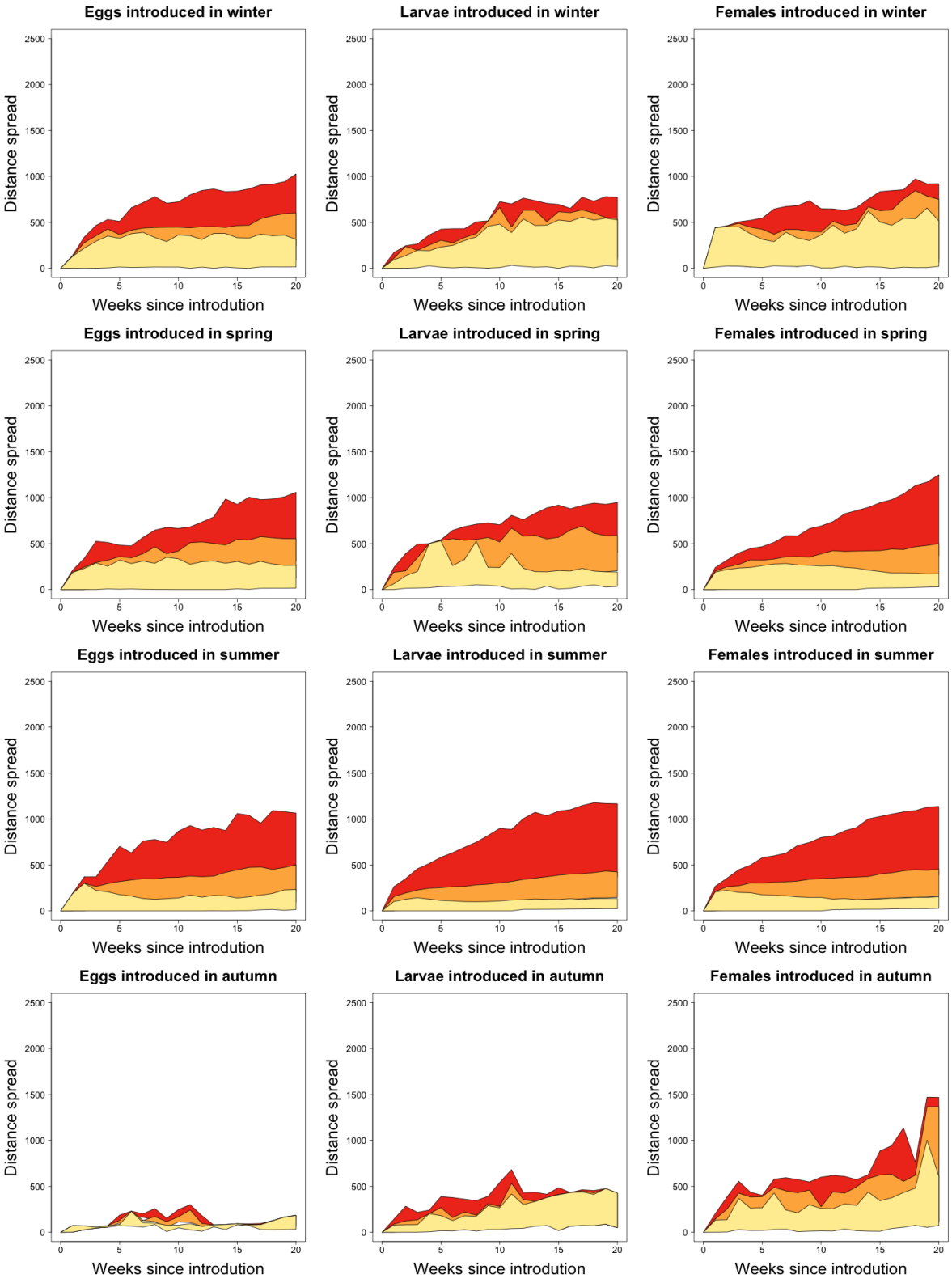

Figure 4.8: The temporal trend of the distance (m) travelled by *Ae. albopictus* adults for the first 20 weeks for each introduction scenario. The yellow, orange and red areas represents the 95 % inter-quantile range of the low (2.5 %), median (50.0 %) and high (97.5 %) quantile of weekly travelled distance distribution for that scenario.

When using the model to study the invasion patterns in El Monte villages under 12 introduction scenarios (eggs, larvae or adults introduced in each season), the simulations showed a shared similar spatio-temporal pattern of population abundances, dispersal and extinction rate. Nevertheless, the magnitude of the patterns remarkably varied across the scenarios. Not surprisingly, winter introductions led to a low invasion success. However, it is noteworthy that *Ae. albopictus* non-diapausing eggs could survive, in a reduced proportion of the simulations, the coldest winter temperatures in the study areas [Thomas et al., 2012; Delatte et al., 2009], causing the infrequent successful winter introductions. Less surprisingly, adults introduced in spring and larvae and adults introduced in summer often resulted in successful introductions (over 50 % success). In the study area in 2010, spring temperatures were around 21 °C, meaning an optimal survival conditions for *Ae. albopictus* adults. The further summer increase in temperature, with an average around 25 °C, favours an optimal larval survival [Waldock et al., 2013]. Indeed, larvae introduced in summer emerge as adults after the season's temperature peak, when the temperature are optimal for the survival of this stage. This allows *Ae. albopictus* to reproduce and establish populations big enough so that some individuals can survive through the following winter. As a result, and in partial contrast with what sometimes is reported in the literature (e.g. Washburn and Hartmann [1992]; Benedict et al. [2007]), temperatures during summer in the study area may be optimal for *Ae. albopictus* successful introduction when larvae are the introduced propagule. In the case of adults introduced in summer, the temperature in the study area decreases the daily adult survival rate, but shortens the gonotrophic period, which actually reaches the optimum [Delatte et al., 2009]. This scenario reduces the number of adults but, based on the reproductive capacity of mosquitoes, a well sized population that is able to survive the following winter is established. Introductions in autumn had a very low probability of starting a successful invasion. The low *Ae. albopictus* introduction success for these scenarios can be explained by considering the species life history in combination with the less favourable climatic conditions that mosquitoes experienced just after introduction in late autumn and winter. As a result, all the stages undergone high daily mortality rates due to the sub-optimal temperatures.

We are aware that our results may have underestimated the probability of a successful invasion since the model did not consider the photoperiodic diapause response as adaptation to adverse climatic conditions. Diapause induction is a complex physiological process triggered by a combination of photoperiod and temperature [Armbruster, 2016]. Thirteen hours is the Critical Photo Period (CPP) for the latitude of the study area (36°N, Urbanski et al. [2012]), reached from the end of August to the beginning of April. However, we did not consider diapause in the model because Pumpuni et al. [1992] reported a reduction of diapause incidence at 26 °C and a complete disruption when the temperature is higher than 29 °C. Temperatures

over these thresholds are common in the study area during spring and autumn (Monrovia weather station), potentially decreasing the incidence of diapause in *Aedes* mosquitoes. More importantly, *Ae. albopictus* invasion population in El Monte villages may have been founded by individuals from Southern China [Zhong et al., 2013] which, being tropical *Ae. albopictus* populations, do not undergo photoperiodic diapause [Hawley, 1988].

An important novelty of the dynamical model structure is that it integrates the spatial dynamics of *Ae. albopictus* population combining habitat suitability, shape of the urban landscape components, and a kernel function of spread distance decay. This feature of the developed model allowed to consider and track the dispersion of the simulated mosquito populations together with their demographic evolution.

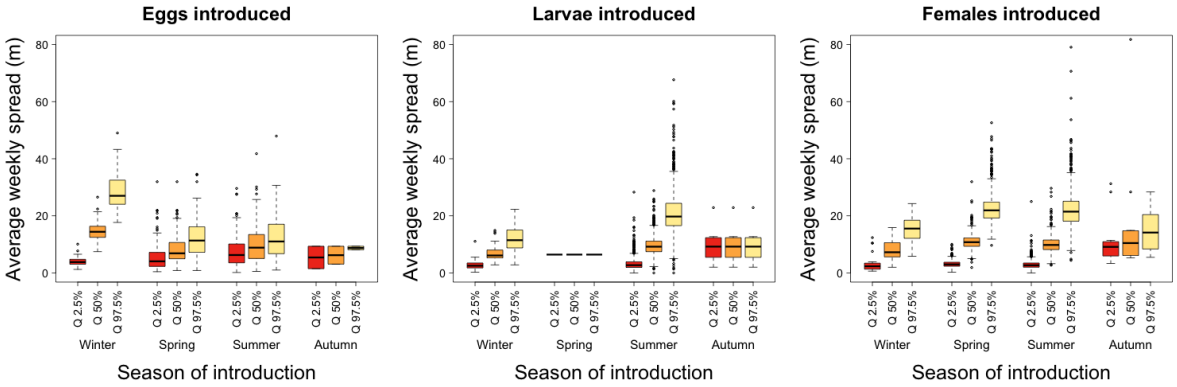

Figure 4.9: The boxplots represent *Ae. albopictus* weekly spread distribution for each introduction scenario. Each scenario is reported as a group of a yellow, orange and red boxplots representing the low (2.5 %), median (50.0 %) and high (97.5 %) quantile of weekly spread distribution for that scenario.

Despite the simulated scenarios consider different seasons and physiological stages of introduction, the pattern of *Ae. albopictus* density at the parcel level was relatively consistent, with extremely low density until summer when it increased until a maximum of 6 adults/parcel. However, the density magnitude was clearly different across scenarios. In winter for example, the introduction of eggs, caused the highest densities of adults per parcel across all scenarios. Eggs are the dry and cold-resistant life stage of *Ae. albopictus* and, as mentioned previously, temperatures in El Monte villages can sustain the development of this mosquito. Therefore, during the 20 weeks prior to summer, eggs were laid at low rates but consistently, they survived cold weather, and developed when temperatures increased. Similarly occurred with larvae and adults introduced in this season, but with a markedly lower adult density per parcel.

Regardless of the scenario, we found a relatively low median dispersal capacity of ~ 400 m in 20 weeks. In the most successful scenarios, the introduction of gravid adults or larvae in summer, the dispersal capacity of the derived populations had a maximum dispersal distance of

less than 1 km. When considering the entire period of observation for each season, we found that the travelled distance was $\sim$10 m week^{-1}, with no difference between seasons or life stages introduced, except for eggs introduced in winter that reached 20 m week^{-1}. The demographic and spatial trends across scenarios translated in a low number of new invaded parcels per week, with a maximum of 3.4 invaded parcels/week. Therefore, in spite of a high probability that a summer introduction of gravid adults or larvae was successful, the dispersal capacity of the derived population and subsequently the number of invaded households remained relatively low for all the considered period.

Mosquito populations at low density in urban areas are not easy to be discovered, due to the complexity of the urban landscape as well as the low sensitivity of mosquito population monitoring tools (e.g. ovitraps) and activities (e.g. door to door search). As a consequence, we hypothesise that the introduction of *Ae. albopictus* gravid adults or larvae during the summer or spring months are the most likely scenarios underpinning the invasion of this species in El Monte villages. However, our results suggested that any successfully introduced population would have remained localised in space and at low density for a long time, therefore, being difficult to discover. The species discovery would have been possible only when the corresponding population had reached a critical density, beyond the detectability threshold of the surveillance system. Our findings could also support the hypothesis that the introduction of *Ae. albopictus* in the study area happened in the years before 2011, as this species could have remained at low undetectable densities. Zhong et al. [2013] found a close genetic match between *Ae. albopictus* individuals collected in El Monte in 2011 and in L.A. harbour in 2001 during a previous and supposedly eradicated incursion of *Ae. albopictus* in Southern California. Based on these genetic similarities and other anecdotal evidences, they suggested that El Monte *Ae. albopictus* population is a carryover of the population introduced in 2001 in L.A. However, further analysis are needed to clarify the most likely time span from introduction to *Ae. albopictus* populations reaching density detectable by mosquito control activities in the study area.

The model framework proposed in this study can be applied to investigate different facets of *Ae. albopictus* invasion dynamics in L.A. areas as well as generalised to model and predict the invasion spatio-temporal pattern in other urban areas worldwide or under different climatic scenarios. However, some limitations have to be considered when interpreting the reported results. The population dynamics model assumed that breeding habitat and mate availability were not limiting factors for the survival of mosquitoes population. On the one hand, *Ae. albopictus* ecological plasticity [Waldock et al., 2013] justifies the first model assumption, especially when modelling its dynamics in urban areas where artificial breeding habitats are almost unlimited [Paupy et al., 2009]. On the other hand, the second assumption may have

led to overestimated population densities and spread rates. Indeed, at low population density, finding a suitable mate can be hard enough to limit the fitness of the invading population (one of the factors contributing to the inverse density dependence at low density or Allee effects; Courchamp et al. [1999]; McDermott and Finnoff [2016]), thus slowing the invasion process and decreasing the introduction success probability [Veit and Lewis, 1996]. Despite these limitations, we believe that the developed *Ae. albopictus* population dynamical model is a valuable, powerful and flexible tool to investigate the invasion mechanisms of this species that can bring important advances in knowledge to improve and target control actions.

Chapter 5

The configuration of urban vegetation affects the invasion dynamics of the Asian tiger mosquito

Marcantonio, M, Baldacchino, M, Montecino, D, Rizzoli A, Barker C, (in prep.). The configuration of urban vegetation affects the invasion dynamic of the Asian tiger mosquito.

Abstract

The Asian tiger mosquito, *Aedes albopictus*, is among the world's most invasive species. This species represents a threat to human health, being a day-biting pest, a competent vector of the dengue, chikungunya viruses and a bridge vector of several other arboviruses. *Aedes albopictus* has a wide ecological plasticity, a feature that has allowed it to adapt rapidly to urban ecosystems. Today, *Ae. albopictus* occurs in rural and suburban areas, and the species has been reported as abundant in several major urban areas. Invasion dynamics following introduction in a new urban landscape is the product of a combination of social, economic and ecological factors. For example, neighbourhood economic status affects the arrangement and type of green areas in the urban matrix, as well as urban connectivity, which in turn may significantly influence *Ae. albopictus* spread. In this study, we considered the impacts of the configuration of urban vegetation on *Ae. albopictus* spread immediately following introduction, and explored the subsequent implications for the establishment of the mosquito. We used field data and hierarchical modelling to characterise mosquito suitability in a recently invaded city, then we applied the model to generate realistic household-level suitability estimates in synthetic urban areas, with specific vegetation configurations. We subsequently modelled the stochastic spread of *Ae. albopictus* on each synthetic landscape using a temperature-dependent, dynamical model for mosquito reproduction and movement. Vegetation configuration did affect the spatial dynamics of the mosquito population. The spatial movement of simulated *Ae. albopictus* populations depended on the characteristics of the urban landscape with which they interacted, where vegetation homogeneously spread across the urban landscape favoured longer dispersal distances and higher population density. This trend was observed and was particularly evident at very low urban vegetation coverages which still supported highly localised mosquito densities, if the vegetation was evenly spread across the matrix. These findings, based on simulations of urban landscape and mosquito population dynamics, may have significant implications for mosquito control activities or when planning urban areas. However, detailed ground-truth entomological data are needed to confirm the inferred patterns.

5.1 Introduction

The spatial mobility of many species is dramatically rising, mirroring the increased movement of goods and people [Floerl et al., 2016]. At the same time, the geographical volume suitable for many species is expanding given the additive and interactive simultaneous effect of global warming and land use change [Hellmann et al., 2008]. Among these species reaching and eventually invading new areas, some are competent hosts for anthropozoonosis [Morens et al., 2004; Vora, 2008]. This set of species is a cause of human sufferance and death worldwide [Daszak et al., 2000].

Invasive species encroaching a new area will or will not colonise it depending on a set of interplaying conditions. Among all Earth's land uses, urban areas have features that make them more prone to attract and host invasive species: *i)* they are hubs for national and international commercial and tourist routes, acting as focal point for broad scale introduction (both intentional and unintentional); *ii)* the "urban heat-island" effect provides distinctive environmental conditions that have allowed many exotic species, *viz.* with high temperature requirements, to become established in urban environments [Ricotta et al., 2010; LaDeau et al., 2015]; *iii)* the high "fractal dimension" of urban areas makes multiple micro-climatic niches available in a relatively small volume [Batty and Longley, 1994; Overgaard et al., 2003]. Urban areas are also hotspots of human, pet and synantropic species populations (more than half of the world's population now lives in cities; Satterthwaite [2009]), providing endless blood meal opportunities to bloodsucking arthropods, such as mosquito vectors of pathogens [Reiter, 2001; Norris, 2004]. Given the rampant urbanisation throughout the tropics and subtropics, and the features of urban areas with respect to human and invasive species distribution, urbanised areas are considered as ticking time bombs for emerging and re-emerging vector-borne pathogens transmission [Patz et al., 2004; Lederberg et al., 1992; Li et al., 2014; Nature, 2016].

Among the many exotic species thriving in urban areas, *Aedes* (Meigen) mosquitoes gained international public attention due to their rapid spread worldwide [Benedict et al., 2007]. They are vectors of all the major vector-borne pathogens in humans, from dengue to Zika virus [Simmons et al., 2012; Charrel et al., 2014; Weaver et al., 2016]. Among *Aedes* species, *Aedes albopictus* (Skuse) has the widest ecological plasticity, thus it is able to colonise and thrive also in apparently hostile environments, such as highly urbanised areas [Hawley, 1988; Medley, 2010; Li et al., 2014; Samson et al., 2015].

The first events in a biological invasion process, are the translocation and introduction of species propagules [Dunn and Hatcher, 2015]. A high propagule pressure, i.e. the rate and size of the introduced agent of reproduction (e.g. eggs), often underlies successful introductions [Williamson and Fitter, 1996]. After introduction, whether species become established or not is a result of complex interactions between the invader and the physical and biological

characteristics of the recipient environment [Davis et al., 2000; Bomford et al., 2008]. A favourable climate ("matching climatic conditions") is a central condition for the establishment of viable invasive population (naturalisation) in new areas [Duncan et al., 2001; Bomford et al., 2008]. *Aedes albopictus* has reached beyond these limits thanks to the ability to exploit human movements to overpass ecological barriers at any scale (from rivers to oceans; Tatem et al. [2006]) and to a wide, partially acquired, temperature niche (achieved through several physiological and behavioural traits, such as diapausing and desiccation-resistant eggs; Rochlin et al. [2013]). As a consequence, this species is potentially able to repeatedly reach any human settlement on Earth and has a widening potential distribution that now spans from as north as Northern Europe to as south as Southern Argentina [Kraemer et al., 2015]. However, its invasion success and speed differs between urban areas or in different neighbourhoods of the same urban area with similar macro-climatic conditions and propagule pressure potential. The variable invasion dynamics is sometimes explained by intra-specific differences in the introduced individuals but is often due to variability in urban land use and urban area structure, which is linked to differences in socio-economical and demographical characteristics [Davis et al., 2000; Unlu et al., 2011; Roche et al., 2015].

Urban vegetation is often considered to be a proxy for neighbourhood socio-economical characteristics, with a strong positive relationship between vegetation cover, income and education level [Liu et al., 2008; Luck et al., 2009]. When considering the invasion of mosquito species, urban vegetation combines a whole set of key features for environment suitability as it provides shelter, hiding places from predators as well as stepping-stones towards new areas for colonisation. Vegetation in urban environments also provides breeding habitats as it promotes water accumulation (mainly in artificial containers such as flowerpots and disposable tins), both actively, as requiring constant watering, or passively, through rainfall interception [Vezzani et al., 2001]. These breeding habitats are optimal since the plant debris improves their attractiveness and organic quality [Schultz, 1989]. In addition, vegetation provides sources of sugar food as well as blood meals for mosquitoes, given the higher plant/host abundance and diversity. Moreover, when the climatic conditions of the host urban environment diverge from the optimal ecological niche of the invader (matching climate), vegetation work as an environmental buffer to "adjust" them [Beier et al., 1983b; Meyer et al., 1990; Benoit and Denlinger, 2007; Bartlett-Healy et al., 2012]. The properties of urban vegetation, such as abundance (coverage), configuration and composition, are extremely variable from city to city, depending on the local climatic, ecological, historical and social context. In the scientific literature, vegetation abundance and composition have often been associated with high abundance of mosquitoes in urban areas. The presence of vegetation (i.e. small green islands) was found to be positively related to *Aedes* infestation in urban areas [Vezzani et al., 2001; Mercado-Hernandez et al.,

2003; Manica et al., 2016]. The presence of trees was positively related to abundance of *Aedes* eggs, while grass vegetation was negatively associated [Vezzani et al., 2005; Cianci et al., 2015]. The negative association with grass vegetation indicates that open areas without dense vegetation are unsuitable for *Ae. albopictus* survivorship [Rey et al., 2006; Honório et al., 2009]. Besides vegetation abundance, vegetation composition could also affect mosquito population dynamics in urban areas. Interestingly, plant species provide different quantities of sugar for mosquito diet [Samson et al., 2013], thus affecting mosquito fitness which, in turn, influences the invasion process. Previous studies mainly focused on the relationships between urban vegetation and mosquito composition and abundance [Vezzani et al., 2001; Rubio et al., 2012; Medeiros-Sousa et al., 2015; Manica et al., 2016]. However, detailed information on the dispersion of *Aedes* mosquitoes is still lacking. For those species with a limited self-dispersal capacity [Marini et al., 2010], the configuration of the urban vegetation may be inferred to play an essential role in their dispersion, particularly after introduction, when avoiding extinction through hiding and acclimatising in patches of suitable habitat is critical. In addition, the dispersion of *Aedes* mosquitoes depends on the availability of oviposition sites, mostly located in vegetation [Reiter, 1996; Vezzani et al., 2001]. Vegetation configuration is defined as the connectivity and spatial arrangement of vegetation patches in the (urban) landscape matrix, regardless of its abundance and specific composition, and can strongly vary among cities. Green areas can be concentrated in a few big patches (i.e. urban parks or wooded areas), or can be widespread among many private gardens. Moreover, they can be sparse and interconnected (e.g. through canals) in the urban matrix or can be clustered and isolated in different districts of the urban area. Amid these extremes lie all the possible configurations that we observe in the today's cities.

We aim to test how *Ae. albopictus* invasion dynamics varies with different configurations of the urban vegetation, which represents a research topic rarely treated in the scientific literature. We are aware that vegetation has multiple positive effects on urban areas, such as: *i)* limiting the urban heat island effect and pollution; *ii)* providing amenities for humans and *iii)* allowing biological diversity to persist [Smardon, 1988; McPherson, 1998; Dimoudi and Nikolopoulou, 2003; Kati and Jari, 2016]. Nevertheless, its role in the invasion dynamic of exotic species noxious for human health, such as *Ae. albopictus*, has yet to be clarified.

We will apply a temperature dependent time-discrete dynamical model of *Ae. albopictus* life cycle and spatial movement to synthetic urban landscapes. These landscapes have a varying vegetation configuration, from high vegetation coverage grouped in public parks to low coverage spread throughout the city. The simulated urban landscapes have properties mirroring modern urban areas. The rate of introduction success as well as population dynamic spatial and temporal trends will be tracked for each simulated urban landscape. Due to species biology and

ecology, we hypothesise that *i)* the invasion success, abundance and spread of *Ae. albopictus* populations in urban landscapes — the other conditions held constant, are facilitated by a higher vegetation abundance, and/or *ii)* a homogeneous configuration of vegetation throughout the urban landscape.

We conceived this study certain that identifying those urban vegetation properties which facilitate the establishment, spread and invasion of *Ae. albopictus* may have a double-fold positive outcome. It may help to understand observed invasion patterns in order to mitigate *Ae. albopictus* spread more efficiently [Unlu et al., 2016] and at the same time may contribute to better plan future "smart" urban environments, more "resistant" to *Aedes* mosquito invasion.

5.2 Methods

5.2.1 Deriving landscape characteristics of real urban areas

We identified 5 fundamental urban landscape units: *i)* Roads (Rd); *ii)* Apartment, offices and industrial buildings (Ho); *iii)* Public large green areas (Vp); *iv)* Private and other green small areas (Vo) and *v)* Open areas (Op). Given the purpose of the study, we focused on Vp and Vo, and gathered information on their configuration in real urban landscapes. We found that the most representative source of data on public parks coverage in cities is "The Trust for Public Land's ParkScore® index" which, making use of an advanced GIS, has mapped the park coverage and needing for the 75 biggest cities in the United States for 2015 (parkscore.tpl.org). This index ranks the considered cities using multiple criteria. We chose the criterion "Parkland as percent of Adjusted City Area" and utilised the first and last city as ranked by the index, San Francisco and Fresno respectively, in order to define the extremes of the range in the percentage of public green areas in real urban landscapes. Public green areas are usually arranged in big vegetation patches which have different characteristics (species composition, density, management, etc.) from private green areas. The two reference cities are located in California which has been recently re-invaded by *Ae. albopictus*. As a result, California is facing risks of importation of *Aedes*-borne disease agents such as, dengue and chikungunya viruses, from Central America endemic areas [Fredericks and Fernandez-Sesma, 2014]. All the other data on mosquito population and vegetation used in the following analysis were also derived from Californian urban areas.

According to the ParkScore index, 19 % of San Francisco urban area is covered by parks which have an average size of about 8 km^2. On the contrary, 3.2 % of Fresno urban area is covered by parks with an average size of 20 km^2. We checked these figures using the National Land Cover Database 2011 (NLCD; Homer et al. [2015]) and found an adequate match. Once

known the approximate percentage of urban area covered by public parks in the two reference cities, we derived the percentage coverage of other green areas using a GIS approach. In GRASS GIS 7 [Neteler et al., 2012], we overlaid the park areas of the two cities (downloaded from https://data.sfgov.org/ and http://www.fresno.gov/) with all the NLCD land uses that included vegetation (NLCD categories 21, 41, 42, 43, 51, 52, 90, 95). Then we clipped the overlapping sections and the remaining areas were considered as vegetated urban patches not part of public parks. We assumed that these areas represented private (gardens), or other green areas present in the cities. These areas covered 5.5 % and 9 % of San Francisco and Fresno urban landscape, respectively. We used this information as milestones to define six different scenarios for vegetation configuration in urban areas:

1. High vegetation coverage (25 %) mainly allocated in urban public parks (Vp 18 %; Vo 7 %; i.e. San Francisco);
2. High coverage of vegetation (25 %) spread throughout the urban area (Vp 6.25 %; Vo 18.75 %);
3. Medium vegetation coverage (17.5 %) mainly allocated in a few public urban parks (Vp 13 %, Vo 4.5 %) ;
4. Medium vegetation coverage (17.5 %) spread throughout the urban area (Vo 6 %; Vp 11.5 %) ;
5. Low vegetation coverage (10 %) mainly allocated in a few urban parks (Vp 7 %, Vo 3 %);
6. Low vegetation coverage (10 %) spread throughout the urban area (Vp 3.5 %; Vo 6.5 %, i.e. Fresno);

These scenarios were defined with the aim to cover extreme and intermediate urban vegetation configurations and were consequently used as references to simulate the corresponding urban landscapes.

5.2.2 The simulations of urban landscapes

R functions to simulate roads and urban land use

We developed two R functions to build synthetic representations of roads and urban matrices with customisable spatial relationships among the landscape units. The first R function, *roadsim()*, allows the user to build "road shaped" features in a 2D matrix through a sinusoidal function. The starting point on the matrix, main direction (row or column), approximate length and width (in cells) as well as the shape of the road (frequency and amplitude) are customisable.

The second function *citysim()* starts with an empty 2D matrix of user defined size. This matrix is then iteratively filled with numeric elements in patterns determined by the settings

specified by the user. The matrix can be filled using block of cells (i.e cellular automata approach) or cell by cell. The filled cells are excluded by the next iteration. The coordinates of the cell from where to start to fill the matrix can be defined in the function or picked randomly. A bias to the starting coordinates can be added as a probabilistic drawn from a cut normal distribution. This bias is added to allow the function to find new empty cells, in case of no proximal solutions. Furthermore, through the definition of mean and standard deviation of the distribution from which to pick the bias, the spatial relationship between the matrix units can be customised. It is also possible to define a range of cells around the provided starting coordinates inside which to randomly pick the actual starting coordinates. The search for new cells to be filled is settable to start from cells already filled by another feature.

In brief, several consecutive runs of these two functions allow to build a matrix filled by road-like or clumped basic elongated and squared shapes of different size that are the main elements of a basic simulated urban matrix. Both the functions, enriched with simple examples, are reported and commented in Appendix D.

The definition of urban landscapes

To build the synthetic urban landscapes in the R programming environment [R Core Team, 2016], we firstly defined six 500x500 cells matrices. These matrices were transformed in spatial objects having an unreferenced projection with pixel resolution of 10 m, thus having an extent of 5x5 km. We ran the *roadsim* function to fill each of the matrices with primary and smaller secondary roads. The secondary roads always originated from the main roads. The number of pixels occupied by roads was held constant using as reference the proportion of roads observed in San Francisco and Fresno urban areas (about 0.01 % of the total urban area; road data were derived from openstreetmap.org). Afterwards, through the *citysim* function and using as reference the proportion reported in paragraph 5.2.2, the other land uses were allocated in each of the simulated urban landscape. We started from the public green areas which were built using a cellular automata approach with a very weak spatial relationship between them. Groups of cells representing buildings of various size were then added to the matrix. These cells were allocated with a high spatial autocorrelation between them and with a close spatial relationship with road type cells. Finally, cells representing private green areas (e.g. gardens) were filled. Each pixel of this class was spatially related to building cells, but with a weak spatial relationship between themselves. The unfilled cells were finally assigned to the bare surface category.

Normalised Difference Vegetation Index (NDVI) and *Ae. albopictus* habitat suitability

We used NDVI, a proxy for vegetation biomass, and the proportion of highly developed area to derive *Ae. albopictus* suitability in the simulated urban landscapes [Cianci et al., 2015; Manica et al., 2016; Montecino et al., 2016]. We used a GIS "reverse-engineer approach" to assign each pixel in the simulated matrices to a NDVI value. As first step, we sought for correspondences between the 5 simulated land use classes and the land use classes reported in the NLCD (see Table 5.1).

Table 5.1: Description of each of the Land Use category in the simulated landscapes and corresponding categories in the National Land Cover Database (NLCD) 2011 dataset. Class Ho (Buildings) and Rd (Roads) were assigned to the same NLCD class, 24 (Highly Developed Areas)

Land use	**Description**	**NLCD category**
Ho	Highly developed urban landscape / Barren surfaces	24
Rd	Roads	24
Vp	Low to moderately developed areas	22, 23
Vo	Trees / Shrubs	21, 71, 72, 73, 74, 81, 82
Op	Open areas / Grass / Crops / Hay	41, 42, 43, 51, 52

Secondly, the NDVI distribution for each NLCD class was derived intersecting the NLCD with a NDVI map derived from the National Agriculture Imagery Program (NAIP 2014) for the city of San Francisco. Then, the NDVI distribution of NLCD classes corresponding to the same simulated land use classes were merged. The results represented the NDVI distribution of the 5 simulated land use classes (Figure 5.1). The NDVI value was then assigned to each pixel of the simulated matrices picking it at random from a normal distribution with the average and standard deviation of its land cover category. Each of the 500x500 pixel matrix was divided in 50x50 pixel "city blocks" to control for the effect of highly developed areas in the urban landscapes, known to influence *Ae. albopictus* presence [Montecino et al., 2016; Manica et al., 2016]. We derived the proportion of "highly developed areas" in each block as the proportion of block area covered by Rd and Ho land use classes.

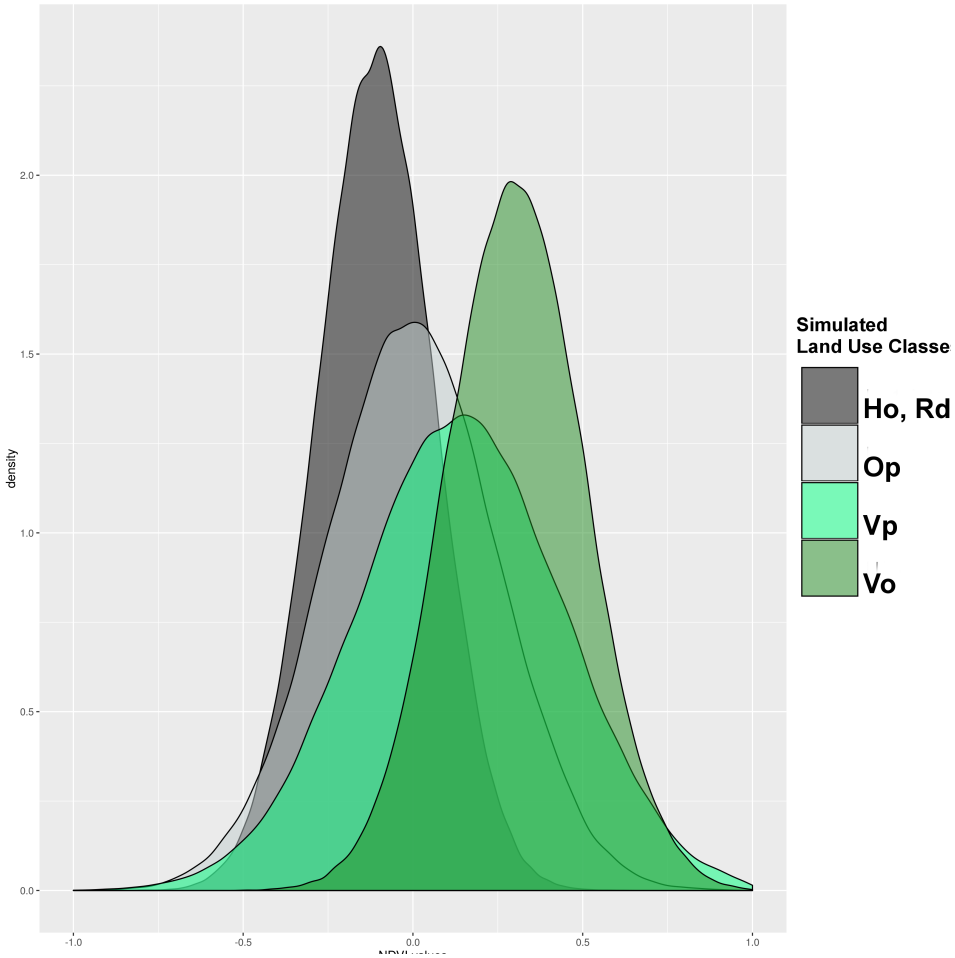

Figure 5.1: The density distribution of NDVI values for the 5 simulated classes. Dark grey = Ho and Rd, Grey = Op, Light green = Vp, Dark green = Vo.

Having an NDVI value and developed area proportion assigned to each pixel in the simulated matrices, we predicted *Ae. albopictus* suitability in each pixel of the 6 simulated urban landscapes through the multilevel logistic regression model proposed in Montecino et al. [2016]. The authors parametrized the model making use of a very wide dataset of *Ae. albopictus* presence/absence data (about 65 000 observations; collected between 2011 and 2016 in El Monte and South El Monte, two cities in the Los Angeles metropolitan area) as response variable. The model had a multilevel structure, with NDVI at pixel level and proportion of highly developed area at block level included as predictor variables. NDVI was credibly positively correlated with the *Ae. albopictus* presence odds ratio, while the percentage of developed area was found to be credibly negatively correlated (see Table 2 in Montecino et al. [2016]). The average of the distribution of suitability surfaces, outcome of the logistic regression models, was then used as input in the population dynamical model. The multilevel model was implemented in JAGS 4.2.0 through runjags [Denwood, 2016] and coda [Plummer et al., 2006] packages in the R software environment [R Core Team, 2016].

5.2.3 The population dynamical model

We modified the time-discrete temperature-dependent model for *Ae. albopictus* population dynamic proposed in Montecino et al. [2016]. This model has a classical stage-structure where mature winged females disperse flying. This dispersal process is macroscopically represented in the model by a daily distance decay process, coupled with a habitat suitability index. We adapted this model to run on a 2D squared matrix, removing the model parts that treated the spatial features (shape and dimension) of land use patches in order to adjust the probability of the mosquitoes to move into it. The resulting new probability θ for an *Ae. albopictus* adult of moving from parcel i to parcel i' is now therefore defined as:

$$\theta_{i'i} = \frac{s_i \times invd_{i'i}}{\sum_{(\mathbf{s_{i'}} \times \mathbf{invd_{i'i}})}} \tag{5.1}$$

where:

s_i = the suitability per parcel informed by the multilevel models.
$invd_{i'i}$ = $d_{i'i}^{-\lambda}$
λ = the exponential decay in probability with respect to distance (d).

In order to adjust the function describing the mosquito dispersal probability $\theta_{i'i}$ to match the observation about mosquito dispersal capacity as reported in Marini et al. [2010], we ran simulations varying the λ parameter $\mathbb{Z}[1,10]$ and introducing 10 females for 10 000 iterations. We checked the distance travelled by the successful introductions after a week and for each of the considered λ values. According to best matching results, we defined $\lambda = 3$. The decay in the capacity of mosquito dispersal decreased with respect to the original model (where $\lambda = 6$) due to the intrinsic higher spatial detail of our analysis (10 m pixels vs. irregular polygons).

We used the temperature time series recorded by the Monrovia weather station, in Los Angeles metropolitan area (34.149°N, −117.989°E) as temperature input in the population dynamical model. This temperature data series is indeed optimal for *Ae. albopictus* development and survival [Delatte et al., 2009; Waldock et al., 2013].

Forty eggs [Hawley, 1988] were released randomly in one of the cells of each simulated urban matrix on the 1st March 2006 and the mosquito population dynamics tracked for 365 d. We chose 2006 as introduction year since it is an average year for temperature in the considered temporal series. The twenty most external cells of the urban matrix were excluded from the releasing process, simulated for 1000 times, to avoid a too strong boundary effect. For further details on the model refer to Montecino et al. [2016]. All the analysis were performed using the R programming language [R Core Team, 2016], the *roadsim* and *citysim* functions are publicly available in the author's GitHub repository: https://github.com/mattmar. The life cycle simulations were run in the cluster computer hosted in the Fondazione Edmund Mach, San Michele all'Adige, Italy.

5.3 Results

5.3.1 The simulated urban landscapes

The 6 simulated Urban Landscapes (UL) shown in Figure 5.2 had a spatial extent of 25 km^2 and a pixel resolution of 10 m (matrices of 500x500 pixel). The land use statistics as well as the Proper Likelihood Adjacencies (PLA) metric, or degree of aggregation, for the vegetation land uses are reported in Table 5.2.

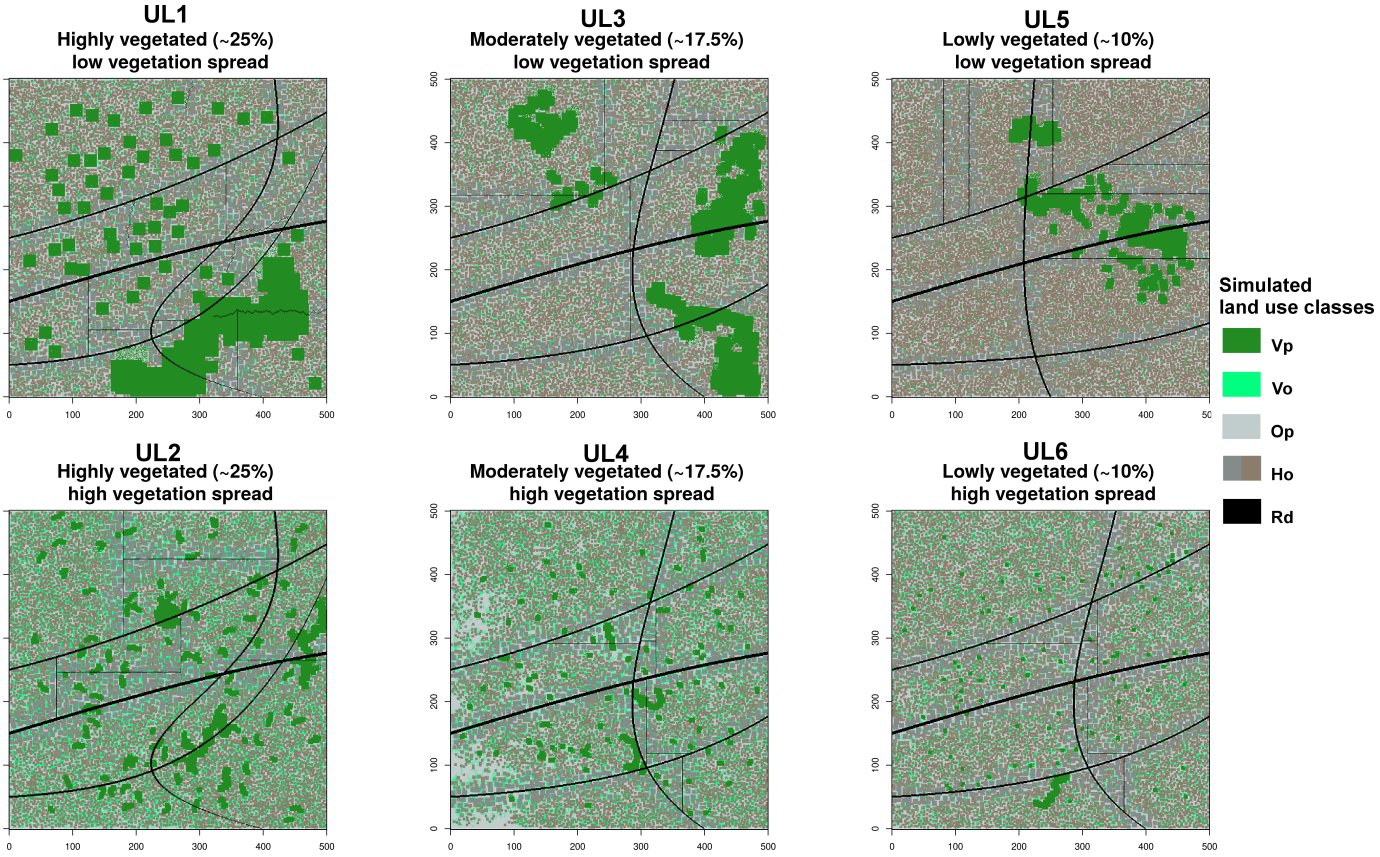

Figure 5.2: The six simulated urban landscapes. The long description of the land use classes is reported in Table 5.1.

The coverage of vegetated area in the simulated ULs varied from 24.8 % (UL1) to 9.7 % (UL5). The PLA statistics, the probability that a vegetation pixel bounds with another vegetation pixel, confirmed that landscape UL1, UL3, UL5 (with clustered vegetation) and UL2, UL4, UL6 (with spread vegetation) formed two groups with opposite vegetation configuration properties.

Using the NDVI distributions reported in Figure 5.1, we transformed the simulated urban land use maps (Figure 5.2) in vegetation (NDVI) maps (Figure 5.3).

Table 5.2: Land use statistics for each of the six simulated urban landscape. Proper Likelihood Adjacencies (PLA) has been calculated for Vp and Vo. This index shows the frequency with which different land use classes (vegetated vs. not vegetated) appear side-by-side on the map.

Urban landscape	Op %	Rd %	Ho %	Vp %	Vo %	Vp+Vo %	PLA
UL1 (High/concentrated)	20.2	3.2	52.0	20	4.8	24.8	0.71
UL2 (High/spread)	16.5	3.2	56.0	10.3	14.1	24.4	0.47
UL3 (Moderate/concentrated)	22.4	3.2	56.0	14.6	3.9	17.5	0.69
UL4 (Moderate/spread)	23.9	3.0	55.8	4.8	12.5	17.3	0.36
UL5 (Low/concentrated)	19.5	3.3	67.4	8.0	1.7	9.7	0.68
UL6 (Low/spread)	18.0	3.2	67.9	3.0	7.3	10.3	0.36

5.3.2 *Aedes albopictus* invasion dynamics

The average distance reached by the mosquito population after a week from introduction was between 30 and 40 m for all the urban matrices, while the maximum distance travelled at the end of the simulations was 4.7 km (UL2). Figure 5.4 shows the average, 0.05 and 0.95 quantile of the daily travelled distance by the mosquito population for each of the simulated urban landscape.

By focusing on the high quantile of the distribution the effect of very short distance travelled by populations that headed towards extinction soon after introduction is somehow minimised. We recorded the 0.95 quantile highest travelled distance in UL2 while in UL6 the lowest. On average, the mosquito population in UL1 and UL2 travelled the longest distance while UL6 the shortest. The decrease in the dispersal distance at the end of the simulated period is due to local (pixel) population extinction linked with the suboptimal climatic conditions in winter.

The temporal trend in the average abundance of *Ae. albopictus* eggs, larvae and adult females per parcel for each urban matrix is reported in Figure 5.5. This figure represent the eggs, larvae or adults observed in a randomly chosen parcel in a day after introduction for each of the simulated urban landscapes. The trend reported in Figure 5.5 indicates that the mosquito population started to grow exponentially in July when the temperature reached the maximum value. The exponential growth slowed in September but exhibited another increase at the end of October when the temperature started to grow again. We reported the temporal trend of the considered temperature data at the bottom of Figure 5.5.

At the peak of *Ae. albopictus* population, UL2, UL4 and UL6 showed the highest population for all the life stages. Eventually the populations started to decrease in half November to reach

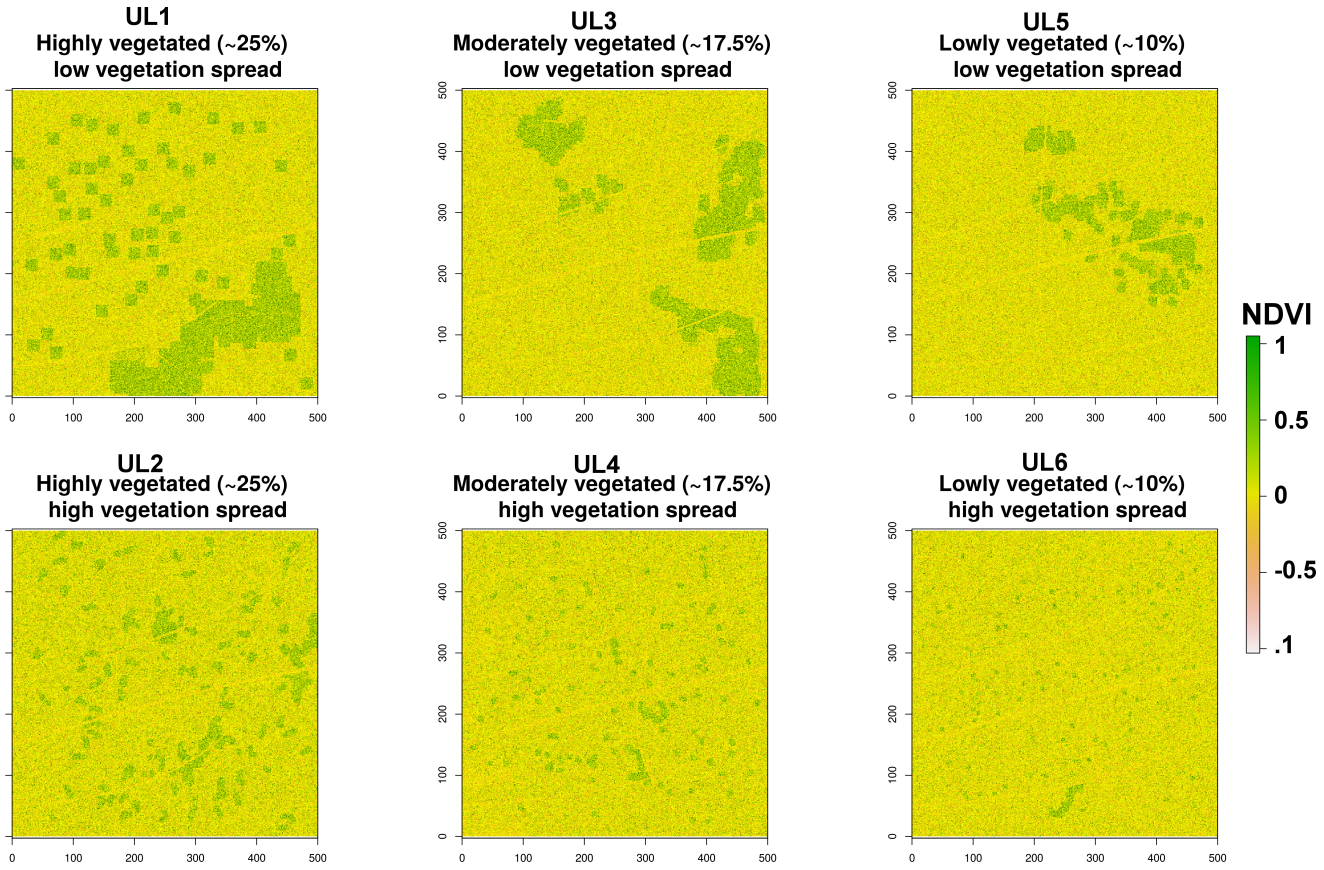

Figure 5.3: NDVI maps for the six simulated landscapes.

very low densities in February. At the very end of the simulations (1st March 2007), the mosquito populations recorded the highest density in UL3 and UL4, while UL6 had the lowest population (Figure 5.5). The urban landscape with higher vegetation spread (UL2, UL4, UL6) systematically showed higher population abundances with respect to the urban landscape with clustered vegetation (UL1, UL3, UL5).

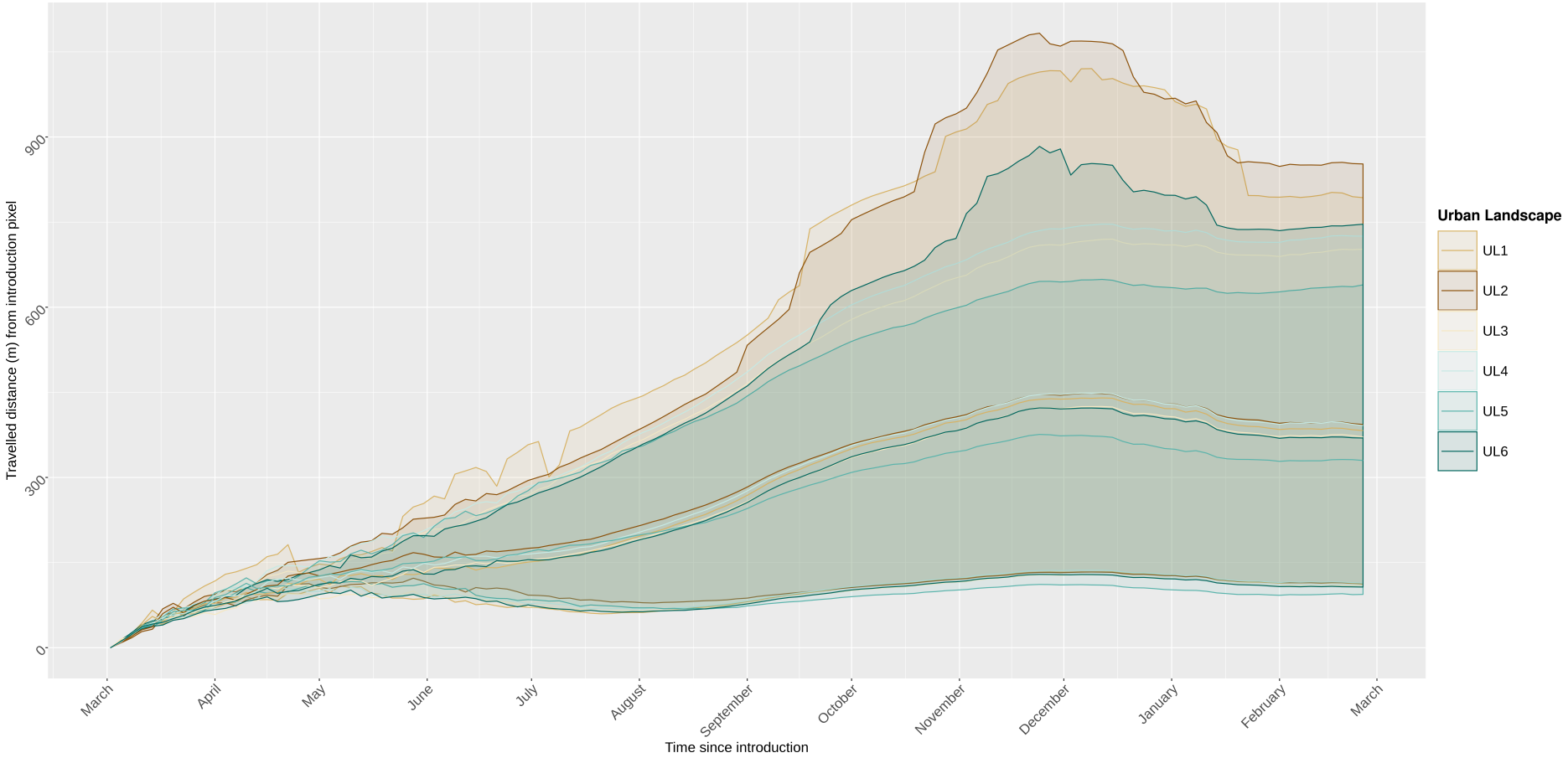

Figure 5.4: The 95 % CI distribution of the dispersal distance for *Ae. albopictus* populations in each of the simulated urban landscape.

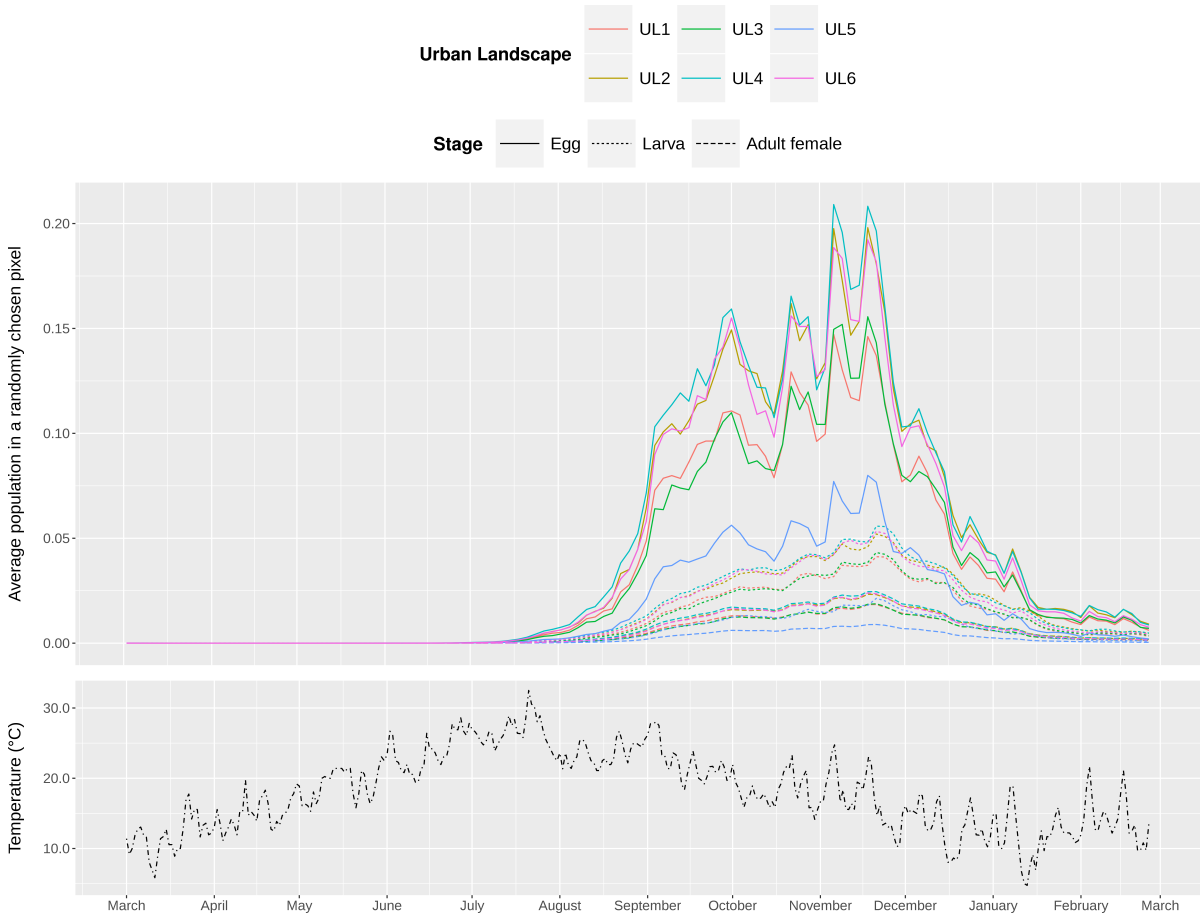

Figure 5.5: The average abundance of *Ae. albopictus* eggs, larvae and adult females per parcel in the whole urban matrix. This statistics represent the eggs, larvae or adults observed in a randomly chosen parcel in a day after introduction for each of the simulated urban landscapes. At the bottom of Figure 5.5 is reported the temporal trend of the considered temperature data.

To show how the mosquito populations expanded in urban landscapes with different vegetation configurations, we plotted the average number of *Ae. albopictus* eggs, larvae and adult females, in each pixel observed every day in a year from introduction (Figure 5.6). This figure reveals that in UL2, the introduction caused the highest number of invaded pixels and the highest population with respect to the other simulated urban landscapes. On the contrary, UL6 showed the lowest spread of mosquito populations which reached high values in only a few pixels. Mosquito populations spread more in those urban landscapes with vegetation distributed across the urban matrix than in the ones with vegetation concentrated in few bigger patches. Figure 5.7a shows the first day of invasion for each pixel in the urban matrices. In the case of pixels invaded multiple times (i.e. in different simulations), we averaged the day of invasion. *Aedes albopictus* populations were able to reach at least once, almost all the pixels in every landscape after a year from introduction (from 86 % to 99 % of all the pixels).

The highest invaded pixel coverage was reported for UL1 and UL6. We noted that mosquito populations in urban landscapes with a more abundant vegetation tended to expand more slowly than landscapes with lower vegetation. However, with vegetation held constant, urban landscapes with more spread vegetation had more pixels occupied by mosquitoes. In Figure 5.7b the percentage of new invaded pixels in each season is shown for all the UL. At the end of the spring, the percentage of invaded pixels was never higher than 2 %. During summer the mosquitoes spread the most, while at the end of autumn, the percentage of new invaded parcels decreased. However, as shown in Figure 5.5 and 5.6, the autumn recorded the peaks in population abundance and spatial expansion for all the simulated ULs. This pattern is a consequence of the the summation of high expansion rate in summer and autumn, that recorded the lowest values in spring just after introduction.

The rate of successful introductions, defined as those with at least one individual at the end of the simulated period (1 yr), was very low for all the urban landscapes. We recorded the highest rate in UL6 (6.0 %) while the lowest in UL5 (4.0 %; other rates, UL1=4.3 %; UL2=5.2 %; UL3=5.3 %; UL4=4.9 %). Figure 5.8 shows the relationship between the average abundance of mosquitoes for all the simulated period of time and the NDVI average value of the area of introduction (defined as introduction pixel plus the 399 nearest neighbours). Each circle represents a different introduction of the 1000 simulated. No evident trend between NDVI value and average mosquito abundance was observed.

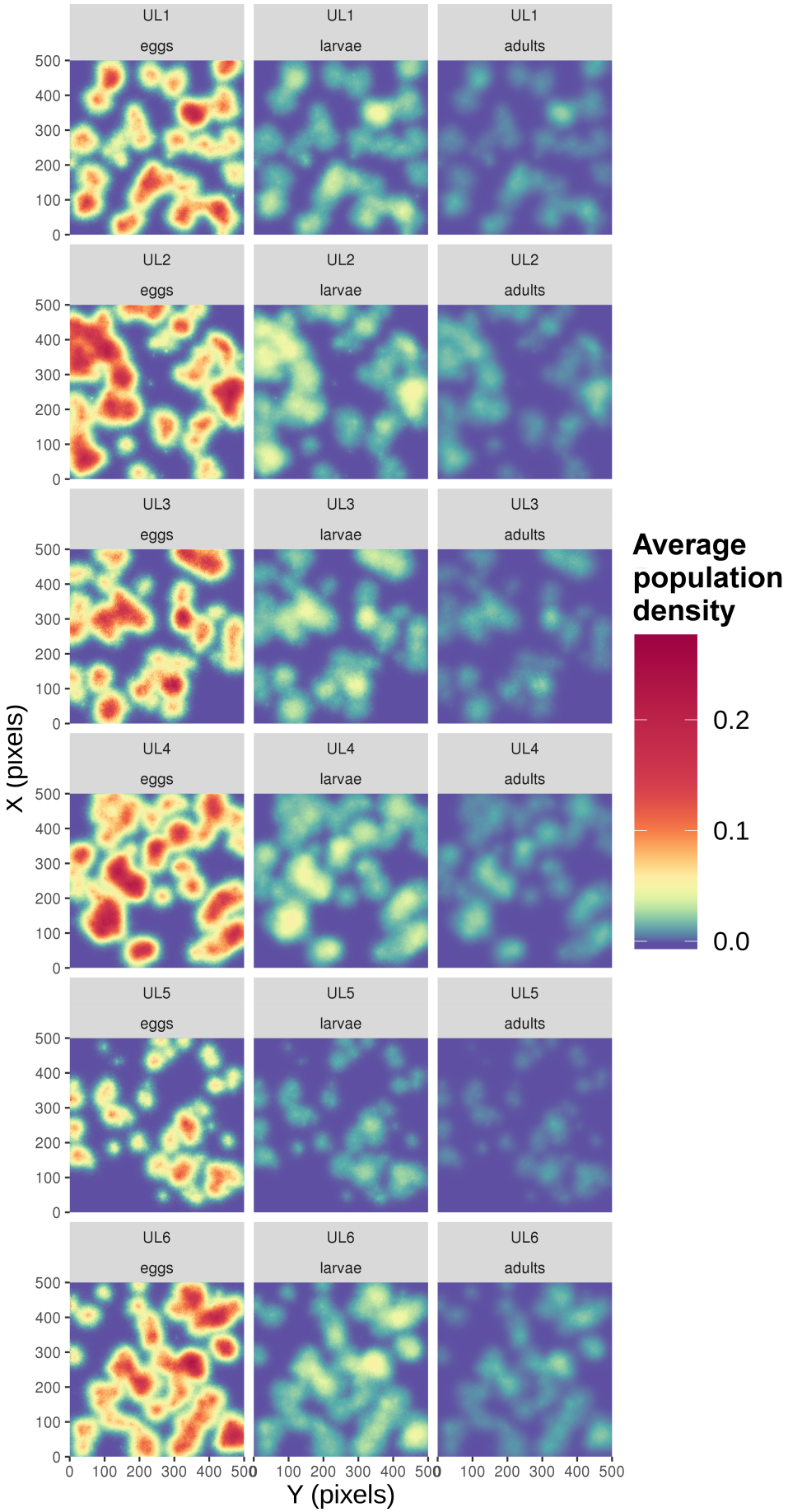

Figure 5.6: The average number of *Ae. albopictus* eggs, larvae and adult females, in each pixel observed every day in a year from introduction

5.4 Discussion

Vegetation in urban areas provides habitats for many organisms including mosquitoes [Alvey, 2006]. The impact of urban vegetation on *Aedes* mosquito invasion and dispersal dynamics is relatively understudied. We tested how the configuration of vegetation affects *Ae. albopictus* invasion dynamics after introduction in urban areas.

The success of the introduction event did not correlate with the average NDVI in the introduction areas, whatever the vegetation features were in the urban landscape. This does not contradict the relationship between *Aedes* mosquito and urban vegetation reported in the scientific literature [Vezzani et al., 2001; Mercado-Hernandez et al., 2003; Cianci et al., 2015; Manica et al., 2016]. Indeed, while an introduced population can be initially favoured by the vegetation abundance and configuration in the surroundings of the introduction area, in the long term other factors, including stochastic events, have a greater effect on the introduction success, mosquito population abundance and spread. A population introduced in a favourable (i.e. vegetated) patch in a urban area but surrounded by a landscape matrix with low suitability can reach a steady state at low abundances and even move towards local extinction due to reaching carrying capacity and/or stochastic events, being unable to emigrating [Suzán et al., 2015]. A similar setting may underpin the trend observed for an *Aedes koreicus* (Edwards) population which invaded a village in Belgium in 2008 and, despite the population being viable and the favourable climatic conditions [Montarsi et al., 2013], no expansion has been recorded since then [Versteirt et al., 2012].

Vegetation configuration did affect the spatial dynamics of the mosquito populations. According to our findings, the dispersion pattern of an invading *Ae. albopictus* population depends on the characteristics of the urban vegetation with which it interacts (see also Maneerat and Daudé [2016]). The model outputs showed that populations in urban landscapes with a homogeneous spread of vegetation, dispersed for longer distances than population within a landscape characterised by clustered vegetation, such as big urban parks. Furthermore, in urban landscapes with a spread vegetation, we observed invaded pixels at further distance from the introduction locations at the end of the winter (end of simulations). When favourable habitat is clustered in isolated patches, *Ae. albopictus* mosquitoes do not need to move for long distances to find new suitable habitats. Moreover, at the edge of the favourable patch, we may assume that a mosquito avoids moving in the hostile urban matrix, and remains in the favourable patch of suitable habitat. On the contrary, when suitable patches (i.e. densely vegetated) are evenly spread across the urban matrix, mosquito populations more easily move to exploit new unoccupied patches. In brief, an urban landscape with vegetation spread across the matrix is more permeable to *Ae. albopictus* dispersion. Interestingly, this trend was also observed, and even particularly evident, for very low vegetation abundances.

The flight dispersal and local *Aedes* mosquitoes population density play important roles in mosquito-borne pathogen such as dengue virus in urban environments [Kim et al., 2006; Raghwani et al., 2011; Karl et al., 2014; Guzzetta et al., 2016]. We found that the *Aedes* abundance trend was strictly related to the air temperature, with the population starting to grow when temperature reached a peak and decreasing drastically when the temperature dropped below 15 °C [Delatte et al., 2009]. However, despite a similar trend, the average abundance distribution amplitude was highly variable across the considered urban landscapes. As a consequence, the structure of the urban landscape has to underlay the observed variability in *Aedes* abundances. Differences in vegetation coverage in the urban landscape did not directly affect the average mosquito population density. Conversely, mosquito density was always higher in landscapes with vegetation evenly spread compared to landscapes with vegetation concentrated in large isolated patches. This trend was particularly evident when the vegetation abundance was held very low. It derives that low vegetation coverages in urban landscapes can still support moderate to high localised mosquito density, given that the vegetation is evenly spread across the matrix. We can further speculate, using population ecology concepts, that large isolated vegetation patches act as ”magnet“ habitats for introduced mosquito populations. These patches are highly attractive for mosquitoes and as such they have low rates of emigration. On the contrary, when the vegetation is spread across the urban landscape, mosquitoes have a higher chance of finding new unoccupied suitable patches in the nearest neighbour set, increasing the total mosquito abundance in the urban landscape.

Our results demonstrated that vegetation abundance in urban landscapes does not directly affect the success of invasion as well as density and spread of *Ae. albopictus* population after a year from introduction. On the other hand, vegetation configuration seems to have an important role in affecting *Ae. albopictus* invasion dynamics. Our simulations indicate that vegetation scattered across the landscape may positively affect the invasion and population dynamics of *Ae. albopictus* in urban areas. Small wooded vegetation patches evenly distributed across the urban landscape may act as stepping stones and facilitate an introduced *Aedes* population in finding new suitable unoccupied breeding sites [Reiter, 1996; Vezzani et al., 2001]. As a result, the mosquito population will have higher chances to survive periods of adverse weather conditions as well as other potential mortality factors. This configuration of urban vegetation may also have consequences on mosquito control activities. Indeed, having many small patches of suitable habitat across the landscape (i.e. private gardens) makes public *Ae. albopictus* control strategies expensive and hard to implement. Thus, organised control (by public agencies) interventions may fail to decrease mosquito abundances. In the absence and/or failure of public control interventions, private citizens self-organise to control high mosquito densities in their private yards, implementing peri-domestic insecticide spraying which, despite being effective

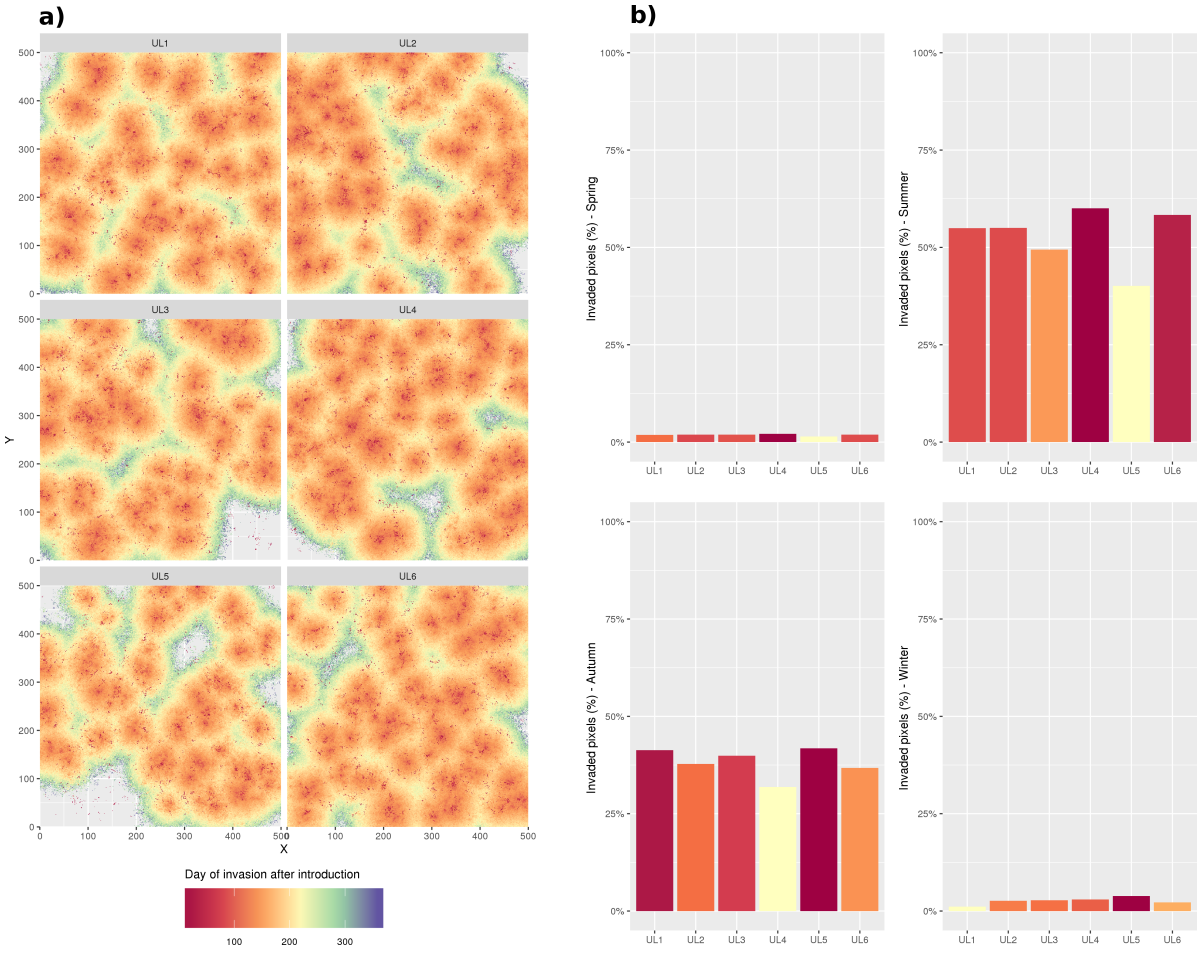

Figure 5.7: *a)* The spatial distribution of first day of invasion from introduction date (2006-03-01) across all the 1000 simulated introductions is reported with a red-blue palette. In the case of a pixel invaded more than once, i.e. in different simulations, the reported first day of invasion was calculated as the average value of all the first invasion days. *b)* The percentage of new invaded pixels in each season for all the simulated urban landscapes.

on the short run, fails to keep low mosquito abundance for a long period. The uncontrolled frequency of insecticide treatments, besides having obvious risks to environment and human health, may boost development of mosquito resistance [Caputo et al., 2015]. Implications on the transmission of mosquito-borne pathogens are also expected, since the distributions of mosquito populations in urban areas (i.e. skewed vs uniform) has been shown to have a significant effect on mosquito-borne disease incidence [Adams and Kapan, 2009]. For example, large mosquito populations in places that are visited by a large fraction of the human population, such as public park, may cause higher disease incidence in urban areas.

We are aware of the limitations of this study, based on the simulation of urban landscapes which may not fully represent the variability observed in current cities. Furthermore, the

considered modelling approach, despite being validated and rooted in real data, is still a partial representation of life cycle and spatial dynamics of *Ae. albopictus*. However, the theoretical framework presented in this work remains valid and can be extensively further developed to explore other facets of the Asian tiger mosquito urban invasion dynamics [Suzán et al., 2015].

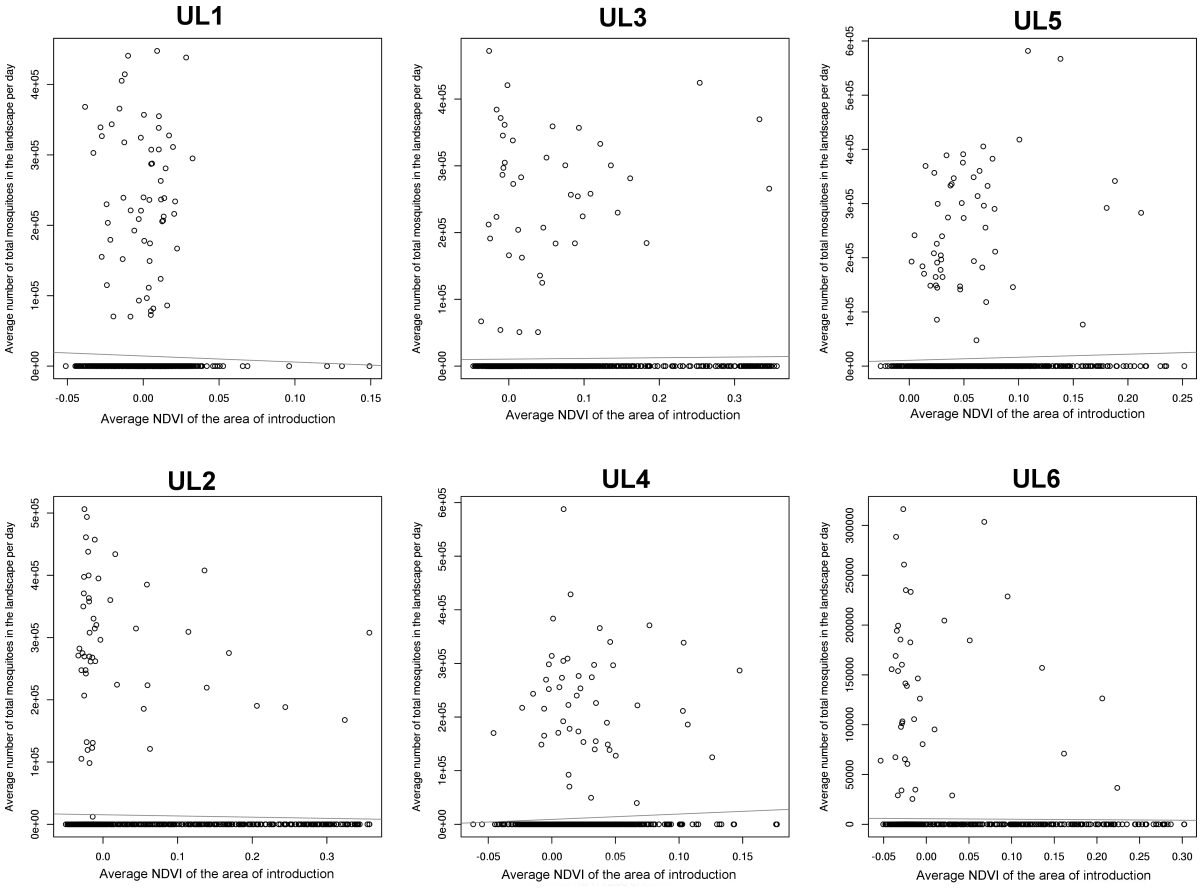

Figure 5.8: The relationship between the average abundance of mosquitoes for all the simulated period of time and the NDVI average value of the area of introduction (defined as introduction pixel plus the 399 nearest neighbours). Each circle represents a different introduction of the 1000 simulated.

5.5 Conclusion

Climate change will undoubtedly boost the geographical range expansion of *Aedes* mosquitoes. Indeed, climatic factors will represent the major constraints on their expansion extent at very large spatial scales. However, despite the widespread mitigation efforts to decrease the climate change rate, the effect of human population growth on *Aedes* mosquitoes invasion and *Aedes*-borne pathogen transmission dynamics will likely be larger [Monaghan et al., 2016]. Population growth is closely linked with urbanisation, a trend predicted to increase in the next decades. Hence there is small doubt that urban areas will be critical spots for controlling transmission of *Aedes*-borne viruses [Karl et al., 2014; Unlu et al., 2016]. Thus, a firm understanding of urban ecological mechanisms becomes of paramount importance to design more resilient cities through informed environmental and smart planning [Steiner, 2014].

We suggest that conceiving urban environments with few large natural vegetated areas may not only lower *Ae. albopictus* mosquito invasion risk but may also facilitate prevention, mitigation and control actions. At the best of our knowledge, we are not aware of drawbacks of this vegetation configuration with respect to the others evaluated in this study. Davis et al. [2016] found that vegetation scattered in the matrix in urban areas is important for mitigating urban area temperatures. However, as they state in the manuscript, this pattern was due to the fact that this type of vegetation was by far the most abundant in the urban matrix and not due to a particular property of this vegetation configuration itself.

To conclude we want to highlight that large urban green areas also contribute to human well-being, as well as maintaining higher biodiversity than smaller vegetation patches [MacArthur and Wilson, 1967; Szlavecz et al., 2011]. We call for more studies and *ad hoc* data collections on the effect of vegetation configuration in urban areas respect to *Aedes* invasion dynamics to confirm the findings achieved in this study.

Chapter 6

Aedes albopictus Skuse aboveground micro-habitat: quantifying temperature variability and the mismatch with regional data

Marcantonio, M, Baldacchino, M, Montecino, D, Arnoldi D, Barker C, Rizzoli A, (in prep.). *Aedes albopictus* aboveground micro-habitat: quantifying temperature variability and the mismatch with regional data.

Abstract

The worldwide spread of *Aedes* mosquitoes is among the biggest threats for public health posed by environmental changes. Mitigation actions are effective when targeted in space and time, therefore we need to pre-locate the spatio-temporal conditions suitable for *Aedes* populations using statistical or mathematical models. Temperature data is widely used for model parameterisation as it is the main factor driving the mosquito life cycle, however it is usually chosen opportunistically (e.g. nearest weather station). Mosquitoes have an "amphibious" life history, and exploit a variety of micro-habitats. The characteristics of these micro-habitats can strongly vary and are highly localised such that they may diverge from the surrounding conditions. As such the thermal properties of these micro-habitats are unique and consequently modelling efforts can be hindered by the input temperature data. Here, we present data from an experimental cross factorial design, performed for one year in Northern Italy to assess the thermal characteristics of aboveground *Aedes albopictus* micro-habitats for all life stages. Artificial breeding habitats were built, and internal water, external water and air temperature of putative resting sites was measured under semi-controlled environmental conditions. The aims of this project were to: *i)* define the thermal characteristics of aboveground *Ae. albopictus* micro-habitats; *ii)* estimate temperature difference distributions between micro-habitats; *iii)* investigate how the use of micro-habitat rather than generic temperature data changes estimated *Ae. albopictus* life cycle durations. Data were pre-processed to minimise errors and the differences examined using a Bayesian Analysis Of Variance. The micro-habitat temperature variability was quantitatively characterised, providing probability distributions of their differences. These data are now available to be implemented in mathematical and statistical models for different facets of *Aedes* invasion processes and patterns. A high variation in temperatures was observed between different micro-habitats and also between micro-habitat, weather station and remotely sensed temperatures. As a result, when applied to temperature-dependent functions describing the processes of *Ae. albopictus* life cycle, the duration of these processes drastically changed. Considering the variability in micro-habitat temperatures as well as differences between micro-habitat and other commonly used temperature data in *Ae. albopictus* modelling improves our ability to predict the mosquito life cycle duration or habitat suitability, with potential positive consequences for control actions.

6.1 Introduction

The Asian tiger mosquito, *Aedes albopictus* (Skuse), is a highly invasive species which commonly inhabits man-made containers, and has a global distribution [Benedict et al., 2007]. *Aedes albopictus* is a competent vector of at least three globally important mosquito-borne viruses such as chikungunya, dengue, and Zika virus [Grard et al., 2014]. The control of population density and mitigation of mosquito spread are critical for limiting the risk of disease agent transmission worldwide. Control actions are more effective when a diverse set of tools are integrated and when they are targeted in both space and time [Faraji and Unlu, 2016; Unlu et al., 2016; Baldacchino et al., 2016]. To target a control action requires an understanding of the spatio-temporal conditions which are highly suitable for *Aedes* populations, in order to anticipate population density hotspots and potential spread pathways. Statistical or mathematical models have long been used for this purpose, from local to worldwide geographical extensions (e.g. Benedict et al. [2007]; Neteler et al. [2013]; Kraemer et al. [2015]). Mosquitoes are poikilothermic animals, meaning that their life cycle is heavily driven by temperature variations, therefore temperature data underpins any model parameterisation. This data is often opportunistic, such as from the weather station nearest to the study area or temperature surfaces derived from spatio-temporal interpolation of several sparse weather stations. In the last decades satellite remote sensors such as MODIS or AVHRR have allowed the derivation of spatially and temporally continuous temperature data, enriching the available temperature datasets [Metz et al., 2014]. Due to its unprecedented characteristics, this data is more and more used in the modelling scientific literature [Roiz et al., 2011; Brady et al., 2014; Cianci et al., 2015; Marcantonio et al., 2016]. Despite its broad application, remotely sensed temperature data has limitations such as missing data due to cloud gaps, moderate spatio-temporal resolution and inhomogeneity due to sensors turnover. These issues, which are sometimes overcome using data harmonisation, gap-filling and spatio-temporal downscaling algorithms but are often simply ignored, limit the application of remote sensing temperature data in ecological modelling. Moreover, remote sensing instruments do not directly measure temperature, but radiances in the thermal infrared region which are then converted into surface temperature using split-window techniques [Li et al., 2013].

Mosquitoes have an “amphibious” life history, experiencing surface, water and air temperatures, by having terrestrially fixed eggs, aquatic immature larvae and flying adults [Becker, 2010]. Moreover, among mosquitoes, *Aedes* species are ecologically very plastic [Waldock et al., 2013] being able to exploit a variety of micro-habitats, including those which are human-made, during their lifetime [Paupy et al., 2009]. The characteristics of the micro-habitats colonised during a life cycle can strongly vary and, at the same time, diverge from the surrounding conditions [Becker, 2010; Yee, 2016]. The thermal properties of *Aedes* micro-habitats are

unique too and, as a result, the efforts to model *Aedes* mosquito distributions can be jeopardised by the consideration of sub-optimal temperature data series [Paaijmans et al., 2010; Yee, 2016]. In this regard, Vallorani et al. [2015], modelling *Ae. albopictus* population dynamics, found that applying catch basin temperature, among *Ae. albopictus* breeding habitats in Central Italy, rather than generic air temperature, induces an increase in the estimated length of development season of the mosquito. An increasing number of scientific studies call for a better estimation of the thermal characteristics of mosquito micro-habitats in order to achieve more reliable life cycle and distribution models [Paaijmans et al., 2010; Vallorani et al., 2015; Asare et al., 2016].

Energy budget models can be used to simulate temperature in mosquito micro-habitat conditions. In spite of some interesting attempts made for *Anopheles* breeding habitats in Africa and Southern-East Asia [Ohta and Kag, 2011; Asare et al., 2016], or for the pitcher plant mosquito (*Wyeomyia smithii*; Kingsolver [1979]), there is a lack of similar studies applied to *Aedes* species micro-habitats. This lack of studies is linked to the species strong preferences for artificial breeding and resting habitats, from cans to containers with a capacity of several hundred litres, which are partially detached from the surrounding environmental conditions [Waldock et al., 2013]. An alternative and empirical strategy to improve our understanding of *Ae. albopictus* micro-habitat thermal property can be the implementation of a semi-controlled experimental design, that allows us to characterise and generalise micro-habitat properties, controlling for the desired environmental conditions [Watt and van den Berg, 2002; Thomas et al., 2012].

Here, we present data from a semi-controlled experimental design carried out in Northern Italy to gain knowledge on the thermal characteristics of aboveground *Ae. albopictus* micro-habitats for all life stages. Aboveground man-related breeding habitats are among the main breeding habitats for *Ae. albopictus* in urban and rural areas worldwide [Yee, 2008; Paupy et al., 2009; Bartlett-Healy et al., 2012; Baldacchino et al., 2016]. With the help of expert entomologists, we built artificial breeding habitats and located putative resting sites to set up a cross factorial experimental design to measure water, just above water and air temperature of putative resting sites in different environmental settings. Gravid *Aedes* females lay eggs inside water filled containers just outside the water, where they will hatch after flooding. As a consequence, temperature just outside the water impacts on eggs mortality and maturation process. After hatching, larvae pass through 5 different immature aquatic stages. Water temperature in the container influences the development of each of these aquatic stages as well as the size of female adults that can affect their capacity to transmit pathogens [Haramis, 1984; Lounibos, 2002; Westbrook et al., 2009; Carrington and Simmons, 2014]. *Aedes albopictus* are mainly exophilic, and air temperature of putative resting sites determines their survival and

development, their capacity to transmit pathogens, and also drives other physiological phases such as oviposition and gonotrophic cycle duration [Hawley, 1988].

We compared the recorded temperature data among them, focusing on winter, spring and summer seasons. Furthermore, we applied the recorded temperature, the temperature time series from the nearest weather station (hereafter, WS) and remote sensed Land Surface Temperature (LST) to *Ae. albopictus* life cycle temperature-dependent functions. The main aims of this project were to: *i)* define the thermal characteristics of aboveground *Aedes* micro-habitats in the study area; *ii)* estimate temperature difference distributions between micro-habitats that can be generalisable to other locations and *iii)* investigate how the use of micro-habitat rather than generic temperature data changes estimated *Ae. albopictus* life cycle durations.

6.2 Materials and Methods

6.2.1 Study area and experimental design

The study area was located inside the Fondazione Edmund Mach (FEM) research centre estate in San Michele all'Adige, Italy (46.2°E, 11.13°N). The location was chosen as it has been colonised by *Ae. albopictus*, which first became established in the area in 2001 [Ferrarese, 2010]. Across the study area, we built a 3x4x2 crossed experimental design with repetitions to reproduce mosquito micro-habitats under different environmental settings. Thus, temperature time series were recorded for 18 different semi controlled experimental conditions (Figure 6.1).

A micro-habitat was defined as an artificial, hard plastic, water filled container (for eggs, larvae, emerged adults) or a resting site (developed adults). The controlled environmental conditions (experimental factors) were solar exposure (or openness, Ex), water amount (Wa) and location respect to the water (Wp). The levels of each experimental factor were chosen in order to include the full range of conditions experienced by *Ae. albopcitus* during a life cycle. These three environmental factors can be considered as the main sources of variability of temperature in *Ae. albopictus* artificial micro-habitats [Beier et al., 1983b; Berry and Craig, 1984]. The openness of a micro-habitat affects both the available energy, by affecting the total amount of direct solar radiation, and the input of organic detritus. The water volume determines the flux of absorbed, stored and released energy. As we know that these factors do have an effect on the micro-habitat temperature, this project aimed to quantify the distribution of differences due to the levels of each environmental factor, as well as to their interactions, rather than testing the null hypotheses that they cause a change in temperature.

The Ex factor had three levels representing the extremes and a midpoint for micro-habitat solar exposure: *i)* Full shadow (ExLv1). We defined the "full shadow" or "sheltered" condition

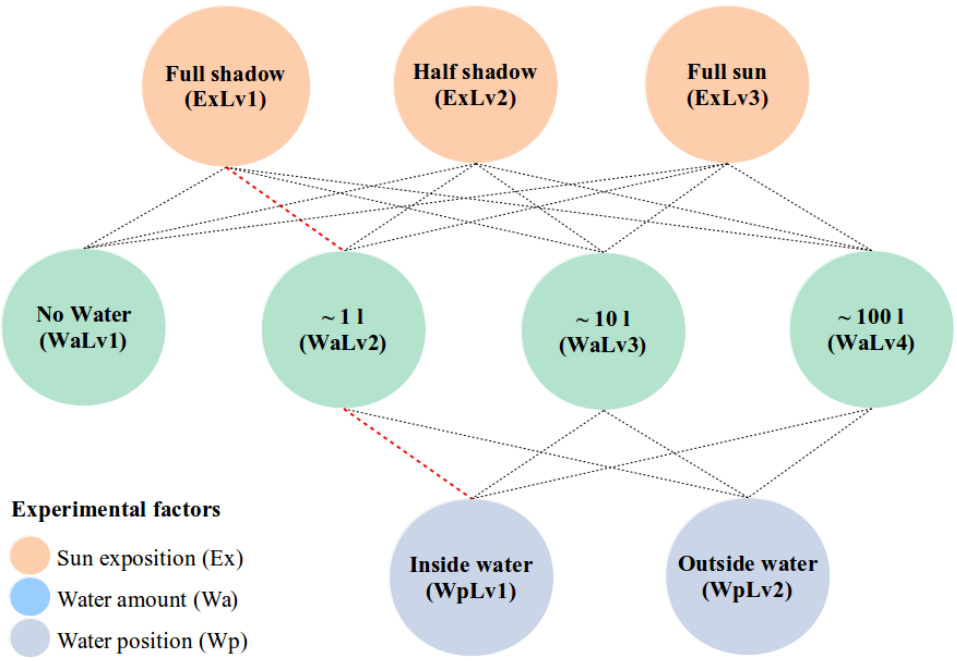

Figure 6.1: Experimental design. The circles represent the levels of each experimental factor. Levels of the same experimental factor are reported on the same row and in the same colour. Each dashed line connects circles that result in each of the 18 different experimental conditions for which a sensor was a temperature sensor was placed. As an example, the sensor in ExLv1-WaLv2-WpLv1 (highlighted in red) measures the temperature inside 1 l of water in full shadow.

as a location that did not receive direct solar radiation from sunrise to sunset for at least 95 % of the day on average with clear sky conditions; *ii)* Half shadow (ExLv2), defined as a location that received direct solar radiation for about 50 % of the day on average; *iii)* Full sun (ExLv3) or "open habitat", defined as a location that received direct solar radiation for at least 95 % of the day on average (Figure 6.2). The three levels of the Ex factor were represented by three different sites in the study area, located not more than 500 m apart (Figure 6.2). In order to facilitate reproducibility, we further characterised the openness and amount of solar radiation reaching each site using fish-eye photography processed with an imaging software, data from the Photovoltaic Geographical Information System (PVGIS; http://re.jrc.ec.europa.eu/pvgis/) and a sun-path model (refer to Appendix F for further details).

The factor Wa had 4 levels representing water volume in the vicinity of the micro-habitat container or the resting site (no water). The range of water volume in an artificial micro-habitat was decided based on the scientific literature on the topic [Hawley, 1988; Bartlett-Healy et al., 2012; Baldacchino et al., 2016; Faraji and Unlu, 2016] and expert entomologist opinions, as follows: *i)* Resting site (WaLv1), resting sites were selected as sheltered locations hidden in

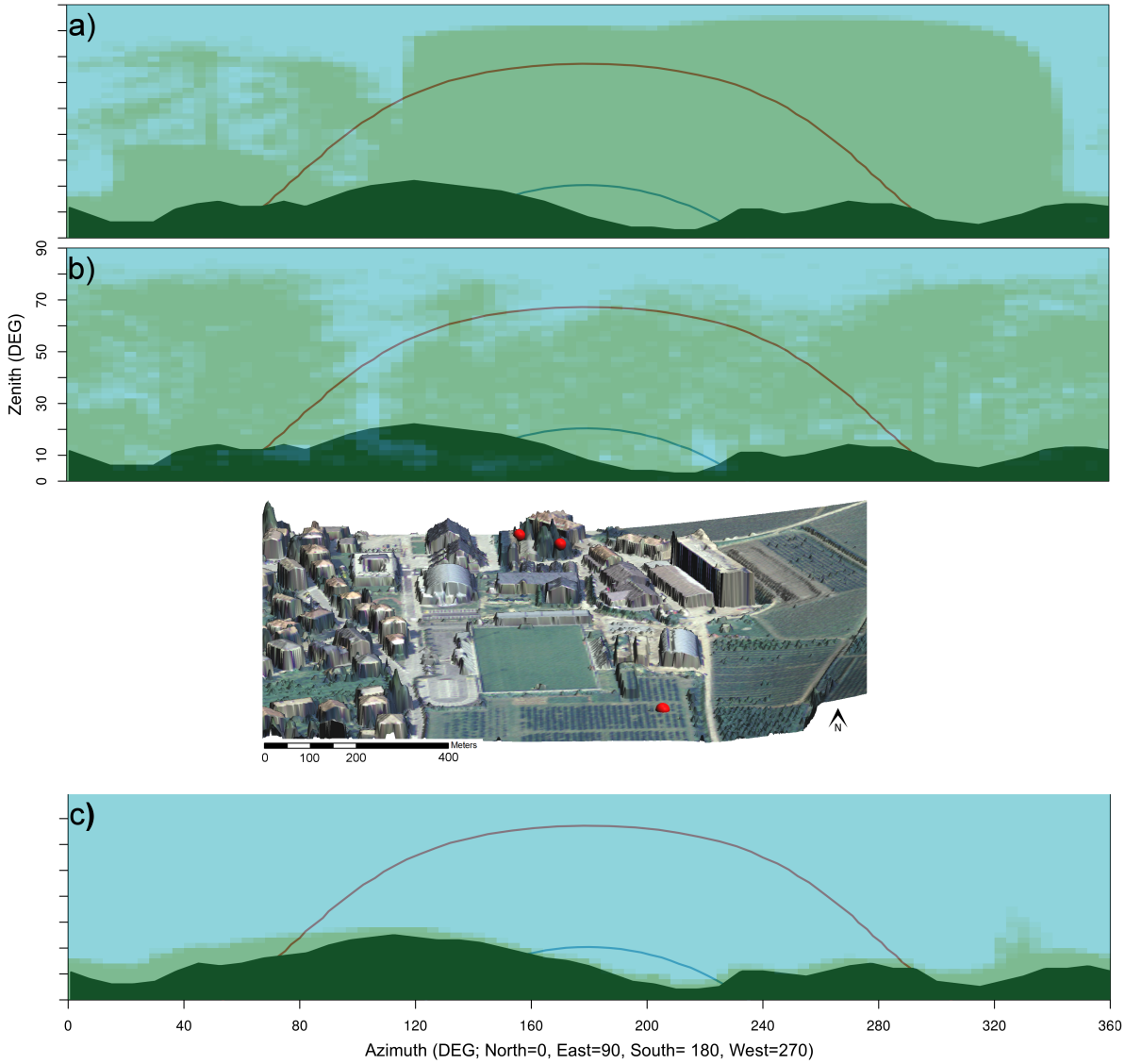

Figure 6.2: At the centre of the figure is reported a 3D representation of the study area (FEM) obtained by overlapping a natural colour orthophoto to a digital surface model. The 3 red spheres indicate the locations of the three experimental sites, representing *Ae. albopictus* micro-habitats with different solar exposures. The openness of each experimental site was firstly qualitatively determined and later quantitatively described as reported in Appendix F and in Figure *a)*, *b)*, and *c)* for full shadow, half shadow and full sun conditions, respectively. In this Figure, the "openness" represents the percentage of open sky seen from the centre of each experimental site and is plotted against the azimuth angle with a light blue–dark green continuous palette. As such, the dark green pixels represent topographical obstacles (i.e. hills, mountains), while the light green pixels represent semi-permanent non-topographic obstacles (e.g. trees, shrubs, buildings). The light blue pixels are clear sky areas, therefore they represent gaps where direct solar radiation can penetrate and reach the experimental site (i.e. an *Ae. albopictus* micro-habitat). The red parabolic curve is the sun path at its peak (summer solstice) while the blue curve is the sun path at the winter solstice.

vegetation pockets in the vicinity of the water tanks (e.g. bushes or shrubs; Panella et al. [2011]; ECDC [2012]); *ii)* ∼1 l of water (WaLv2); *iii)* ∼10 l (WaLv3); *iv)* ∼100 l (WaLv4). Finally, the experimental factor Wp had two levels: *i)* Just outside water (5–10 cm; WpLv1); *ii)* Inside water (10–50 cm; WpLv2). The containers were all made of hard plastics with colour consistent at least among blocks.

A total of 18 experimental combinations were therefore defined. We repeated twice each of the experimental combinations. The repetitions were placed as near as possible (never more than 5 m), to avoid unwanted spatial variability in the experimental conditions. As a result, a total of 36 temperature sensors were placed. The containers were checked weekly and refilled with tap water when the water volume had decreased by more than 15 %. Half hourly temperature data was collected from the 1st December 2015 to the 31st August 2016.

6.2.2 Temperature sensors and data organisation

Temperature sensors were two different model of iButton® (Maxim Integrated, US), DS1923 and DS1921G-F5 respectively. The first sensor model measures only temperature, has a resolution of 0.5 °C and an accuracy of 1 °C, while the second measures temperature and humidity, has a resolution of 0.1 °C and accuracy of 0.5 °C. Humidity was recorded but not considered in this study. These sensors are water resistant but not waterproof, thus in order to ensure their duration under water, we placed them in 50 ml Falcon™ tube (for 10 l and 100 l water volumes) or a 35x10 mm Falcon™Petri dish (for the 1 l water volume), sealed with parafilm. We tested for potential bias in the recorded temperature due to the shells, leaving two sensors (one each for the two models) inside the two type of shells under ice for 24 h. The measured temperature stayed constant at 0.0 °C for all the experiment duration, revealing no shell influence on the recorded temperature.

The two sensor models have an integrated memory of 16 and 64 kB, resulting in 2048 and 8192 8 bit readings, respectively. The recorded data was downloaded through 1-Wire iButton reader once per month and stored in a PostgreSQL geo-database (https://www.postgresql.org/), freely available by request to the corresponding author.

6.2.3 Other temperature data source

Two other temperature data series for the period from the 1st December 2015 to the 31st August 2016 were also recorded: *i)* hourly data from the weather station nearest to the study area (46.18°N, 11.10°E) and *ii)* 4 daily (at 01:30, 10:30, 13:30, 22:30, respectively) Land Surface Temperatures (LST) from the Moderate Resolution Imaging Sensor (MODIS) instruments on board the Terra and Aqua satellites (from the 1st December 2015 to the 10th August 2016).

The MOD11A1 and MYD11A1 MODIS products were downloaded from a NASA server (https://lpdaac.usgs.gov/data_access), and then gap-filled through a harmonic analysis of time series [Roerink et al., 2000]. Afterwards, a temperature time series was extracted from the same coordinates of the weather station. All the spatial analysis were performed in GRASS GIS 7 [Neteler et al., 2012]. The four LST daily data were interpolated using a linear interpolation in order to achieve hour temporal grain. The weather station and LST temperature time series were used to assess the mismatch between *Ae. albopictus* life cycle duration estimated using micro-habitat temperature and generic temperature data.

6.2.4 Statistical analysis

Firstly, we averaged the temperatures recorded by the iButton sensors in the two repetitions carried out for each crossed experimental condition. This step was performed in order to marginalise outliers due to errors in the temperature recording process (manipulation by humans, temporal sensor failure, etc.). The repetitions were not treated as random deviates from an unknown distribution ("random effects") as we assumed that the random variation in temperature sensors placed few meters each other, and under the same "controlled" conditions, is not-influential for our scientific questions. Repetitions were performed merely to assure that temperature were recorded continuously along all the considered period. Afterwards, the iButton temperature series were averaged to an hourly basis and the missing values were filled using a linear interpolation. Finally all the iButton temperature data series were smoothed using a rolling mean with a 3 h rolling interval. Besides error filtering, the temperature data averaging on an hourly basis was performed since sub-hourly fluctuations in temperature can be considered as marginally important for *Aedes* mosquitoes life cycle durations [Paaijmans et al., 2010; Carrington and Simmons, 2014].

We learned the relative importance of different sources of variation in micro-habitat temperatures focussing on winter (December to February), spring (March to May) and summer (June to August) months using a Hierarchical Bayesian Analysis of Variance (BANOVA; Kruschke [2015a]). The goal of this analysis was to describe temperatures as a function of three nominal predictors (experimental factors) and to provide information about the trends in the data as well as the uncertainty in these trends. The Bayesian approach is a hierarchical generalisation of the traditional ANOVA, which accommodates for outliers and heterogeneous variance in the different groups. We implemented a BANOVA hierarchical model in R and JAGS 4.2.0 following Gelman and Hill [2006] and Kruschke [2015b]. The implemented hierarchical model assumes that the recorded temperature data are t-distributed around the predicted value. The predicted value is composed of a baseline value (overall average) plus the group (experimental factors and levels) and interaction (between levels) deflections, which come from a gamma

distribution different for each group and interaction. The mode and scale of the gamma distributions are estimated by the model, with priors that are vague on the scale of the data. This model hierarchical structure causes the standard deviation of each group to mutually inform the standard deviation of other groups. We ran 10000 iterations to allow JAGS to find an optimal set of initial values for the sampler. After further 10000 burn-in iterations, we sampled 100000 times the Posterior Probability Distribution (PPD) of the model parameters from 10 different chains to estimate the main and interactions (non additive influence of the factors) deflection for each factor. Visual and diagnostic inspections were then performed to check the chains representativeness and accuracy.

We calculated main and interaction contrasts for our set of data. The contrasts were calculated considering that each step of the MCMC chain provides a credible difference between groups. To avoid bias due to potential autocorrelation of parameters, we calculated contrasts between groups cancelling out the baseline, so that the credible difference (δ) between two hypothetical groups A and B is defined as:

$$\delta AB = \mu A - \mu B = (\beta 0 + \beta A) - (\beta 0 + \beta B) \tag{6.1}$$

where:

$\beta 0$ = baseline value.
βA = deflection parameters for group A
βB = deflection parameters for group B

The model parameter PPDs were therefore summarised and listed using their average value and the 95 % High Density Interval (HDI). Moreover, the PPD of main and interaction contrasts were reported through histograms. We defined a deflection or a contrast to be credibly different from zero when the 95 % HDI did not include zero. The HDI indicates which points of a distribution are most credible, so that at any point inside the interval it has higher credibility than any point outside the interval. The BANOVA was performed using mainly the runjags [Denwood, 2016] and coda [Plummer et al., 2006] packages in R [R Core Team, 2016].

6.2.5 *Aedes albopictus* estimated life cycle duration

In order to assess how different temperature data series affect the estimation of *Ae. albopictus* life history, we applied two temperature-dependent functions describing *Ae. albopictus* life cycle process duration. Firstly, the function describing the temperature-dependent adult survival rate was derived fitting a parametric survival regression to lab temperature-dependent survival

data from Armijos [Armijos, 2016]. We considered the temperature and its square as predictors, after performing model selection. Secondly, we estimated *Ae. albopictus* temperature-dependent immature to adult development rate applying the temperature-dependent enzyme kinetic function proposed by Sharpe and DeMichele [1977] to *Ae. albopictus* temperature-dependent development data retrieved from the literature Delatte et al. [2009] and an optimisation method as in Nelder and Mead [1965]. In order to exploit the (hourly) temporal resolution of the recorded temperature series, the *Ae. albopictus* life cycle data reported in Delatte et al. [2009] and Armijos [2016] were transformed from daily to hourly. The daily rate of survival was considered as a binomial random variable and thus converted to hourly survival probability through the following equation:

$$p_h = {p_d}^{1/N} \tag{6.2}$$

where:

p_h = the hourly survival probability (hereafter *rate* for the sake of simplicity).
p_d = the daily survival rate.
N = the number of Bernoulli trials (in this case 24, representing 24 h).

Afterwards, we used these two functions to derive the adult survival and immature to adult development hourly probabilities for each of the recorded temperature data series. Sharp changes in life cycle duration are key to investigate *Ae. albopictus* population dynamics. For example, a decrease in the gonotrophic cycle duration and larvae to adult development time at the end of the cold season may underlie physiological changes which allow an overwintering mosquito population to rapidly increase in abundance.

To study how different temperature data series influence the temporal location of these important changes in *Ae. albopictus* life cycle, we made use of changepoint detection analysis. Changepoint detection is the problem of estimating the points at which one or multiple statistical properties of a sequence of observations change [Killick and Eckley, 2014]. Applying this concept to the scientific questions considered in this study, this statistics helped find the temporal location of changes in two *Ae. albopictus* demographic and physiologic processes (hourly adult survival and larvae to adult development rates), which lead to significant shifts in population dynamics. We used the segment neighbourhood algorithm for the change points search due to its "exact" nature and due to its flexibility in setting the number of searched changepoints [Auger and Lawrence, 1989]. This algorithm uses dynamic programming to optimise over a cost function for a given number of segments K, based on the optimal solution found for $K-1$. We assumed that, for each of the considered temporal series, there were two

change points (or three neighbourhood segments) in *Ae. albopictus* life cycle probabilities: *i)* end of winter-start of spring, *ii)* end of spring-start of summer. To assess where these two change points were located along the life cycle rates time series, we estimated joint change points for the mean and variance parameters. This joint changepoint analysis was chosen in order to locate segments with similar property in the distribution of their values and was performed using the R package changepoint [Killick and Eckley, 2014].

6.3 Results

We reported the recorded temperature series from the 1st December 2015 to the 31st August 2016 per each combination of experimental factors in Figure 6.3, on which WS and LST time series were also superimposed. The estimated overall micro-habitat average temperature was 3.2 °C (sd 3.9), 13.6 °C (sd 6.0), 22.7 °C (sd 5.8) for the three considered seasons, respectively. The maximum and minimum overall recorded temperatures were −10.3 °C (open site; January) and 54.0 °C (open site; July). Strong temperature variations were observed between the semi-controlled experimental conditions. Variability increased from ExLv1 to ExLv3, and from water (i.e. larvae micro-habitat) to resting site (i.e. adults micro-habitat) to just outside water (i.e. eggs micro-habitat) temperature, while less variation was observed between different water volumes. Moreover, temperature variability remained moderately constant between different seasons for all the cross-conditions but not for ExLv3, whose temperature variation markedly increased from winter to summer, being particularly evident for the small water size (1 l). The differences between inside and external water temperature was very weak for ExLv1 conditions throughout the year.

The BANOVA analysis allowed us to quantify the variability observed between micro-habitat average temperatures during the three considered seasons. The model diagnostics showed that the MCMC converged, while a moderate autocorrelation for the sampled values was found only for model parameters with a high hierarchy in the model (not reported). Thus we could assume the MCMC sampled values as representative of the model PPDs.

The main effects of the environmental factors showed that ExLV3 recorded a credible decrease of 0.55 °C in winter respect to the baseline temperature, while an increase of 0.12 and 1.40 °C in spring and summer time (Table 6.1). ExLv1 and ExLv2 had an inverse trend. Different water amounts did not show any credible deflections but for WaLv4 (100 l) during winter, which was 0.62 °C higher than the baseline. WpLv1 was 0.42 °C higher in winter, while 0.31 and 0.65 °C colder in spring respect to WpLv2.

Importantly, the temperature of each experimental cross-combination of conditions was also affected by interaction deflections (non-additive portions of the explained variability), reported

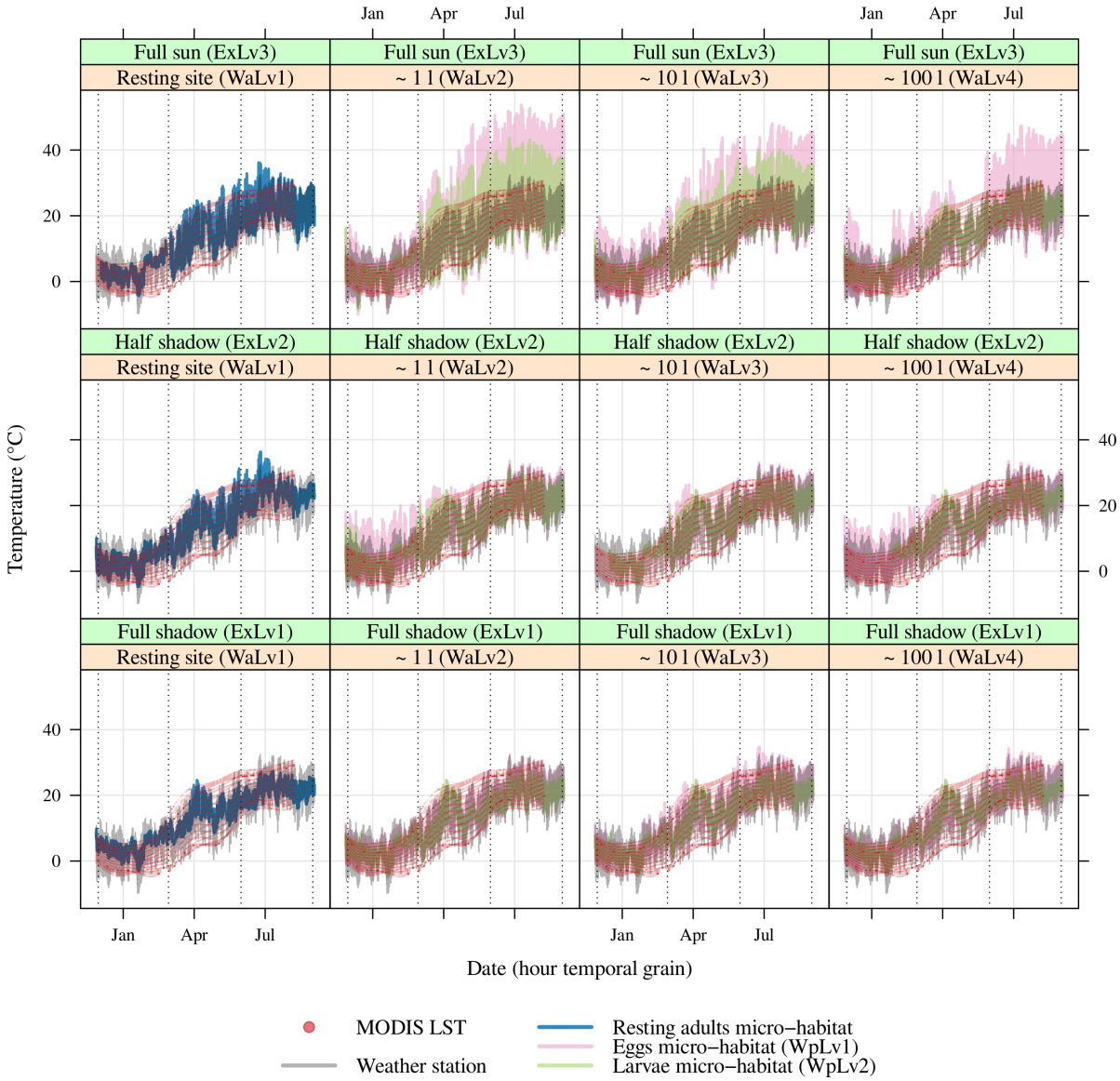

Figure 6.3: the temperature series from the 1st December 2015 to the 31st August 2016 per each combination of experimental factors.

in Appendix G. Despite not bearing credible deflections as main factors, Wa interacted with Ex, reporting credible temperature interaction deflections. The WaLv4 reported temperature always lower than the other levels in ExpLv3, while, when interacting with ExLv1, its influence on temperature was negative in winter, but positive in spring and summer. Considering ExLv3 temperature was higher for WaLv2 in spring and summer, while WaLv4 for ExpLv2 reported higher temperature than any other levels. WaLv1 did not show credible deflections from the baseline.

Table 6.1: The main effect deflections in °C from the baseline temperature for each level of the experimental factors, for each considered season. The second row from the top shows the estimated average temperature in °C (baseline) and HDI of the temperature posterior probability distribution for each season.

		Winter			**Spring**			**Summer**		
		baseline = 3.27			baseline = 13.70			baseline = 22.70		
		(2.86–3.67)			(13.28–14.12)			(22.41–22.98)		
		Main effect deflections								
Factor	Level	Mean	HDI_{low}	HDI_{high}	Mean	HDI_{low}	HDI_{high}	Mean	HDI_{low}	HDI_{high}
Exposition	ExLv1	0.23	0.13	0.34	−0.29	−0.37	−0.21	−1.16	−1.29	−1.05
	ExLv2	0.32	0.19	0.43	0.17	0.09	0.26	−0.23	−0.39	−0.09
	ExLv3	−0.55	−0.65	−0.43	0.12	0.01	0.21	1.40	1.25	1.56
Water amount	WaLv1	−0.02	−1.41	1.44	0.07	−0.91	1.23	0.02	−1.71	1.77
	WaLv2	−0.25	−0.91	0.38	−0.22	−0.77	0.30	−0.11	−0.75	0.55
	WaLv3	−0.35	−1.00	0.30	0.10	−0.43	0.61	0.21	−0.43	0.83
	WaLv4	0.62	0.10	1.23	0.06	−0.48	0.59	−0.12	−0.78	0.52
Water position	WpLv1	0.42	0.15	0.69	−0.31	−0.93	0.01	−0.65	−1.28	0.32
	WpLv2	−0.42	−0.88	−0.01	0.31	−0.41	0.72	0.65	0.04	1.49

The credible temperature difference distributions between the levels of each experimental factor, or main contrasts, were calculated and reported for each season in Figure 6.4, 6.5 and 6.6 (for Ex) and Appendix G (for factors Wa and Wp). ExLv3 had the lowest estimated average temperature for winter, with a credible decrease in temperature of 0.8 °C with respect to ExLv2 and 0.9 °C more than ExLv2. On the other hand, in spring ExLv3 average temperature was lower than ExLv1, and slightly higher (not a credible difference, however) than ExLv2. The three Ex levels strongly differentiated in summer, when ExLv3 was 2.76 and 1.75 °C higher than the ExLv1 and ExLv2.

No significant difference was reported between WaLv1 and the other levels of Wa experimental factor. In winter, WaLv4 recorded the highest temperature, with an increase of 0.7–1.0 °C with respect to the other factor levels. In spring WaLv3 estimated temperature was credibly higher than WaLv2 and WaLv4, while summer did not show any credible difference.

The levels of factor Wp reported WpLv1 with temperature 0.75 °C higher on average in winter, while 0.43 °C and 1.18 °C lower in spring and summer respectively.

Interaction contrasts were also calculated and those between ExLv1 and ExpLv3 were further explored and reported. The difference between these two experimental conditions was about 0.9 °C less when interacting with WaLv2 (presence of small amount of water) than with WaLv4 (large amount of water) in spring (Figure 6.7). Moreover, this difference was 0.6 and 0.4 °C lower when inside than just outside water in winter (Figure 6.8a) and spring (Figure 6.8b) but 0.9 °C higher in summer (Figure 6.8c).

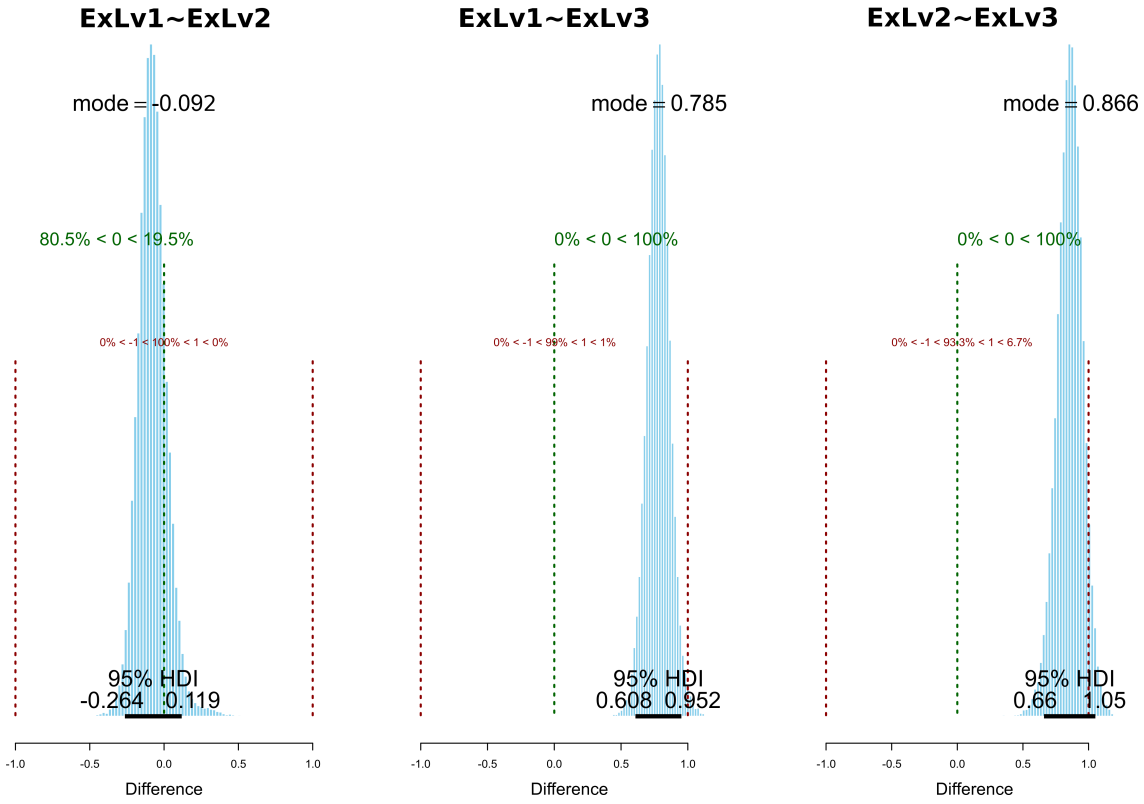

Figure 6.4: The credible temperature difference distributions between the levels of Ex in winter. The percentage of the distribution mass located at the right and left of 0 is reported in green, while the percentage at the left of -1, between -1–1 and at the right of 1 is shown in red.

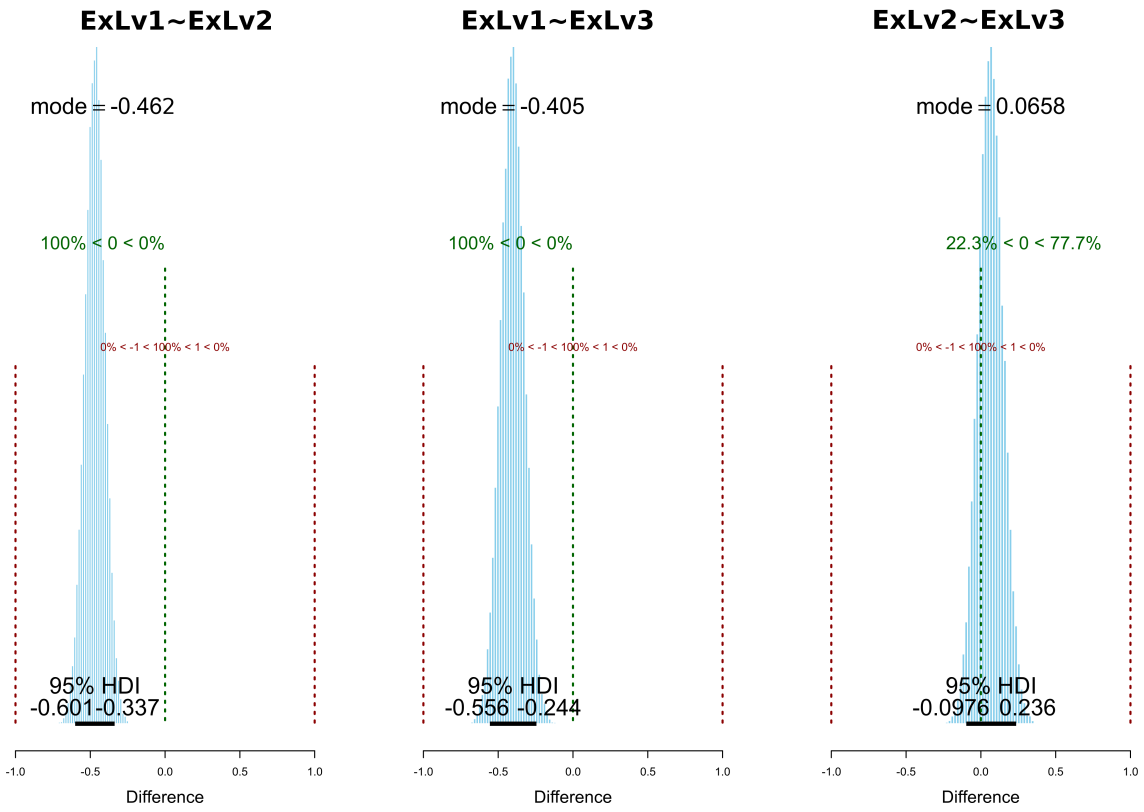

Figure 6.5: The credible temperature difference distributions between the levels of Ex in spring. The percentage of the distribution mass located at the right and left of 0 is reported in green, while the percentage at the left of -1, between -1–1 and at the right of 1 is shown in red.

The estimated hourly life cycle rates ranged between 0–0.01 (larvae to adult) and 0.7–1.0 (adult survival), respectively. Seasonal change points in the estimated larvae to adult development and adult survival rates were reported in Figure 6.9 and 6.10 for the three Ex levels and seasons. Concerning the larvae to adult development rate (Figure 6.9), it always increased from winter to summer, no matter the considered temperature series. Temperature derived from remote sensing (LST) brought about a higher estimated adult to larvae development rate than WS in spring and summer while lower in winter. The WaLv4 had the maximum average rate during spring and summer in ExLv2 and ExLv3. For the ExLv3 conditions, we noticed earlier change points in the larvae to adult rate temporal trend for WaLv2 and WaLv3; ExLv1 showed the same trend but for WaLv3 and WaLv4.

The estimated average adult survival rate varied markedly in winter and spring but less during summer, except for ExLv3. The winter/spring change point in the average adult survival rate was always shifted forward in the seasons when considering WS and LST with respect to the other temperature series. ExLv3 recorded the lowest estimated survival rates when interacting with WaLv2 both in winter and summer. During summer time, the survival rate in the ExLv3 was lower than spring and similar to winter values. All the estimated rate average values as well as the change dates for each estimated change point are listed in Appendix H.

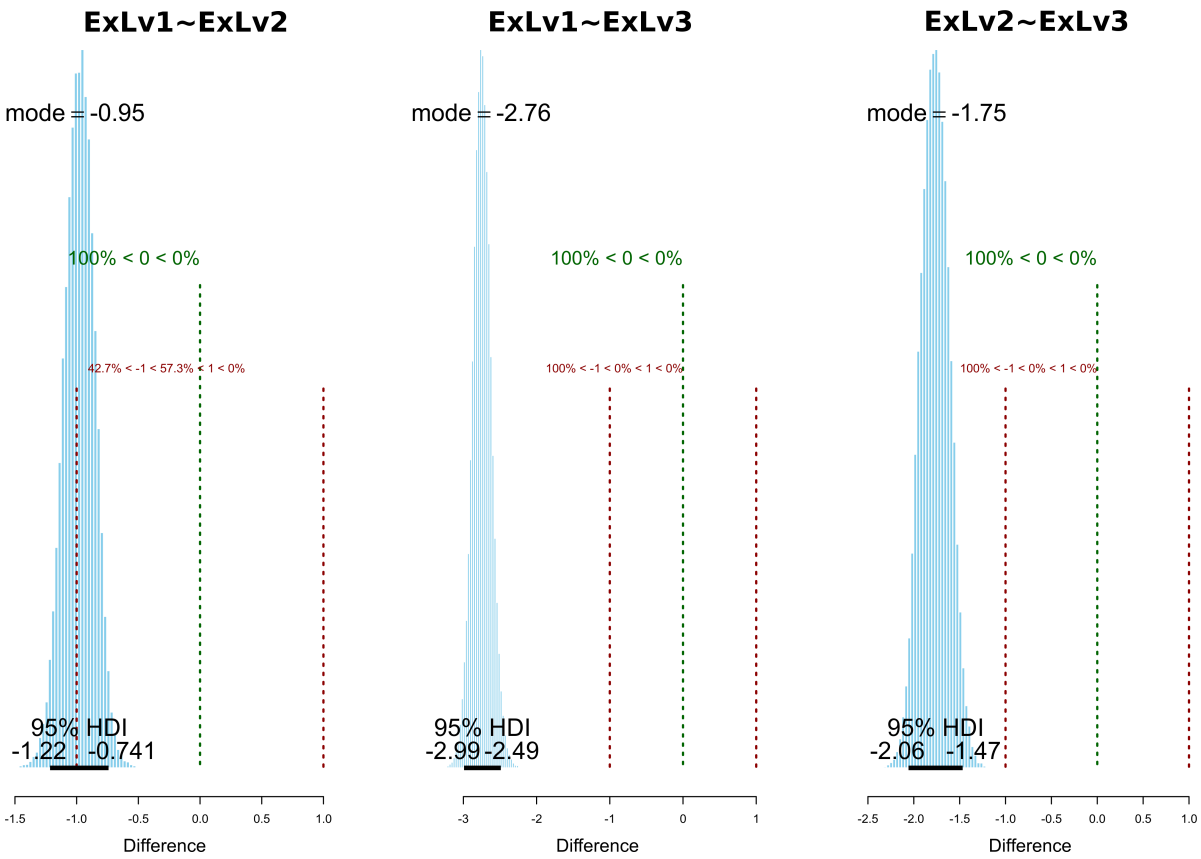

Figure 6.6: The credible temperature difference distributions between the levels of Ex in summer. The percentage of the distribution mass located at the right and left of 0 is reported in green, while the percentage at the left of -1, between -1–1 and at the right of 1 is shown in red.

6.4 Discussion

We recorded temperature in artificial *Ae. albopictus* micro-habitats under semi-controlled environmental conditions. Ambient air temperature, usually averaged across long time spans, is routinely used in mosquitoes population dynamics research, despite the complex ecology of many mosquito species and the known critical role of relatively small temperature change in shaping their life cycle [Waldock et al., 2013]. The semi-controlled experimental approach proposed in this study represents a step towards shedding light on the thermal characteristics of *Ae. albopictus* micro-habitats, crucial to improve our ability to understand their population and spatial dynamics. Differences in micro-habitat temperature were explained by both solar exposure (Ex) and water volumes (Wa) as well as their interactions [Bartlett-Healy et al., 2012]. In spite of this apparently simple trend, a complex interplay of interactions between environmental conditions shaped the temperatures of the simulated *Ae. albopictus* micro-habitat, with ramifications on the estimation of *Ae. albopictus* life history duration [Paaijmans et al., 2010; Vallorani et al., 2015]. Open habitats showed lower temperatures in winter but higher temperatures in spring and summer. This pattern is due to the heat dispersion during winter of open sites and the higher availability of direct solar radiation in spring and summer. Even though warmer temperatures are associated with higher adult mosquito abundance and activity, extremely high temperatures (i.e. above 30 °C) can decrease some development rates and increase adult mortality. The estimated survival rates indicated that the temperature recorded in open conditions (ExLv1) are sub-optimal for *Ae. albopictus* adult survival during summer.

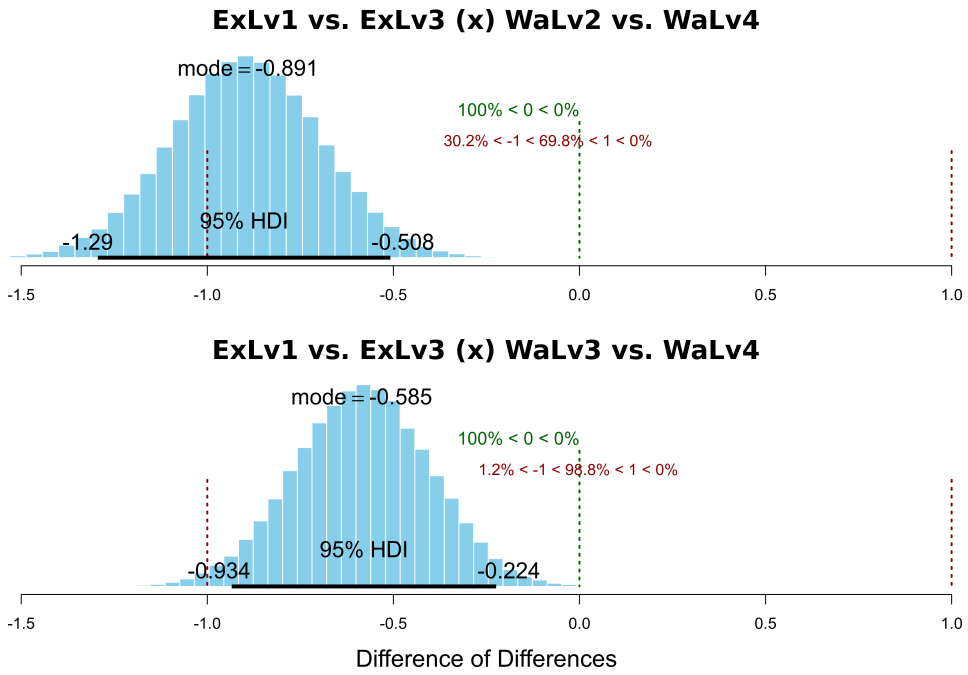

Figure 6.7: Interaction contrasts between ExLv1, ExLv3 and WaLv2, WaLv4 for winter. The percentage of the distribution mass located at the right and left of 0 is reported in green, while the percentage at the left of -1, between -1–1 and at the right of 1 is shown in red.

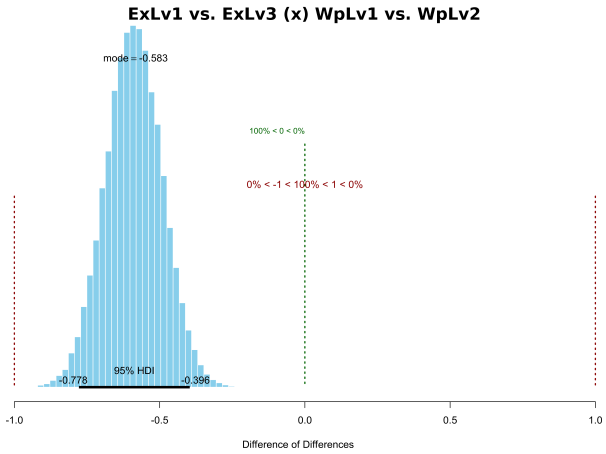

(a) Winter

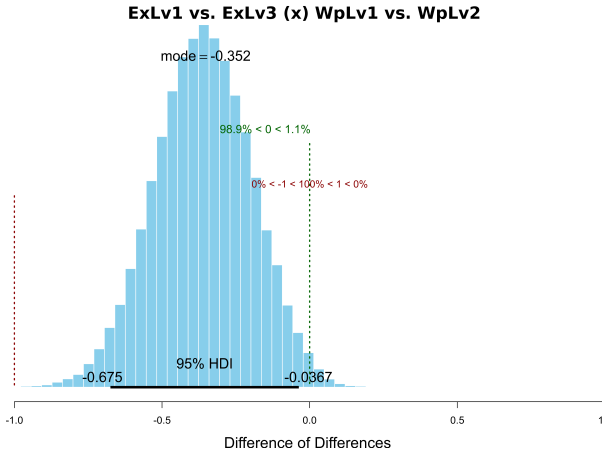

(b) Spring

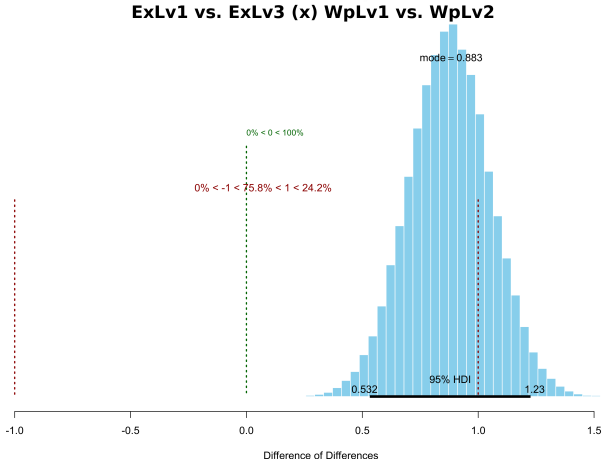

(c) Summer

Figure 6.8: Interaction contrasts among experimental levels ExLv1, ExLv2 and WpLv1, WpLv2. The percentage of the distribution mass located at the right and left of 0 is reported in green, while the percentage at the left of -1, between -1–1 and at the right of 1 is shown in red.

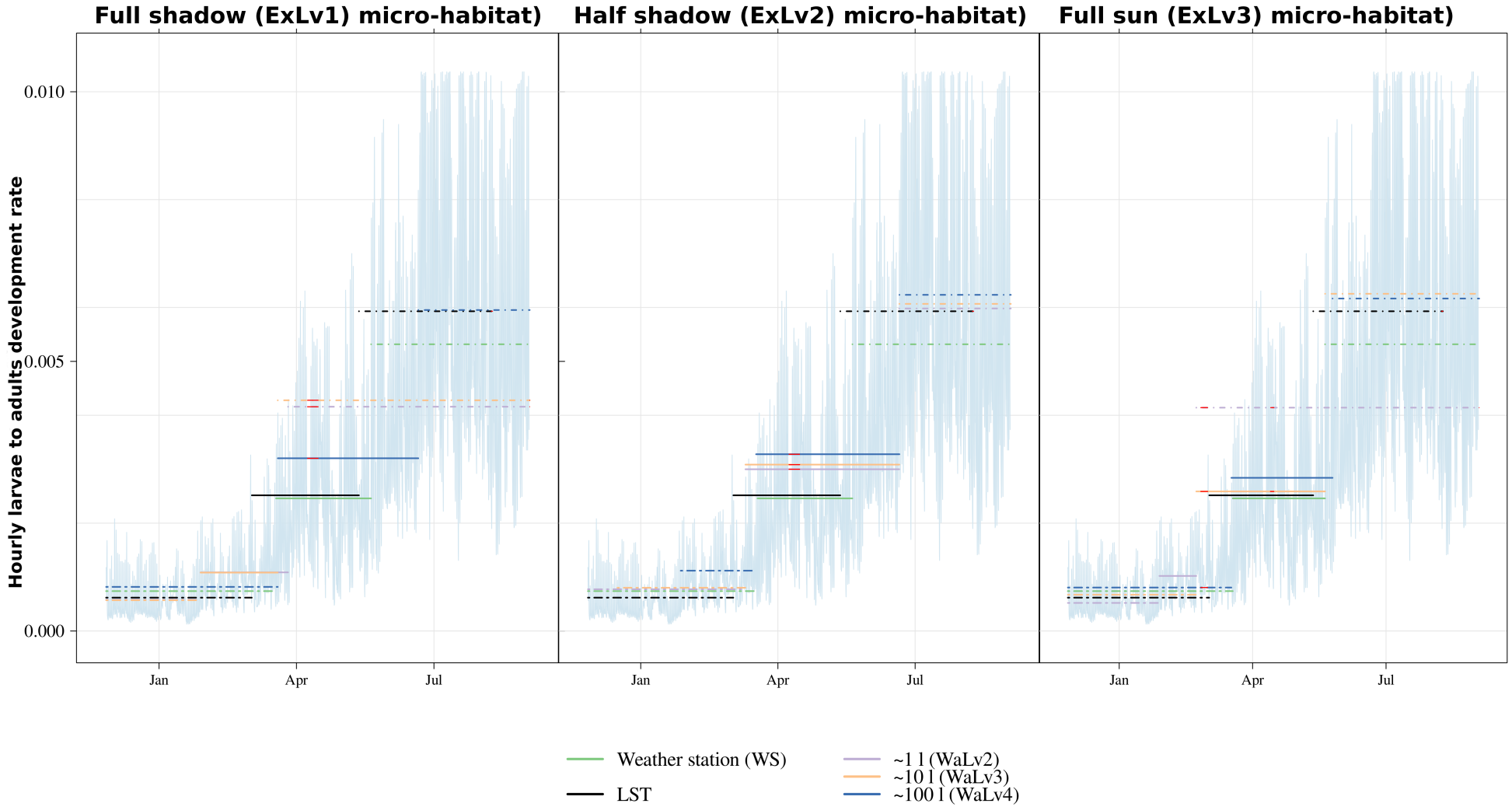

Figure 6.9: Change points in the estimated larvae to adult development rate trend for the three solar exposure (Ex) conditions. The trend derived using the temperature time series from the nearest weather station is reported in grey in the background. The three groups of horizontal lines in each box represent the average rate estimated from one change point to the next for weather station (WS) and LST temperature as well as all water temperature recorded for the Ex conditions (ExLv1, ExLv2 and ExLv3) and three Wa levels (WaLv2, WaLv3, WaL4). WaLv4 was not considered due to the lack of credible differences with the other experimental combinations. The red thicker lines show period of missing data in the temporal trend.

The strong difference in temperature between the full-, half-shadow and open micro-habitats was decreased by the presence of water during spring and summer, so that the difference in temperature between open and closed micro-habitats decreased when a 100 l water volume was present. Micro-habitats with a low water volume (1 l) reported the highest water temperature in all the solar exposure, potentially contributing to limit *Ae albopictus* fitness and survival [Wynn and Paradise, 2001] during summer time, but being advantageous during spring time (we found very early change points in the estimated life cycle rates temporal trend). Indeed, small containers are indicated as the most productive artificial breeding sites in the literature (e.g. planter dishes, buckets; [Bartlett-Healy et al., 2012; Baldacchino et al., 2016]).

The difference between shadowed and open habitats decreased passing from inside to external water temperature in winter and spring, but this difference increased during summer. The relationship between air and water temperature is generally non-linear; 1 °C increases in the former temperature typically cause smaller increases in the latter. However, when direct solar radiation is available (i.e. in summer), water is prone to accumulate more heat than air (high heat capacity). This complex set of interactions indicates that different environmental breeding micro-habitats may be optimal in different seasons. In spring and summer, the recorded water and just outside water temperature was the highest, averaging 14.2 and 26.2 °C, in small tanks in the open site. Higher breeding habitat temperatures during spring and early summer translate into a more suitable habitat for *Ae. albopictus* eggs and larvae. Bartlett-Healy et al. [2012] found that the average temperature of artificial containers with *Ae. albopictus* larvae had an average temperature of 17.2 °C, while lab experiments reported the optimal temperature for larval development between between 15 and 25 °C [Delatte et al., 2009; Waldock et al., 2013]. As a result, open micro-habitats can become sub-optimal or deadly for *Aedes* mosquitoes when direct solar radiation is at its yearly peak. Poikilothermic insects suffer from a disproportionate use of energy per unit body mass at high temperatures, and consequently, more energy is expended in maintenance [Gillooly et al., 2001], imposing bioenergetic constrains on individuals [Evans et al., 2015]. The estimated life cycle rates and the knowledge on poikilotherms bioenergetic constraints thus indicates full sun conditions as potentially suboptimal in summer, when, on the contrary, half shadow conditions resulted in the highest development and survival rates. Temperature in the half-shadow micro-habitat was rather dynamical, being more similar to one or to the other solar exposure in the different seasons, but being cooler than open habitats during spring and summer (2–6 °C less), yet warmer than full shadow (1–2 °C). In the scientific literature it is often reported that shadowed micro-habitats support greater mosquito abundance or richness than sunlit breeding habitats (i.e. Bartlett-Healy et al. [2012]). Generalising the findings in this project, we can speculate that breeding sites in half-shadow may represent optimal conditions for *Ae. albopictus* larval development. The partial mismatch between this

statement and the scientific literature may be due to the always subjective definition of solar exposure conditions. Hence, we decided to better define the exposure conditions considered in this study through a quantitative procedure. This procedure, routinely used in forest sciences [Cescatti and Zorer, 2003], consisted of the integration of hemispherical picture, topographical analysis and sun-path modelling. Being easy to implement and reliable, it helps to define the "openness" and direct (transmitted) solar radiation received by a determined point location, such as an *Ae. albopictus* micro-habitat. We described in detail this procedure, reporting the results for the three solar exposures considered in this study, in Appendix F. We propose that this relatively easy toolbox to estimate openness and solar radiation reaching breeding sites is implemented in future studies on this topic.

Concerning micro-habitats in half-shadow, they have the advantage of full shadow micro-habitats (high organic matter input, low evaporation rates, etc; Beier et al. [1983a]; Baumgartner [1988]; Lampman et al. [1997]; Kling et al. [2007]), but at the same time they receive a moderate amount of solar radiation. This additional energy input can considerably increase the larvae to adult development rate [Beier et al., 1983a; Berry and Craig, 1984; Haramis, 1984; Kling et al., 2007]. Half shadowed micro-habitats may be optimal also for overwintering eggs. Indeed this condition reported the mildest temperatures among all the experimental combinations during winter, when a 100 l volume was present (ExLv2WaLv4, average temperature = $\sim$6 °C). As such, this environmental setting may improve the viability of overwintering eggs, being sheltered by cold winds and, at the same time, receiving a moderate amount of solar radiation which increases the micro-habitat temperature.

Investigating the life cycle rate trends, the considered weather station or remotely sensed temperatures resulted sub-optimal to reliably estimate *Ae. albopictus* physiological and demographic rates [Paaijmans et al., 2010]. By using these generic temperature data, the temporal trend of the two estimated life cycle rates resulted markedly different, with delayed shifts in life history durations and underestimated population growth rates (see Appendix H). However, temperature data from weather stations or remote sensors is undoubtedly useful when exploring mosquito suitability at large spatial extensions and at course spatial resolutions, or when investigating the mechanisms of *Aedes* population dynamics is not the main aim of the project [Waldock et al., 2013].

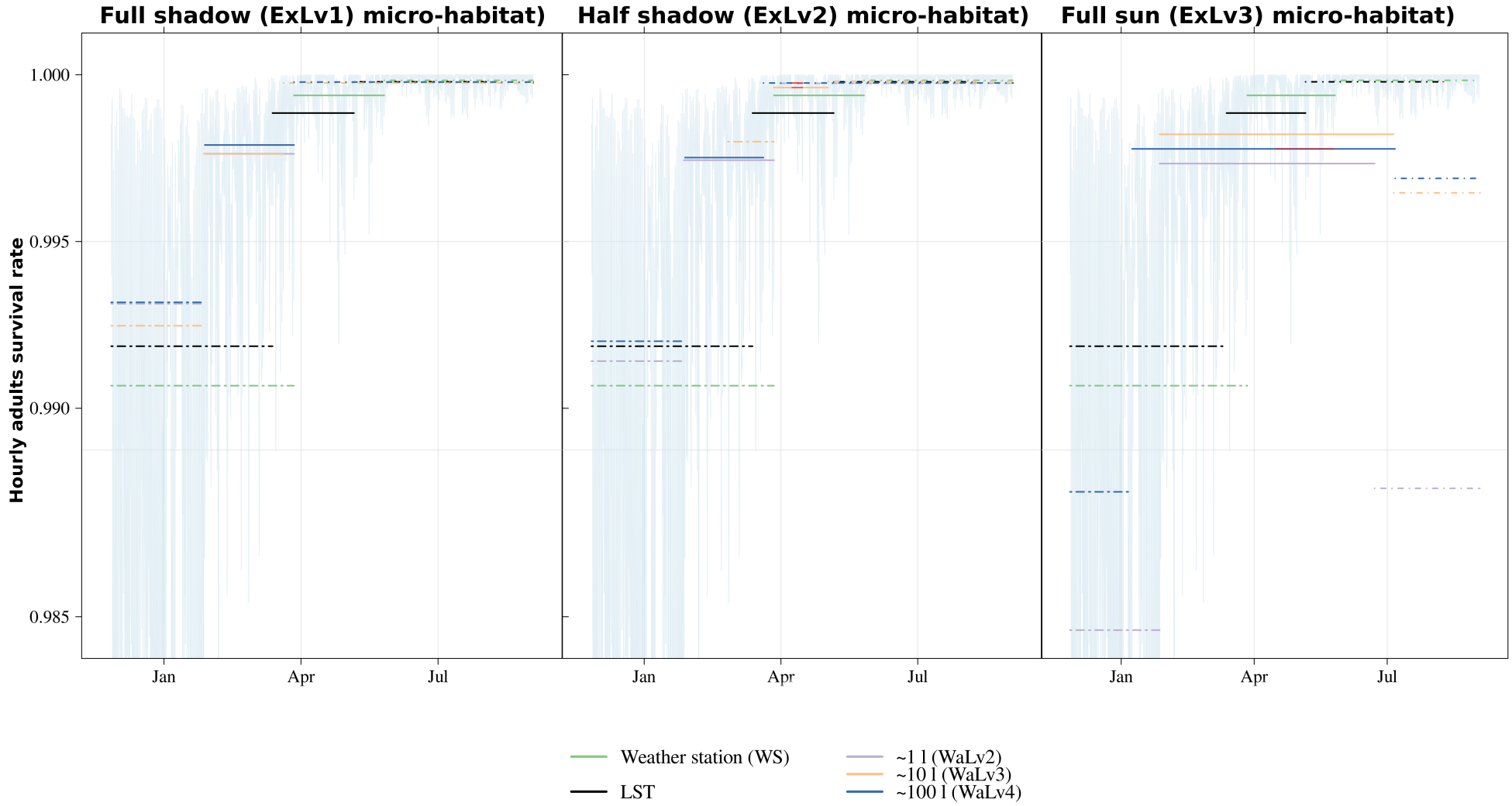

Figure 6.10: Change points in the estimated adult survival rate trend for the three solar exposure (Ex) conditions. The trend derived using the temperature time series from the nearest weather station is reported in grey in the background. The three groups of horizontal lines in each box represent the average rate estimated from one change point to the next for weather station (WS) and LST temperature as well as all water temperature recorded for the Ex conditions (ExLv1, ExLv2 and ExLv3) and three Wa levels (WaLv2, WaLv3, WaL4). WaLv4 was not considered due to the lack of credible differences with the other experimental combinations. The red thicker lines show period of missing data in the temporal trend.

The recorded micro-habitat temperatures and estimated physiological and demographic rates give information on how the environmental characteristics of the micro-habitat affect *Ae. albopictus* life history. However, they should be integrated in population dynamical models that consider the complex interactions between performance curves of different physiological processes [Evans et al., 2015]. In this regard, the temperature difference distributions provided in this project can be used as input for population models applied to any geographical location. Indeed, they are credible estimates of the variability in micro-habitat temperature experienced by a putative *Ae. albopictus* individual during its life cycle. As such, they are generalisable to other environmental settings which are similar to the ones investigated here. As an example, assuming that the baseline temperature time series of an area is known (e.g. a weather station temperature time series may be an assumed representative of the climatic conditions of a determined area), one could derive the relative temperature of a potential artificial breeding site with associated uncertainties for each season making use of Table 6.1 (reporting the main effects of each experimental factor) and Table (for simple effects). Indeed, the temperature of this putative breeding site (T_{f2f2f1}) would be the baseline temperature b_0 (i.e. the weather station temperature) plus the main (b_n) and simple deflections ($b_n b_n$) due to environmental factors and their interactions, so that:

$$T_{f2f2f1} = b_0 + b_1 + b_2 + b_3 + b_1 b_2 + b_1 b_3 + b_2 b_3 \tag{6.3}$$

The same concept is valid if the temperature of any particular *Aedes* micro-habitat is known. As an example, if the average temperature of a resting site in half shadow is known for a given location, the temperature of a breeding site in full sun with a determined water amount is derivable applying the right deflection estimates.

In conclusion, considering detailed micro-habitat temperature for each *Ae. albopictus* life stage, rather than temperature derived from generic data sources, considerably changes the estimated *Ae. albopictsu* life history timing and duration. Although generic temperature data are nowadays relatively easy to acquire, this convenience comes at the price of potential low accuracy of *Aedes* mosquitoes suitability and spread assessment as well as of vector-borne pathogen transmission and risk evaluation. We suggest that by choosing a representative baseline temperature for the area of interest and applying the appropriate deflections, such as those provided in this project, better estimates of *Ae. albopictus* population dynamics could be enabled, leading to an improved understanding of their spread. This improved knowledge is needed to support control programs which aim to mitigate *Ae. albopictus* continuous geographical expansion.

The experiment was performed in a single location and thus the collection of temperature data in other geographical locations may improve the estimated deflections. More projects aimed at defining *Ae. albopictus* breeding and resting micro-habitat temperatures are needed to refine the provided estimates. Future projects should consider the measurement of micro-habitat humidity together with temperature, due to its key role in *Ae. albopictus* adult and egg survival.

Chapter 7

General summary and outlook

7.1 General summary

The overarching aim of this thesis was to gain insights into re-emerging mosquito-borne pathogens and invasive vector species, their interaction with major environmental drivers and the mechanisms underpinning some less explored facets of their invasion dynamics. Vector-borne pathogens and their vector species are a major cause of disease and death worldwide [WHO, 2016]. Their global spread is a result of a complex interplay between socio-economic trends and environmental factors [Brown et al., 2014]. Moreover invasive vector species possess ecological traits that make them extremely well adapted for exploiting human related environments and thus are problematic to control [Paupy et al., 2009].

Here, environmental modelling has been used as a tool to explore and predict the spatio-temporal processes and patterns of vector-borne pathogens and invasive vector species. In this thesis, opinions from modellers, mosquito species experts and public health practitioners were fused to build models and experiments, interpret results and consider their potential impact on control actions. The subsequent results carry advances in research theory and application. In addition, some of the results and their interpretations, may be combined with invasive mosquito surveillance, monitoring and control method guidelines [ECDC, 2012; Baldacchino et al., 2016] to support public health personnels and policy makers in designing effective plans for mitigation against vector populations and potential outbreaks of invasive pathogens [Unlu et al., 2016].

7.2 West Nile Virus re-emergence in the Old World, are interpretations limited by data?

The study of vector-borne pathogen ecology and epidemiology in areas where they have been endemic for a long time provides clues on what can be expected in newly invaded areas [Petersen and Roehrig, 2001]. This thesis considered the re-emerging epidemiological trend of WNV across the Old World as a model for emergent pathogens. Research into the ecological determinants of pathogen epidemiological patterns, including climatic and environmental factors, help in determining geographic areas at higher risk [Hayes et al., 2005]. Through an automatic statistical approach and exploiting a wide set of potential predictors we found that warm, dry summers and wet springs are positively associated with WNV incidence in human population. Here, for the first time, landscape ecology data and concepts were fused with WNV epidemiology in the Old World. Forests fragmented by human settlements and irrigated croplands were the land uses that had the strongest association with WNV incidence. Landscape fragmentation favours generalist species, including many mosquito vector species which have

amplified contact with humans, so that the transmission of pathogens may be augmented [Suzán et al., 2015]. Irrigated crop-lands can favour the transmission of pathogens to humans since this land use may attract birds, mosquitoes and humans in the same spatio-temporal unit [Schöning et al., 2013]. These associations confirm and expand what has previously been found in the WNV scientific literature [Semenza, 2015].

At the current time however, a number of weaknesses in the available data make the model results and predictive modelling limited in accuracy. While the complexity of the WN viral transmission cycle remains poorly understood in the Old World and human epidemics continue to be sporadic, WNV data is limited by geographic variation in the accuracy of diagnosis, the establishment of surveillance, and the organisation of national reporting systems. On the one hand, the utilisation of opportunistic datasets coupled with data dredging algorithms can provide information on potential processes underpinning re-emerging pathogen epidemiology. Due to the importance of landscape structure for the dynamics of both the pathogens and vectors, landscape ecology concepts should be integrated more frequently [Suzán et al., 2015]. On the other hand, results from these applications may not be optimal for understanding and controlling pathogen transmission in endemic or newly invaded territories. The outcome from chapter 4 together with the latest scientific literature on the topic (i.e. Chevalier et al. [2014]; Semenza et al. [2016]) suggest that efforts now need to be concentrated on the collection of data on WNV host and vector population abundance, competence, seroprevalence as well as cases of human infection, rather than modelling using provisional datasets. The relatively easy implementation of some statistical modelling algorithms which are able to provide attractive results, including with sub-optimal data, should not be abused [Carneiro et al., 2016]. Simple model generalisations about environmental conditions made with opportunistic datasets suffer from poor predictive values in any given area [Reiter, 2001; Kearney and Porter, 2009; Carneiro et al., 2016]. These generalisations may be especially deleterious when applied to climate change scenarios [Reiter, 2001; Evans et al., 2015]. We suggest that a more robust collection of information on WNV ecology and epidemiology should be implemented for public health standards. Whenever adequate, this information should be combined with spatio-temporal locations and associated a degree of uncertainty [Rocchini et al., 2013]. This latter information is of paramount importance for human case reporting, since it is well established that disease does not develop at the site of transmission and indeed, not even necessarily close to this site [Connor and Monroe, 1923]. The ECDC European Environment and Epidemiology (E3) Network is a step towards the development of such a dataset, which in the long run will contribute to uncovering the root of mechanisms behind the global WNV and other vector-borne pathogens re-emergence.

7.3 *Aedes koreicus* as the next global mosquito invader

The early detection of invasive species is by no means the most effective control method that we can use to limit biological invasions [Simberloff, 2014]. *Aedes koreicus* was first reported in Northeast Italy in 2011, in an area already colonised by *Ae. albopictus* [Capelli et al., 2011]. The geographical expansion of *Ae. koreicus* was tracked using a network of traps and larvae surveys [Montarsi et al., 2015b]. The subsequent dataset was used in this thesis to assess *Ae. koreicus* distribution through SDMs, which predicted that 30 % of the study area is highly suitable for this species. The velocity of *Ae. koreicus* spread was simulated for the study area, thus predicting that 30 yr following introduction the population is expected to fill all the suitable niches (see section 3.4.5). The predicted area of invasion largely overlaps with the current distribution of *Ae. albopictus*, which may result in the two species interacting. *Aedes albopictus* and *Ae. koreicus* are both container breeding species, thus compete for the same resources. On the one hand, *Ae. koreicus* has a higher resistance to cold temperatures and it has a lower competition potential, which may result in a differentiation of its spatial niche. The emerging pattern can be simplified thus; *Ae. koreicus* may thrive in colder areas, while *Ae. albopictus* could be more abundant in warmer areas. On the other hand, Montarsi et al. [2015b] observed that *Ae. koreicus* larvae emergence is anticipated in late winter, allowing this species to occupy an empty temporal niche, implying a partial spatial coexistence with *Ae. albopictus*. However, with some degree of uncertainty due to biotic interactions, this thesis demonstrated that there is little doubt that Northeast Italy and potentially other parts of Northern Europe will be invaded by *Ae. koreicus*, complicating the entomological landscape and mosquito control strategies. As confirmation of these results, this species has been recently found in new localities across Europe [Suter et al., 2015; Ganushkina et al., 2016; Werner et al., 2016; Kurucz et al., 2016].

Despite the known role of *Ae. koreicus* as a minor vector of pathogens, there is a lack of studies which systematically investigate its vectoring capabilities [Montarsi et al., 2015a]. Thus, considering the rapid change in biological interactions among species due to rapid environmental changes (e.g. novel ecosystems; Hobbs et al. [2006]), together with the lessons learnt from *Ae. albopictus* [Gratz, 2004], the mitigation of *Ae. koreicus* spread should be of primary public health importance. Undoubtedly, the collection of more detailed information on the physiological and ecological requirements of this species is critical to reproduce its population dynamics and spread at a fine spatial scale. However, until this information is available, the suitability assessment and the simulation of the potential velocity of spread which was developed in chapter 3 can support control methods and risk evaluations to achieve an integrated mosquito control strategy [Baldacchino et al., 2015; Unlu et al., 2016]. For example, the constrained dispersal routes that *Ae. koreicus* is expected to follow in order to disperse within the study area according to our results, can be monitored to break the invasion wavefront.

Even after the eco-physiological requirements of this species are unravelled, suitability surfaces, like the one developed in chapter 3, in combination with population dynamical models help to forecast with higher accuracy the spatio-temporal dynamics of vector species at fine spatio-temporal scale.

7.4 *Aedes albopictus* micro-geographical dynamics

The final three chapters of this thesis are devoted to expanding the knowledge on processes which influence *Ae. albopictus* invasion in urban areas, which is facilitated by its ecological plasticity. Control strategies, such as the promising release of *Wolbachia* infected sterile-males, would benefit from more accurate knowledge on invasion mechanisms and invasion spatio-temporal predictions [Hancock et al., 2016; Ogden and Lindsay, 2016]. With this in mind, chapter 4 was dedicated to developing a new tool, aimed at reproducing the fine scale invasion and dispersal patterns immediately following introduction in urban areas. The developed model integrated detailed information on *Ae. albopictus* occurrence together with laboratory and literature data on its survival and development rates. The spatial dynamics of the mosquito population was included in the model structure, then used to simulate different introduction scenarios in two villages in Southern California, which have recently been invaded by *Ae. albopictus* [Fujioka and et al., 2012]. It was indicated that the most likely introduction scenario was the introduction of larvae during summer, or of adults during spring. However, the mosquito population was found to remain at very low densities after introduction. This finding supports the hypotheses that *Ae. albopictus* was actually introduced years before it was observed in Southern California, resulting from a carry-over of a previous introduction which occurred in 2001 [Zhong et al., 2013]. The model outputs effectively reproduced the spatio-temporal dynamics of introduced *Ae. albopictus* populations, giving insights into the mechanisms contributing to the invasion pattern in urban areas. Hence, it can be considered a valuable and flexible tool for investigating the invasion mechanisms of this species, and with further development and implementation will contribute to knowledge for operational control actions [Faraji and Unlu, 2016].

The developed model was thus used to explore the effect of urban vegetation on the spread of *Ae. albopictus*, a topic rarely touched upon in the scientific literature. Vegetation contributes to shaping habitat suitability for *Ae. albopictus* in urban areas [Manica et al., 2016]. Some studies targeted (mostly indirectly) the role of vegetation abundance or composition (see Cianci et al. [2015]; Manica et al. [2016]) but, to the best of my knowledge, this is the first attempt to directly target the role of urban vegetation configuration in *Ae. albopictus* invasion dynamics. In chapter 5, urban landscapes with different vegetation configuration were simulated, based on

information derived from real cities. *Aedes albopictus* introduction was then simulated for each of the urban landscapes using the model developed in chapter 4. Vegetation configuration did affect the spatial dynamics of the mosquito population. The spatial movement of simulated *Ae. albopictus* populations depended on the characteristics of the urban landscape with which they interacted [Maneerat and Daudé, 2016], where vegetation homogeneously spread across the urban landscape favoured longer dispersal distances and higher population density. This trend was observed and was particularly evident at very low urban vegetation coverages which still supported highly localised mosquito densities, if the vegetation was evenly spread across the matrix. We can further speculate, using population ecology concepts, that large isolated vegetation patches act as "magnet" habitats for introduced mosquito populations. These patches are highly attractive for mosquitoes and as such have low rates of emigration. On the contrary, when the vegetation is spread across the urban landscape, mosquitoes have a higher chance of finding new unoccupied suitable patches in the nearest neighbour set, increasing the total mosquito abundance in the urban landscape. These findings, based on simulations of urban landscape and mosquito population dynamics, may have significant implications for mosquito control activities or when planning urban areas [Steiner, 2014]. For example the adoption of vegetated roof tops in highly urbanised area [Manfred Köhler et al., 2002] should be carefully designed, such as implementing aggregated configurations in some blocks of the urban matrix which would limit the potential spread of *Aedes* mosquitoes. In addition, the achieved results may serve to stimulate further research on the role of the configuration of urban vegetation in *Ae. albopictus* invasion dynamics, for example considering the interactions between urban vegetation configuration and its vertical structure. The effectiveness of different control actions in urban areas with different vegetation characteristics is another interesting topic worthwhile of further research. All of these potential research topics need to be supported, and their results validated by, field observations coming from entomological experimental designs aimed at disentangling the roles of climatic, socio-economic and landscape factors in *Ae. albopictus* population urban dynamics.

The model presented in chapter 4 and applied in chapter 5 was employed a series of temperature-dependent functions reproducing larvae to adult development and adult survival rate. The input temperature data was taken from the nearest weather station. Opportunistic temperature data are routinely used in ecological modelling of invasive mosquitoes due to the lack of more accurate temperature data [Waldock et al., 2013]. This data is indeed difficult to collect and complex to model, given the peculiar characteristics of the micro-habitats preferred by invasive mosquitoes such as *Ae. albopictus* [Waldock et al., 2013]. Given these premises, in chapter 6, we implemented an experimental design to collect data from artificial breeding sites and putative resting sites. Data coming from this cross-factorial design were then analysed

using a Bayesian analysis of variance, in order to capture the distribution of temperature differences among micro-habitats. The resulting estimated temperature deflections due to the prevalence of one or another controlled environmental condition are thus generalisable to other areas with similar climatic characteristics. The sampled temperature and other generic sources of data were then used to estimate *Ae. albopictus* life cycle rates. As a consequence of the complex interplay between the controlled environmental conditions, different micro-habitats were optimal depending on the season, however half-shadow micro-habitats generally showed the highest development and survival rate. In the scientific literature it is often reported that shadowed habitats are the most productive for *Ae. albopictus*, however the meaning of open, half- or full-shadowed conditions is unclear and never quantitatively characterised. Therefore, we exploited a methodology based on hemispherical picture, topographical analysis and a sun-path model that, being effective and easy to implement, helps to define the amount of direct transmitted solar radiation received by the micro-habitats. I propose that this procedure, reported in detail in Appendix E, is more often integrated when studying *Ae. albopictus* larval micro-habitats.

Concerning the considered source of temperature data, data collected by weather stations or remote sensing equipment resulted in sub-optimal estimates of *Ae. albopictus* demographic and physiological rates [Paaijmans et al., 2010]. Indeed, the temporal trend of these rates were markedly different, with delayed shifts in life history durations and underestimated population growth rates, when compared to the recorded micro-habitat temperatures. I am aware that satellite and weather station data are often the only available source of temperature data when exploring invasive mosquito suitability at large spatial extensions, at course spatial resolutions [Benedict et al., 2007], or when investigating the mechanisms of mosquito population dynamics is not the main aim of the project. However, the difference between temperature from generic data sources and *Ae. albopictus* micro-habitats should be considered when interpreting model results, especially if these results drive public health policies [Evans et al., 2015]. Otherwise, model outputs risk to provide biased spatio-temporal predictions, which in the best case scenario will result in the outputs playing only marginal roles in the development of early-warning systems or forecasting tools, or at worst, will generate underachieving public health actions. Even better than just considering data bias, I suggest that by choosing a representative baseline temperature for the area of interest and applying the appropriate deflections, such as those provided in this project, better estimates of *Ae. albopictus* population dynamics can be enabled, leading to an improved understanding of their spread and control through forecasting tools.

7.5 Outlook

Insights derived here from modelling WNV at continental scales, together with the recent literature on the topic lay the basis for reliable predictions with more consistent sets of data. Even though a set of potential environmental factors emerged as conditions potentially underpinning WNV spatio-temporal dynamics in the Old World [Paz et al., 2013; Tran et al., 2014; Marcantonio et al., 2015; Semenza et al., 2016], accurate data is a *sine-qua-non* for developing robust and effective re-emergent pathogen predictive models. More accurate information on WNV circulation can be retrieved from country level monitoring and prevention activities. For example, Greece, being among the most impacted countries by WNV re-emergence, stimulated the collection of a number of datasets that, if integrated, may serve as a reference to predict WNV future trends in other countries within the Old World. Existing data on the seroprevalence in human [Hadjichristodoulou et al., 2015] and host populations (Charalambos Billinis, personal communication) may be integrated in a hierarchical framework to inform, together with the outlined potential environmental drivers, the modelling of WNV human case spatio-temporal trends. In spite of new re-emergent pathogens menacing human health (e.g. Zika virus), and a somewhat decreased activity in the Old World (210, 301, and 254 cases in 2014, 2015 and until the 9th September 2016 respectively, compared to 935, 785 in 2012 and 2013 respectively; ecdc [2016]), constant attention on the circulation of WNV should be maintained until its epidemiological trends are fully understood [Reisen, 2013].

The spatio-temporal variation in the circulation and transmission of vector-borne pathogens, such as WNV, is a consequence of the distribution of host and vector species. SDMs help to gain knowledge on the current and future distribution of a vector, which can be applied to prioritise limited resources which are available for vector control. Making use of correlative SDMs we found that *Ae. koreicus* will rapidly expand its distribution in Northeast Italy and potentially Europe within a relatively short time. The collection of further data on the physiological constraints of *Ae. koreicus* will clarify its ecological requirements and interactions with *Ae. albopictus*. When this data is available, models that integrate suitability surfaces with demographic and spatial dynamics of the vector, as well as interactions between the two mosquito species should be developed, to shed light on niche partitioning and interspecific competition mechanisms. Two possible scenarios can be hypothesised; partitioning of the spatial niche (geographical differentiation) or of the temporal niche (temporal differentiation), through both resource (larval stage; Juliano [2007]) and/or conditional (adult stage) partitioning. Both scenarios, and all the intermediate possibilities, will lead to a new epidemiological landscape, more complex to interpret than the current situation. One possible outcome of these scenarios may be that the minor vector *Ae. koreicus* (which is more resistant to cold temperatures) out-competes *Ae. albopictus* (which is known to vector more pathogen species)

in colder areas, thus potentially decreasing the transmission risk of vector-borne pathogens. Notably, another vector mosquito species, *Ae. japonicus*, has recently been collected close to the study area [Seidel et al., 2016]. The ecology of this species [Kaufman and Fonseca, 2014] suggests that *Ae. japonicus* will rapidly reach Northeast Italy. The transdisciplinary integration of remotely sensed, field and laboratory data in modelling frameworks will be the only tool able to disentangle the future epidemiological landscapes, composed by several interacting invasive vector species.

The above-mentioned integration has already demonstrated effectiveness in reproducing *Ae. albopictus* invasion dynamics in newly invaded areas. The integrated model framework developed in chapter 4 provided quantitative support for delineating *Ae. albopictus* invasion dynamics in Southern California. The flexibility of the developed tool was therefore exploited to investigate how vegetation configuration affects the introduction and spread of *Ae. albopictus* in urban areas, supplying new stimulating hypotheses which need to be confirmed through the implementation of specific data collection designs or experiments (chapter 5). A firm understanding of urban ecological mechanisms is of paramount importance to design cities more resilient to invasion through informed environmental and smart planning [Steiner, 2014]. New perspectives in the diverse facets of invasive vector ecology in urban areas can be explored by applying the proposed model framework. Among the most exciting future directions is the exploration of the multivariate interactions [Armstrong and McGehee, 1980] between two or more invasive container breeding vectors [Ho et al., 1989], conditions which are already occurring in many urban areas [Armistead et al., 2008; Montarsi et al., 2015b; Seidel et al., 2016] and the effectiveness of control strategies [Baldacchino et al., 2015]. Nevertheless, there is room for further improvements in the model structure. The definition of more accurate suitability surfaces, which underpin the attractiveness and carrying capacity of individual features of the urban landscape (*viz.* cadastral units, lots, parcels, blocks) would be beneficial. In this regard, information on the spatial and temporal availability of artificial breeding habitats are challenging to retrieve, but their implementation would have a strong positive impact on the reliability of model outputs. Remote sensing, enriched by field data, is perhaps the only tool that has a real potential to provide this information, however only indirect inferences are currently possible [McFeeters, 2013; Cleckner and Allen, 2014]. The consideration of imperfect detection and survey bias derived from *Ae. albopictus* data collection would also improve the accuracy of suitability estimates [Low et al., 2016]. Statistical techniques which make use of few high quality data from planned surveys are being developed to correct opportunistic and less accurate datasets [Dorazio, 2014]. Human movements (i.e. road traffic) and wind speed are significant dispersal means for mosquitoes in urban areas and as such should be integrated in the kernel functions underlying *Ae. albopictus* simulated spatial dynamics [Garrett-Jones,

1950; Service, 1997; Tatem et al., 2006]. Excessive road traffic in urban areas is amongst the issues associated with rapid urbanisation occurring throughout the world [Wang et al., 2015]. As such traffic data are becoming more readily available, e.g. through passive sensors and the ubiquitous spread of digital mobile devices, that allow the aggregation of location history data [González et al., 2008]. Wind direction and speed in the urban landscape often abruptly vary from street to street due to the inhomogeneous heat and moisture patterns resulting from human activities, topographic characteristics and urban surface roughness [Britter and Hanna, 2003]. Consequently, wind speed modelling in urban areas is rarely implemented or, when it is, the predictions are suboptimal [Great Britain et al., 2012]. However, the rapid development of remote sensing technology, such as LIDAR and SODAR devices, may soon allow more detailed spatio-temporal data on this important mosquito dispersal agent in urban areas. The pioneering work of Takahashi et al. [2004] on *Ae. aegypti* dispersal dynamics represents a theoretical keystone which can be applied using data as that related to road traffic and wind. This extension would increase the reliability of the expected velocity of mosquito spread.

What is not currently provided by models or remote sensing technology, with little chances for the future, is data on the variability of *Ae. albopictus* urban micro-habitat thermal properties [Waldock et al., 2013]. Micro-habitat temperature must be considered a key property when modelling ectotherm habitat suitability or population dynamics. Ectotherms such as *Ae. albopictus* are indeed incapable of surviving in open habitats through physiological thermal tolerance alone, and thus, survival depends on access to thermal refugia to survive (i.e. shade; Sunday et al. [2014]). Estimates of temperature variability in the range of *Ae. albopictus* artificial micro-habitat conditions as well as their effect on estimated life durations were reported in chapter 6. These estimates can potentially be applied to account for the variability in micro-habitat conditions in other geographical areas and can therefore be a step towards defining urban micro-habitat thermal properties for *Ae. albopictus* [Vallorani et al., 2015]. Despite being generalisable, the presented data was however limited to 36 temperature sensors placed in a single geographical location. The collection of further data as well as the integration of humidity measures (advanced iButton models measure humidity together with temperature) would benefit the proposed deflection estimates and the generation of model outputs operational for public health purposes. Towards this direction, the OpenSignal's battery temperature data (http://opensignal.com/sensors/), or ambient temperature gathered directly from some new smart-phone models (Samsung Galaxy SG4, South Korea) deserve to be further explored [Budello and Ziv, 2016].

Bibliography

Adams, B and Kapan, DD (2009). Man Bites Mosquito: Understanding the Contribution of Human Movement to Vector-Borne Disease Dynamics. *PLOS ONE*, 4(8):p. e6763.

Adams, VM, Petty, AM, Douglas, MM, Buckley, YM, Ferdinands, KB et al. (2015). Distribution, demography and dispersal model of spatial spread of invasive plant populations with limited data. *Methods in Ecology and Evolution*.

Adhami, J and Reiter, P (1998). Introduction and establishment of Aedes (Stegomyia) albopictus skuse (Diptera: Culicidae) in Albania. *Journal of the American Mosquito Control Association*, 14(3):pp. 340–343.

Adler, P and Laurenroth, W (2003). The power of time: spatiotemporal scaling of species diversity. *Ecology Letters*, pp. 749–756.

Aharonson-Raz, K, Lichter-Peled, A, Tal, S, Gelman, B, Cohen, D et al. (2014). Spatial and Temporal Distribution of West Nile Virus in Horses in Israel (1997–2013) - from Endemic to Epidemics. *PLOS ONE*, 9(11):p. e113149.

Allouche, O, Tsoar, A, and Kadmon, R (2006). Assessing the accuracy of species distribution models : prevalence , kappa and the true skill statistic (TSS). *Journal of Applied Ecology*, pp. 1223–1232.

Alto, BW and Juliano, SA (2001). Temperature effects on the dynamics of Aedes albopictus (Diptera: Culicidae) populations in the laboratory. *Journal of Medical Entomology*, 38(4):pp. 548–556.

Alvey, AA (2006). Promoting and preserving biodiversity in the urban forest. *Urban Forestry & Urban Greening*, 5(4):pp. 195–201.

Analytics, R and Weston, S (2015). *foreach: Provides Foreach Looping Construct for R*. R package version 1.4.3.

Ancona, V, Appel, DN, and de Figueiredo, P (2010). Xylella fastidiosa: A Model for Analyzing Agricultural Biosecurity. *Biosecurity and Bioterrorism: Biodefense Strategy, Practice, and Science*, 8(2):pp. 171–182.

Araújo, MB and New, M (2007). Ensemble forecasting of species distributions. *Trends in Ecology & Evolution*, 22(1):pp. 42–47.

Armbruster, PA (2016). Photoperiodic Diapause and the Establishment of Aedes albopictus (Diptera: Culicidae) in North America. *Journal of Medical Entomology*, p. tjw037.

Armijos, V (2016). *Aedes albopictus life rates*. PhD thesis, UC Davis.

Armistead, JS, Arias, JR, Nishimura, N, and Lounibos, LP (2008). Interspecific Larval Competition Between Aedes albopictus and Aedes japonicus (Diptera: Culicidae) in Northern Virginia. *Journal of medical entomology*, 45(4):pp. 629–637.

Armstrong, RA and McGehee, R (1980). Competitive Exclusion. *The American Naturalist*, 115(2):pp. 151–170.

Arnold, C (2012). West Nile virus bites back. *The Lancet Neurology*, 11(12):pp. 1023–1024.

Artsob, H, Gubler, DJ, Enria, DA, Morales, MA, Pupo, M et al. (2009). West Nile Virus in the New World: Trends in the Spread and Proliferation of West Nile Virus in the Western Hemisphere. *Zoonoses and Public Health*, 56(6-7):pp. 357–369.

Asare, EO, Tompkins, AM, Amekudzi, LK, and Ermert, V (2016). A breeding site model for regional, dynamical malaria simulations evaluated using in situ temporary ponds observations. *Geospatial Health*, 11(1s).

Auger, IE and Lawrence, CE (1989). Algorithms for the optimal identification of segment neighborhoods. *Bulletin of Mathematical Biology*, 51(1):pp. 39–54.

Bakonyi, T, Ferenczi, E, Erdélyi, K, Kutasi, O, Csörgő, T et al. (2013). Explosive spread of a neuroinvasive lineage 2 West Nile virus in Central Europe, 2008/2009. *Vet Microbiol*, 165(1-2):pp. 61–70.

Baldacchino, F, Bussola, F, Arnoldi, D, Marcantonio, M, Montarsi, F et al. (2016). An integrated pest control strategy against the Asian tiger mosquito in northern Italy: a case study. *Pest Management Science*, pp. n/a–n/a.

Baldacchino, F, Caputo, B, Chandre, F, Drago, A, della Torre, A et al. (2015). Control methods against invasive Aedes mosquitoes in Europe: a review. *Pest Management Science*.

Barker, C, Montecino, D, and Marcantonio, M (2015). Modeling the Spread and Control of the Asian Tiger Mosquito in Los Angeles. San Francisco, California, USA.

Bartlett-Healy, K, Unlu, I, Obenauer, P, Hughes, T, Healy, S et al. (2012). Larval Mosquito Habitat Utilization and Community Dynamics of Aedes albopictus and Aedes japonicus (Diptera: Culicidae). *Journal of Medical Entomology*, 49(4):pp. 813–824.

Bartoń, K (2013). MuMIn: Multi-model inference; R package version 1.9.13.

Barzon, L, Pacenti, M, Franchin, E, Pagni, S, Lavezzo, E et al. (2013). Large Human Outbreak of West Nile Virus Infection in North-Eastern Italy in 2012. *Viruses*, 5(11):pp. 2825–2839.

Bates, D and Maechler, M (2016). *Matrix: Sparse and Dense Matrix Classes and Methods*. R package version 1.2-6.

Batty, M and Longley, P (1994). *Fractal Cities: A Geometry of Form and Function*. Academic Press, San Diego, CA and London.

Baumgartner, D (1988). Suburban accumulations of discarded tires in northeastern Illinois and their associated mosquitoes. *Journal of the American Mosquito Control Association*.

Becker, N (2010). *Mosquitoes and their control*. Springer.

Beier, JC, Patricoski, C, Travis, M, and Kranzfelder, J (1983a). Influence of Water Chemical and Environmental Parameters on Larval Mosquito Dynamics in Tires. *Environmental Entomology*, 12(2):pp. 434–438.

Beier, JC, Travis, M, Patricoski, C, and Kranzfelder, J (1983b). Habitat Segregation Among Larval Mosquitoes (Diptera: Culicidae) in Tire Yards in Indiana, USA. *Journal of Medical Entomology*, 20(1):pp. 76–80.

Bellini, R, Veronesi, R, Venturelli, G, and Angelini, P (2005). Guidelines for surveillance and control of the Asian tiger mosquito (Aedes albopictus). Technical report, Regione Emiia-Romagna.

Benedict, MQ, Levine, RS, Hawley, WA, and Lounibos, LP (2007). Spread of The Tiger: Global Risk of Invasion by The Mosquito Aedes albopictus. *Vector-Borne and Zoonotic Diseases*, 7(1):pp. 76–85.

Benoit, JB and Denlinger, DL (2007). Suppression of water loss during adult diapause in the northern house mosquito, Culex pipiens. *Journal of Experimental Biology*, 210(2):pp. 217–226.

Berry, JK (2007). Beyond Mapping III – Map Analysis. *University of Denver, Geo Tec Media*.

Berry, W and Craig, G (1984). Bionomics of Aedes-Atropalpus Breeding in Scrap Tires in Northern Indiana. *Mosquito News*, 44(4):pp. 476–484. WOS:A1984AAP4300007.

Bhatt, S, Gething, PW, Brady, OJ, Messina, JP, Farlow, AW et al. (2013). The global distribution and burden of dengue. *Nature*, 496(7446):pp. 504–507.

Bivand, R and Lewin-Koh, N (2016). *maptools: Tools for Reading and Handling Spatial Objects*. R package version 0.8-39.

Boehringer, S (2013). *parallelize.dynamic: Automate parallelization of function calls by means of dynamic code analysis*. R package version 0.9-1.

Bomford, M, Kraus, F, Barry, SC, and Lawrence, E (2008). Predicting establishment success for alien reptiles and amphibians: a role for climate matching. *Biological Invasions*, 11(3):pp. 713–724.

Bowden, SE, Magori, K, and Drake, JM (2011). Regional Differences in the Association Between Land Cover and West Nile Virus Disease Incidence in Humans in the United States. *Am J Trop Med Hyg*, 84(2):pp. 234–238.

Bradley, CA and Altizer, S (2007). Urbanization and the ecology of wildlife diseases. *Trends in Ecology & Evolution*, 22(2):pp. 95–102.

Brady, OJ, Golding, N, Pigott, DM, Kraemer, MUG, Messina, JP et al. (2014). Global temperature constraints on Aedes aegypti and Ae. albopictus persistence and competence for dengue virus transmission. *Parasites & Vectors*, 7:p. 338.

Brady, OJ, Johansson, MA, Guerra, CA, Bhatt, S, Golding, N et al. (2013). Modelling adult Aedes aegypti and Aedes albopictus survival at different temperatures in laboratory and field settings. *Parasites & Vectors*, 6(1):p. 351.

Britter, RE and Hanna, SR (2003). Flow and Dispersion in Urban Areas. *Annual Review of Fluid Mechanics*, 35(1):pp. 469–496.

Brotons, L, Thuiller, W, Araújo, MB, and Hirzel, AH (2004). Presence-absence versus presence-only modelling methods for predicting bird habitat suitability. *Ecography*, 27(4):pp. 437–448.

Brown, HE, Childs, JE, Diuk-Wasser, MA, and Fish, D (2008a). Ecologic Factors Associated with West Nile Virus Transmission, Northeastern United States. *Emerging Infectious Diseases*, 14(10):pp. 1539–1545.

Brown, H, Diuk-Wasser, M, Andreadis, T, and Fish, D (2008b). Remotely-Sensed Vegetation Indices Identify Mosquito Clusters of West Nile Virus Vectors in an Urban Landscape in the Northeastern United States. *Vector-Borne and Zoonotic Diseases*, 8(2):pp. 197–206.

Brown, JE, Evans, BR, Zheng, W, Obas, V, Barrera-Martinez, L et al. (2014). Human Impacts Have Shaped Historical and Recent Evolution in Aedes Aegypti, the Dengue and Yellow Fever Mosquito. *Evolution*, 68(2):pp. 514–525.

Buck, C (1988). *The Challenge of Epidemiology: Issues and Selected Readings*. Pan American Health Org.

Buckland, ST, Burnham, KP, and Augustin, NH (1997). Model Selection: An Integral Part of Inference. *Biometrics*, 53(2):pp. 603–618.

Budello, L and Ziv, G (2016). Utilising smart phone sensors and crowdsourcing to monitor temperature change. In *Urban-Alert (U-Alert) Scoping Exercise Report*.

Bureau, UC (2014). 2014 TIGER/Line Shapefiles (machinereadable data files). Prepared by the Census Bureau. Technical report.

Burnham, K and Anderson, DR (2002). *Model selection and multimodel inference: A practical Information-Theoretic Approach*. Springer, second edition.

Calcagno, V and de Mazancourt, C (2010). glmulti: An R Package for Easy Automated Model Selection with (Generalized) Linear Models. *Journal of Statistical Software*, 34(12):pp. 1–29.

Calder, C, Lavine, M, Müller, P, and Clark, JS (2003). Incorporating Multiple Sources of Stochasticity into Dynamic Population Models. *Ecology*, 84(6):pp. 1395–1402.

Calzolari, M, Monaco, F, Montarsi, F, Bonilauri, P, Ravagnan, S et al. (2013). New incursions of West Nile virus lineage 2 in Italy in 2013: the value of the entomological surveillance as early warning system. *Vet Ital*, 49(3):pp. 315–319.

Cambridge Dictionary, T (2016). the Old World.

Caminade, C, Medlock, JM, Ducheyne, E, McIntyre, KM, Leach, S et al. (2012). Suitability of European climate for the Asian tiger mosquito Aedes albopictus: recent trends and future scenarios. *J R Soc Interface*, 9(75):pp. 2708–2717.

Capelli, G, Drago, A, Martini, S, Montarsi, F, Soppelsa, M et al. (2011). First report in italy of the exotic mosquito species Aedes (Finlaya) koreicus, a potential vector of arboviruses and filariae. *Parasites & Vectors*, 4(1):p. 188.

Caputo, B, Ienco, A, Manica, M, Petrarca, V, Rosà, R et al. (2015). New adhesive traps to monitor urban mosquitoes with a case study to assess the efficacy of insecticide control strategies in temperate areas. *Parasites & Vectors*, 8:p. 134.

Carneiro, LRdA, Lima, AP, Machado, RB, and Magnusson, WE (2016). Limitations to the Use of Species-Distribution Models for Environmental-Impact Assessments in the Amazon. *PLOS ONE*, 11(1):p. e0146543.

Carrieri, M, Bacchi, M, Bellini, R, and Maini, S (2003). On the Competition Occurring Between Aedes albopictus and Culex pipiens (Diptera: Culicidae) in Italy. *Environmental Entomology*, 32(6):pp. 1313–1321.

Carrington, LB and Simmons, CP (2014). Human to Mosquito Transmission of Dengue Viruses. *Frontiers in Immunology*, 5.

Cescatti, A and Zorer, R (2003). Structural acclimation and radiation regime of silver fir (Abies alba Mill.) shoots along a light gradient. *Plant, Cell & Environment*, 26(3):pp. 429–442.

Charrel, RN, Leparc-Goffart, I, Gallian, P, and de Lamballerie, X (2014). Globalization of Chikungunya: 10 years to invade the world. *Clinical Microbiology and Infection*, 20(7):pp. 662–663.

Chase, JM and Knight, TM (2003). Drought-induced mosquito outbreaks in wetlands. *Ecology Letters*, 6(11):pp. 1017–1024.

Chevalier, V, Tran, A, and Durand, B (2014). Predictive Modeling of West Nile Virus Transmission Risk in the Mediterranean Basin: How Far from Landing? *Int J Environ Res Public Health*, 11(1):pp. 67–90.

Chianucci, F, Chiavetta, U, and Cutini, A (2014). The estimation of canopy attributes from digital cover photography by two different image analysis methods. *iForest - Biogeosciences and Forestry*, 7(4):pp. 255–259.

Chuang, TW, Hockett, CW, Kightlinger, L, and Wimberly, MC (2012). Landscape-Level Spatial Patterns of West Nile Virus Risk in the Northern Great Plains. *Am J Trop Med Hyg*, 86(4):pp. 724–731.

Chuang, TW and Wimberly, MC (2012). Remote Sensing of Climatic Anomalies and West Nile Virus Incidence in the Northern Great Plains of the United States. *PLoS ONE*, 7(10):p. e46882.

Cianci, D, Hartemink, N, and Ibáñez-Justicia, A (2015). Modelling the potential spatial distribution of mosquito species using three different techniques. *International Journal of Health Geographics*, 14(1):p. 10.

CIESIN - Columbia University (2015). Gridded Population of the World, Version 4 (GPWv4): Population Density Grid, Future Estimates.

Cini, A, Ioriatti, C, and Anfora, G (2012). A review of the invasion of Drosophila suzukii in Europe and a draft research agenda for integrated pest management. *Bulletin of Insectology-Bulletin of Insectology*, 65:pp. 149–160.

Cleckner, H and Allen, TR (2014). Dasymetric Mapping and Spatial Modeling of Mosquito Vector Exposure, Chesapeake, Virginia, USA. *ISPRS International Journal of Geo-Information*, 3(3):pp. 891–913.

Clements, AN (1992). *The Biology of Mosquitoes: Development, nutrition, and reproduction*. Chapman & Hall.

Coker, R, Rushton, J, Mounier-Jack, S, Karimuribo, E, Lutumba, P et al. (2011). Towards a conceptual framework to support one-health research for policy on emerging zoonoses. *The Lancet Infectious Diseases*, 11(4):pp. 326–331.

Colborn, JM, Smith, KA, Townsend, J, Damian, D, Nasci, RS et al. (2013). West Nile virus outbreak in Phoenix, Arizona–2010: entomological observations and epidemiological correlations. *J Am Mosq Control Assoc*, 29(2):pp. 123–132.

Connor, ME and Monroe, WM (1923). Stegomyia Indices and Their Value in Yellow Fever Control. *The American Journal of Tropical Medicine and Hygiene*, s1-3(1):pp. 9–19.

Corlett, RT (2015). The Anthropocene concept in ecology and conservation. *Trends in Ecology & Evolution*, 30(1):pp. 36–41.

Cornel, AJ and Hunt, RH (1991). Aedes albopictus in Africa? First records of live specimens in imported tires in Cape Town. *Journal of the American Mosquito Control Association*, 7(1):pp. 107–108.

Courchamp, F, Clutton-Brock, T, and Grenfell, B (1999). Inverse density dependence and the Allee effect. *Trends in ecology & evolution (Personal edition)*, 14(10):pp. 405–410.

Crowl, TA, Crist, TO, Parmenter, RR, Belovsky, G, and Lugo, AE (2008). The spread of invasive species and infectious disease as drivers of ecosystem change. *Frontiers in Ecology and the Environment*, 6(5):pp. 238–246.

Cunze, S, Kochmann, J, Koch, LK, and Klimpel, S (2016). Aedes albopictus and Its Environmental Limits in Europe. *PLOS ONE*, 11(9):p. e0162116.

Daszak, P, Cunningham, aa, and Hyatt, aD (2000). Emerging infectious diseases of wildlife–threats to biodiversity and human health. *Science (New York, NY)*, 287(5452):pp. 443–9.

Dauphin, G, Zientara, S, Zeller, H, and Murgue, B (2004). West Nile: worldwide current situation in animals and humans. *Comparative Immunology, Microbiology and Infectious Diseases*, 27(5):pp. 343–355.

Davis, MA, Grime, JP, and Thompson, K (2000). Fluctuating resources in plant communities: a general theory of invasibility. *Journal of Ecology*, 88(3):pp. 528–534.

Davis, AY, Jung, J, Pijanowski, BC, and Minor, ES (2016). Combined vegetation volume and "greenness" affect urban air temperature. *Applied Geography*, 71:pp. 106–114.

De Clercq, EM, Leta, S, Estrada-Peña, A, Madder, M, Adehan, S et al. (2015). Species distribution modelling for Rhipicephalus microplus (Acari: Ixodidae) in Benin, West Africa: Comparing datasets and modelling algorithms. *Preventive Veterinary Medicine*, 118(1):pp. 8–21.

Deichmeister, JM and Telang, A (2011). Abundance of West Nile virus mosquito vectors in relation to climate and landscape variables. *Journal of Vector Ecology*, 36(1):pp. 75–85.

Delatte, H, Desvars, A, Bouétard, A, Bord, S, Gimonneau, G et al. (2010). Blood-feeding behavior of Aedes albopictus, a vector of Chikungunya on La Réunion. *Vector Borne and Zoonotic Diseases (Larchmont, NY)*, 10(3):pp. 249–258.

Delatte, H, Gimonneau, G, Triboire, A, and Fontenille, D (2009). Influence of temperature on immature development, survival, longevity, fecundity, and gonotrophic cycles of Aedes albopictus, vector of chikungunya and dengue in the Indian Ocean. *Journal of Medical Entomology*, 46(1):pp. 33–41.

Delatte, H, Paupy, C, Dehecq, J, Thiria, J, Failloux, A et al. (2008). *Aedes albopictus* , vecteur des virus du chikungunya et de la dengue à la Réunion : biologie et contrôle. *Parasite*, 15(1):pp. 3–13.

Denwood, MJ (2016). runjags: An R Package Providing Interface Utilities, Model Templates, Parallel Computing Methods and Additional Distributions for MCMC Models in JAGS. *Journal of Statistical Software*, 71(9):pp. 1–25.

Dimoudi, A and Nikolopoulou, M (2003). Vegetation in the urban environment: microclimatic analysis and benefits. *Energy and Buildings*, 35(1):pp. 69–76.

Dobson, A and Foufopoulos, J (2001). Emerging infectious pathogens of wildlife. *Philos Trans R Soc Lond, B, Biol Sci*, 356(1411):pp. 1001–1012.

Dohm, DJ, O'Guinn, ML, and Turell, MJ (2002). Effect of environmental temperature on the ability of Culex pipiens (Diptera: Culicidae) to transmit West Nile virus. *J Med Entomol*, 39(1):pp. 221–225.

Dorazio, RM (2014). Accounting for imperfect detection and survey bias in statistical analysis of presence-only data. *Global Ecology and Biogeography*, 23(12):pp. 1472–1484.

Dormann, CF, Schymanski, SJ, Cabral, J, Chuine, I, Graham, C et al. (2012). Correlation and process in species distribution models: bridging a dichotomy. *Journal of Biogeography*, 39(12):pp. 2119–2131.

Dowling, Z, Ladeau, SL, Armbruster, P, Biehler, D, and Leisnham, PT (2013). Socioeconomic status affects mosquito (Diptera: Culicidae) larval habitat type availability and infestation level. *J Med Entomol*, 50(4):pp. 764–772.

Drake, JA (1989). *Biological Invasions: A Global Perspective*. Wiley. Google-Books-ID: If0TAQAAIAAJ.

Drake, JM (2015). Range bagging: a new method for ecological niche modelling from presence-only data. *Journal of The Royal Society Interface*, 12(107):p. 20150086.

Duncan, RP, Bomford, M, Forsyth, DM, and Conibear, L (2001). High predictability in introduction outcomes and the geographical range size of introduced Australian birds: a role for climate. *Journal of Animal Ecology*, 70(4):pp. 621–632.

Dunn, AM and Hatcher, MJ (2015). Parasites and biological invasions: parallels, interactions, and control. *Trends in Parasitology*.

Eads, R (1972). Recovery of Aedes albopictus from used tires shipped to United States ports. *Mosquito News*, 32(1):pp. 113–114.

Eaton, JS, Likens, GE, and Bormann, FH (1973). Throughfall and Stemflow Chemistry in a Northern Hardwood Forest. *Journal of Ecology*, 61(2):pp. 495–508.

ECDC, ECfDPaCE (2012). Development of *Aedes albopictus* risk maps.

ecdc (2016). West Nile fever maps.

Effler, PV, Pang, L, Kitsutani, P, Vorndam, V, Nakata, M et al. (2005). Dengue fever, Hawaii, 2001-2002. *Emerging Infectious Diseases*, 11(5):pp. 742–749.

Eisen, L, Barker, CM, Moore, CG, Pape, WJ, Winters, AM et al. (2010). Irrigated agriculture is an important risk factor for West Nile virus disease in the hyperendemic Larimer-Boulder-Weld area of north central Colorado. *Journal of medical entomology*, 47(5):pp. 939–951.

Eisen, L, Wong, D, Shelus, V, and Eisen, RJ (2013). What is the Risk for Exposure to Vector-Borne Pathogens in United States National Parks? *Journal of Medical Entomology*, 50(2):pp. 221–230.

Elith, J, H. Graham, C, P. Anderson, R, Dudík, M, Ferrier, S et al. (2006). Novel methods improve prediction of species' distributions from occurrence data. *Ecography*, 29(2):pp. 129–151.

Elith, J and Leathwick, JR (2009). Species Distribution Models: Ecological Explanation and Prediction Across Space and Time. *Annual Review of Ecology, Evolution, and Systematics*, 40(1):pp. 677–697.

Elith, J, Phillips, SJ, Hastie, T, Dudík, M, Chee, YE et al. (2011). A statistical explanation of MaxEnt for ecologists. *Diversity and Distributions*, 17(1):pp. 43–57.

Ellis, EC and Ramankutty, N (2008). Putting people in the map: anthropogenic biomes of the world. *Frontiers in Ecology and the Environment*, 6(8):pp. 439–447.

Ellison, AM (2004). Bayesian inference in ecology. *Ecology Letters*, 7(6):pp. 509–520.

Elvidge, C, Baugh, K, Hobson, V, Kihn, E, Kroehl, H et al. (1997). Satellite inventory of human settlements using nocturnal radiation emissions: a contribution for the global toolchest. *Global Change Biology*, 3(5):pp. 387–395.

Enserink, M (2008). Entomology. A mosquito goes global. *Science (New York, NY)*, 320(5878):pp. 864–866.

Epstein, PR (2001). Climate change and emerging infectious diseases. *Microbes and Infection*, 3(9):pp. 747–754.

Eritja, R, Escosa, R, Lucientes, J, Marquès, E, Roiz, D et al. (2005). Worldwide invasion of vector mosquitoes: present European distribution and challenges for Spain. *Biological Invasions*, 7(1):pp. 87–97.

Evans, TG, Diamond, SE, and Kelly, MW (2015). Mechanistic species distribution modelling as a link between physiology and conservation. *Conservation Physiology*, 3(1):p. cov056.

Fang, J (2010). Ecology: A world without mosquitoes. *Nature News*, 466(7305):pp. 432–434.

Faraji, A and Unlu, I (2016). The Eye of the Tiger, the Thrill of the Fight: Effective Larval and Adult Control Measures Against the Asian Tiger Mosquito, Aedes albopictus (Diptera: Culicidae), in North America. *Journal of Medical Entomology*, p. tjw096.

Feng, L (1930). Experiments with dirofilaria immitis and local species of mosquitoes in peiping, north china. *Ann Trop Med Parasit*, 24:pp. 347–366.

Ferrarese, U (2010). Monitoraggio di Aedes albopictus (Skuse) nel comune di Rovereto (Trento) nel 2009. *Annali del Museo Civico di Rovereto*, 25(2009):pp. 287–296.

Fischer, D, Thomas, S, Neteler, M, Tjaden, N, and Beierkuhnlein, C (2014). Climatic suitability of Aedes albopictus in Europe referring to climate change projections: comparison of mechanistic and correlative niche modelling approaches. *Eurosurveillance*, 19(6).

Floerl, O, Inglis, GJ, and Diettrich, J (2016). Incorporating human behaviour into the risk–release relationship for invasion vectors: why targeting only the worst offenders can fail to reduce spread. *Journal of Applied Ecology*, pp. n/a–n/a.

Foley, JA, DeFries, R, Asner, GP, Barford, C, Bonan, G et al. (2005). Global Consequences of Land Use. *Science*, 309(5734):pp. 570–574.

Forattini, OP (1986). Aedes (Stegomyia) Alboptctus (Skuse) identification in Brazil. *Revista de Saúde Pública*, 20(3):pp. 244–245.

Frazer, GW, Canham, CD, and Lertzman, KP (1999). Gap Light Analyzer (GLA), Version 2.0: Imaging software to extract canopy structure and gap light transmission indices from true-colour fisheye photographs, users manual and program documentation. *Simon Fraser University, Burnaby, British Columbia, and the Institute of Ecosystem Studies, Millbrook, New York*, 36.

Fredericks, AC and Fernandez-Sesma, A (2014). The burden of dengue and chikungunya worldwide: implications for the southern United States and California. *Annals of Global Health*, 80(6):pp. 466–475.

Fujioka, K and et al. (2012). Aedes albopictus (Skuse) in the city of El Monte and the initial response. In *Proc. Papers Mosq. Vect. Control. Assoc. Calif.*, volume 80, pp. 27–29.

Ganushkina, LA, Patraman, IV, Rezza, G, Migliorini, L, Litvinov, SK et al. (2016). Detection of Aedes aegypti, Aedes albopictus, and Aedes koreicus in the Area of Sochi, Russia. *Vector-Borne and Zoonotic Diseases*, 16(1):pp. 58–60.

Gao, Bc (1996). NDWI—A normalized difference water index for remote sensing of vegetation liquid water from space. *Remote Sensing of Environment*, 58(3):pp. 257–266.

Gardner, AM, Lampman, RL, and Muturi, EJ (2014). Land Use Patterns and the Risk of West Nile Virus Transmission in Central Illinois. *Vector-Borne and Zoonotic Diseases*, 14(5):pp. 338–345.

Garrett-Jones, C (1950). A Dispersion of Mosquitoes by Wind. *Nature*, 165(4190):pp. 285–285.

Gates, B (2016). The Deadliest Animal in the World.

Gelman, A and Hill, J (2006). *Data Analysis Using Regression and Multilevel/Hierarchical Models*. Cambridge University Press.

Gelman, A and Rubin, D (1992). Inference from iterative simulation using multiple sequences. *Statistical Science*, 7:pp. 457–511.

Gerhardt, RR, Gottfried, KL, Apperson, CS, Davis, BS, Erwin, PC et al. (2001). First isolation of La Crosse virus from naturally infected Aedes albopictus. *Emerging Infectious Diseases*, 7(5):pp. 807–811.

Gillooly, JF, Brown, JH, West, GB, Savage, VM, and Charnov, EL (2001). Effects of Size and Temperature on Metabolic Rate. *Science*, 293(5538):pp. 2248–2251.

Gilpin, ME and McClelland, GA (1979). Systems analysis of the yellow fever mosquito Aedes aegypti. *Fortschritte Der Zoologie*, 25(2-3):pp. 355–388.

Ginzburg, LR, Jensen, CXJ, and Yule, JV (2007). Aiming the "unreasonable effectiveness of mathematics" at ecological theory. *Ecological Modelling*, 207(2–4):pp. 356–362.

Goedde, N (1998). The poisoning of lake davis: weighting the risks. *Environs*, 21:pp. 3–24.

Gomes, B, Sousa, CA, Novo, MT, Freitas, FB, Alves, R et al. (2009). Asymmetric introgression between sympatric molestus and pipiens forms of Culex pipiens (Diptera: Culicidae) in the Comporta region, Portugal. *BMC Evol Biol*, 9:p. 262.

Gomes, B, Sousa, CA, Vicente, JL, Pinho, L, Calderón, I et al. (2013). Feeding patterns of molestus and pipiens forms of Culex pipiens (Diptera: Culicidae) in a region of high hybridization. *Parasit Vectors*, 6:p. 93.

González, MC, Hidalgo, CA, and Barabási, AL (2008). Understanding individual human mobility patterns. *Nature*, 453(7196):pp. 779–782.

Grard, G, Caron, M, Mombo, IM, Nkoghe, D, Ondo, SM et al. (2014). Zika Virus in Gabon (Central Africa) – 2007: A New Threat from Aedes albopictus ? *PLOS Negl Trop Dis*, 8(2):p. e2681.

Gratz, NG (2004). Critical review of the vector status of Aedes albopictus. *Med Vet Entomol*, 18(3):pp. 215–227.

Great Britain, Department of Energy and Climate Change, Great Britain, and Parliament (2012). *Annual energy statement 2012*. Stationery Office, London. OCLC: 822992293.

Guisan, A and Thuiller, W (2005). Predicting species distribution: offering more than simple habitat models. *Ecology Letters*.

Guisan, A and Zimmermann, NE (2000). Predictive habitat distribution models in ecology. *Ecological Modelling*, 135(2–3):pp. 147–186.

Guzzetta, G, Montarsi, F, Baldacchino, FA, Metz, M, Capelli, G et al. (2016). Potential Risk of Dengue and Chikungunya Outbreaks in Northern Italy Based on a Population Model of Aedes albopictus (Diptera: Culicidae). *PLOS Negl Trop Dis*, 10(6):p. e0004762.

Gómez, A, Kilpatrick, AM, Kramer, LD, Dupuis, AP, Maffei, JG et al. (2008). Land Use and West Nile Virus Seroprevalence in Wild Mammals. *Emerging Infectious Diseases*, 14(6):pp. 962–965.

Hadjichristodoulou, C, Pournaras, S, Mavrouli, M, Marka, A, Tserkezou, P et al. (2015). West Nile Virus Seroprevalence in the Greek Population in 2013: A Nationwide Cross-Sectional Survey. *PLoS ONE*, 10(11).

Haenke, S, Kovács-Hostyánszki, A, Fründ, J, Batáry, P, Jauker, B et al. (2014). Landscape configuration of crops and hedgerows drives local syrphid fly abundance. *Journal of Applied Ecology*, 51(2):pp. 505–513.

Hair, JF (2009). *Multivariate Data Analysis*.

Hancock, PA, Linley-White, V, Callahan, AG, Godfray, HCJ, Hoffmann, AA et al. (2016). Density-dependent population dynamics in Aedes aegypti slow the spread of wMel Wolbachia. *Journal of Applied Ecology*, pp. n/a–n/a.

Hannah, L, Flint, L, Syphard, AD, Moritz, MA, Buckley, LB et al. (2014). Fine-grain modeling of species' response to climate change: holdouts, stepping-stones, and microrefugia. *Trends in Ecology & Evolution*, 29(7):pp. 390–397.

Hanson, SM and Craig, GB (1995). Relationship between cold hardiness and supercooling point in Aedes albopictus eggs. *Journal of the American Mosquito Control Association*, 11(1):pp. 35–38.

Haramis, L (1984). Aedes-Triseriatus - a Comparison of Density in Tree Holes Vs Discarded Tires. *Mosquito News*, 44(4):pp. 485–489. WOS:A1984AAP4300008.

Harbach, RE (2012). Culex pipiens: species versus species complex taxonomic history and perspective. *Journal of the American Mosquito Control Association*, 28(4 Suppl):pp. 10–23.

Harrigan, RJ, Thomassen, HA, Buermann, W, Cummings, RF, Kahn, ME et al. (2010). Economic Conditions Predict Prevalence of West Nile Virus. *PLOS ONE*, 5(11):p. e15437.

Hatcher, MJ, Dick, JTA, and Dunn, AM (2012). Disease emergence and invasions. *Functional Ecology*, 26(6):pp. 1275–1287.

Hawley, WA (1988). The biology of Aedes albopictus. *Journal of the American Mosquito Control Association Supplement*, 1:pp. 1–39.

Hawley, WA, Reiter, P, Copeland, RS, Pumpuni, CB, and Craig, GB (1987). Aedes albopictus in North America: probable introduction in used tires from northern Asia. *Science*, 236(4805):pp. 1114–1116.

Hayes, EB, Komar, N, Nasci, RS, Montgomery, SP, O'Leary, DR et al. (2005). Epidemiology and transmission dynamics of West Nile virus disease. *Emerging Infectious Diseases*, 11(8):pp. 1167–1173.

Haylock, MR, Hofstra, N, Klein Tank, AMG, Klok, EJ, Jones, PD et al. (2008). A European daily high-resolution gridded data set of surface temperature and precipitation for 1950–2006. *J Geophys Res*, 113(D20):p. D20119.

Hejda, M, Pyšek, P, and Jarošík, V (2009). Impact of invasive plants on the species richness, diversity and composition of invaded communities. *Journal of Ecology*, 97(3):pp. 393–403.

Hellmann, JJ, Byers, JE, Bierwagen, BG, and Dukes, JS (2008). Five Potential Consequences of Climate Change for Invasive Species. *Conservation Biology*, 22(3):pp. 534–543.

Hijmans, RJ (2016). *raster: Geographic Data Analysis and Modeling*. R package version 2.5-8.

Hijmans, RJ, Phillips, S, Leathwick, J, and Elith, J (2015). *dismo: Species Distribution Modeling*. R package version 1.0-12.

Hirzel, AH, Hausser, J, Chessel, D, and Perrin, N (2002). Ecological-niche factor analysis: how to compute habitat-suitability maps without absence data? *Ecology*, 83(7):pp. 2027–2036.

Ho, BC, Ewert, A, and Chew, LM (1989). Interspecific competition among Aedes aegypti, Ae. albopictus, and Ae. triseriatus (Diptera: Culicidae): larval development in mixed cultures. *Journal of Medical Entomology*, 26(6):pp. 615–623.

Hobbs, RJ, Arico, S, Aronson, J, Baron, JS, Bridgewater, P et al. (2006). Novel ecosystems: theoretical and management aspects of the new ecological world order. *Global Ecology and Biogeography*, 15(1):pp. 1–7.

Homer, C, Dewitz, J, Yang, L, Jin, S, Danielson, P et al. (2015). Completion of the 2011 National Land Cover Database for the Conterminous United States – Representing a Decade of Land Cover Change Information. *Photogrammetric Engineering and Remote Sensing*, 81(5):pp. 345–354.

Honório, NA, Castro, MG, Barros, FSMd, Magalhães, MdAFM, and Sabroza, PC (2009). The spatial distribution of Aedes aegypti and Aedes albopictus in a transition zone, Rio de Janeiro, Brazil. *Cadernos de Saúde Pública*, 25(6):pp. 1203–1214.

Hooten, MB and Wikle, CK (2007). A hierarchical Bayesian non-linear spatio-temporal model for the spread of invasive species with application to the Eurasian Collared-Dove. *Environmental and Ecological Statistics*, 15(1):pp. 59–70.

Hughes, MT, Gonzalez, JA, Reagan, KL, Blair, CD, and Beaty, BJ (2006). Comparative potential of Aedes triseriatus, Aedes albopictus, and Aedes aegypti (Diptera: Culicidae) to transovarially transmit La Crosse virus. *Journal of Medical Entomology*, 43(4):pp. 757–761.

Hulme, PE (2006). Beyond control: wider implications for the management of biological invasions. *Journal of Applied Ecology*, 43(5):pp. 835–847.

Hulme, PE (2015). European Union: New law risks release of invasive species. *Nature*, 517(7532):pp. 21–21.

Hutchinson, GE (1957). Concluding Remarks. *Cold Spring Harbor Symposia on Quantitative Biology*, 22:pp. 415–427.

IPCC (2013). *Climate Change 2013: The Physical Science Basis. Contribution of Working Group I to the Fifth Assessment Report of the Intergovernmental Panel on Climate Change*. Cambridge University Press.

Iyer, AV and Kousoulas, KG (2013). A Review of Vaccine Approaches for West Nile Virus. *International Journal of Environmental Research and Public Health*, 10(9):pp. 4200–4223.

Jimenez-Clavero, MA (2012). Animal viral diseases and global change: bluetongue and West Nile fever as paradigms. *Front Gene*, 3:p. 105.

Johnson, BJ, Munafo, K, Shappell, L, Tsipoura, N, Robson, M et al. (2012). The roles of mosquito and bird communities on the prevalence of West Nile virus in urban wetland and residential habitats. *Urban Ecosyst*, 15(3):pp. 513–531.

Johnson, JB and Omland, KS (2004). Model selection in ecology and evolution. *Trends in Ecology & Evolution*, 19(2):pp. 101–108.

Joyce, RJ, Janowiak, JE, Arkin, PA, and Xie, P (2004). CMORPH: A Method that Produces Global Precipitation Estimates from Passive Microwave and Infrared Data at High Spatial and Temporal Resolution. *Journal of Hydrometeorology*, 5(3):pp. 487–503.

Juliano, SA (2007). Population Dynamics. *Journal of the American Mosquito Control Association*, 23(2 Suppl):pp. 265–275.

Juliano, SA, Lounibos, LP, and O'Meara, GF (2004). A field test for competitive effects of Aedes albopictus on A. aegypti in South Florida: differences between sites of coexistence and exclusion? *Oecologia*, 139(4):pp. 583–593.

Karesh, WB, Dobson, A, Lloyd-Smith, JO, Lubroth, J, Dixon, MA et al. (2012). Ecology of zoonoses: natural and unnatural histories. *Lancet*, 380(9857):pp. 1936–1945.

Karl, S, Halder, N, Kelso, JK, Ritchie, SA, and Milne, GJ (2014). A spatial simulation model for dengue virus infection in urban areas. *BMC Infectious Diseases*, 14:p. 447.

Kati, V and Jari, N (2016). Bottom-up thinking-Identifying socio-cultural values of ecosystem services in local blue-green infrastructure planning in Helsinki, Finland. *Land Use Policy*, 50:pp. 537–547.

Kaufman, MG and Fonseca, DM (2014). Invasion biology of Aedes japonicus japonicus (Diptera: Culicidae). *Annu Rev Entomol*, 59:pp. 31–49.

Kearney, M and Porter, W (2009). Mechanistic niche modelling: combining physiological and spatial data to predict species' ranges. *Ecology Letters*, 12(4):pp. 334–350.

Killick, R and Eckley, IA (2014). changepoint : An R Package for Changepoint Analysis. *Journal of Statistical Software*, 58(3).

Kilpatrick, AM (2011). Globalization, Land Use, and the Invasion of West Nile Virus. *Science*, 334(6054):pp. 323–327.

Kilpatrick, AM, Daszak, P, Jones, MJ, Marra, PP, and Kramer, LD (2006). Host heterogeneity dominates West Nile virus transmission. *Proceedings of the Royal Society of London B: Biological Sciences*, 273(1599):pp. 2327–2333.

Kilpatrick, AM, Meola, MA, Moudy, RM, and Kramer, LD (2008). Temperature, Viral Genetics, and the Transmission of West Nile Virus by Culex pipiens Mosquitoes. *PLOS Pathog*, 4(6):p. e1000092.

Kim, HC, Chong, ST, Nunn, PV, and Klein, TA (2010). Seasonal prevalence of mosquitoes collected from light traps in the Republic of Korea, 2007. *Entomological Research*, 40(2):pp. 136–144.

Kim, HC, Chong, ST, O'brien, LL, O'guinn, ML, Turell, MJ et al. (2006). Seasonal prevalence of mosquitoes collected from light traps in the Republic of Korea in 2003. *Entomological Research*, 36(3):pp. 139–148.

Kingsolver, JG (1979). Thermal and Hydric Aspects of Environmental Heterogeneity in the Pitcher Plant Mosquito. *Ecological Monographs*, 49(4):pp. 357–376.

Kleinschmidt, I, Bagayoko, M, Clarke, GP, Craig, M, and Le Sueur, D (2000). A spatial statistical approach to malaria mapping. *International Journal of Epidemiology*, 29(2):pp. 355–361.

Kling, LJ, Juliano, SA, and Yee, DA (2007). Larval mosquito communities in discarded vehicle tires in a forested and unforested site: detritus type, amount, and water nutrient differences. *Journal of vector ecology : journal of the Society for Vector Ecology*, 32(2):pp. 207–217.

Kraemer, MU, Sinka, ME, Duda, KA, Mylne, AQ, Shearer, FM et al. (2015). The global distribution of the arbovirus vectors Aedes aegypti and Ae. albopictus. *eLife*, 4:p. e08347.

Krishna, YC, Krishnaswamy, J, and Kumar, NS (2008). Habitat factors affecting site occupancy and relative abundance of four-horned antelope. *Journal of Zoology*, 276(1):pp. 63–70.

Kruschke, JK (2010). *Doing Bayesian Data Analysis*. 1st edition edition.

Kruschke, JK (2015a). *Doing Bayesian Data Analysis*. 2nd edition edition.

Kruschke, JK (2015b). Metric predicted variable with multiple nominal predictors. In *Doing Bayesian Data Analysis*, pp. 621–646. Academic Press, 2st edition edition.

Kuno, G, Chang, GJJ, Tsuchiya, KR, Karabatsos, N, and Cropp, CB (1998). Phylogeny of the Genus Flavivirus. *Journal of Virology*, 72(1):pp. 73–83.

Kurucz, K, Kiss, V, Zana, B, Schmieder, V, Kepner, A et al. (2016). Emergence of Aedes koreicus (Diptera: Culicidae) in an urban area, Hungary, 2016. *Parasitology Research*, pp. 1–3.

Kwan, JL, Park, BK, Carpenter, TE, Ngo, V, Civen, R et al. (2012). Comparison of Enzootic Risk Measures for Predicting West Nile Disease, Los Angeles, California, USA, 2004–2010. *Emerging Infectious Diseases*, 18(8).

La Ruche, G, Souarès, Y, Armengaud, A, Peloux-Petiot, F, Delaunay, P et al. (2010). First two autochthonous dengue virus infections in metropolitan France, September 2010. *Euro Surveill*, 15(39):p. 19676.

LaBeaud, AD, Gorman, AM, Koonce, J, Kippes, C, McLeod, J et al. (2008). Rapid GIS-based profiling of West Nile virus transmission: defining environmental factors associated with an urban outbreak in Northeast Ohio, USA. *Geospatial health*, 2(2):p. 215.

LaDeau, SL, Allan, BF, Leisnham, PT, and Levy, MZ (2015). The ecological foundations of transmission potential and vector-borne disease in urban landscapes. *Functional Ecology*, pp. n/a–n/a.

Lampman, R, Hanson, S, and Novak, R (1997). Seasonal abundance and distribution of mosquitoes at a rural waste tire site in Illinois. *Journal of the American Mosquito Control Association*, 13(2):pp. 193–200.

Landesman, WJ, Allan, BF, Langerhans, RB, Knight, TM, and Chase, JM (2007). Inter-Annual Associations Between Precipitation and Human Incidence of West Nile Virus in the United States. *Vector-Borne and Zoonotic Diseases*, 7(3):pp. 337–343.

Landis, JR and Koch, GG (1977). The Measurement of Observer Agreement for Categorical Data. *Biometrics*, 33(1):pp. 159–174.

Lederberg, J, Shope, RE, and Oaks, SC (1992). *Emerging Infections: Microbial Threats to Health in the United States*. National Academies Press, Washington, D.C.

Lehane, M (2005). The Biology of Blood-Sucking in Insects.

Lenoir, J and Svenning, JC (2014). Climate-related range shifts – a global multidimensional synthesis and new research directions. *Ecography*, pp. no–no.

Leroux, SJ, Larrivée, M, Boucher-Lalonde, V, Hurford, A, Zuloaga, J et al. (2013). Mechanistic models for the spatial spread of species under climate change. *Ecological Applications*, 23(4):pp. 815–828.

Li, Y, Kamara, F, Zhou, G, Puthiyakunnon, S, Li, C et al. (2014). Urbanization Increases Aedes albopictus Larval Habitats and Accelerates Mosquito Development and Survivorship. *PLoS Negl Trop Dis*, 8(11):p. e3301.

Li, ZL, Tang, BH, Wu, H, Ren, H, Yan, G et al. (2013). Satellite-derived land surface temperature: Current status and perspectives. *Remote Sensing of Environment*, 131:pp. 14–37.

Link, W and Sauer, J (2002). A hierarchical analysis of population change with application to Cerulean Warblers. *Ecology*, 83(10):p. 9.

Linthicum, KJ, Kramer, VL, Madon, MB, Fujioka, K, and Surveillance-Control Team (2003). Introduction and potential establishment of Aedes albopictus in California in 2001. *Journal of the American Mosquito Control Association*, 19(4):pp. 301–308.

Liu, H, Weng, Q, and Gaines, D (2008). Spatio-temporal analysis of the relationship between WNV dissemination and environmental variables in Indianapolis, USA. *International Journal of Health Geographics*, 7(1):pp. 1–13.

Lockwood, JL, Cassey, P, and Blackburn, T (2005). The role of propagule pressure in explaining species invasions. *Trends in Ecology & Evolution*, 20(5):pp. 223–228.

Lounibos, LP (2002). Invasions by insect vectors of human disease. *Annual Review of Entomology*, 47:pp. 233–266.

Lourenço, PM, Sousa, CA, Seixas, J, Lopes, P, Novo, MT et al. (2011). Anopheles atroparvus density modeling using MODIS NDVI in a former malarious area in Portugal. *Journal of Vector Ecology: Journal of the Society for Vector Ecology*, 36(2):pp. 279–291.

Low, M, Tsegaye, AT, Ignell, R, Hill, S, Elleby, R et al. (2016). The importance of accounting for larval detectability in mosquito habitat-association studies. *Malaria Journal*, 15:p. 253.

Lowe, S, Browne, M, Boudjelas, S, and De Poorter, M (2000). 100 of the world's worst invasive alien species: a selection from the global invasive species database.

Lozier, JD, Aniello, P, and Hickerson, MJ (2009). Predicting the distribution of Sasquatch in western North America: anything goes with ecological niche modelling. *Journal of Biogeography*, 36(9):pp. 1623–1627.

Lucientes-Curdi, J, Molina-Moreno, R, Amela-Heras, C, Simon-Soria, F, Santos-Sanz, S et al. (2014). Dispersion of Aedes albopictus in the Spanish Mediterranean Area. *The European Journal of Public Health*, 24(4):pp. 637–640.

Luck, GW, Smallbone, LT, and O'Brien, R (2009). Socio-Economics and Vegetation Change in Urban Ecosystems: Patterns in Space and Time. *Ecosystems*, 12(4):pp. 604–620.

MacArthur, RH and Wilson, EO (1967). *The Theory of Island Biogeography*. Princeton University Press. Google-Books-ID: a10cdkywhVgC.

Mack, RN, Simberloff, D, Mark Lonsdale, W, Evans, H, Clout, M et al. (2000). Biotic Invasions: Causes, Epidemiology, Global Consequences, and Control. *Ecological Applications*, 10(3):pp. 689–710.

Maneerat, S and Daudé, E (2016). A spatial agent-based simulation model of the dengue vector Aedes aegypti to explore its population dynamics in urban areas. *Ecological Modelling*, 333:pp. 66–78.

Manel, S, Ceri Williams, H, and Ormerod, S (2001). Evaluating presence-absence models in ecology: The need to account for prevalence. *Journal of Applied Ecology*, 38(5):pp. 921–931.

Manfred Köhler, Marco Schmidt, Friedrich Wilhelm Grimme, Michael Laar, Vera Lúcia de Assunção Paiva et al. (2002). Green roofs in temperate climates and in the hot-humid tropics — far beyond the aesthetics. *Environmental Management and Health*, 13(4):pp. 382–391.

Manica, M, Filipponi, F, D'Alessandro, A, Screti, A, Neteler, M et al. (2016). Spatial and Temporal Hot Spots of Aedes albopictus Abundance inside and outside a South European Metropolitan Area. *PLOS Negl Trop Dis*, 10(6):p. e0004758.

Marcantonio, M, Metz, M, Baldacchino, F, Arnoldi, D, Montarsi, F et al. (2016). First assessment of potential distribution and dispersal capacity of the emerging invasive mosquito Aedes koreicus in Northeast Italy. *Parasites & Vectors*, 9(1):p. 63.

Marcantonio, M, Rizzoli, A, Metz, M, Rosà, R, Marini, G et al. (2015). Identifying the Environmental Conditions Favouring West Nile Virus Outbreaks in Europe. *PLoS ONE*, 10(3):p. e0121158.

Marchand, E, Prat, C, Jeannin, C, Lafont, E, Bergmann, T et al. (2013). Autochthonous case of dengue in France, October 2013. *Euro Surveill*, 18(50):p. 20661.

Marini, F, Caputo, B, Pombi, M, Tarsitani, G, and della Torre, A (2010). Study of Aedes albopictus dispersal in Rome, Italy, using sticky traps in mark-release-recapture experiments. *Medical and Veterinary Entomology*, 24(4):pp. 361–368.

Martinez, EZ and Achcar, JA (2014). Trends in epidemiology in the 21st century: time to adopt Bayesian methods. *Cadernos De Saúde Pública*, 30(4):pp. 703–714.

Martín-Acebes, MA (2012). West Nile virus: A re-emerging pathogen revisited. *World Journal of Virology*, 1(2):p. 51.

May, FJ, Davis, CT, Tesh, RB, and Barrett, ADT (2011). Phylogeography of West Nile Virus: from the Cradle of Evolution in Africa to Eurasia, Australia, and the Americas. *J Virol*, 85(6):pp. 2964–2974.

McCarthy, MA and Masters, P (2005). Profiting from prior information in Bayesian analyses of ecological data. *Journal of Applied Ecology*, 42(6):pp. 1012–1019.

McDermott, SM and Finnoff, DC (2016). Impact of repeated human introductions and the Allee effect on invasive species spread. *Ecological Modelling*, 329:pp. 100–111.

McFeeters, SK (2013). Using the Normalized Difference Water Index (NDWI) within a geographic information system to detect swimming pools for mosquito abatement: a practical approach. *Remote Sensing*, 5(7).

McGarigal, K and Marks, BJ (1995). *Fragstats: spatial pattern analysis program for quantifying landscape structure*, volume 351. U.S. Department of Agriculture, Forest Service, Pacific Northwest Research Station, Portland, OR.

McPherson, EGUoC (1998). Atmospheric carbon dioxide reduction by Sacramento's urban forest. *Journal of arboriculture (USA)*.

Medeiros-Sousa, AR, Ceretti-Júnior, W, de Carvalho, GC, Nardi, MS, Araujo, AB et al. (2015). Diversity and abundance of mosquitoes (Diptera:Culicidae) in an urban park: Larval habitats and temporal variation. *Acta Tropica*, 150:pp. 200–209.

Medley, KA (2010). Niche shifts during the global invasion of the Asian tiger mosquito, Aedes albopictus Skuse (Culicidae), revealed by reciprocal distribution models. *Global Ecology and Biogeography*, 19(1):pp. 122–133.

Medlock, JM, Avenell, D, Barrass, I, and Leach, S (2006). Analysis of the potential for survival and seasonal activity of Aedes albopictus (Diptera: Culicidae) in the United Kingdom. *Journal of Vector Ecology: Journal of the Society for Vector Ecology*, 31(2):pp. 292–304.

Medlock, JM, Hansford, KM, Schaffner, F, Versteirt, V, Hendrickx, G et al. (2012). A review of the invasive mosquitoes in Europe: ecology, public health risks, and control options. *Vector Borne Zoonotic Dis*, 12(6):pp. 435–447.

Medlock, JM, Hansford, KM, Versteirt, V, Cull, B, Kampen, H et al. (2015). An entomological review of invasive mosquitoes in Europe. *Bulletin of Entomological Research*, pp. 1–27.

Mercado-Hernandez, R, Fernández-Salas, I, and Villarreal-Martinez, H (2003). Spatial distribution of the larval indices of Aedes aegypti in Guadalupe, Nuevo León, Mexico, with circular distribution analysis. *Journal of the American Mosquito Control Association*, 19(1):pp. 15–18.

Merow, C, Smith, MJ, Edwards, TC, Guisan, A, McMahon, SM et al. (2014). What do we gain from simplicity versus complexity in species distribution models? *Ecography*, 37(12):pp. 1267–1281.

Metz, M, Rocchini, D, and Neteler, M (2014). Surface Temperatures at the Continental Scale: Tracking Changes with Remote Sensing at Unprecedented Detail. *Remote Sensing*, 6(5):pp. 3822–3840.

Meyer, RP, Hardy, JL, and Reisen, WK (1990). Diel changes in adult mosquito microhabitat temperatures and their relationship to the extrinsic incubation of arboviruses in mosquitoes in Kern County, California. *Journal of Medical Entomology*, 27(4):pp. 607–614.

Miles, JAR (1964). Some ecological aspects of the problem of arthropod-borne animal viruses in the Western Pacific and South-East Asia regions. *Bull World Health Organ*, 30(2):pp. 197–210.

Mitchell, CJ, Niebylski, ML, Smith, GC, Karabatsos, N, Martin, D et al. (1992). Isolation of eastern equine encephalitis virus from Aedes albopictus in Florida. *Science*, 257(5069):pp. 526–527.

Monaghan, AJ, Sampson, KM, Steinhoff, DF, Ernst, KC, Ebi, KL et al. (2016). The potential impacts of 21st century climatic and population changes on human exposure to the virus vector mosquito Aedes aegypti. *Climatic Change*, pp. 1–14.

Montarsi, F, Ciocchetta, S, Devine, G, Ravagnan, S, Mutinelli, F et al. (2015a). Development of Dirofilaria immitis within the mosquito Aedes (Finlaya) koreicus, a new invasive species for Europe. *Parasites and Vectors*, 8(1).

Montarsi, F, Drago, A, Martini, S, Calzolari, M, De Filippo, F et al. (2015b). Current distribution of the invasive mosquito species, Aedes koreicus [Hulecoeteomyia koreica] in northern Italy. *Parasites & Vectors*, 8:p. 614.

Montarsi, F, Martini, S, Dal Pont, M, Delai, N, Ferro Milone, N et al. (2013). Distribution and habitat characterization of the recently introduced invasive mosquito Aedes koreicus [Hulecoeteomyia koreica], a new potential vector and pest in north-eastern Italy. *Parasites & Vectors*, 6(1):p. 292.

Montecino, D, Marcantonio, M, Perkins, A, and Barker, C (2016). Modeling *Aedes albopictus* Skuse population dynamics and spatial behavior in urban landscapes, an integrated approach. *In prep*, 81.

Moore, CG (1999). Aedes albopictus in the United States: current status and prospects for further spread. *Journal of the American Mosquito Control Association*, 15(2):pp. 221–227.

Morchón, R, Carretón, E, González-Miguel, J, and Mellado-Hernández, I (2012). Heartworm Disease (Dirofilaria immitis) and Their Vectors in Europe – New Distribution Trends. *Frontiers in Physiology*, 3.

Morens, DM and Fauci, AS (2013). Emerging Infectious Diseases: Threats to Human Health and Global Stability. *PLOS Pathog*, 9(7):p. e1003467.

Morens, DM, Folkers, GK, and Fauci, AS (2004). The challenge of emerging and re-emerging infectious diseases. *Nature*, 430(6996):pp. 242–249.

Morin, CW and Comrie, AC (2013). Regional and seasonal response of a West Nile virus vector to climate change. *Proc Natl Acad Sci USA*, 110(39):pp. 15620–15625.

Moudy, RM, Meola, MA, Morin, LLL, Ebel, GD, and Kramer, LD (2007). A Newly Emergent Genotype of West Nile Virus Is Transmitted Earlier and More Efficiently by Culex Mosquitoes. *Am J Trop Med Hyg*, 77(2):pp. 365–370.

Mulatti, P, Ferguson, HM, Bonfanti, L, Montarsi, F, Capelli, G et al. (2014). Determinants of the population growth of the West Nile virus mosquito vector Culex pipiens in a repeatedly affected area in Italy. *Parasit Vectors*, 7:p. 26.

Murray, KO, Walker, C, and Gould, E (2011). The virology, epidemiology, and clinical impact of West Nile virus: a decade of advancements in research since its introduction into the Western Hemisphere. *Epidemiology and Infection*, 139(06):pp. 807–817.

Nature, E (2016). Viral complacency. *Nature*, 532(7597):p. 5.

Nayar, JK and Sauerman, DM (1975). The effects of nutrition on survival and fecundity in Florida mosquitoes. Part 1. Utilization of sugar for survival. *Journal of Medical Entomology*, 12(1):pp. 92–98.

Nelder, JA and Mead, R (1965). A Simplex Method for Function Minimization. *The Computer Journal*, 7(4):pp. 308–313.

Neteler, M, Bowman, MH, Landa, M, and Metz, M (2012). GRASS GIS: A multi-purpose open source GIS. *Environmental Modelling & Software*, 31:pp. 124–130.

Neteler, M and Metz, M (2014). MODIS and Vector-Borne Diseases.

Neteler, M, Metz, M, Rocchini, D, Rizzoli, A, Flacio, E et al. (2013). Is switzerland suitable for the invasion of *Aedes albopictus*? *PLoS ONE*, 8(12):p. e82090.

Neteler, M, Roiz, D, Rocchini, D, Castellani, C, and Rizzoli, A (2011). Terra and Aqua satellites track tiger mosquito invasion: modelling the potential distribution of Aedes albopictus in north-eastern Italy. *International Journal of Health Geographics*, 10(1):p. 49.

Niebylski, ML, Savage, HM, Nasci, RS, and Craig, GB (1994). Blood hosts of Aedes albopictus in the United States. *Journal of the American Mosquito Control Association*, 10(3):pp. 447–450.

Norris, K (2004). Managing threatened species: the ecological toolbox, evolutionary theory and declining-population paradigm. *Journal of Applied Ecology*, 41(3):pp. 413–426.

Nunes, MSwcfT, Heuer, C, Marshall, J, Sanchez, J, Thornton, R et al. (2016). *epiR: Tools for the Analysis of Epidemiological Data*. R package version 0.9-77.

Ogden, NH and Lindsay, LR (2016). Effects of Climate and Climate Change on Vectors and Vector-Borne Diseases: Ticks Are Different. *Trends in Parasitology*, 32(8):pp. 646–656.

Ohta, S and Kag, T (2011). Possible Effects of Future Climate Changes on the Maximum Number of Generations of Anopheles in Monsoon Asia. In JA Blanco (Ed.), *Climate Change - Geophysical Foundations and Ecological Effects*. InTech.

Osório, HC, Zé-Zé, L, Amaro, F, Nunes, A, and Alves, MJ (2013). Sympatric occurrence of Culex pipiens (Diptera, Culicidae) biotypes pipiens, molestus and their hybrids in Portugal, Western Europe: feeding patterns and habitat determinants. *Med Vet Entomol*.

Overgaard, HJ, Ekbom, B, Suwonkerd, W, and Takagi, M (2003). Effect of landscape structure on anopheline mosquito density and diversity in northern Thailand: Implications for malaria transmission and control. *Landscape Ecology*, 18(6):p. 605.

Ozdenerol, E, Taff, GN, and Akkus, C (2013). Exploring the Spatio-Temporal Dynamics of Reservoir Hosts, Vectors, and Human Hosts of West Nile Virus: A Review of the Recent Literature. *International Journal of Environmental Research and Public Health*, 10(11):pp. 5399–5432.

Paaijmans, KP, Imbahale, SS, Thomas, MB, and Takken, W (2010). Relevant microclimate for determining the development rate of malaria mosquitoes and possible implications of climate change. *Malaria Journal*, 9:p. 196.

Pacifici, M, Foden, WB, Visconti, P, Watson, JEM, Butchart, SHM et al. (2015). Assessing species vulnerability to climate change. *Nature Climate Change*, 5(3):pp. 215–224.

Pagel, J and Schurr, FM (2012). Forecasting species ranges by statistical estimation of ecological niches and spatial population dynamics. *Global Ecology and Biogeography*, 21(2):pp. 293–304.

Panella, NA, Crockett, RJK, Biggerstaff, BJ, and Komar, N (2011). The Centers for Disease Control and Prevention resting trap: a novel device for collecting resting mosquitoes. *Journal of the American Mosquito Control Association*, 27(3):pp. 323–325.

Papa, A (2013). West nile virus infections in humans-focus on greece. *J Clin Virol*, 58(2):pp. 351–353.

Patrice, B, Pierre, D, Carsten, B, Leon, S, Christelle, V et al. (2008). *GlobCover - Products Description and Validation Report*.

Patz, JA, Daszak, P, Tabor, GM, Aguirre, AA, Pearl, M et al. (2004). Unhealthy landscapes: Policy recommendations on land use change and infectious disease emergence. *Environ Health Perspect*, 112(10):pp. 1092–1098.

Paupy, C, Delatte, H, Bagny, L, Corbel, V, and Fontenille, D (2009). Aedes albopictus, an arbovirus vector: From the darkness to the light. *Microbes and Infection*, 11(14-15):pp. 1177–1185.

Paz, S, Malkinson, D, Green, MS, Tsioni, G, Papa, A et al. (2013). Permissive Summer Temperatures of the 2010 European West Nile Fever Upsurge. *PLOS ONE*, 8(2):p. e56398.

Paz, S and Semenza, JC (2013). Environmental drivers of West Nile fever epidemiology in Europe and Western Asia–a review. *Int J Environ Res Public Health*, 10(8):pp. 3543–3562.

Pecoraro, HL, Day, HL, Reineke, R, Stevens, N, Withey, JC et al. (2007). Climatic and landscape correlates for potential West Nile virus mosquito vectors in the Seattle region. *Journal of Vector Ecology*, 32(1):pp. 22–28.

Petersen, LR and Marfin, AA (2002). West Nile virus: a primer for the clinician. *Ann Intern Med*, 137(3):pp. 173–179.

Petersen, LR and Roehrig, JT (2001). West Nile virus: a reemerging global pathogen. *Emerging Infectious Diseases*, 7(4):pp. 611–614.

Petersen LR, Brault AC, and Nasci RS (2013). West nile virus: Review of the literature. *JAMA*, 310(3):pp. 308–315.

Phillips, S, Anderson, R, and Schapire, R (2006). Maximum entropy modeling of species geographic distributions. *Ecological Modelling*, 190(3-4):pp. 231–259.

Phillips, SJ and Dudı, M (2008). Modeling of species distributions with Maxent : new extensions and a comprehensive evaluation. *Ecography*, (December 2007):pp. 161–175.

Pielou, EC (1966). The measurement of diversity in different types of biological collections. *Journal of Theoretical Biology*, 13:pp. 131–144.

Pimentel, D (2011). *Biological Invasions: Economic and Environmental Costs of Alien Plant, Animal, and Microbe Species, Second Edition*. CRC Press. Google-Books-ID: wDbNBQAAQBAJ.

Pimentel, D, Zuniga, R, and Morrison, D (2005). Update on the environmental and economic costs associated with alien-invasive species in the United States. *Ecological Economics*, 52(3):pp. 273–288.

Pita, R, Mira, A, Moreira, F, Morgado, R, and Beja, P (2009). Influence of landscape characteristics on carnivore diversity and abundance in Mediterranean farmland. *Agriculture, Ecosystems & Environment*, 132(1–2):pp. 57–65.

Platonov, AE, Fedorova, MV, Karan, LS, Shopenskaya, TA, Platonova, OV et al. (2008). Epidemiology of West Nile infection in Volgograd, Russia, in relation to climate change and mosquito (Diptera: Culicidae) bionomics. *Parasitol Res*, 103(1):pp. 45–53.

Plummer, M (2003). *JAGS: A program for analysis of Bayesian graphical models using Gibbs sampling*.

Plummer, M (2015). *rjags: Bayesian Graphical Models using MCMC*. R package version 4-4.

Plummer, M, Best, N, Cowles, K, and Vines, K (2006). CODA: Convergence Diagnosis and Output Analysis for MCMC. *R News*, 6(1):pp. 7–11.

Popović, N, Milošević, B, Urošević, A, Poluga, J, Lavadinović, L et al. (2013). Outbreak of west Nile virus infection among humans in Serbia, August to October 2012. *Eurosurveillance*, 18(43).

Pradier, S, Leblond, A, and Durand, B (2008). Land Cover, Landscape Structure, and West Nile Virus Circulation in Southern France. *Vector-Borne and Zoonotic Diseases*, 8(2):pp. 253–264.

Pratt, JJ and Heterick, RH (1946). Tires as a factor in the transportation of mosquitoes by ships. *Military Surgeon*, 99(6):pp. 785–788.

Proestos, Y, Christophides, GK, Ergüler, K, Tanarhte, M, Waldock, J et al. (2015). Present and future projections of habitat suitability of the Asian tiger mosquito, a vector of viral pathogens, from global climate simulation. *Phil Trans R Soc B*, 370(1665):p. 20130554.

Prow, NA, Edmonds, JH, Williams, DT, Setoh, YX, Bielefeldt-Ohmann, H et al. (2016). Virulence and Evolution of West Nile Virus, Australia, 1960–2012. *Emerging Infectious Diseases*, 22(8):pp. 1353–1362.

Pumpuni, CB, Knepler, J, and Craig, GB (1992). Influence of temperature and larval nutrition on the diapause inducing photoperiod of Aedes albopictus. *Journal of the American Mosquito Control Association*, 8(3):pp. 223–227.

Pyšek, P, Jarošík, V, Hulme, PE, Kühn, I, Wild, J et al. (2010). Disentangling the role of environmental and human pressures on biological invasions across Europe. *PNAS*, 107(27):pp. 12157–12162.

Pérez-Rodríguez, A, Fernández-González, S, de la Hera, I, and Pérez-Tris, J (2013). Finding the appropriate variables to model the distribution of vector-borne parasites with different environmental preferences: climate is not enough. *Glob Change Biol*, 19(11):pp. 3245–3253.

R Core Team (2014). *R: A Language and Environment for Statistical Computing*. R Foundation for Statistical Computing, Vienna, Austria.

R Core Team (2015). *R: A Language and Environment for Statistical Computing*. R Foundation for Statistical Computing, Vienna, Austria.

R Core Team (2016). *R: A Language and Environment for Statistical Computing*. R Foundation for Statistical Computing, Vienna, Austria.

Raghwani, J, Rambaut, A, Holmes, EC, Hang, VT, Hien, TT et al. (2011). Endemic Dengue Associated with the Co-Circulation of Multiple Viral Lineages and Localized Density-Dependent Transmission. *PLOS Pathog*, 7(6):p. e1002064.

Reinert, JF, Harbach, RE, and Kitching, IJ (2004). Phylogeny and classification of Aedini (Diptera: Culicidae), based on morphological characters of all life stages. *Zoological Journal of the Linnean Society*, 142(3):pp. 289–368.

Reinert, JF, Harbach, RE, and Kitching, IJ (2009). Phylogeny and classification of tribe Aedini (Diptera: Culicidae). *Zoological Journal of the Linnean Society*, 157(4):pp. 700–794.

Reisen, WK (2013). Ecology of West Nile Virus in North America. *Viruses*, 5(9):pp. 2079–2105.

Reiter, P (1996). [Oviposition and dispersion of Aedes aegypti in an urban environment]. *Bulletin De La Société De Pathologie Exotique (1990)*, 89(2):pp. 120–122.

Reiter, P (2001). Climate change and mosquito-borne disease. *Environmental Health Perspectives*, 109(Suppl 1):pp. 141–161.

Reiter, P (2010). West Nile virus in Europe: understanding the present to gauge the future. *Eurosurveillance*.

Revolution Analytics and Weston, S (2015). *doSNOW: Foreach Parallel Adaptor for the 'snow' Package*. R package version 1.0.14.

Rey, JR, Nishimura, N, Wagner, B, Braks, MA, O'connell, SM et al. (2006). Habitat Segregation of Mosquito Arbovirus Vectors in South Florida. *Journal of medical entomology*, 43(6):pp. 1134–1141.

Rezza, G, Nicoletti, L, Angelini, R, Romi, R, Finarelli, AC et al. (2007). Infection with chikungunya virus in Italy: an outbreak in a temperate region. *Lancet*, 370(9602):pp. 1840–1846.

Richards, SL, Ponnusamy, L, Unnasch, TR, Hassan, HK, and Apperson, CS (2006). Host-feeding patterns of Aedes albopictus (Diptera: Culicidae) in relation to availability of human and domestic animals in suburban landscapes of central North Carolina. *Journal of Medical Entomology*, 43(3):pp. 543–551.

Ricotta, C, Godefroid, S, and Rocchini, D (2010). Invasiveness of alien plants in Brussels is related to their phylogenetic similarity to native species. *Diversity and Distributions*, 16(4):pp. 655–662.

Rizzoli, A, Jimenez-Clavero, MA, Barzon, L, Cordioli, P, Figuerola, J et al. (2015). The challenge of West Nile virus in Europe: knowledge gaps and research priorities. *Euro Surveillance: Bulletin Européen Sur Les Maladies Transmissibles = European Communicable Disease Bulletin*, 20(20).

Rocchini, D, Foody, GM, Nagendra, H, Ricotta, C, Anand, M et al. (2013). Uncertainty in ecosystem mapping by remote sensing. *Computers & Geosciences*, 50:pp. 128–135.

Roche, B, Léger, L, L'Ambert, G, Lacour, G, Foussadier, R et al. (2015). The Spread of Aedes albopictus in Metropolitan France: Contribution of Environmental Drivers and Human Activities and Predictions for a Near Future. *PLoS ONE*, 10(5):p. e0125600.

Rochlin, I, Ninivaggi, DV, Hutchinson, ML, and Farajollahi, A (2013). Climate Change and Range Expansion of the Asian Tiger Mosquito (Aedes albopictus) in Northeastern USA: Implications for Public Health Practitioners. *PLoS ONE*, 8(4):p. e60874.

Roerink, GJ, Menenti, M, and Verhoef, W (2000). Reconstructing cloudfree NDVI composites using Fourier analysis of time series. *International Journal of Remote Sensing*, 21(9):pp. 1911–1917.

Roiz, D, Neteler, M, Castellani, C, Arnoldi, D, and Rizzoli, A (2011). Climatic Factors Driving Invasion of the Tiger Mosquito (Aedes albopictus) into New Areas of Trentino, Northern Italy. *PLoS ONE*, 6(4):p. e14800.

Rosà, R, Marini, G, Bolzoni, L, Neteler, M, Metz, M et al. (2014). Early warning of West Nile virus mosquito vector: climate and land use models successfully explain phenology and abundance of Culex pipiens mosquitoes in north-western Italy. *Parasites & Vectors*, 7:p. 269.

Rouse, JW (1974). Monitoring the vernal advancement and retrogradation (green wave effect) of natural vegetation. Technical report.

Rubio, A, Bellocq, MI, and Vezzani, D (2012). Community structure of artificial container-breeding flies (Insecta: Diptera) in relation to the urbanization level. *Landscape and Urban Planning*, 105(3):pp. 288–295.

Rueda, LM, Patel, KJ, Axtell, RC, and Stinner, RE (1990). Temperature-Dependent Development and Survival Rates of Culex quinquefasciatus and Aedes aegypti (Diptera: Culicidae). *Journal of Medical Entomology*, 27(5):pp. 892–898.

Sabatini, A, Raineri, V, Trovato, G, and Coluzzi, M (1990). Aedes albopictus in Italy and possible diffusion of the species into the Mediterranean area. *Parassitologia*, 32(3):pp. 301–304.

Sambri, V, Capobianchi, M, Charrel, R, Fyodorova, M, Gaibani, P et al. (2013). West nile virus in europe: emergence, epidemiology, diagnosis, treatment, and prevention. *Clin Microbiol Infect*, 19(8):pp. 699–704.

Samson, DM, Archer, RS, Alimi, TO, Arheart, KK, Impoinvil, DE et al. (2015). New baseline environmental assessment of mosquito ecology in northern Haiti during increased urbanization. *Journal of vector ecology : journal of the Society for Vector Ecology*, 40(1):pp. 46–58.

Samson, DM, Qualls, WA, Roque, D, Naranjo, DP, Alimi, T et al. (2013). Resting and energy reserves of Aedes albopictus collected in common landscaping vegetation in St. Augustine, Florida. *Journal of the American Mosquito Control Association*, 29(3):pp. 231–236.

Saponari, M, Boscia, D, Nigro, F, and Martelli, GP (2013). Identification of Dna Sequences Related to Xylella Fastidiosa in Oleander, Almond and Olive Trees Exhibiting Leaf Scorch Symptoms in Apulia (southern Italy). *Journal of Plant Pathology*, (3).

Satterthwaite, D (2009). The implications of population growth and urbanization for climate change. *Environment and Urbanization*, 21(2):pp. 545–567.

Saupe, EE, Barve, V, Myers, CE, Soberón, J, Barve, N et al. (2012). Variation in niche and distribution model performance: The need for a priori assessment of key causal factors. *Ecological Modelling*, 237–238:pp. 11–22.

Schultz, GW (1989). Cemetery vase breeding of dengue vectors in Manila, Republic of the Philippines. *Journal of the American Mosquito Control Association*, 5(4):pp. 508–513.

Schöning, JM, Cerny, N, Prohaska, S, Wittenbrink, MM, Smith, NH et al. (2013). Surveillance of Bovine Tuberculosis and Risk Estimation of a Future Reservoir Formation in Wildlife in Switzerland and Liechtenstein. *PLOS ONE*, 8(1):p. e54253.

Scott, J (2003). *The Ecology of the Exotic Mosquito Ochlerotatus (Finlaya) japonicus japonicus (Theobald 1901) (Diptera: Culicidae) and an Examination of its Role in the West Nile Virus Cycle in New Jersey.* Ph.D. thesis, Rutgers University.

Seidel, B, Montarsi, F, Huemer, HP, Indra, A, Capelli, G et al. (2016). First record of the Asian bush mosquito, Aedes japonicus japonicus, in Italy: invasion from an established Austrian population. *Parasites & Vectors*, 9.

Semenza, JC (2015). Prototype Early Warning Systems for Vector-Borne Diseases in Europe. *International Journal of Environmental Research and Public Health*, 12(6):pp. 6333–6351.

Semenza, JC and Domanović, D (2013). Blood supply under threat. *Nature Clim Change*, 3(5):pp. 432–435.

Semenza, JC, Tran, A, Espinosa, L, Sudre, B, Domanovic, D et al. (2016). Climate change projections of West Nile virus infections in Europe: implications for blood safety practices. *Environmental Health*, 15(1):pp. 125–136.

Service, MW (1997). Mosquito (Diptera: Culicidae) dispersal–the long and short of it. *Journal of Medical Entomology*, 34(6):pp. 579–588.

Shaman, J, Day, JF, and Komar, N (2010). Hydrologic Conditions Describe West Nile Virus Risk in Colorado. *International Journal of Environmental Research and Public Health*, 7(2):pp. 494–508.

Shaman, J, Day, JF, and Stieglitz, M (2005). Drought-induced amplification and epidemic transmission of West Nile virus in southern Florida. *J Med Entomol*, 42(2):pp. 134–141.

Sharpe, PJH and DeMichele, DW (1977). Reaction kinetics of poikilotherm development. *Journal of Theoretical Biology*, 64(4):pp. 649–670.

Simberloff, D (2003). How Much Information on Population Biology Is Needed to Manage Introduced Species? *Conservation Biology*, 17(1):pp. 83–92.

Simberloff, D (2014). Biological invasions: What's worth fighting and what can be won? *Ecological Engineering*, 65:pp. 112–121.

Simberloff, D, Martin, JL, Genovesi, P, Maris, V, Wardle, DA et al. (2013). Impacts of biological invasions: what's what and the way forward. *Trends in Ecology and Evolution*, 28(1):pp. 58–66.

Simmons, CP, Farrar, JJ, van Vinh Chau, N, and Wills, B (2012). Dengue. *New England Journal of Medicine*, 366(15):pp. 1423–1432.

Sinclair, SJ, White, MD, and Newell, GR (2010). How Useful Are Species Distribution Models for Managing Biodiversity under Future Climates? *Ecology and Society*, 15.

Small, C, Elvidge, CD, Balk, D, and Montgomery, M (2011). Spatial scaling of stable night lights. *Remote Sensing of Environment*, 115(2):pp. 269–280.

Smardon, RC (1988). Special Issue: Urban Forest EcologyPerception and aesthetics of the urban environment: Review of the role of vegetation. *Landscape and Urban Planning*, 15(1):pp. 85–106.

Smith, G and Eliason, D (1989). Use of elevated temperatures to kill Aedes albopictus and Ae. aegypti. *Journal of the American Mosquito Control Association*, 4(4):pp. 557–8.

Smith, DL, Perkins, TA, Reiner, RC, Barker, CM, Niu, T et al. (2014). Recasting the theory of mosquito-borne pathogen transmission dynamics and control. *Transactions of the Royal Society of Tropical Medicine and Hygiene*, 108(4):pp. 185–197.

Smithburn, K, Hughes, T, Burke, A, and Paul, J (1940). A neurotropic virus isolated from the blood of a native of Uganda. *The American Journal of Tropical Medicine and Hygiene*, 20:pp. 471–492.

Soverow, JE, Wellenius, GA, Fisman, DN, and Mittleman, MA (2009). Infectious Disease in a Warming World: How Weather Influenced West Nile Virus in the United States (2001-2005). *Environ Health Perspect*, 117(7):pp. 1049–1052.

Spiegelhalter, DJ, Best, NG, Carlin, BP, and Van Der Linde, A (2002). Bayesian measures of model complexity and fit. *Journal of the Royal Statistical Society: Series B (Statistical Methodology)*, 64(4):pp. 583–639.

Sprenger, D and Wuithiranyagool, T (1986). The discovery and distribution of Aedes albopictus in Harris County, Texas. *Journal of the American Mosquito Control Association*, 2(2):pp. 217–219.

Steiner, F (2014). Frontiers in urban ecological design and planning research. *Landscape and Urban Planning*, 125:pp. 304–311.

Stenseth, NC, Ottersen, G, Hurrell, JW, Mysterud, A, Lima, M et al. (2003). Studying climate effects on ecology through the use of climate indices: the North Atlantic Oscillation, El Niño Southern Oscillation and beyond. *Proceedings of the Royal Society B: Biological Sciences*, (April):pp. 2087–2096.

Sullivan, MF, Gould, DJ, and Maneechai, S (1971). Observations on the host range and feeding preferences of Aedes albopictus (Skuse). *Journal of Medical Entomology*, 8(6):pp. 713–716.

Sunday, JM, Bates, AE, Kearney, MR, Colwell, RK, Dulvy, NK et al. (2014). Thermal-safety margins and the necessity of thermoregulatory behavior across latitude and elevation. *Proceedings of the National Academy of Sciences*, 111(15):pp. 5610–5615.

Suter, T, Flacio, E, Fariña, B, Engeler, L, Tonolla, M et al. (2015). First report of the invasive mosquito species Aedes koreicus in the Swiss-Italian border region. *Parasites and Vectors*, 8(1).

Suzán, G, García-Peña, GE, Castro-Arellano, I, Rico, O, Rubio, AV et al. (2015). Metacommunity and phylogenetic structure determine wildlife and zoonotic infectious disease patterns in time and space. *Ecol Evol*, pp. n/a–n/a.

Szlavecz, K, Warren, P, and Pickett, S (2011). Biodiversity on the Urban Landscape. In RP Cincotta and LJ Gorenflo (Eds.), *Human Population*, number 214 in Ecological Studies, pp. 75–101. Springer Berlin Heidelberg. DOI: 10.1007/978-3-642-16707-2_6.

Tabachnick, WJ (1991). Evolutionary Genetics and Arthropod-borne Disease: The Yellow Fever Mosquito. *American Entomologist*, 37(1):pp. 14–26.

Takahashi, LT, Maidana, NA, Ferreira, WC, Pulino, P, and Yang, HM (2004). Mathematical models for the Aedes aegypti dispersal dynamics: Travelling waves by wing and wind. *Bulletin of Mathematical Biology*, 67(3):pp. 509–528.

Tanaka, T, Mizusawa, K, and Saugstad, E (1979). *Mosquitoes of Japan and Korea*, volume 16 of *Contributions of the AmericanEntomological Institute*.

Tatem, AJ, Hay, SI, and Rogers, DJ (2006). Global traffic and disease vector dispersal. *Proceedings of the National Academy of Sciences*, 103(16):pp. 6242–6247.

Teng, HJ and Apperson, CS (2000). Development and Survival of Immature Aedes albopictus and Aedes triseriatus (Diptera: Culicidae) in the Laboratory: Effects of Density, Food, and Competition on Response to Temperature. *Journal of Medical Entomology*, 37(1):pp. 40–52.

Thomas, SM, Obermayr, U, Fischer, D, Kreyling, J, and Beierkuhnlein, C (2012). Low-temperature threshold for egg survival of a post-diapause and non-diapause European aedine strain, Aedes albopictus (Diptera: Culicidae). *Parasites & Vectors*, 5(1):p. 100.

Thuiller, W, Lafourcade, B, Engler, R, and Arau, MB (2009). BIOMOD: a platform for ensemble forecasting of species distributions. *Ecography*, (December 2008):pp. 369–373.

Townson, H (1993). The biology of mosquitoes. Volume 1. Development, nutrition and reproduction. By A.N. Clements. (London: Chapman & Hall, 1992). viii + 509 pp. Hard cover £50. ISBN 0-412-40180-0. *Bulletin of Entomological Research*, 83(02):p. 307.

Tran, A, Sudre, B, Paz, S, Rossi, M, Desbrosse, A et al. (2014). Environmental predictors of West Nile fever risk in Europe. *International Journal of Health Geographics*, 13:p. 26.

Trpis, M, Haufe, WO, and Shemanchuk, JA (1973). Embryonic development of aedes (o.) Sticticus (diptera: culicidae) in relation to different constant temperatures. *The Canadian Entomologist*, 105(01):pp. 43–50.

Tsai, T, Popovici, F, Cernescu, C, Campbell, G, and Nedelcu, N (1998). West nile encephalitis epidemic in southeastern romania. *The Lancet*, 352(9130):pp. 767–771.

Turell, MJ, Beaman, JR, and Neely, GW (1994). Experimental transmission of eastern equine encephalitis virus by strains of Aedes albopictus and A. taeniorhynchus (Diptera: Culicidae). *Journal of Medical Entomology*, 31(2):pp. 287–290.

Turell, MJ, Dohm, DJ, Sardelis, MR, Oguinn, ML, Andreadis, TG et al. (2005). An update on the potential of north American mosquitoes (Diptera: Culicidae) to transmit West Nile Virus. *Journal of Medical Entomology*, 42(1):pp. 57–62.

Uden, DR, Allen, CR, Angeler, DG, Corral, L, and Fricke, KA (2015). Adaptive invasive species distribution models: a framework for modeling incipient invasions. *Biological Invasions*, pp. 1–20.

Unlu, I, Farajollahi, A, Healy, SP, Crepeau, T, Bartlett-Healy, K et al. (2011). Area-wide management of Aedes albopictus: choice of study sites based on geospatial characteristics, socioeconomic factors and mosquito populations. *Pest Management Science*, 67(8):pp. 965–974.

Unlu, I, Klingler, K, Indelicato, N, Faraji, A, and Strickman, D (2016). Suppression of Aedes albopictus, the Asian tiger mosquito, using a 'hot spot' approach. *Pest Management Science*, 72(7):pp. 1427–1432.

Urbanski, J, Mogi, M, O'Donnell, D, DeCotiis, M, Toma, T et al. (2012). Rapid Adaptive Evolution of Photoperiodic Response during Invasion and Range Expansion across a Climatic Gradient. *The American Naturalist*, 179(4):pp. 490–500.

Valerio, L, Marini, F, Bongiorno, G, Facchinelli, L, Pombi, M et al. (2010). Host-Feeding Patterns of *Aedes albopictus* (Diptera: Culicidae) in Urban and Rural Contexts within Rome Province, Italy. *Vector-Borne and Zoonotic Diseases*, 10(3):pp. 291–294.

Valiakos, G, Papaspyropoulos, K, Giannakopoulos, A, Birtsas, P, Tsiodras, S et al. (2014). Use of Wild Bird Surveillance, Human Case Data and GIS Spatial Analysis for Predicting Spatial Distributions of West Nile Virus in Greece. *PLOS ONE*, 9(5):p. e96935.

Vallorani, R, Angelini, P, Bellini, R, Carrieri, M, Crisci, A et al. (2015). Temperature Characterization of Different Urban Microhabitats of Aedes albopictus (Diptera Culicidae) in Central–Northern Italy. *Environmental Entomology*, p. nvv067.

Veit, RR and Lewis, MA (1996). Dispersal, Population Growth, and the Allee Effect: Dynamics of the House Finch Invasion of Eastern North America. *The American Naturalist*, 148(2):pp. 255–274.

Versteirt, V, De Clercq, EM, Fonseca, DM, Pecor, J, Schaffner, F et al. (2012). Bionomics of the Established Exotic Mosquito Species Aedes koreicus in Belgium, Europe. *Journal of Medical Entomology*, 49(6):pp. 1226–1232.

Vezzani, D, Rubio, A, Velázquez, SM, Schweigmann, N, and Wiegand, T (2005). Detailed assessment of microhabitat suitability for Aedes aegypti (Diptera: Culicidae) in Buenos Aires, Argentina. *Acta Tropica*, 95(2):pp. 123–131.

Vezzani, D, Velázquez, SM, Soto, S, and Schweigmann, NJ (2001). Environmental characteristics of the cemeteries of Buenos Aires City (Argentina) and infestation levels of Aedes aegypti (Diptera: Culicidae). *Memórias do Instituto Oswaldo Cruz*, 96(4):pp. 467–471.

Villard, MA, Trzcinski, MK, and Merriam, G (1999). Fragmentation Effects on Forest Birds: Relative Influence of Woodland Cover and Configuration on Landscape Occupancy. *Conservation Biology*, 13(4):pp. 774–783.

Vora, N (2008). Impact of Anthropogenic Environmental Alterations on Vector-Borne Diseases. *Medscape J Med*, 10(10):p. 238.

Waldock, J, Chandra, NL, Lelieveld, J, Proestos, Y, Michael, E et al. (2013). The role of environmental variables on Aedes albopictus biology and chikungunya epidemiology. *Pathogens and Global Health*, 107(5):pp. 224–241.

Wang, J, Mao, Y, Li, J, Xiong, Z, and Wang, WX (2015). Predictability of Road Traffic and Congestion in Urban Areas. *PLoS ONE*, 10(4).

Ward, DF (2006). Modelling the potential geographic distribution of invasive ant species in New Zealand. *Biological Invasions*, 9(6):pp. 723–735.

Warner, RD, Kimbrough, RC, Alexander, JL, Rush Pierce Jr., J, Ward, T et al. (2006). Human West Nile Virus Neuroinvasive Disease in Texas, 2003 Epidemic: Regional Differences. *Annals of Epidemiology*, 16(10):pp. 749–755.

Washburn, JO and Hartmann, EU (1992). Could Aedes albopictus (Diptera: Culicidae) become established in California tree holes? *Journal of Medical Entomology*, 29(6):pp. 995–1005.

Watt, JH and van den Berg, S (2002). Semi-Controlled Environments: Field Research. In *Research Methods for Communication Science*.

Weaver, SC, Costa, F, Garcia-Blanco, MA, Ko, AI, Ribeiro, GS et al. (2016). Zika virus: History, emergence, biology, and prospects for control. *Antiviral Research*, 130:pp. 69–80.

Wells, JM, Raju, BC, Hung, HY, Weisburg, WG, Mandelco-Paul, L et al. (1987). Xylella fastidiosa gen. nov., sp. nov: Gram-Negative, Xylem-Limited, Fastidious Plant Bacteria Related to Xanthomonas spp. *International Journal of Systematic and Evolutionary Microbiology*, 37(2):pp. 136–143.

Werner, D, Zielke, D, and Kampen, H (2016). First record of Aedes koreicus (Diptera: Culicidae) in Germany. *Parasitology Research*, 115(3):pp. 1331–1334.

Westbrook, CJ, Reiskind, MH, Pesko, KN, Greene, KE, and Lounibos, LP (2009). Larval Environmental Temperature and the Susceptibility of Aedes albopictus Skuse (Diptera: Culicidae) to Chikungunya Virus. *Vector-Borne and Zoonotic Diseases*, 10(3):pp. 241–247.

WHO (2016). World Health Organization, fact sheet on Vector-borne diseases; http://www.who.int/mediacentre/factsheets/fs387/en/.

Williamson, MH and Fitter, A (1996). Invasion Biology. the characters of successful invaders. *Biological Conservation*, 78(1):pp. 163–170.

Wilson, JRU, Dormontt, EE, Prentis, PJ, Lowe, AJ, and Richardson, DM (2009). Something in the way you move: dispersal pathways affect invasion success. *Trends Ecol Evol (Amst)*, 24(3):pp. 136–144.

Wynn, G and Paradise, CJ (2001). Effects of microcosm scaling and food resources on growth and survival of larval Culex pipiens. *BMC Ecology*, 1:p. 3.

Xian, G, Homer, C, Dewitz, J, Fry, J, Hossain, N et al. (2011). Change of impervious surface area between 2001 and 2006 in the conterminous United States. *Photogrammetric Engineering and Remote Sensing*, 77(8):p. 5.

Yee, DA (2008). Tires as Habitats for Mosquitoes: A Review of Studies Within the Eastern United States. *Journal of Medical Entomology*, 45(4):pp. 581–593.

Yee, DA (2016). Thirty Years of Aedes albopictus (Diptera: Culicidae) in America: An Introduction to Current Perspectives and Future Challenges. *Journal of Medical Entomology*, p. tjw063.

Young, SG, Tullis, JA, and Cothren, J (2013). A remote sensing and GIS-assisted landscape epidemiology approach to West Nile virus. *Applied Geography*, 45:pp. 241–249.

Yu, H (2002). Rmpi: Parallel Statistical Computing in R. *R News*, 2(2):pp. 10–14.

Zhang, L, Liu, S, Sun, P, Wang, T, Wang, G et al. (2015). Consensus Forecasting of Species Distributions: The Effects of Niche Model Performance and Niche Properties. *PLOS ONE*, 10(3):p. e0120056.

Zhong, D, Lo, E, Hu, R, Metzger, aE, Cummings, R et al. (2013). Genetic Analysis of Invasive Aedes albopictus Populations in Los Angeles County, California and Its Potential Public Health Impact. *PLoS ONE*, 8(7):p. e68586.

Zhuo, L, Ichinose, T, Zheng, J, Chen, J, Shi, PJ et al. (2009). Modelling the population density of china at the pixel level based on dmsp ols non–radiance–calibrated night–time light images. *International Journal of Remote Sensing*, 30(4):pp. 1003–1018.

Zorer, R, Moffat, T, Strever, A, and Hunter, JJ (2013). Hourly simulation of grape bunch light microclimate using hemispherical photography. pp. 748–752.

Zorer, R, Volschenk, C, and Hunter, J (2016). Integrating Geographic Information Systems and hemispherical photography in the assessment of canopy light profiles in a vineyard. *Agricultural And Forest Meteorology*.

Zuur, AF, Ieno, EN, Walker, N, Saveliev, A, and Smith, G (2009). *Mixed Effects Models and Extensions in Ecology with R*.

Šúri, M, Huld, TA, and Dunlop, ED (2005). PV-GIS: a web-based solar radiation database for the calculation of PV potential in Europe. *International Journal of Sustainable Energy*, 24(2):pp. 55–67.

Appendix A

Correlation matrix and MaxEnt response curves

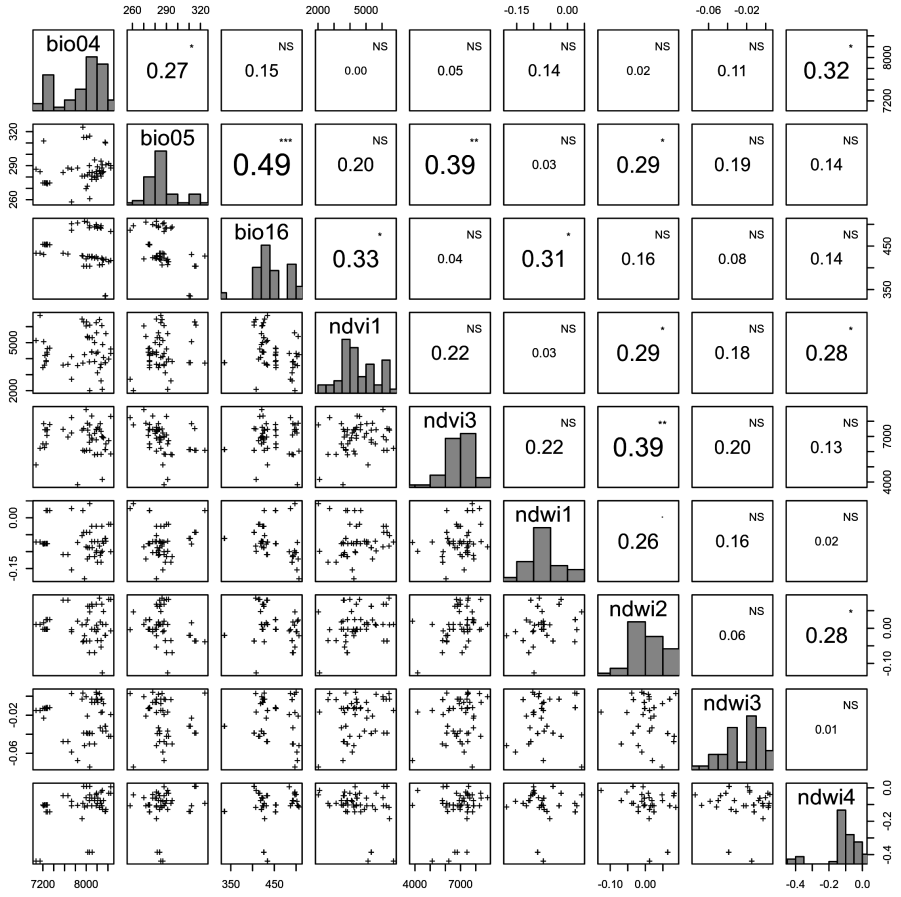

Figure A.1: Correlation matrix for the predictors set, input of MaxEnt model

Table A.1: Ranking of the 5 most important variables for MaxEnt model. We assigned a score ranging from 5 to 1 to the first 5 predictors for each of the three measurements of variable importance provided by MaxEnt. Afterwards, we summed the rank to provide an overall metric for variable importance.

PC	rank contribution	rank permutation	rank training gain	overall rank
PCA03	4	4	5	13
PCA05	3	5	3	11
PCA09	2	–	4	6
PCA22	5	–	–	5
PCA20	–	3	–	3
PCA23	–	2	–	2
PCA07	–	–	2	2
PCA17	–	1	–	1
PCA02	–	–	1	1
PCA13	1	–	–	1

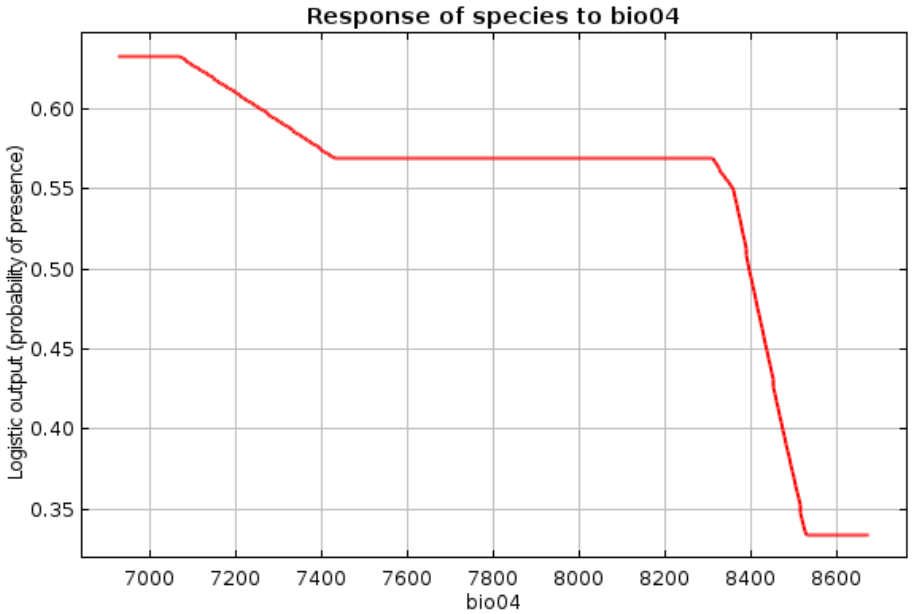

(a) MaXent response curve for PCA03

(b) MaXent response curve for PCA05

Figure A.2: MaxEnt response curve for the two predictors with the highest overall ranking (as calculated in Table A.1).

Appendix B

Posterior Probability Distributions (PPDs) for the best model

Figure B.1: Posterior Probability Distribution for the best model parameters. The red dashed lines represent the distribution of the priors while the black horizontal line is the 95 % High Density Interval of the distribution. The distribution average, lower and upper bound of 95% HDI were also reported in the figure.

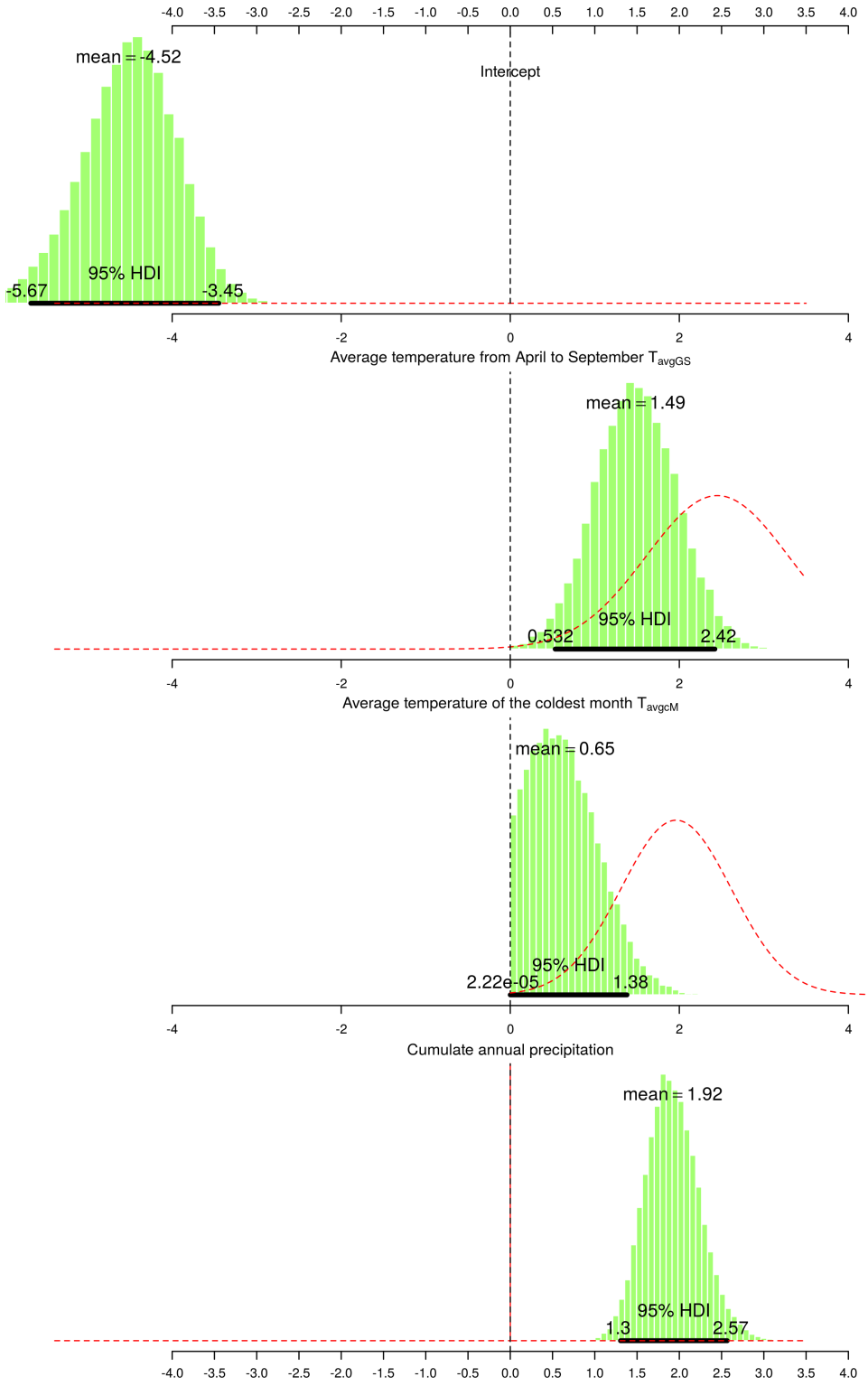

Appendix C

Sigmoid curves

Figure C.1: Sigmoid curves for PHY model: We present the three sigmoid functions used to transform the environmental parameters to separate suitability indices

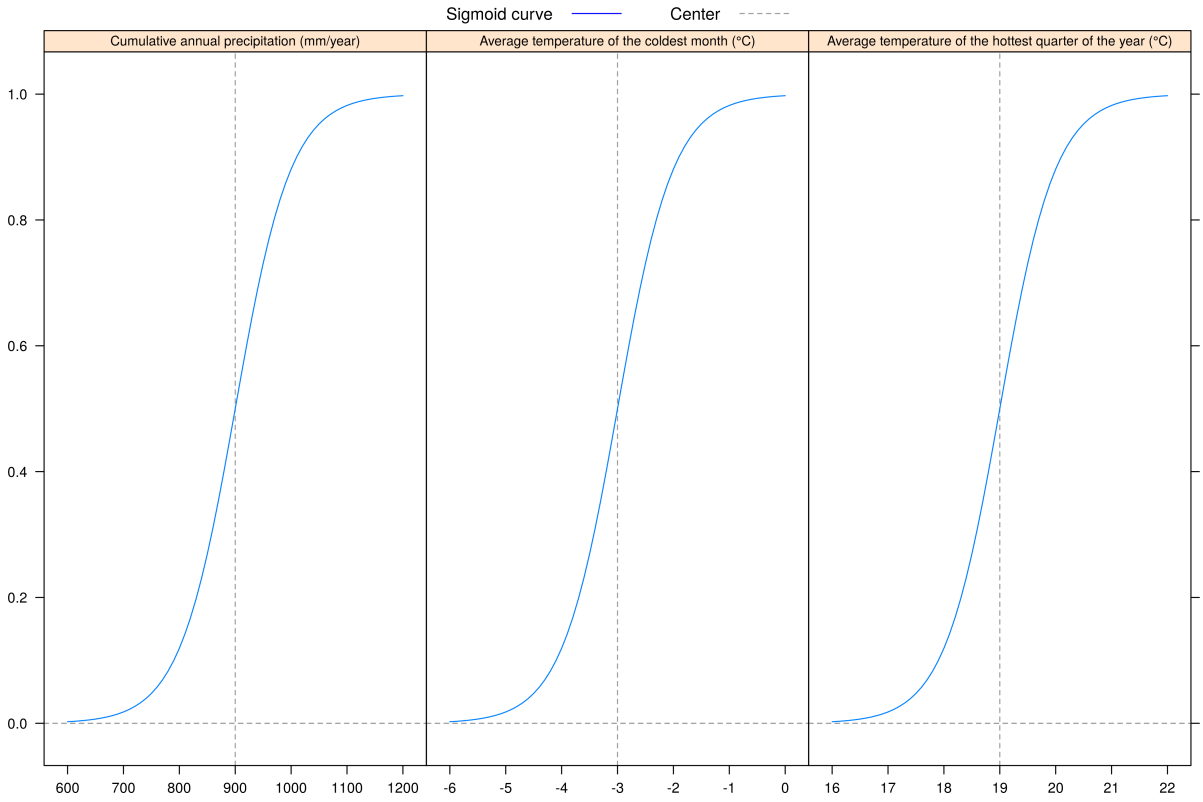

Appendix D

R functions to simulate roads and urban land use

roadsim, a R function to simulate road-like shapes

```
roadsim <- function(x,n1,n2,rvalue=-1,method="row",sl=0.5,fr=0.5,scaling
    =0.5,increase=0) {
    if( method=="row" & increase==0 ) {
        ij <- sapply(1:n2, function(i)
         c(ceiling(n1 * scaling * (1 + exp(sl*i/n2) * sin(fr*i/n2))), i))
        x[t(ij)] <- rvalue; x[t(ij - c(1,0))] <- rvalue; x[t(ij + c(1,0))]
    <- rvalue
    } else if( method=="row" & increase!=0 ) {
     ij <- sapply(1:n2, function(i)
         c(ceiling(n1 * scaling * (1 + exp(sl*i/n2) * sin(fr*i/n2))) ,i))
     for (i in seq(-increase,increase)) {
         ij1 <- rbind(ij[1,]+i,ij[2,])
         x[t(ij1)] <- rvalue; x[t(ij1 - c(1,0))] <- rvalue; x[t(ij1 + c
    (1,0))] <- rvalue
     }
} else if( method=="column" & increase==0 ) {
    ij <- sapply(1:n2, function(i)
     c(i,ceiling(n1 * scaling * (1 + exp(sl*i/n2) *sin(fr*i/n2)))))
    x[t(ij)] <- rvalue; x[t(ij - c(0,1))] <- rvalue; x[t(ij + c(0,1))] <-
    rvalue
} else if( method=="column" & increase!=0 ) {
     ij <- sapply(1:n2, function(i)
         c(i,ceiling(n1 * scaling * (1 + exp(sl*i/n2) * sin(fr*i/n2)))))
     for (i in seq(-increase,increase)) {
         ij1 <- rbind(ij[1,],ij[2,]+i)
```

```
        x[t(ij1)] <- rvalue; x[t(ij1 - c(0,1))] <- rvalue; x[t(ij1 + c(0,1))] <- rvalue
    }
}
return(x)
}

# sc<-0.1;sl<-1.5;j<-0.5; x<-c(); for (i in 1:300){x[i]<-300*sc*(1 + exp(sl*i/300)*sin(j/300)*ifelse(rbinom(1,1,0.2),rnorm(1,1,0.5),1))};plot(x,type="l")
# j<-4; x<-c(); for (i in 1:300){x[i]<-300*j*(1+exp(j*i/300))};plot(x)
# j<-15; x<-c(); for (i in 1:300){x[i]<-300*j*sin(j*i/300)};plot(x)
```

citysim, a R function to simulate urban landscapes

```
multiexpand <- function(x, cluster.number, cluster.size, cluster.size.prob=0, start, count.max, range=1,contiguity, mode="px", nbr.matrix="NA", ww=5, xnnoise=-1, ynnoise=-1, along=FALSE, along.value=0, debug=0) {
#
##Required packages
#
  require(msm)
#
##Neighboroud matrices
#
  if(nbr.matrix=="nn2y") {
    nbr.matrix <- matrix(c(0,-1, 0,1), nrow=2)
  } else if(nbr.matrix=="nn2x") {
    nbr.matrix <- matrix(c(-1,0, 1,0), nrow=2)
  } else if(ww!=0 & ww%%2==0) {
    nbr.matrix.raw <- matrix(1,nrow=ww,ncol=ww)
    nbr.matrix <- rbind((which(nbr.matrix.raw==1,arr.ind=T)-(ww/2))[,1],(which(nbr.matrix.raw==1,arr.ind=T)-(ww/2))[,2])
  } else {
    stop("provide a known nn matrix or an even window size")
  }
#
##Prepare output objects and temporary vectors
#
  n.rows <<- nrow(x)
  n.cols <<- ncol(x)
  nbrhood <- nbr.matrix
  n <- n.rows * n.cols
```

```
26    cells.left <- 1:n
27    cells.left[x!=1 | x==along.value] <- -1 # Occ of cells
28    i <- 2 # index for cluster.size comparison
29    indices <- c() # vector for occupied cells
30    ids <- c()
31    out <- matrix(NA, n.rows, n.cols)
32    busy_cells <- 0
33    fc <- rep(NA,cluster.size)
34    state <- data.frame(occupied=which(x==-1 | x==along.value))
35    add_sd_storage <- c()
36    h <- 1 # counter for synusoidal growth
37    cluster.size.i<-cluster.size
38
39  #
40  ##If `cells_selected` is missing
41  #
42    if( missing(start) ) {
43      rst <- which(x==1,arr.ind=T)
44      start <- rst[sample(1:nrow(rst), 1),]
45    }
46  #
47  #Start the loop
48  #
49    while( i < cluster.number+2 && length(cells.left[x!=-1]) >= cluster.size
        && count.max > 1 ) {
50
51      if(count.max==2) break("No solution found to build the planned number
       of clusters")
52
53  #
54  #Check if cluster size exceed the limit
55  #
56        if(cluster.size>=n/2)break("cluster.size must be less then the cells
       number/2")
57  #
58  #Preparation of the starting cell; for every while loop the new seed is
      randomly drawn from a truncated normal distribution which average=
      previous column and row coordinates while sd=defined by the user.
      Furthermore, if "range">0, the new seed is randomly picked from all the
       neighbourous cells in range.
59  #
60          count.max <- count.max-0.5
61        cells_start <- cells.left[which(cells.left > 0)]
62        cells_selected <- 0
```

```
63
64      if(debug==1 & i>2){
65        print(paste("bench_1: 1st loop","fc",length(fc),"cluster",cluster.
    size-1,"count.max", count.max,start[1],start[2],cells_selected))
66      }
67
68      std_c<-10000
69
70      while( cells_selected == 0 | length(fc) < cluster.size-1 & count.max
    > 0 ) {
71
72        count.max <- count.max-1
73        std_c <- std_c - 10
74
75        if(std_c==1 ) break("No solution found: Seed coords constantly
    outside matrix extent or cluster size not respected")
76
77         if( cluster.size<=1 & cluster.size.prob==0 ) stop("Mean<=1 and SD
    ==0; impossible to draw values from rtnorm")
78
79          cluster.size<-round(rtnorm(1,cluster.size.i,cluster.size.prob,
    lower=1, upper=n.rows*n.cols/2),0)
80
81        if( i !=2 & along!=TRUE ) {
82          start=which(tail(state$occupied, 1)==matrix(seq(1,n),nrow=n.rows
    ,ncol=n.cols,byrow=F),arr.ind=T)
83        }
84
85        if( along==TRUE & exists("along.value") ) {
86          start=which(x==along.value,arr.ind=T)[sample(1:length(which(x==
    along.value)),range),]
87        }
88
89        add_sd <- rbinom(1,50,1/log(ifelse(std_c<2,2,std_c),2))
90
91        if( all(start<=1) & any(contiguity + add_sd==0 )) break("Mean<=1
    and SD==0; impossible to draw values from rtnorm")
92
93          start_coords <- round(rtnorm(2, mean=as.numeric(start), sd=
    contiguity + add_sd, lower=1, upper=min(dim(x))+1),0) #start seed from
    TND
94
95        matrix_start_coords <- matrix(cells.left,nrow=n.rows,ncol=n.cols,
    byrow=FALSE)
```

```
96
97          if(debug==1){
98            print(paste("bench_2: 1st loop","fc",length(fc),"c size:",
      cluster.size-1,"count max: ",count.max, "count std: ",std_c, "start
      coords: ",start_coords[1],start_coords[2]))
99          }
100 #
101 # Check if seeds range is outside x
102 #
103         std_c1 <- 10000
104         while( count.max>0 & start_coords[1]+range > nrow(x) | start_
      coords[2]+range > ncol(x) | start_coords[1]-range <= 0 | start_coords
      [2]-range <= 0 ) {
105
106           if(debug==1){
107            print(paste("bench_3: 3rd loop","fc",length(fc),"cluster",
      cluster.size-1,"range",range, "start coords:",start_coords[1],start_
      coords[2],"std_c1",std_c1))
108          }
109 #
110 # If the seed gets stuck in not valid coordinates, apply a further sd to
      the folded normal distribution to help finding valid coordinates; the
      additional sd is function of count.max
111 #
112          count.max <- count.max - 1
113          std_c1 <- std_c1 - 1
114
115          if( count.max<2 | std_c1==1 ) break("No solution found: Seed
      coords constantly outside matrix extent")
116
117           add_sd1 <- rbinom(1,5,1/log(ifelse(count.max<2,2,std_c1), 2))
118
119          if( all(start<=1) & any(contiguity + add_sd1==0) ) break("Mean<=1
       and SD==0; impossible to draw values from rtnorm")
120
121           start_coords <- round(rtnorm(2, mean=as.numeric(start), sd=
      contiguity + add_sd1, lower=1, upper=min(dim(x))+1),0)
122 #
123 ##Check if the new start is still inside
124 #
125          if ( any((start_coords+range)>500) | any((start_coords-range)<=0)
       ) {
126           message("Coords out of matrix boundaries; bringing them back
      inside...")
```

```
127           if( any((start_coords+range)>500) ) start_coords[(start_coords+
    range)>500] <- ncol(x)/2
128           if( any((start_coords-range)<=0) ) start_coords[(start_coords-
    range)<=0] <- ncol(x)/2
129         }
130       }
131       cells_selected <- matrix_start_coords[(start_coords[1]-range):(start
    _coords[1]+range),(start_coords[2]-range):(start_coords[2]+range)] #
    Neighborhood cell_selected
132       cells_selected<-cells_selected[cells_selected>0]
133 #
134 #If range>0 randomly pick a seed cell in the neighborhood set
135 #
136       if( length(cells_selected)==0 ) cells_selected<-0;
137
138       if( length(cells_selected)>1 ){
139         cells_selected<- sample(cells_selected, 1)
140         start_coords<-which(cells_selected==matrix_start_coords,arr.ind=T)
141       }
142 #
143 # If ca then cluster.size must be respected
144 #
145       if( mode=="ca" & cluster.size.prob==0 ){
146         fc <- c((cells_selected-1)%%n.rows+1, floor((cells_selected-1)/n.
    rows+1)) + nbrhood
147         fc <- fc[, fc[1,] >= 1 & fc[2,] >= 1 & fc[1,] <= n.rows & fc[2,]
    <= n.cols,
148         drop=FALSE]
149         fc <- fc[1,] + (fc[2,]-1)*n.rows
150         fc <- fc[matrix_start_coords[fc]!=-1]
151         fc <- setdiff(fc,state$occupied)
152       } else {fc <- rep(0,cluster.size-1)
153     }
154   }
155
156   if(count.max<2) break("No solution found: Seed coords constantly outside
      matrix extent")
157
158 #
159 #Expand a patch randomly within indicator array `x` (1=unoccupied) by `
    cluster.size` cells beginning at index `start_coords`.
160 #
161 #
```

```
#Adjoin one more random cell and update 'state', which records (1) the
    immediately available cells and (2) already occupied cells.
#
    grow <- function(state,cells_selected) {
#
# Find all available neighbors that lie within the extent of 'x' and
# are unoccupied.
#

      neighbors <- function(i) {

#
# In case of syn growth
#
        if( xnnoise> -1 | ynnoise> -1 ){
          nbr <- as.matrix(nbrhood[,nbrhood[1,]>=0 & nbrhood[2,]>=0])
        }

        if( ynnoise> -1 ){
          n <- c((i-1)%%n.rows+1, floor((i-1)/n.rows+1)) + nbr # extract
    nn matrix
          noise<-round(ifelse(ynnoise_r> -1, 1 + exp(ynnoise_r*h/h) * sin(
    h),0))
          noise<-ifelse(noise>1,1,ifelse(noise<-1,-1))
          n[1,] <- if(rbinom(1,1,0.50)==0) {
            n[1,] + noise
          } else{n[1,] - noise # add synusoidal noise
        }
      } else {
        if( xnnoise> -1 ) {
          n <- c((i-1)%%n.rows+1, floor((i-1)/n.rows+1)) + nbr # extract
    nn matrix
          noise<-round(ifelse(xnnoise_r>0, 1 + exp(xnnoise_r*h/h) * sin(h)
    ,0))
          noise<-ifelse(noise>1,1,ifelse(noise<-1,-1))
          n[2,] <- if(rbinom(1,1,0.50)==0) {
            n[2,] + noise
          } else{n[2,] - noise # add synusoidal noise
        }
      } else { n <- c((i-1)%%n.rows+1, floor((i-1)/n.rows+1)) + nbrhood
    } # extract nn matrix
  }

```

```
200   n <- n[, n[1,] >= 1 & n[2,] >= 1 & n[1,] <= n.rows & n[2,] <= n.cols,
        drop=FALSE] # Remain inside the extent of `x`.
201   n <- n[1,] + (n[2,]-1)*n.rows  # Convert to *vector* indexes into `x`.
202   n <- n[x[n]==1] # Stick to valid cells in `x`.
203   n <- setdiff(n, state$occupied)# Remove any occupied cells.
204
205   return (n)
206 }
207 #
208 ## Select one available cell uniformly at random.  Return an updated state
      .
209 #
210 if( mode=="ca" ){
211
212   if( length(state$occupied)>1 & length(state$available)>1 ) {
213     j <- ceiling(runif(1) * length(state$available))
214     a <- state$available[j]
215     return(list(index=a,
216       available = state$available[-j],
217       occupied = c(state$occupied, a)))
218   }
219
220   a <- state$available
221   return(list(index=a,
222     available = union(state$available[-1], neighbors(a)),
223     occupied = c(state$occupied, a)))
224 }
225
226 if( mode=="px" ){
227   j <- ceiling(runif(1) * length(state$available))
228   a <- state$available[j]
229   return(list(index=a,
230     available = union(state$available[-j], neighbors(a)),
231     occupied = c(state$occupied, a)))
232 }
233 }
234
235 state <- list(available=cells_selected, occupied=busy_cells)
236 #
237 ##Grow for as long as possible and as long as needed.
238 #
239 a <- 1
240 indices.c <- c(NA, cluster.size)
241 while( length(state$available) >= 1 && a <= cluster.size ) {
```

```
242
243   if(xnnoise > -1 | ynnoise > -1){ xnnoise_r <- runif(1,0,xnnoise);
      ynnoise_r <- runif(1,0,ynnoise)}
244
245   h <- h+1 # counter for syn
246   state <- grow(state,cells_selected)
247   indices.c[a] <- state$index
248   a <- a+1 # index for cluster size comparison
249   count.max <- count.max-0.5
250
251   if( debug==1 ) {
252     print(paste("bench_4: 4th loop","available cells",length(state$
      available),"cluster.size",cluster.size-1,a,"cluster n",i,"count max",
      count.max))
253   }
254 }
255 #
256 ##Return a grid of generation numbers from 1, 2, ... through cluster.size.
257 #
258 indices.c <- indices.c[!is.na(indices.c)]
259 y <- matrix(NA, n.rows, n.cols)
260 y[indices.c] <- 1:length(indices.c)
261
262 #
263 ##If not syn growth set then check if the cluster respects cluster.size
264 #
265 if(xnnoise==0 & ynnoise==0){
266   if ( length(y[!is.na(y)])==cluster.size ) {
267     i <- i+1
268     ids <- c(ids, rep(i, cluster.size))
269     indices <- c(indices, which(!is.na(y)))
270     cells.left[indices] <- -1 #Indicate occupacy
271
272     cat(paste(i-2,"cluster(s) created. Cluster size=",cluster.size,"x=",
      start_coords[1],"y=",start_coords[2],length(which(cells.left>0)),"cells
      unoccupied \n", sep=" "))
273
274   } else {
275    next("No cluster created. Cluster smaller than cluster.size. Jumping to
      the next iteration")
276    count.max <- count.max-1
277  }
278 } else {
279   i <- i+1
```

```
280   ids <- c(ids, rep(i, length(y[!is.na(y)])))
281   indices <- c(indices, which(!is.na(y)))
282   cells.left[indices] <- -1 #Indicate occupacy
283   count.max <- count.max -1
284   cat(paste(i-2,"cluster(s) created. Cluster size=",length(y[!is.na(y)]),"
        x=",start_coords[1],"y=",start_coords[2],length(which(cells.left >0)),"
        cells unoccupied \n", sep=" "))
285 }
286 #
287 ##Check if the left cells are enough for the next cluster
288 #
289 if( length(which(cells.left!=-1))<=cluster.size ) {
290   break(paste("Unoccupied cells are not enough","only",i-2,"cluster(s)
        created out of",cluster.size,"\n",sep=" "))
291   i=cluster.number
292   count.max <- count.max-1
293 }
294
295 busy_cells<-indices
296 }
297 out[indices] <- ids
298 out[out %in% NA] <- 1
299 return(out)
300 }
```

Appendix E

The parameters of the *Ae. albopictus* dynamical model

Table E.1: Summary of the dynamical model parameters defining the biological cycle and the movement of adult *Ae. albopictus* in the study area.

Stage	Parameter name	Parameter description	Parameter value/distribution	Reference
E_{it}	W_{ELt}	The temperature dependent egg-development time.	$W_{ELt} \sim G(\alpha,\beta)$, $\alpha = 1.2, \beta = 0.1$	This study
	$\mu_{\varepsilon t}$	The egg daily mortality probability.	$\mu_{\varepsilon t} \sim Beta(\alpha,\beta)$, $\alpha = 4.772, \beta = 1.199$	Juliano [2007]; Delatte et al. [2008]
	λ_{ε}	Expected number of eggs to be laid by females.	$\lambda_{\varepsilon} = 40$	This study
L_{it}	$1/W_{LFt}$(T)	The temperature dependent rate of larvae-development.	$\frac{W_{LFt}(T) = \frac{0.201(T+273)/298 exp[(14792.5/R)(1/298)-1/(T+273)]}{1+exp[(105759.7/R)1/(34.88+273)-1/(T+273)]}}$	This study
	μ_{Lt}	The daily larval mortality probability.	$\mu_{Lt} = 1 - exp(-(-log(1 - \mu\ di_L)_t + \mu\ dd_{Lit} \times L_{it}))$	Delatte et al. [2008]; Marini et al. [2010]
	$\mu\ di_{Lt}$	The daily density independent larval mortality probability.	$\mu\ di_{Lt} \sim Beta(\alpha,\beta)$, $\alpha = 5.115, \beta = 0.1.358$	Hawley [1988]; Delatte et al. [2008]
	$\mu\ dd_{Lit}$	The density dependent larval daily mortality rate.	$\mu\ dd_{Lit} = (EL_{it} - (-(log(1 - \mu\ di_{Lt})) + W_{LF}(T)^{-1}) \times K) \times K^{-2}$	Hawley [1988]; Delatte et al. [2008]
	K	The parcel carrying capacity for *Ae. albopictus* larvae.	$K = 40$	Hawley [1988], This study

Stage	Parameter name	Parameter description	Parameter value/distribution	Reference
F_{it}	$1/Gp(T)$	The temperature dependent rate of the gonotrophic cycle.	$\frac{1/Gp(T) = \frac{0.091(T+273)/298exp[(13601.05/R)(1/298)-1/(T+273)]}{1+exp[(91171.43/R)1/(34.17+273)-1/(T+273)]}}{}$	Delatte et al. [2008]; Sharpe and DeMichele [1977]
	$1-\mu_F(T)$	The temperature dependent adult survival probability.	$1-\mu_F(T) = (1-\mu_{LAB}(T))-\mu_{FIELDt}$	This study
	$1-\mu_{LAB}(T)$	The experimental temperature dependent adult survival probability.	$1-\mu_{LAB}(T) = exp(-\lambda_{LAB})$	This study
	$\lambda_{LAB}(T)$	The temperature dependent laboratory-based mortality rate.	$log(\lambda_{LAB}) = -(\alpha_0+\beta_1\times T+\beta_2\times T^2$	This study
	μ_{FIELDt}	The daily field adult mortality probability.	$\mu_{FIELDt} \sim Beta(\alpha,\beta)$, $\alpha = 3.761.2, \beta = 44.256$	Brady et al. [2013]
	$\theta_{i'i}$	Probability to move from i' neighbour parcel of parcel i into parcel i.	$\theta_{i'i} = \frac{s_i \times invd_{i'i}}{\sum(\mathbf{s_{i'}}\times \mathbf{invd_{i'i}})}$	This study
	s_i	Suitability of parcel i.	$s_i \sim N(,)$	This study based on the Bayesian hierarchical logistic regression.
	$invd_{i'i}$	Inverse distance weighting from parcel i' to parcel i.	$invd_{i'i} = d_{i'i}^{-\lambda}$	Marini et al. [2010]
	$d_{i'i}$	Distance between the i' neighbour parcel of parcel i.	Variable, but within 200 m, assumed to be the maximum self-dispersal distance for adults *Ae. albopictus*	This study
	λ_D	Parameter for the exponential decay in dispersal probability with respect to distance	$\lambda_D = 6$	This study
	$S_{i'}$	The vector of suitability values of the neighbour parcels of parcel i'. This vector contains also the suitability of parcel i.	The set of $s_{i'}$	This study

Appendix F

Quantifying openness and fraction of transmitted direct solar radiation for *Aedes albopictus* micro-habitats

To quantify the openness and the fraction of transmitted direct solar radiation reaching each experimental site, representing *Ae. albopictus* micro-habitats in different sun exposures, we re-adapted the procedure proposed in Zorer et al. [2013, 2016] to assess grapevine light-profile within the canopy and on the bunch zone. This procedure consisted in the integration of hemispherical photography, topographical analysis and sun-path modelling.

F.1 Hemispherical picture

Hemispherical pictures have been acquired on the 28th July 2016 at each experimental site using a Nikon Coolpix 4500 digital camera, equipped with a Nikon FC-E8 fish-eye converter (Nikon Corp., Tokyo, Japan). The pictures were taken from the centre of each experimental site, facing upwards by keeping the lens horizontal. The back side of the camera body was oriented perpendicular to the magnetic North. This setup is routinely applied in forestry research (i.e. Cescatti and Zorer [2003]; Chianucci et al. [2014]) and it allows to obtain a full-frame hemispherical picture. A professional light stand (051NB 190 Pro equipped with a 486RC2 compact ball head, Manfrotto, Italy) was used to maintain the camera stable and at horizontal level during image acquisition. The resulting pictures gave a 180° view in all directions, with the zenith at the centre and the horizon at the edges of the photograph.

F.2 Derivation of the topographical horizon

To account for the effect of topographic obstacles at each experimental sites, a 360° sky-ground profile was obtained by using the web application "Photovoltaic Geographical Information System" (PVGIS; http://re.jrc.ec.europa.eu/pvgis/apps4/pvest.php?map=africa), generally used for the estimation of the performance of photovoltaic systems in Europe, Africa and Asia [Šúri et al., 2005]. To obtain the raw data for the topographical horizon, the position of each of the three experimental site on the map was first selected and then the "Text file" radio-button in the "Output options" section of the "PV estimation" toolbox checked. In the saved text file the "Hh" data represent the horizon height in decimal degrees, corresponding to the azimuth angles.

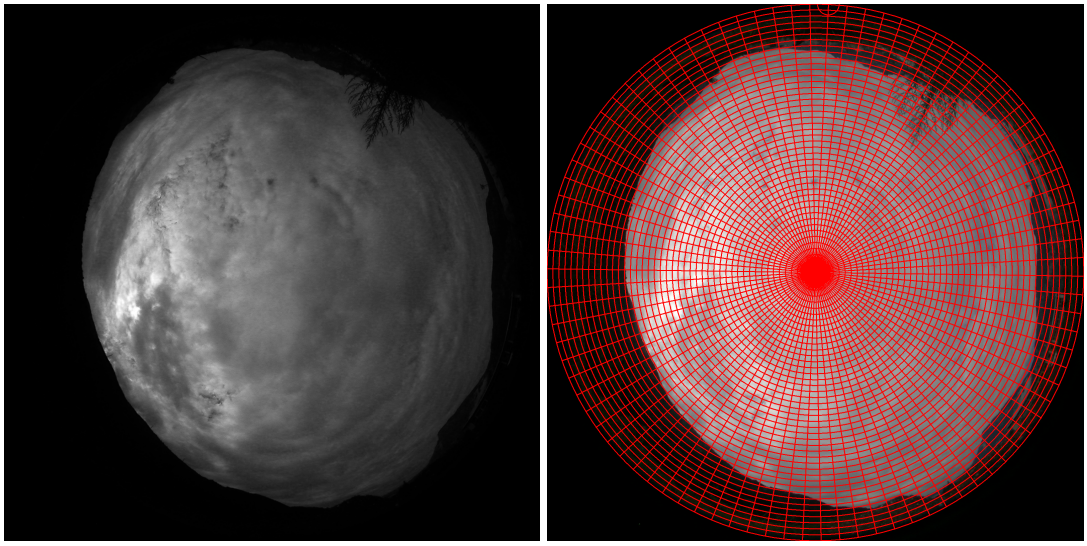

(a) Blue channel of the hemispherical picture. (b) The 4x2° grid superimposed in GLA.

Figure F.1: The elaboration in GLA of the open site (ExLv1) hemispherical picture.

F.3 Assessment of site openness and direct solar radiation

The software Gap Light Analyzer 2.0 (GLA; Frazer et al. [1999]) was used to process the hemispherical pictures. The procedure began with the definition of latitude, longitude and elevation of each site, setting the day that the picture was taken and the maximum working resolution. The image coordinates for the "Image registration" were set for all the images as "Initial Point: 367 (X) 863 (Y)" "Final Point 1971 (X) 863 (Y)". These values were based on empirical estimates [Zorer et al., 2013, 2016]. Afterwards, the sky was divided into the maximum number of allowed regions in GLA (90 Azimuth and 45 Zenith), resulting in a grid of 4x2° (Figure F.1b). The colour images were split into their component parts, with the

"Choose a Colour Plane..." command under the "Image menu". Then the blue channel, which maximizes the contrast between sky and non-sky pixels, was chosen to classify the picture (Figure F.1a). The classification in gap and filled classes was performed visually, by choosing a threshold value for each hemispherical picture that best separated the sky pixel from canopy and topographic mask.

F.4 Daily sunpath calculation and visualisation

A solar position and solar radiation calculator for Excel/VBA (http://www.ecy.wa.gov/programs/eap/models/solrad.zip), developed by the Washington State Department of Ecology, was used to determine the sun path. Latitude and longitude of each exposition condition were added to the Excel worksheet to calculate the daily sun position in the sky. Afterwards, for each experimental site, the summer and winter solstice sunpath was derived and plotted against azimuth angles. Then the topographical profile and the openness of each angular sector, derived from GLA, were added to the plot. The final output, reported in Figure 6.2a, b and c, represents the openness of each experimental site. In these Figures, which are a rectangular view of the classified hemispherical pictures, pixels, grouped by angular sectors (see Figure F.1b), are coloured with a green-blue continuous palette. Light blue colours indicates sky (open) pixels, light green non-sky pixels covered by non-topographic obstacles (i.e., vegetation or buildings) and dark-green pixels covered by topographical obstacles. The Figures 6.2a, b and c were made importing data from GLA, PVGIS and the Excel workbook in the R software [R Core Team, 2016].

F.5 Results for the experimental sites

Table F.1: The openness and direct solar radiation reaching each of the experimental site on the 28th July 2016. The openness represents the percentage of open sky seen from the centre of the experimental site. "Tot. dir. sun radiation - above" and "Tot. dir. solar radiation - transmitted" are the gross and net direct solar radiation reaching the experimental site.

Experimental site (Solar Exposure Level)	**Openness** (%)	**Tot. dir. solar radiation** above ($mol\,m^{-2}\,d^{-1}$)	**Tot. dir. solar radiation** trans ($mol\,m^{-2}\,d^{-1}$)
Full shadow (ExLv1)	12	22.41	0.74
Half shadow (ExLv2)	18	22.41	10.89
Full sun (ExLv3)	70	22.41	21.59

Appendix G

Simple effect deflections from the baseline temperature and temperature difference distributions for factor Wa and Wp

G.1 Simple effect deflections from baseline temperature

Table G.1: Simple effect deflections from the baseline temperature for each interaction between the experimental factors, for each season. The second row from the top shows the average (baseline) and HDI of the temperature posterior probability distribution.

	Winter			**Spring**			**Summer**		
	Average = 3.30			Average = 13.70			Average = 22.70		
	Simple effect deflections								
Interaction term	Mean	HDI_{low}	HDI_{high}	Mean	HDI_{low}	HDI_{high}	Mean	HDI_{low}	HDI_{high}
ExLv1∼WaLv1	0.20	−0.61	1.02	−0.03	−0.34	0.27	−0.02	−0.97	0.95
ExLv2∼WaLv1	−0.45	−1.28	0.48	0.16	−0.18	0.49	0.68	−0.55	1.93
ExLv3∼WaLv1	0.25	−0.62	1.08	−0.13	−0.45	0.21	−0.66	−1.82	0.54
ExLv1∼WaLv2	0.20	−0.08	0.48	−0.18	−0.33	−0.03	−0.33	−0.67	−0.01
ExLv2∼WaLv2	−0.24	−0.55	0.05	−0.08	−0.24	0.08	−0.37	−0.80	0.06
ExLv3∼WaLv2	0.05	−0.23	0.36	0.26	0.08	0.45	0.70	0.27	1.12
ExLv1∼WaLv3	0.19	−0.10	0.46	0.02	−0.13	0.16	−0.15	−0.48	0.18
ExLv2∼WaLv3	−0.45	−0.77	−0.15	−0.16	−0.32	−0.00	−0.51	−0.93	−0.08
ExLv3∼WaLv3	0.26	−0.03	0.56	0.14	−0.03	0.31	0.66	0.24	1.07
ExLv1∼WaLv4	−0.59	−0.87	−0.31	0.19	0.05	0.34	0.50	0.17	0.83
ExLv2∼WaLv4	1.14	0.82	1.43	0.09	−0.06	0.24	0.20	−0.22	0.62
ExLv3∼WaLv4	−0.55	−0.83	−0.25	−0.27	−0.44	−0.11	−0.70	−1.11	−0.31
WaLv2∼WpLv1	−0.21	−0.78	0.33	−0.24	−0.79	0.28	−0.04	−0.38	0.26
WaLv3∼WpLv1	0.01	−0.55	0.54	−0.03	−0.57	0.49	0.03	−0.25	0.38
WaLv4∼WpLv1	0.23	−0.29	0.80	0.25	−0.27	0.79	−0.02	−0.34	0.29
WaLv2∼WpLv2	0.17	−0.38	0.71	0.20	−0.32	0.74	0.03	−0.29	0.34
WaLv3∼WpLv2	−0.05	−0.61	0.47	0.07	−0.48	0.60	−0.04	−0.35	0.27
WaLv4∼WpLv2	−0.16	−0.69	0.41	−0.22	−0.75	0.31	0.02	−0.29	0.35
ExLv1∼WpLv1	−0.38	−0.75	−0.02	−0.11	−0.27	0.04	0.12	−0.30	0.56
ExLv2∼WpLv1	0.52	0.14	0.93	0.00	−0.17	0.16	−0.12	−0.67	0.43
ExLv3∼WpLv1	−0.13	−0.53	0.24	0.11	−0.05	0.29	0.00	−0.51	0.55
ExLv1∼WpLv2	0.27	−0.09	0.64	0.12	−0.02	0.29	−0.07	−0.49	0.37
ExLv2∼WpLv2	−0.21	−0.57	0.21	−0.10	−0.28	0.06	−0.67	−1.23	−0.11
ExLv3∼WpLv2	−0.07	−0.47	0.30	−0.02	−0.19	0.16	0.73	0.20	1.29

G.2 Temperature difference distributions for Wa and Wp

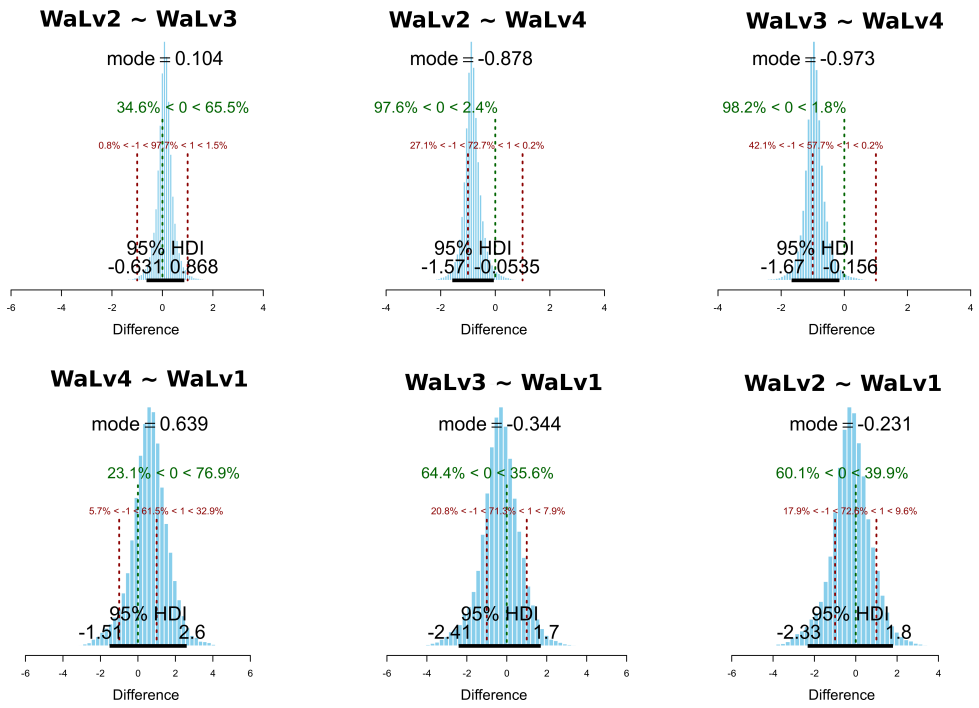

(a) Wa - Winter.

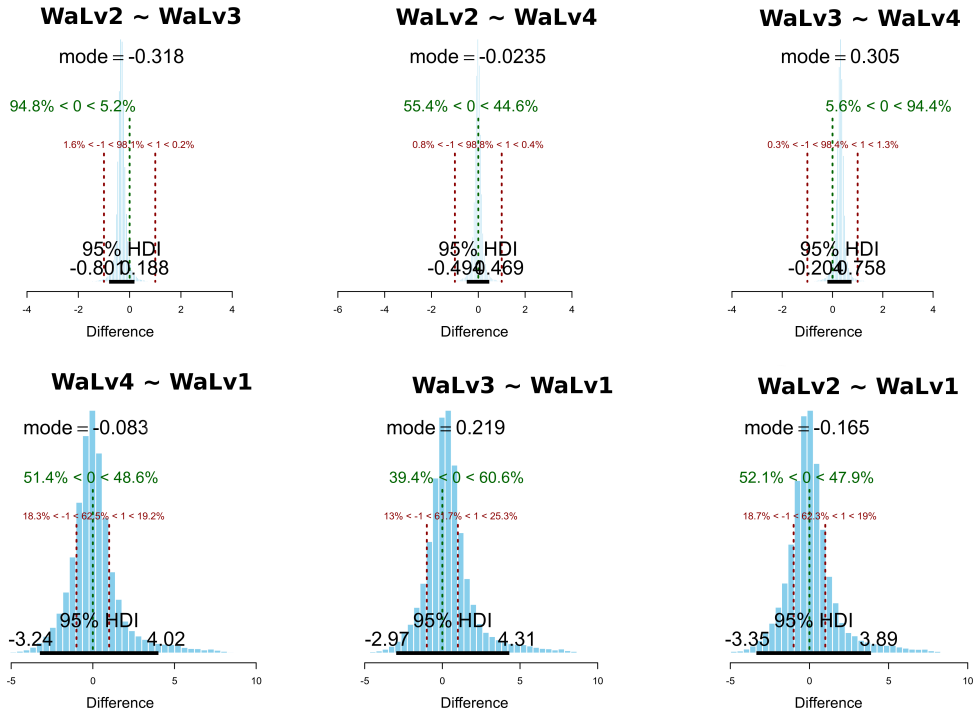

(b) Wa - Spring.

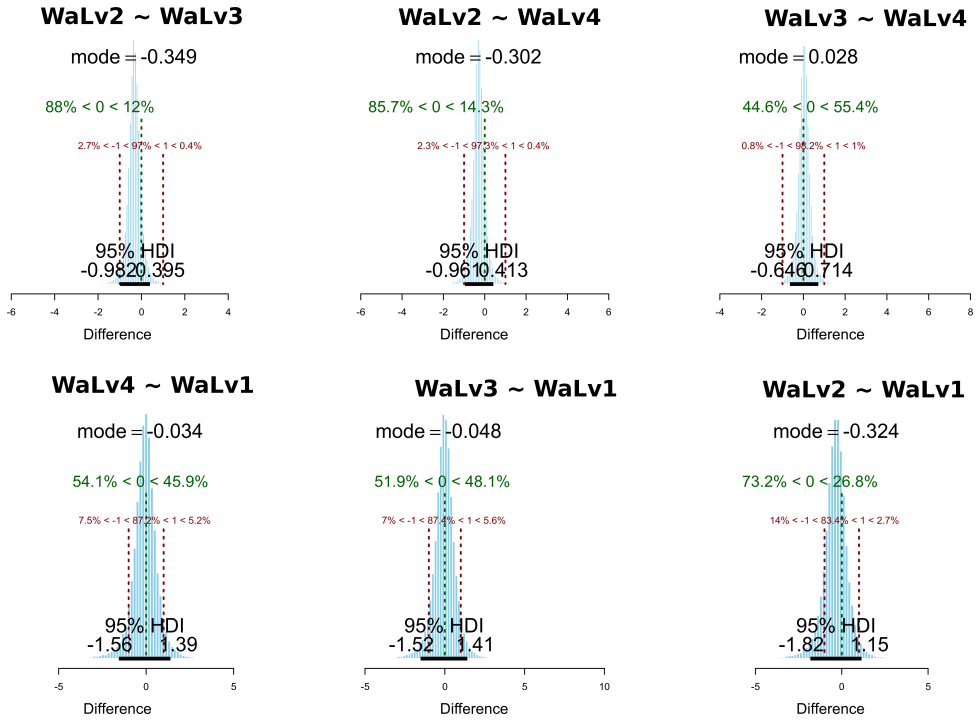

(c) Wa - Summer.

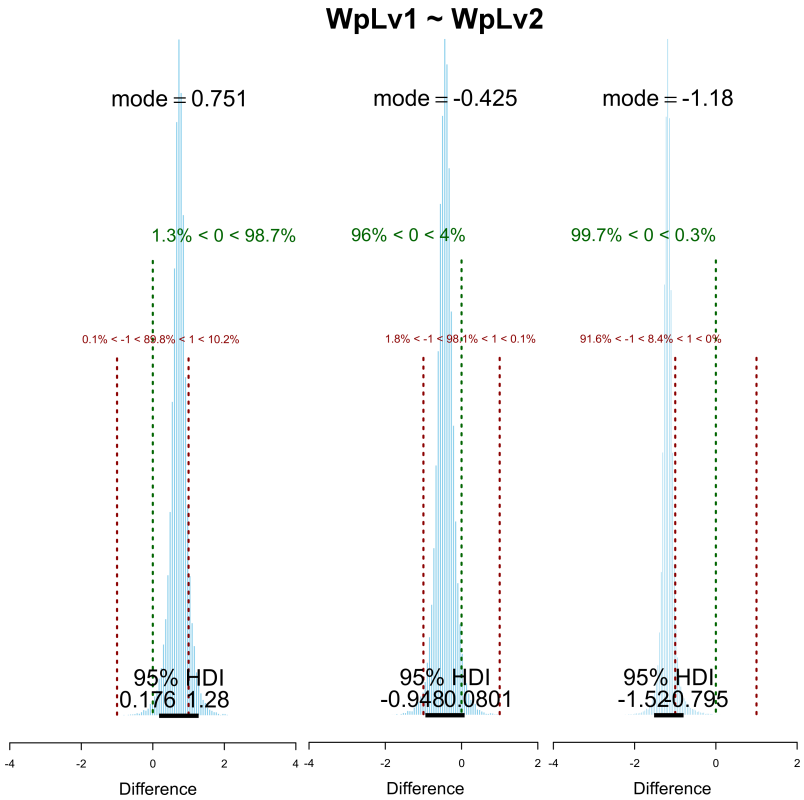

(d) Wp - Winter (left), summer (centre), spring (right).

Figure G.1: The credible temperature difference distributions between the levels of Wa (a,b,c) and Wp (d). The percentage of the distribution mass located at the right and left of 0 is reported in green, while the percentage at the left of -1, between -1–1 and at the right of 1 is shown in red.

Appendix H

The estimated rate averages and dates for each detected change point

Table H.1: The estimated average larvae to adult development rate (avg) and the change date (number of days from the beginning of the experiment, the 1st November 2015) for each estimated change point. The estimated hourly rates were back-transformed in daily rates using the inverse of Equation 6.2.5, to facilitate their interpretation and comparison.

		LST/WS			**WaLv2WpLv1**			**WaLv3WpLv1**			**WaLv4WpLv1**		
		wi	sp	su	wi	sp	su	wi	sp	su	wi	sp	su
LST	avg	0.01	0.04	0.07									
	day	92	163	-									
WS	avg	0.01	0.03	0.06									
	day	108	171	-									
ExLv1	avg				0.01	0.03	0.07	0.01	0.01	0.05	0.01	0.01	0.06
	day				110	202	-	58	109	-	55	107	-
ExLv2	avg				0.01	0.03	0.07	0.01	0.04	0.08	0.01	0.04	0.08
	day				100	202	-	100	202	-	107	202	-
ExLv3	avg				0.01	0.01	0.04	0.01	0.02	0.05	0.01	0.03	0.07
	day				58	83	-	61	85	-	100	176	-

Table H.2: The estimated adult survival rate (avg) and the change date (number of days from the beginning of the experiment, the 1st November 2015) for each estimated change point. The estimated hourly rates were back-transformed in daily rates using the inverse of Equation 6.2.5, to facilitate their interpretation and comparison.

		LST/WS			**WaLv2WpLv2**			**WaLv3WpLv2**			**WaLv4WpLv2**		
		wi	sp	su	wi	sp	su	wi	sp	su	wi	sp	su
LST	avg	0.83	0.95	0.97									
	day	103	157	-									
WS	avg	0.73	0.92	0.97									
	day	58	117	-									
ExLv1	avg				0.89	0.97	0.97	0.84	0.93	0.97	0.86	0.93	0.97
	day				110	153	-	57	110	-	57	110	-
ExLv2	avg				0.83	0.93	0.97	0.84	0.97	0.97	0.84	0.93	0.97
	day				57	117	-	117	153	-	58	110	-
ExLv3	avg				0.71	0.93	0.74	0.68	0.94	0.90	0.77	0.93	0.91
	day				57	204	-	57	217	-	38	218	-

Declaration / Eidesstaatliche Versicherung

I hereby declare that except where specific reference is made to the work of others, the contents of this dissertation are original and have not been submitted in whole or in part for consideration for any other degree or qualification in this, or any other university. This dissertation is my own work and contains nothing which is the outcome of work done in collaboration with others, except as specified in the text and Acknowledgements.

Matteo Marcantonio
March 2017